Characterisation of two mouse mutant lines generated by transgene insertional mutagenesis

Paisley, Derek John

Award date:
2000

Awarding institution:
University of Bath

CHARACTERISATION OF TWO MOUSE MUTANT LINES GENERATED BY TRANSGENE INSERTIONAL MUTAGENESIS

Submitted by Derek John Paisley

for the degree of PhD of the University of Bath

2000

ProQuest LLC
789 East Eisenhower Parkway
P.O. Box 1346
Ann Arbor, MI 48106-1346

Characterisation of Two Mouse Mutant Lines Generated By Transgene Insertional Mutagenesis

Derek John Paisley, PhD

University of Bath, 2000

ABSTRACT

Some 74 lines of transgenic mice were screened for insertional mutant phenotypes using a two-step breeding strategy. A number of interesting developmental mutations were identifed and confirmed as resulting from transgene insertional mutagenesis. The further characterisation of two of these lines is described.

The Ann line displayed a severe ataxic phenotype, leading to death at an early age. Histological analysis of the brains of these mice revealed abnormal neuronal patterning in the cerebellum, cerebral cortex and hippocampus. The site of transgene insertion was mapped on Chromsome 4 by a combination of Fluorescence *In-Situ* Hybridisation (FISH) and backcross linkage mapping. The expression of several candidate genes mapping close to the transgene was tested. Expression of the mouse disabled (*mdab1*) gene was completely ablated in the brains of Ann mutants. Several mutant alleles of this gene have already been described that result in a phenotype indistinguishable from that seen in Ann mutants. The Ann mutant thus represents a new member of a pre-existing allelic series at this locus.

Male homozygotes of the Ob transgenic line have never been identified. That a significant proportion of Ob transgenic males did not breed strongly suggested that this line was affected by male sterility. Non-breeding males were confirmed as homozygous transgenics by FISH on interphase chromosome spreads. Additionally, histological studies showed abnormalities in testicular morphology as well as a reduction in a subset of spermatogenic cell types. Again the site of transgene insertion was mapped by FISH and linkage mapping. No strong candidate genes are present around the site of transgene integration on chromosome 8 suggesting that a novel mutation could be present in the Ob line.

I wish to dedicate this thesis to my parents,

Kathleen and Alexander Paisley.

ACKNOWLEDGMENTS

Firstly, I would like to give my warmest thanks to my supervisor Dr. Andrew Ward. Not just for his excellent supervision but also for taking me on when I most needed a break. The contribution made by Dr. Bill Bennett to my PhD cannot be understated. Bill not only led the way but also set an extremely high standard that I could only hope to live up to. Thanks to everyone else in lab 0.76 and the rest of the Developmental Biology Programme for generating an enjoyable, challenging and often exhilarating atmosphere in which to work. I must also mention the staff of the University of Bath animal facility for their camaraderie.

I thank my Mother and Father for their unstinting personal support. I also cannot forget Claire Adams for sharing the mostly good times with me during our tenure in Bath. A special mention must go to Eamon Mallon for putting up with me and still managing to be my favourite ever flatmate/lunchtime companion. More than thanks go to Lucy Allen for providing me with the best ever excuse to take a break from writing-up.

Thanks to Benjamin Cravatt for providing the *faah* cDNA clone and to Chris Walsh and Jonathan Cooper for the *mdab1* clones. Janet Smith provided guidance for perfusion fixation. Thanks also to Professor Chris Graham who assisted me in re-deriving a number of lines in Bath. Muriel Lee provided technical advice for *FISH* and G-banding and also an expert opinion on chromosomal assignments.

ABBREVIATIONS

A	adenosine
bp	base pairs
BSA	bovine serum albumin, fraction V
C	cytosine
cDNA	complimentary DNA
CCD	centrally conserved domain (*Igf2/H19* intergenic region)
CCD	charge-coupled device (camera)
Chr	chromosome
cM	centimorgan(s)
CNS	central nervous system
DEPC	diethylpyrocarbonate
DMR	*Igf2* 5′ differentially methylated region
DNA	deoxyribonucleic acid
EDTA	ethylene diamine tetra-acetic acid, sodium salt
ENU	ethylnitrosourea
ES cells	embryonic stem cells
EtBr	ethidium bromide
EtOH	ethanol
FITC	fluorescein isothiocyanate
H&E	haematoxylin and eosin
IAP	intracisternal A particle
Igf-2	gene encoding insulin-like growth factor-II
IMS	industrial methylated spirit
kb	kilobase(s)
LB	Luria-Bertani medium
Luc	luciferase coding region
M	molar

MOPS	3-[N-Morpholino]propanesulfonic acid
mRNA	messanger ribonucleic acid
nt	mucleotide(s)
NTD	neural tube defect
OD	optical density
PAC	phage (P1) artificial chromosome
PBS	phosphate buffered saline
PCR	polymerase chain reaction
QTL	quantitative trait locus
RFLP	restriction fragment length polymorphism
RI	recombinant inbred
rpm	revolutions per minute
Rnase	ribonuclease
RT	reverse transcriptase
SDS	sodium dodecyl sulfate
SSC	150mM NaCl, 15mM Na citrate
SSCT	4xSSC containing 0.05% Tween-20
SSCTM	SSCT + 5% non-fat milk
SSPE	20mM NaH_2PO_4, 0.3M NaCl, 2mM EDTA
SV40	simian virus 40
TBE	tris/boric acid/EDTA
TE	10mM Tris.HCl pH 8.0, 1mM EDTA
YAC	yeast artificial chromosome

TABLE OF CONTENTS

LIST OF TABLES

LIST OF FIGURES

CHAPTER 1: INTRODUCTION

1.1 The Laboratory Mouse As A Model System

The study of mouse genetics originated at the beginning of the 20th century with the demonstration that Mendel's laws could be applied to mammalian species. This was done by Cuenot who, along with two other forefathers of the field, Castle and Bateson, conducted their work on mouse coat colour phenotypes (reviewed in Mouse Genetics by L. M. Silver [1]).

The small size, short gestation period and prolific breeding rate of the mouse, made it an ideal model for the study of mammalian genetics. Mouse genetics only really though began to flourish with the advent of recombinant DNA technology. Early mouse genetics focused on the generation of inbred lines of the *Mus musculus* sub-species, and the study of a small number of 'classical' loci which had a readily identifiable phenotype.

The ability to manipulate genes using molecular biology, coupled with existing embryology, facilitated the generation, or improvement, of a wide range of techniques useful for studying mouse genetics, development and cell biology. Mouse genes can now be cloned, sequenced, mapped (both genetically and physically) and manipulated in a variety of ways. Laboratory mice can now be generated in which genes are deleted, subtly changed or missexpressed. This has enabled us to learn much about the mouse genome and how it functions, yet despite this a great deal of questions remain unanswered. The sequencing of the entire mouse genome, which should be completed within the forthcoming months, will ensure that further progress proceeds at an astonishing rate.

1.2 Tools For studying The Mouse Genome - Genotype Based Analysis

The original genetics of Mendel investigated naturally occurring, visible mutations. Today, the ability to manipulate the mouse genome means that both a genetic and a 'reverse genetic' approach can be employed by investigators. As well as going from a mutant phenotype to identification of the gene involved, one can now, with the DNA sequence of a mouse gene in-hand, investigate what the phenotypic effects are of artificially manipulating this gene. This can facilitate the elucidation of a gene's wild-type function. The technology available for manipulation of the mouse genome has evolved so rapidly that alterations ranging from vast chromosomal rearrangements to point mutations can now be introduced with relative ease.

1.2.1 Gene targeting

The cloning of a gene facilitates the manipulation of that gene by means of targeted gene replacement. This involves the replacement of the endogenous wild-type gene with a gene copy bearing the desired mutation. Gene targeting, as this technology is known, involves the manipulation of the mouse genome using embryonic stem (ES) cells in culture. Cells bearing an altered genetic code are then used to generate mice carrying only the altered copy of the gene of interest.

Derived from the inner cell mass of mouse blastocyst stage embryos, embryonic stem (ES) cells can be maintained in culture, where treatment with leukaemia inhibitory factor/differentiation inhibitory activity (LIF/DIA) allows them to retain their totipotency [2-4]. On re-introduction into mouse embryos these cells contribute to normal embryonic development [5]. During culture, ES cells can be subjected to genetic

manipulation through homologous recombination with specially designed gene-targeting constructs. These constructs contain a region of homology to the gene being targeted, which is essential for homologous recombination to take place. The homologous region incorporates the desired modification that will be introduced into the endogenous gene upon successful targeting. When the aim of a targeting experiment is the introduction of a null mutation into an endogenous gene, the region of homology used in the targeting vector will most often be disrupted with a positive selectable marker such as a neomycin resistance cassette. This serves two functions. Firstly, expression of this marker can be used to select ES clones, into the genomes of which the targeting vector has been introduced. Secondly, depending upon the homology region used, the selectable cassette will create a null mutation by replacing or interrupting the desired segment of the endogenous gene (most often the protein coding region of the gene) [6].

In the vast majority of cases, such an exogenous DNA construct, upon introduction into an ES cell culture, will integrate randomly into the genome of these cells. It has been found that only around 1 in 1000 integration events take place by homologous recombination [7]. A procedure to enrich for homologous recombination events is therefore desirable. This is achieved through the incorporation of a negative selectable marker (such as the Herpes Simplex Virus Thymidine Kinase (HSV TK) cassette) in the targeting vector, outwith the gene homology region. This cassette will not be incorporated into the host genome, following homologous recombination, allowing selection of targeted ES cell clones [6].

Successfully targeted clones can then be microinjected into the blastocoel cavity of a blastocyst stage embryo that is then introduced into a surrogate mother [6]. Alternatively, ES cells can be incorporated into a cleavage stage embryo by means of aggregation [8]. Being totipotent, ES cells are able to contribute to both the somatic and germ cell lineages of the host embyo, to generate a chimera [5]. Chimeric mice produced in this manner are identifiable through the use of coat colour genetics. ES cell lines are generally derived from the 129 inbred strain of laboratory mice, which has an agouti (or in the case of the 129/Ola substrain, chinchilla) coat colour. Chimeric mice display patches of agouti coloured fur (derived from 129 cells) interspersed with the blastocyst derived colour (often white from the BALB/c line or black from the C57BL/6J line). Chimeras are then bred, with the aim of passing the targeted genome through the germline to produce pure-bred offspring which will be heterozygous for the targeted alteration. Crossing of heterozygotes will then generate homozygous animals, the phenotype of which can be studied in detail.

The basic gene-targeting technology used to introduce straightforward null mutations at a specific gene has been adapted to facilitate the introduction of more subtle mutations i.e. point mutations, into an endogenous gene. One such method, 'hit and run' gene targeting, involves a two-step recombination strategy [9]. Conventional gene targeting (as described above) is used to replace the endogenous gene with a specially designed targeting vector. A second, intrachromosomal recombination event (which is also selectable), then eliminates the selectable marker and leaves behind an engineered copy of the gene.

Another two-step targeting strategy that can be used to introduce subtle alterations to genes is double replacement gene targeting [10, 11]. Again, a conventional targeting step is used to replace the endogenous gene with a targeting vector that includes a marker that is both positively and negatively selectable (usually HPRT). A second targeting step is then used to replace the newly introduced sequence with an identical copy of the original gene except for the subtle alteration of choice. This step is also selectable through the loss of the positive/negative selectable marker. An advantage this method has over 'hit and run' gene targeting is that following the original targeting step, separate mouse lines bearing different mutant alleles can be produced by carrying out the second targeting stage with different constructs.

An alternative to both of the two-step targeting methods for introducing subtle mutations is the generation of transgenic lines with the transgene consisting of a subtly altered gene copy, on a null genetic background generated by conventional gene targeting. This approach can often prove more efficient for generation of multiple mutant alleles but does require that the expression of the transgene is correctly regulated.

1.2.2 Cre/lox P technology

The ability to study the function of a gene of interest, by introducing a null mutation into this gene, is often impeded by the embryonic lethality of the mutant mice generated by gene targeting. It is, though, possible to introduce mutations into genes in a spatially or temporally restricted manner that may enable animals to survive to term if not adulthood. This can be achieved through the use of the bacteriophage P1-derived loxP sequence for site-specific recombination, in conjunction with the Cre

recombinase enzyme that catalyses the recombination reaction. Introduction of the short (23bp in length) loxP sites at the desired location is possible through gene targeting in ES cells. To generate a conditional null mutation, loxP sites are often introduced flanking the protein coding region of the gene of interest. These gene-targeted mice, bearing a so-called 'floxed' gene, can then be bred with a transgenic mouse line that expresses the Cre recombinase enzyme either in a spatially or temporally restricted manner [12]. Cre-mediated recombination of loxP sites will then take place, generating a recombined null allele in the offspring produced only in the tissues or at the time at which the enzyme is expressed. This allows the effects of loss of gene expression only in particular tissues or at particular time periods to be studied where, in a conventional gene-knockout, the mouse may have died early in embryogenesis.

Cre/loxP technology has also been applied to uses other than the generation of conditional knockout mice. The introduction of loxP sites at specific chromosomal locations has facilitated the generation of chromosomal rearrangements unattainable by means of conventional gene targeting. This 'chromosome engineering' has been successfully used to introduce defined chromosomal deficiencies, inversions and duplications into the mouse genome [13]. Such technology can be applied to create useful models of human diseases that involve chromosomal rearrangements as well as other tools such as mouse strains carrying balancer chromosomes [14]. Another use of the Cre/loxP system is the accurate replacement of a specific gene with a gene of choice. In such a 'knock-in' mouse an endogenous gene can be simultaneously disrupted and replaced with another gene. The expression pattern of the introduced gene should recapitulate that of the original. 'Knock-in' mice can be useful

in demonstrating the functional redundancy of closely related genes (e.g. the muscle-specific transcription factors myogenin and Myf-5 [15]).

1.3 Tools For Studying The Mouse Genome - Phenotype Based Analysis

In addition to the introduction of specific genetic alterations following the isolation of the DNA sequence of a gene, the laboratory mouse also lends itself to more traditional genetic investigation where one can progress from the discovery of a phenotypic mutation to the isolation of the gene responsible for this phenotype. A variety of techniques have been successfully used to produce novel mutants without prior knowledge of gene sequence. The genes involved in these, as well as the vast number of naturally occurring mouse mutants in existence, can then be isolated through gene mapping and cloning.

1.3.1 Gene traps

In addition to the targeted alteration of genes, embryonic stem cells have successfully been used in the generation of random mutations by 'gene trapping'. Upon their introduction to ES cells, gene trap vectors integrate into the host genome at random. These vectors are designed so that their insertion into an actively transcribed gene can be identified and they can then be used as a means to isolate the endogenous gene involved [16]. This is achieved through the presence of two genes in the gene trap vector: a selectable marker (e.g. *neo*, encoding resistance to the antibiotic G418) [17], that allows the selection of integration events, and a reporter gene (e.g. β–galactosidase), that enables lines carrying a successful gene-trap event to be identified [18]. In the generic gene trap vector the reporter gene does not have any associated control elements meaning that it will only be expressed upon integration of the vector into an exon of a transcribed gene.

Modification of the basic vector by the addition of a splice acceptor site upstream of the reporter allows expression upon integration of the vector into either an intron or an exon [19].

Succesful 'trapping' of a gene in this manner serves multiple functions. The endogenous gene will usually be rendered dysfunctional, constituting a null mutation. Gene trapped ES cells can be used to generate mouse lines in an identical manner to gene targeted ES lines, therefore the phenotypic effects of a gene trap mutation can be studied. Furthermore, the inclusion of the reporter gene in the gene trap vector means that the expression pattern of the 'trapped' gene can be followed. Finally, the vector itself facilitates the cloning of the 'trapped' gene, often by RACE (rapid amplification of cDNA ends); a technique used to amplify unknown stretches of cDNA flanking a region of known sequence [20].

Additional modifications to the basic gene trap vector have been developed, facilitating the successful isolation of unknown enhancers [21] and secreted and membrane-spanning proteins [22] in addition to gene coding sequences.

1.3.2 Transgene insertional mutagenesis

A further method of mutating the mouse genome at random is through the production of transgene insertional mutants. DNA constructs introduced into the mouse genome either through pronuclear microinjection of fertilised eggs [23], electroporation of ES cells [24] or infection with a retrovirus based vector [25] integrate randomly into the host genome. It has been estimated that in 5 to 10% of transgenics the function of an endogenous gene is disrupted [26]. Such mutants are suitable for further

characterisation using the transgene sequence as a molecular handle. Indeed a variety of interesting mouse mutants have been generated and characterised in this way. Transgenic insertional mutagenesis will be discussed in greater detail in section 1.6.

1.3.3 Mutagenic agents

Both ionising radiation and chemical mutagens have been used to induce germline mutations in the mouse. Whilst exposure to radiation of one of the three commonly used types (X-rays, gamma rays or neutrons) frequently creates large deletions or other chromosomal rearrangements [1], chemical mutagens are available that, upon delivery to the gonads, can induce both large and discrete mutations in the mouse germline. Furthermore, chemical mutagens have a much higher mutational yield than any radiation type tested, making them more suitable for small scale screening programmes.

Ethylnitrosourea (ENU) is a chemical mutagen that induces discrete lesions which are often point mutations [27]. ENU has been used in a number of screens for mutations across the whole genome [28] or at specific chromosomal sites [29]. Rapid throughput, whole genome mutagenic screens are being carried out using ENU treatment. Such studies usually involve screening for detectable dominant mutant phenotypes that are expressed in heterozygous animals generated by a single point mutation in a gene. The number and variety of dominant mutant phenotypes identified in this way can depend upon the screening strategy used to identify mutant animals. One such study being carried out by the MRC Mammalian Genetics Unit involves the use of the SHIRPA (SmithKline Beecham, Harwell, Imperial College, Royal London Hospital, Phenotype

Assesment) protocol for detecting even the most subtle dominant mutant phenotypes with a special emphasis being placed on neurological phenotypes [30].

ENU mutagenesis has also been used in screening for recessive point mutations in chromosomal regions that have been defined by deletions. The existence of mouse strains carrying characterised deletions spanning single or multiple genes, allows the expression of recessive mutant phenotypes following a single point mutation in one of these genes. ENU is now being used to saturate such regions with point mutations (e.g. the *t* region [31]). Unfortunately only a limited number of these regions exist throughout the genome. Most deletion complexes available in the mouse were generated by X-ray irradiation. It is hoped that the discovery of a chemical mutagen, chlorambucil, that induces deletion mutations at a high rate in the mouse may lead to an increase in the number of genomic regions in the mouse that are defined by deletions [32]. Alternatively, Cre/loxP chromosomal engineering can be employed for the same purpose [13].

1.4 Analysing The Mutant Resource

1.4.1 Bridging the phenotype gap

With a panopoly of techniques now available for the generation of both targeted and random mutations in the mouse genome, perhaps the major bottle-neck in the progression of murine functional genomics rests with the phenotypic analysis of the array of mutants which have been, or are being, generated.

Whilst new mutants have been produced at a phenomenal rate, often through high throughput, systematic mutagenesis programmes, until recently, phenotypic analysis of mutants was only conducted on a mouse to mouse basis. A major aim of mouse functional genomics is now the high throughput analysis of mutant phenotypes that will in turn provide an essential insight into the functions and interactions of a vast number of mammalian genes. Such studies, working in tandem with large scale mutagenesis programmes of a variety of types, are currently in progress [33].

1.4.2 The emergence of microarray technology

Microarray technology is an extremely novel approach to high-throughput genomic analysis based upon the ability to spot high numbers (as much as 10,000) of discrete cDNAs onto a non-porous support (e.g. glass). Expression in a test sample of each gene represented on the array can then be monitored through hybridisation and fluorescent detection [34].

This technology has a variety of applications including the analysis of differential gene expression in disease [35]. In the context of mouse mutant analysis, cDNA microarrays have considerable potential for investigating the effects of a mutation on the expression of other genes. One could envisage using microarray technology on mouse mutants in order to identify genes up or downregulated in the mutant, implying their interaction in some way with the mutated gene [36]. In this way a clearer picture of gene and protein interactions and expression pathways could be formulated.

1.5 Mapping Genes And Mutations In The Laboratory Mouse

The mapping of genes and mutations represents an extremely important tool in modern mouse genetics. Obtaining the map position of a phenotype-causing mutation is often the fist step in the molecular cloning of the causative gene. Alternatively, DNA clones of unknown function can be associated with characterised mutant phenotypes by means of gene mapping. Recently, mapping has been increasingly applied to the dissection of complex traits and the identification and cloning of loci contributing quantitatively or qualitatively to such traits [37].

Mapping studies can be subdivided into three tiers: chromosomal mapping allows the assignment of a locus to a specific chromosme or chromosomal segment, whilst linkage mapping involves the ordering of loci through recombinational distance. At the highest level of resolution, physical mapping is based upon the direct analysis of DNA, either in the form of overlapping clones or nucleotide sequence itself.

1.5.1 Linkage mapping in the mouse

Linkage mapping centres upon the premise that meiotic recombination takes place at random sites across the genome and the further two linked loci are apart the greater the likelihood of recombination events taking place in the intervening region. The frequency of recombination between two linked loci therefore provides a measurement of the genetic distance between these sites.

In the laboratory mouse, breeding experiments of different types can be performed and offspring tested to identify whether parental or recombinant combinations of genes being mapped have been inherited.

For this to be possible it is essential that the loci of interest exist in multiple identifiable forms or alleles.

Originally, linkage mapping was carried out only on a small number of phenotypically defined loci. The dawn of the recombinant DNA era has meant that now polymorphic DNA sequences, such as microsatellite markers, can be linkage mapped [38].

An extremely detailed linkage map now exists for the laboratory mouse, containing thousands of polymorphic genes and DNA sequences ordered across the whole genome, with new markers being added on a daily basis [39].

1.5.2 Chromosomal mapping

Chromosomal mapping involves the assignment of loci to a specific mouse chromosomal or sub-chromosomal region. Whilst not providing the same level of resolution as linkage mapping, chromosomal mapping does circumvent the need for mouse breeding excercises.

Individual chromosomes can be defined cytogenetically, according to their size and the banding pattern obtained following staining with dyes such as Geimsa. If a probe specific to the locus of interest is to hand (e.g. a cDNA clone), then fluorescence *in situ* hybridisation (FISH) can be performed in concert with chromosomal banding to allow a sub-chromosomal assignment for the locus to be made [40].

The use of somatic cell hybrid lines, containing a portion of a mouse chromosome in combination with the complete karyotype of another

species, allows loci to be assigned to a sub-chromosomal interval [41]. Radiation hybrid panels are derived from somatic cell hybrid lines but contain even smaller portions of mouse chromosome, allowing a higher degree of resolution to be obtained [42].

1.5.3 Physical mapping

Physical maps are concerned with the molecular constitution of the locus of interest, and as such provide the highest level of resolution of the various mapping strategies. Such maps are usually found as a contiguous series of of overlapping DNA clones, or contig. Owing to their greater cloning capacity, contigs are usually constructed using YAC (yeast artificial chromosome) cloning vectors [43], although BAC (bacterial artificial chromosome) and PAC (P1 artificial chromosome) vectors have been used [44].

The nucleotide sequence of a genomic region can also be considered a form of physical map. Indeed, the complete physical mapping of the mouse genome is currently underway [45], with the production of contigs covering each mouse chromosome facilitating the nucleotide sequencing of the chromosome [46].

Positional cloning involves the progression from high-resolution linkage mapping, in which markers closely flanking the gene of interest have been identified, to the cloning of the sequence separating the two markers (chromosome walking) through the construction of a contig. A variety of methodologies can then be utilised to isolate the gene in question such as exon trapping [47] and CpG island identification [48] as well as direct sequencing.

1.6 Transgene Insertional Mutagenesis

1.6.1 Making transgenics

The ability to culture mouse eggs and early stage embryos that could subsequently develop as normal following re-introduction into the uterus, opened the way for the creation of genetically altered mouse lines. The generation of adult 'transgenic' mice carrying exogenous DNA, introduced by the genetic manipulation of cultured mouse embryos, was first achieved through the injection of viral particles into the blastocoel cavity of blastocyst stage mouse embryos [49]. Soon after it was discovered that microinjection of DNA into fertilized mouse eggs could also be used to produce transgenic lines [23]. A variety of techniques are now available for making transgenic mouse lines. The most widely used technique is microinjection of DNA into the pronucleus of a fertilised oocyte. Alternatively, DNA can be introduced into embryonic stem cells that can then be microinjected into the inner cell mass of a blastocyst [24]. In both cases the genetically altered embryo can then be taken through development by re-introduction into a pseudopregnant surrogate mother. Founder animals produced in this manner can then be bred in order to establish a new transgenic line.

The life cycle of retroviruses makes them ideal candidates for use in making transgenics. The double stranded DNA provirus integrates into the genome of an infected cell as a single copy without accompanying genomic rearrangements [50]. Genetically engineered viruses can thus be used to introduce exogenous genes into the genome of pre-implantation embryos [25] or ES cells [51], again facilitating the generation of a transgenic founder.

Transgenic mice have a variety of important applications in modern biology. One common use is in the study of regulatory regions controlling gene expression. By generating a range of transgenic lines, each bearing a different segment of a regulatory region in combination with a suitable reporter gene, the effects of each segment upon gene expression can be elucidated. In this way the composition of regulatory regions can be dissected accurately.

Another reason for making transgenic mouse lines is to determine the effects of gene missexpression. This can be achieved by combining the gene of interest with regulatory regions that will cause it to be expressed in a different tissue, at a different developmental stage or at a different level than normal. Any mutant phenotype created through such missexpression may provide some insight into the normal function of the gene in question [52].

Transgenic technology can also be used to ascertain whether a cloned candidate gene is responsible for a mutant disease phenotype. To discover if a cloned gene complements a recessive mutation, a transgene rescue experiment can be performed. The success of such a test may depend upon an accurate recapitulation of the gene expression pattern. The fact that gene regulatory regions can sometimes be located hundreds of kilobases upstream of a gene can now be overcome by making BAC or YAC transgenics in which the transgene may be large enough to encompass all regulatory regions [53, 54].

Two problems that can hamper transgenic studies arise due to the tendancy of microinjected transgene DNA to integrate into the host

genome at random. Firstly, levels of transgene expression can be affected by local chromatin conformation, depending upon the site of insertion, or de-novo methylation. This can often cause a reduction in expression or silencing of a transgene [55]. Secondly, integration into an endogenous gene can occur and may result in the production of a mutant phenotype [26]. Care must be taken not to confuse such a mutation with one resulting from the expression of the transgene.

1.6.2 Mechanisms of microinjected transgene insertion

Although the integration mechanism of microinjected DNA into the host genome is unknown, a number of features of the integration event are widely recognised. It is the commonly held view that transgene integration into the mouse genome is random or at least near-random [55, 56]. Despite the fact that evidence in favour of preferential integration into genes or other 'hot spots' does exist it would be premature to eliminate a model of random insertion [26].

In the majority of cases, transgene insertion is thought to take place at a single site in the genome, although multiple sites of integration have been reported in transgenics generated by iontophoretic techniques [57] or pronuclear microinjection (A. Ward, personal communication). A transgene can insert as single or multiple copies. Multiple copy arrays are normally found with individual transgene units orientated as 'head-to-tail' repeats [58]. It has been proposed that such arrays are generated through extra-chromosomal homologous recombination between individual transgene units. The concatamer formed could then insert into the genome, resulting in a multiple copy array with transgene elements orientated predominantly in a 'head-to-tail' fashion [59]. Supporting

evidence exists with an experiment in which microinjection of two MT-hGH genes with non-overlapping deletions gave rise to functional recombinant hGH copies in transgenic mice [60]. Such a model also accounts for the high frequency of incomplete transgene copies found at the terminal ends of such arrangements.

Finally, a mechanism of transgene integration into the host genome has been suggested that involves the ends of DNA molecules initiating integration at the site of randomly generated chromosomal breaks [61]. This might explain why the integration efficiency of linear molecules have been observed at fivefold that of circular species.

1.6.3 Chromosomal rearrangements associated with transgene insertion

Transgene integration is often accompanied by chromosomal rearrangements with deletions [62], inversions [63] or translocations [64] frequently occurring at the same site. Surprisingly, novel DNA sequences, found neither in the injected DNA nor around the integration site, have also been identified in some transgene junctions [55]. Studies of breakpoints at naturally occurring chromosomal translocations yield similar observations [65], suggesting a common mechanism for both phenomena.

The probability of disruption to somatic gene function is likely to be increased by the frequent occurrence of chromosomal rearrangements at the site of transgene insertion. Such alterations, whilst increasing the distance from the transgene itself at which endogenous genes may be susceptible to alteration, can also make the identification of these genes more difficult.

Transgene DNA is thought to transmit stably from generation to generation without further possibility of rearrangement. Reports have, though, shown that rearrangement is possible in rare cases where partial deletions and amplifications have been observed [66-69].

1.6.4 Disruption of somatic gene function by insertional mutagenesis

The insertion of transgene DNA into the genome at random means that the disruption of an endogenous gene is a distinct possibility. It has been estimated that between 5% and 10% of transgenic mice will display some form of transgene insertional mutation through disruption of endogenous gene function [26]. This figure is probably an underestimate given the fact that a number of dominant insertional mutations probably go unidentified due to embryonic lethality. Furthermore, subtle phenotypes may also escape detection. Insertional mutants are often generated as a by-product of transgenesis studies but have proved useful in the identification and characterisation of novel genes and mutants [26]. As well as constituting the mutagenic agent, integrated transgene DNA can act as a useful starting point for the further characterisation of the mutant locus at the molecular level.

1.6.5 Using transgene mutagenesis as a method for identifying new mutants

Transgene insertional mutagenesis has proved to be a useful tool for the study of many biological processes by providing a wide variety of novel mutant phenotypes and making their relatively rapid characterisation, especially at the molecular level, a realistic possibility [26].

On identification of a mutant phenotype in a group of transgenic mouse lines, how should one proceed with a more in depth characterisation?

It is important to acknowledge the possibility for spontaneous mutants to appear in such transgenic studies. The in-breeding of lines creates a population 'bottle-neck' in which reinforcement of spontaneous, or indeed pre-existing mutant alleles, could occur. Therefore, in the characterisation of insertional mutants it is important to identify a causal relationship between the transgene and the mutant phenotype. The involvement of the transgene is important since it provides a possible means for the mapping and isolation of the mutant allele.

The ability to use the transgene as a probe for Fluorescent *in situ* Hybridisation (FISH), on Metaphase chromosome spreads, greatly improves the ease of mapping the allele in question. Any map position obtained this way can be further refined through the use of Simple Sequence Length Polymorpism (SSLP) microsatellite markers in association with a suitable breeding strategy [1]. Once a map position has been confidently assigned, it becomes possible to determine if the insertional mutant represents a novel allele of a pre-exisiting mouse mutant. The Mouse Genome Database, which contains information on greater than five thousand mapped genes, provides a means by which possible allelism can be determine relatively quickly [39].

With mutation of a novel gene confirmed, the identification and subsequent characterisation of this locus can be undertaken using the transgene as a molecular tag. Attempts at cloning genomic DNA flanking the site of transgene integration can be complicated by the chromosomal rearrangements that are often found at this site, not to mention complicated arrangements of transgene copies within multiple arrays [55]. Nevertheless, successful isolation of flanking sequence can serve as a

starting point in cloning the wild-type allele by chromosome walking.

1.6.6 The advantages of retroviral transgenics

Production of transgenic lines by retroviral infection is somewhat more straightforward than the technically demanding technique of pronuclear DNA microinjection. Retroviral insertion into the host genome can be accomplished simply through the incubation of pre-implantation embryos or ES cells with virus-producing fibroblasts [25]. Furthermore, retroviruses integrate as single copies and, as often happens with microinjected DNA, integration is not accompanied by chromosomal rearrangements [25]. This presents distinct advantages for the use of retroviral transgenesis in the production of insertional mutants, since cloning of endogenous flanking sequence is generally more straightforward than in the case of injection transgenesis [70].

Retroviral transgenics do have disadvantages including the generation of mosaic founder animals at a higher rate than the 30% estimated in transgenics generated by pronuclear microinjection [71]. This results from infection taking place after the beginning of cell division and necessitates additional breeding steps in order to obtain pure-bred transgenics.

1.7 A systematic screen in the mouse for transgene insertional mutants

1.7.1 Background

Genomic imprinting describes the phenomenon whereby a number of genes are subject to monoallelic expression dependant upon their pattern of inheritance. Different allelic expression of *Igf-2* and *H19* is suspected to involve a number of regulatory elements at these loci. In an attempt to

elucidate the mechanisms behind this imprinting, over 70 lines of transgenic mice were generated [72]. Using the pronuclear microinjection method, individual transgenic lines were founded in Oxford, with one of eight linear DNA constructs. The basic transgene construct consists of the Firefly (*Photinus pyralis*) luciferase coding sequence, coupled to the P3 promoter region of the murine *Igf-2* gene and in seven of the constructs, one or more of regulatory sequences from the *Igf-2/H19* locus (see section 3.1.1). The inclusion of these regions was designed to facilitate the dissection of their functions in genomic imprinting, in isolation from their normal genomic environment and also, importantly, *in vivo*.

Bearing in mind the fact that levels of transgene expression can often be affected by the local chromosomal constitution, each construct was used to generate multiple, separate, transgenic lines. As determined by Southern blotting and breeding analysis, each line represented integration of one or more transgene copies at a single genomic site.

Given a documented frequency of between 5% and 10% of transgenics being insertional mutants [26], the observation of a number of mutant phenotypes was expected. This expectation was realised upon Caesarian rederivation of most of the lines during their transfer from Oxford to Bath.

During this procedure a number of developmental abnormalities were observed which otherwise might have escaped detection due to peri-natal lethality or canabalism by parents. As a result, it was decided that a screen for other developmental abnormalities, within this mouse population, be carried out.

1.7.2 Rationale of this project

A strategy to screen for insertional mutant phenotypes in this population was developed involving two different types of mouse cross. It is normal to expect the majority of mutations in developmentally important genes to be recessive. To test for visible mutations in homozygous offspring, male and female mice, hemizygous for the transgene were thus intercrossed. To detect homozygous mice a second type of cross was utilised. In this case transgenic offspring were backcrossed against non-transgenic animals. Crossing of a test animal homozygous for the transgene would produce litters where every pup is transgenic. If homozygous animals were found not to have a visible phenotype, this line was eliminated. If homozygotes displayed a mutant phenotype or if an abnormally low number of homozygous animals were identified the line would be subjected to further analysis.

In this way a number of transgenic lines bearing putative insertional mutations were found to display visible recessive phenotypes, whilst putative embryonic lethal, variably penetrant and sex-linked mutations have also been identified. Following confirmation that transgene insertional mutagenesis was the basis of the mutation in the mutants displaying visible reccesive phenotypes, these lines were characterised both at the phenotypic and molecular levels. Attempts to elucidate the physiological basis of the mutant phenotypes involved histopatholgical analysis. The inserted transgene provided a vital handle on the molecular basis of the mutations and facilitated gene mapping and attempted cloning exercises.

This thesis details the screen for transgene insertional mutations and the further characterisation of two lines found to bear recessive mutant phenotypes: Ann; a cerebellar ataxia mutant, and Ob; which exhibits male sterility.

CHAPTER 2: GENERAL METHODS AND MATERIALS

2.1 Materials

2.1.1 Mice

Transgenic mice were generated in Oxford using F1 zygotes resulting from crosses between C57BL/6J males and CBA/Ca females (hereafter abbreviated to F1(C57/CBA)). Transgenic lines were maintained by both incrossing of transgenic mice and outcrossing of transgenic to non-transgenic F1(C57/CBA) mice. Stocks of F1(C57/CBA) and C57BL/6J were maintained in the animal unit in Bath.

2.1.2 Other materials

General laboratory chemicals used were of the Analytical Reagent grade (unless otherwise stated) and were purchased from BDH, Fisher or Sigma.

2.2 General methods

Molecular biology methods were performed according to Sambrook et al [73], except where stated otherwise.

2.2.1 Production of electrocompetent *E.coli*

A modified version of [74, 75] was used. A single, well isolated, bacterial colony was picked from a SOB agar (2% bacto tryptone, 0.5% bacto yeast extract, 0.05% NaCl, 2.5mM KCl, 1.5% agar) plate and dispersed in 1ml of SOB (2% bacto tryptone, 0.5% bacto yeast extract, 0.05% NaCl, 2.5mM NaCl) by vortexing. Using a sterile loop, 50ml of SOB was innoculated with this suspension and cultured in a 500ml flask at 37°C, with shaking, for no greater than 12 hours. Two 4ml aliquots of this culture were used to seed 2x 400ml of SOB in 1 litre flasks. These cultures were incubated at 37°C with agitation (approximately 200rpm) for one hour, after which 1ml aliquots of culture were removed at regular intervals, and the optical

density measured at 550nm. Cultures were incubated until an optical density of 0.75 (corresponding to a density of around 3-6x10^8 cells/ml) was reached, following which, the remaining culture was transferred into 4x 250ml centrifuge pots. Cells were pelleted by centrifugation at 4,500rpm at 4°C in a Sorvall GSA rotor (Sorvall) using an RC-5B (Sorvall) centrifuge. Supernatants were decanted and the centrifuge pots placed on ice in a cold room (4°C). Pellets were gently resuspended in 200ml of chilled, sterile, 10% glycerol solution, using a 10ml pipette. Cells were again pelleted by centrifugation, supernatants decanted and pellets resuspended, all as before. After a further centrifugation step (as before), as much supernatant as possible was decanted and the cell pellet resuspended in any remaining supernatant (approximately 3ml in total). The cell suspension was transferred in 40µl aliquots to 0.5ml microfuge tubes, on ice, and snap frozen in liquid nitrogen.

2.2.2 Transformation of electrocompetent *E.coli*

For each transformation a 40µl aliquot of electrocompetent *E.coli* was thawed on ice and 1ng of purified plasmid DNA solution, in a volume of 2µl, added. This mixture was incubated on ice for 45 seconds and then transferred to a 1mm electroporation cuvette. Each cuvette was pulsed at 1.25kV (12.5kV/cm) using a Bio-rad electroporator. 1ml of warm SOB +Mg medium (SOB, 10mM $MgCl_2$) was immediately added to each cuvette and the bacterial suspension dispersed by pipetting. The bacterial suspension was removed from the cuvette and incubated at 37°C, with shaking, in a 15ml propylene Falcon tube for 1 hour, following which 10µl and 100µl of suspension were spread onto LB agar plates (20µg/ml ampicillin). Cells were cultured overnight at 37°C.

2.2.3 Small scale purification of plasmid DNA

A single, well isolated, bacterial colony was picked from an LB agar plate and inoculated into 1.5ml of LB medium containing the appropriate antibiotic in a 15ml Falcon tube. Cells were cultured overnight in a shaking incubator at 37°C and plasmid DNA extracted using the Wizard Miniprep SV kit (Promega) according to the manufacturers instructions for the spin protocol.

2.2.4 Large scale purification of plasmid DNA

A single, well isolated, bacterial colony was picked from an LB agar plate and innoculated into 250ml of LB medium containing the appropriate antibiotic in a 1L glass flask. Cells were cultured overnight in a shaking incubator at 37°C and then pelleted by centrifugation at 4,500rpm at 4°C in a Sorvall GSA rotor using an RC-5B centrifuge. The supernatant was then discarded and the cell pellet resuspended in 9ml of a 50mM glucose/50mM Tris pH 8.0/10mM 0.5M EDTA solution. Following the addition of 18ml of 0.2M NaOH/1% SDS the contents of each tube were mixed using a 'head-over-heels' motion and then incubated on ice for 5 minutes. 9ml of 3M Sodium Acetate (pH 5.0) were then added and the tubes again mixed in the same manner prior to a further 10 minute incubation on ice. Tubes were then spun at 7,000rpm for 10 minutes at 4°C in a Sorvall GSA rotor using an RC-5B centrifuge. Supernatant was then collected into a fresh tube and 21.6ml isopropanol added before further mixing and a 5 minute incubation on ice. After tubes had again been spun at 7,000rpm for 5 minutes at 4°C, the supernatant was discarded and the pellet resuspended in 2ml of TE pH 8.0. The DNA solution was then incubated with 2µl of 10mg/ml RNAase A (Sigma) at 37°C for 30 minutes. The solution was then transferred to a 50ml glass Corex tube and 2ml of Phenol (Sigma) added prior to vortexing

and centrifugation at 10,000rpm for 10 minutes at 4°C in an RC5-B centrifuge, using an SS34 (Sorval) rotor. The supernatant was then carefully transferred to a fresh Corex tube and 2ml of Chloroform added. Tubes were vortexed and spun as before and the supernatant again transferred to a fresh Corex tube. 200µl of 4M LiCl and 5ml of ice cold absolute ethanol were added and DNA precipitated at –70°C for 3 hours. Tubes were then spun at 10,000 rpm for 10 minutes at 4°C and the supernatant discarded, the DNA pellet washed with 70% ethanol and dried under vacuum. The pellet was then resuspended in 200µl of TE pH 8.0.

2.2.5 Purification of genomic DNA from mouse biopsy

This was carried out according to Hogan *et al*[76] (with modifications) on a 5-15mm tail biopsy either untreated or having previously been processed for luciferase assay (see section 2.2.17). Tail lysis buffer (50mM Tris.HCl pH 8.0, 100mM EDTA, 100mM NaCl, 1% SDS) was added to give a total volume of 525µl followed by the addition of proteinase K (Boeringher Mannheim) to a concentration of 285µg/ml. Samples were incubated for at least 12 hours at 55°C after which they were treated with 0.7µg/ml RNase A for 1 hour at 37°C. NaCl was added to 1.25M, samples briefly mixed by inversion, and an equal volume of chloroform/isoamyl alcohol 24:1 (vol:vol) added prior to gentle mixing at room temperature for 2 hours. Samples were microfuged (i.e. subjected to centrifugation in a bench top Heraeus centrifuge with 24-place, 1.5ml tube, rotor) for 10 minutes and the upper, aqueous, layer transferred to a fresh tube. An equal volume (approximately 700µl) of propan-2-ol was added and samples mixed by inversion to precipitate the DNA. Samples were microfuged for 10 minutes causing the precipitate to form a pellet, allowing the supernatant to be removed. Pellets were washed at 4°C for 1 hour in 300µl ice-cold 70%

ethanol. After brief centrifugation the ethanol was removed and the pellet air dried. The pellet was resuspended in 50µl TE (Tris.HCl pH 8.0, 1mM EDTA) overnight at 4°C.

2.2.6 Agarose gel electrophoresis of DNA

Unless stated otherwise, DNA samples were electrophoresed on a 1% agarose (United States Biochemical) gel containing 0.5µg/ml ethidium bromide at 80V for a suitable length of time (usually 1 – 3 hours). DNA was visualised on a UV lightbox.

2.2.7 Quantitation of DNA

Concentrations of purified genomic DNA, plasmid DNA and DNA fragments were estimated by comparison with DNA markers (100bp and 1kb ladders, Promega) of known concentrations, under UV light, following agarose gel electrophoresis (section 2.2.6).

2.2.8 Restriction endonuclease digestion of DNA

For isolation of DNA probe fragments, 1µg of plasmid DNA was used, whereas for digestion of genomic DNA for Southern blotting approximately 10µg of purified genomic DNA was used. DNA was digested with greater than 10 units of the desired restriction endonucleases (Promega) in a 1x concentration of the recommended restriction endonuclease buffers (Promega), for at least 12 hours at the working temperature for the particular enzyme in use.

2.2.9 Purification of DNA from agarose gels

Endonuclease digested plasmid DNA was electrophoresed on an agarose gel (section 2.2.6) and the appropriate DNA fragment excised with a scalpel blade on a UV lightbox. The DNA fragment was purified into 30µl of dH_2O

using the QIAquick Gel Extraction Kit (Qiagen) according to the manufacturers protocol.

2.2.10 Southern blotting

Genomic DNA samples (5-15μg) were digested overnight with the appropriate restriction endonucleases and electrophoresed on a 1% agarose gel containing 0.5μg/ml ethidium bromide. Transfer of DNA onto Hybond-N (Amersham) membranes was performed under high salt denaturing conditions according to standard procedures [73]. Following transfer, DNA was cross-linked to the membrane using a UV crosslinker (UVP, CL-1000) by exposure to 12,000 $\mu J/cm^2$ ultraviolet radiation.

2.2.11 Isolation of brain total RNA

Total RNA was extracted using TRI reagent (acid guanidinium thiocyanate phenol chloroform [77], Sigma) according to the manufacturers instructions. All equipment used for RNA isolation was soaked in DEPC-treated H_2O for a minimum of 1 hour prior to use.

Animals were sacrificed and 50-100mg of brain tissue dissected and placed immediately in 1ml of TRI reagent on ice. Following homogenisation using the 0.1-0.5ml dispersing tool of an Ultra-Turrax T8 homogeniser (IKA-Labortechnik), samples were centrifuged at 12000g for 10 minutes at 4°C. The supernatant was transferred to a fresh tube and allowed to stand at room temperature for 10 minutes prior to addition of 0.2ml of chloroform. The tube was then shaken vigorously and left standing at room temperature for a further 15 minutes. After centrifugation at 12000g for 15 minutes at 4°C, the upper, aqueous phase was removed to a fresh tube and 1/10 volume of propan-2-ol added. The mixture was again shaken and then left standing at room temperature for 5 minutes. The tube was

centrifuged at 12000g for 10 minutes at 4°C and the supernatant removed. To this, an equal volume of propan-2-ol was added in order to precipitate the RNA. After mixing, tubes were allowed to stand at room temperature for 10 minutes and then centrifuged at 12000g for 10 minutes at 4°C in order to pellet the RNA. The supernatant was removed and the pellet washed with 1ml of 75% EtOH. Tubes were briefly centrifuged again and the supernatant extracted, following which the pellet was allowed to air-dry at room temperature for 10 minutes. The pellet was re-dissolved by incubation in a suitable volume of DEPC-treated H_2O at 55°C for 15 minutes with occasional pipetting using a Gilson pipettman. Samples were incubated with 10 units of Rnasin ribonuclease inhibitor (Promega) at 37°C for 30 minutes prior to use.

2.2.12 RNA quantitation

The concentration of RNA samples was quantified by measuring the optical density (OD) of the RNA sample (diluted 1:1000 in DEPC-treated H_2O) at a wavelength of 260nm. The RNA concentration of the samples was calculated based on 40mg/ml of RNA giving an OD reading of 1.0 at 260nm.

RNA was also checked for integrity by electrophoresis on 1% agarose gel for 15 minutes at 100V (section 2.2.6).

2.2.13 Northern blotting

As with RNA isolation, all equipment used in Northern blotting was soaked in DEPC-treated H_2O for a minimum of 1 hour prior to use. Northern blotting was carried out using a modified version of the standard protocol [73]. A 1.2% agarose gel was prepared by dissolving 4.2g of agarose in 304ml of DEPC-treated H_2O. The agarose was incubated at 65°C

and 35ml 10x MOPS running buffer (200mM MOPS (3-[N-Morpholino] propanesulfonic acid) (Sigma) pH 7.0, 50mM Na Acetate, 10mM EDTA) and 10.5ml 37% formaldehyde (Sigma) added, following which the gel was immediately poured. RNA samples were prepared by adding the desired amount of RNA solution to 5µl 10x MOPS running buffer, 8.75µl of 37% formaldehyde, 25µl formamide (Sigma) and making the volume up to 50µl with DEPC-treated H_2O. This mixture was incubated at 55°C for 15 minutes and 5µl 5x Ficoll loading buffer added. Samples were loaded onto the gel and electrophoresed for 18 hours at 50V in 1x MOPS running buffer. The gel was blotted onto Hybond-N membrane by capillary blotting in the same manner as for Southern blots (section 2.2.10). RNA cross-linking, probe hybridisation and membrane stripping were also carried out exactly as described for Southern blot membranes (section 2.2.10 and 2.2.15).

2.2.14 Radiolabelling of DNA probes

10-50ng purified probe DNA was labelled with redivue α^{32}P-dCTP (Amersham) using the High-Prime labelling kit (Boeringher Mannheim) according to the manufacturers instructions, at 37°C for 30min. Following incubation, unincorporated deoxyribonucleoside-triphosphates were removed by spinning the labelling mixture, made up to 100µl with TE pH 8.0, through a 1ml Sephadex G-50 (Sigma) column (packed and pre-equilibrated with TE pH8.0) at 1200rpm for 4min. A further 100µl of TE pH 8.0 was applied to the column which was spun as before and the eluates pooled. This labelled probe solution was denatured prior to use by boiling at 100°C for 5 minutes.

2.2.15 Hybridisation of radiolabelled DNA to Southern and Northern blots

Blotted and cross-linked membranes were prehybridised in a rotisary oven, at 65°C for 2 hours in 30ml of 'Church and Gilbert' hybridisation buffer

(500mM Na_2HPO_4 pH 7.2, 1mM EDTA, 7% SDS, 1% BSA, 100μg/ml sonicated salmon sperm DNA) [78]. Following this period, denatured, radiolabelled probe DNA was added to the hybridisation mixture and filters incubated for at least 12 hours at 65°C. Filters were then washed twice at 65°C for 15 minutes each in 40mM Na_2HPO_4 pH 7.2, 1mM EDTA, 5% SDS followed by two 1 hour washes in 40mM Na_2HPO_4 pH 7.2, 1mM EDTA. After a brief rinse in 40mM Na_2HPO_4 pH 7.2, filters were wrapped in Saran wrap (GRI) and placed in an autoradiography cassette (including intensifying screens) with either pre-flashed blue sensitive X-ray film (GRI) or with Kodak BIO-Max film (Sigma). Following incubation at -80°C for a suitable exposure time, films were developed using a Compact x2 (X-ograph) X-ray processor.

Membranes were stripped by submerging in boiling 0.1X SSC/1% SDS for a minimum of 5 minutes.

2.2.16 Polymerase chain reaction

All PCR reactions were carried out in a total volume of 20μl consisting of 72mM Tris.HCl pH 9.0, 20mM $(NH_4)_2SO_4$, 0.01% Tween-20 (Reaction buffer IV, Advanced Biosciences), 1.5mM, 3mM or 4.5mM $MgCl_2$ (Promega), 200μM dATP, 200μM dCTP, 200μM dGTP, 200μM dTTP (Amersham Pharmacia), 1U "Red *Taq* " DNA polymerase (Sigma) and 133nM of each primer.

For reactions with microsatellite PCR primers, 5μl (approximately 25ng) of genomic DNA (prepared as above), which had been diluted 1:150 in dH_2O, was added to each reaction. For reverse transcriptase PCR reactions, 1μl of

a 20µl reverse transcriptase reaction mixture was added, along with 5µl of dH_2O, to each PCR reaction.

All PCRs reactions were performed on a PTC-100 thermocycler (MJ research) according to the recommended protocol from the Whitehead Institute [79] for microsatellite primer pairs: 2 minutes at 95°C followed by 30 cycles of 45 seconds at 94°C, 45 seconds at the annealing temperature specified for each primer pair and 60 seconds at 72°C followed by a final extension of 7 minutes at 72°C and cooling to 4°C.

2.2.17 Luciferase assay

This was performed essentially according to Ward *et al*(1997) [72] on a small tail biopsy (2-4mm) taken from pups up to 7 days post partum. Following storage at -20°C, thawed material was added to 100µl of luciferase assay cell lysis buffer (Lysis buffer 4, LabTech), vortexed, and then re-frozen at -20°C for at least 30min. 10µl thawed lysates were then plated, in duplicate, on a white, 96-well microtitre plate. Samples were assayed for luciferase activity using 50µl Genglow-1000 luciferase assay substrate (LabTech) in either an Anthos Lucy 1 luminometer (LabTech) or an E.G. & G. Berthold Autolumat LB953 luminometer (Berthold). Light emission was counted for 10s in each case. A mean reading of greater than 0.3 relative light units constituted a positive result for luciferase activity. Genomic DNA was prepared from biopsy samples giving readings below this value and genotyping was repeated by Southern blotting.

2.2.18 Preparation of metaphase chromosome spreads

This protocol was adapted (by Dr W. R. Bennett) [80] from that used in the MRC Human Genetics Unit, Edinburgh (M. Lee, pers. comm). Mice were sacrificed and spleens dissected into PBS. Following transfer into a 50mm

tissue-culture dish containing 5ml of RPMI-1640 with Glutamax 11 (Gibco-BRL) medium, cells were extruded from spleens by piercing with a 26 gauge needle and then, whilst holding the specimen steady with the needle, another needle used to squirt medium into the spleen. Care was taken not to suck cells back through the needle. Using 10ml of medium, as many cells as possible were flushed out and pooled. Cells were then pelleted by centrifugation at 250g for 6 minutes. It was found that splenocytes proliferate more readily and yield more metaphase chromosome spreads when spleens from two or more animals were pooled, only spleens from animals of the same genotype were pooled. Supernatant was removed and cells resuspended in 5ml lymphocyte culture medium (RPMI-1640 with Glutamax 11, 15% fetal calf serum (Gibco-BRL) and 0.1mg/ml gentamicin sulphate (Sigma). Two 5ml cultures were set up per spleen in round-bottomed, 15ml snap-cap polystyrene tubes (Falcon), one consisting of 1ml of cell suspension plus 4ml lymphocyte culture medium, the other; 2ml cells plus 3ml medium. Lipopolysacharride (from *Salmonella enteriditis*, Sigma #L-6011) was added to each culture at 50μg/ml. Cultures were incubated at 37°C (5% CO_2) with tube caps left loose to allow gas exchange. One 1ml and one 2ml culture was incubated for 44 hours whilst similar cultures were incubated for 46 hours. In a subset of cultures ethidium bromide was added at a concentration of 10μg/ml two hours before harvesting. This acts as an intercalating agent between DNA strands therefore decelerating contraction of metaphase chromosomes, thus yielding more elongated metaphase chromosomes. Following incubation, cells were spun at 250g for 6 minutes and the supernatant removed. Cells were resuspended in hypotonic 75mM KCl solution, the first 1ml being added dropwise, with constant agitation, and then carefully overlaid with a further 9ml. Cells

were incubated at room temperature for 10min prior to further centrifugation at 250g for 6 minutes, and the supernatant removed. Freshly made fixative (3:1, methanol:glacial acetic acid) was added, for the first 1ml, dropwise, with constant agitation to prevent cell clumping, and the remaining 9ml gently overlaid. Cell suspensions were incubated overnight at 4°C. The following day, cells were spun at 250g for 6 minutes, fixative removed, and cells resuspended in 10ml fixative. This was repeated except the cells were resuspended in 0.1-0.5ml of fixative.

Glass microscope slides (Raymond Lamb) were cleaned thoroughly, first with hot soapy water, and then by soaking in absolute ethanol: concentrated HCl, 1:1 (vol:vol). Slides were washed in running tap water, rinsed in dH_2O, and stored in industrial methylated spirit (IMS) with a few drops of HCl added. Just prior to use, slides were transferred to dH_2O for 5 minutes. They were then removed from the water and wiped once with a piece of tissue moistened in dH_2O. Only slides showing a uniform thin film of water were used. Spreads were made by applying 10µl of cell suspension directly to the slide using a Gilson Pipettman. Slides were then air-dried at room temperature and then placed under vacuum, at room temperature, for at least 48 hours. These slides were then ready for G-banding and FISH experiments, although it was found that optimal G-banding was obtained if the slides were left at room temperature for around 14 days following vacuum treatment. This is in accordance with the published observations of E.P Evans [76].

2.2.19 Giemsa banding of metaphase chromosome spreads

Giemsa (G-) banding was performed according to standard protocols with modifications [76]; [80]; [81]. to prepare Giemsa stock, 7.63g Giemsa

powder (BDH) was dissolved in 500ml glycerol by incubation at 50°C for 30 minutes, with occasional mixing, and allowed to cool prior to addition of 500ml methanol. This stock solution was filtered with Whatmann 3MM paper and stored at room temperature. Working Giemsa solution was prepared by addition of 1ml stock to 50ml 10mM sodium phosphate buffer pH 6.8.

Following aging, slides were incubated in 2x SSC at 60°C for 60min in a glass Coplin jar. After cooling to room temperature and a brief equilibration in PBS, slides were incubated for between 5 and 20 seconds (optimised for each set of slides) in fresh trypsin solution. This was made by diluting 0.25ml Difco Bacto-trypsin stock (dissolved in dH_2O and stored at -20°C) (Difco Labs #0153-60-2) in 50ml PBS. After a brief rinse in 10mM phosphate buffer pH 6.8, slides were transferred to working Giemsa solution at room temperature for 15 – 20 minutes. Slides were then rinsed in deionized dH_2O and air dried prior to documentation of G-banded spreads (see section 2.2.22).

Prior to FISH, slides were prewashed with xylene and then 1:1 xylene:ethanol for 1min each, then destained with two 5min washes in 3:1 methanol:glacial acetic acid. Spreads were refixed in 4% paraformaldehyde in PBS for 10 minutes followed by four 5 minute washes in PBS, a brief rinse in dH_2O and air-drying. Slides were then used for FISH within 24 hours.

2.2.20 Labeling of FISH probes

FISH DNA probes were labelled according to a modification of Wilkinson *et. al.* [81] For biotin labelled probes a nick translation mix was assembled

on ice containing 500ng purified probe DNA (6µl), 0.3mM dATP, dCTP, dGTP (Amersham Pharmacia), Bio-16-dUTP (Boeringher Mannheim) (2.5µl of each), nick translation salts (0.5M Tris.HCl pH 7.5; 0.1M $MgSO_4$; 1mM dithiothreitol; 500µg/ml BSA fraction V (all Sigma)) (2µl) and 1µl of Rnase-free Dnase 1 (Amersham Pharmacia) freshly diluted 1:500 in ice-cold dH_2O. The reaction mix (total volume 19µl) was spun briefly and 1µl of *E. coli* DNA polymerase I (Sigma) added (final reaction conditions: 50mM Tris.HCl pH7.5, 10mM $MgSO_4$, 0.1mM DTT, 50µg/ml BSA, 62.5mM dATP, 62.5mM dCTP, 62.5mM dGTP, 62.5mM bio-16-dUTP. This mixture was incubated at 15°C for 90min and then the reaction was stopped by incubation at 65°C for 10 minutes following the addition of 2µl 0.2M EDTA and 1µl 5% SDS. TE pH 8.0 was added to give a total volume of 100µl and unincorporated deoxyribonucleoside-triphosphates removed using a 1ml Sephadex G-50 column (as section 2.2.14). 5µl of 10mg/ml sheared salmon sperm DNA (Sigma), 50µl of 3M NH_4 acetate pH4.6 and 500µl of ice-cold absolute ethanol were added to the 200µl of eluate and the probe DNA precipitated overnight at -20°C. The DNA was pelleted by centrifugation at 12000g for 10 minutes and the supernatant removed. After washing with 1ml of 70 EtOH, the pellet was dried and re-dissolved in 50µl of TE pH 8.0.

Labelling of DNA probes with digoxigenin was performed identically to the biotin labelling procedure except that the bio-16-dUTP was substituted for dig-11-dUTP (Boeringher Mannheim).

2.2.21 FISH of chromosome spreads

FISH was carried out according to a modified version of the protocol used in the MRC Human Genetics Unit, Edinburgh [80]. Slides which had not

been G-banded required a pre-treatment step with RNase in which they were equilibrated for 5 minutes at room temperature in 2x SSC, followed by incubation in 0.1mg/ml Rnase (Sigma) at 37°C for 1 hour. Previously G-banded slides did not require this step.

Probe preparation was carried out in advance, or in the case of non G-banded slides, during the RNase treatment step. For each slide, 50ng of probe DNA was added to 2μg of C_ot-1 DNA (Gibco-BRL) and 2 volumes of absolute ethanol, and dried to a pellet under vacuum. Approximately 30 minutes prior to using on slides, 15μl of FISH hybridisation mixture (50% formamide (Ultra grade, Sigma), 2x SSC, 1% Tween-20 (Sigma) and 10% dextran sulphate (Sigma) was added to the probe DNA pellet. This mixture was incubated at 37°C for 15 minutes and vortexed in order to dissolve the probe DNA, prior to further incubation at 37°C. Just prior to use, the probe DNA was denatured at 70°C for 5 minutes followed by incubation at 37°C for a further 30 minutes to allow pre-annealing of the C_ot-1 DNA to any repetitive sequence elements in the probe.

Slides were equilibrated in 2x SSC for 5 minutes, at room temperature, and then dehydrated by passing through 70%, 80% and 100% absolute ethanol for 2 minutes each and air-dried under vacuum. Dried slides were incubated at 70°C for exactly 2 minutes and then transferred to pre-warmed denaturation solution (70% formamide, 2xSSC) at 70°C for exactly 2 minutes. Slides were then quickly passed into ice-cold 70% absolute ethanol for 2 minutes before dehydration in 90% and 100% absolute ethanol at room temperature as before. Slides were then dried under vacuum.

15µl of hybridisation cocktail was pipetted onto a 22x22mm coverslip (stored in IMS) placed on a hotplate. Slides which had been pre-warmed on the hot-plate for no more than 2 minutes were then used to pick up the probe-carrying coverslip. Tip-Top rubber cement (Cat#5059128, Rema Tip-Top UK, Westland Square, Leeds LS11 5X5) was used to seal the edge of the coverslip, and slides were incubated overnight at 37°C.

Following overnight hybridisation, the Tip-Top rubber seal was removed carefully and coverslips allowed to fall off by immersion in 2x SSC at room temperature. Slides were washed in pre-warmed 50% formamide, 2x SSC, at room temperature, four times for 3 minutes each wash. After four further 3 minute washes in 2x SSC at 45°C, and four 3 minute washes in 0.1x SSC at 60°C, slides were equilibrated in SSCT (4x SSC, 0.1% Tween-20) at room temperature for 10 minutes.

SSCTM blocking buffer was prepared by dissolving 5% powdered milk (Sainsburys) in SSCT and spinning at 300g for 10 minutes, after which clarified blocking solution was removed. Fluorescent antibodies were prepared by addition to clarified SSCTM in the correct concentrations, following which the solution was spun at 15000g for 10 minutes and the supernatant removed and stored at 4°C until required.

All antibody incubations were carried out with 50µl of antibody solution under a coverslip, at 37°C, in a humidity chamber. After incubations, slides were washed three times for 2 minutes in SSCT at 37°C. For detection of biotinylated probes with FITC labelled antibodies, slides were incubated with 50µl of SSCTM for 30 minutes at room temperature, followed by incubations with a 1:500 dilution of avidin FITC (Vector) for 30

minutes, then a 1:100 dilution of biotinylated anti-avidin (Vector) for 30 minutes and finally a further 30 minute incubation with avidin FITC, again diluted 1:500. For detection of digoxigenin-labelled probes with FITC antibodies, slides were incubated firstly in SSCTM for 30 minutes at room temperature, and then in a 1:15 dilution of sheep anti-digoxygenin-FITC (Boeringher Mannheim), followed by anti-sheep FITC (Vector), diluted 1:200.

After completion of antibody incubations and final washes, slides were incubated in the dark for 5 minutes in PBS containing 0.25μg/ml DAPI (4,6-diamidino-2-phenylindole) and then washed twice for 5 minutes each in PBS. Slides were mounted in Vectashield mountant (Vector) and coverslips sealed with clear nail varnish (Boots).

2.2.22 Image capture of chromosome spreads

Slides were examined using a Leica DMRB microscope equipped with epifluorescent illumination and the appropriate filter blocks. Spreads were located at x200 magnification and then examined in more detail at x1000 using an oil immersion x100 objective. Image capture was carried out using a cooled CCD camera (Hamamatsu) linked to a PC equipped with a frame grabber card. The Image Pro Plus V3.0 software (Media Cybernetics) was used to capture images and process them for colour and brightness. False colouring and merging of fluorescent images was done using Photoshop V5.0 software (Adobe).

Following G-banding, images of multiple metaphase chromosome spreads were captured and their respective locations recorded using the X-Y stage ruler. This allowed relocation of the same spreads following FISH. It was

found that by setting up the microscope for Kohler brightfield illumination but using the phase ring at position 1 rather than brightfield, more detailed G-banding could be obtained. A decrease in numerical aperture, resulting in both increased contrast and depth of field is thought to be responsible for this phenomenon (W. Bennett, pers. comm.).

2.2.23 Processing, embedding and sectioning of tissue samples

This was performed according to standard procedures [82]. Tissue blocks were fixed in 4% Paraformaldehyde in PBS for 12 hours with one change of fixative (unless stated otherwise). Fixed tissues were processed using a Leica automated processing machine. Samples were rehydrated by passing through 70%, 80%, 90%. 95%, 100% and 100% EtOH, for a period of 30 minutes or 1 hour (dependent on sample size) in each solution. Tissues were cleared by passing through xylene twice (30 minutes or 1 hour per change) and then incubated in paraffin wax at 60°C for 1 hour prior to embedding in paraffin wax.

Wax blocks were trimmed and tissue sections cut at 7μm using a Leica microtome. Sections were floated on a water bath and transferred onto slides previously treated with TESPA (3-aminopropyltriethoxysilane) (Sigma), as per the standard protocol. Following air-drying, slides were suitable for staining.

2.2.24 Haematoxylin and eosin staining of processed tissue samples

This was performed using a modification of the standard procedures [82]. Slides were dewaxed in two 2 minute changes of Histoclear (National Diagnostics) then rehydrated by passing through 100%, 100%, 95%, 90%, 70% and 50% EtOH for 2 minutes in each solution, followed by 1 minute in dH_2O and 20 minutes in Mayer's haematoxylin (Raymond Lamb).

Following a brief rinse (30 seconds) in dH_2O and washing under cold running tap water for 5 minutes, slides were passed through 50%, 70% and 100% EtOH for 2 minutes in each solution. Slides were then stained for 20 minutes in Eosin Yellow (0.1% in 100% EtOH) and passed through two changes in 100% EtOH (2 minutes each) and two changes of Histoclear (2 minutes each). Slides were then mounted under coverslips with DPX mountant (BDH).

2.2.25 Documentation of stained sections

Slides were viewed using bright field illumination on either a Leica DMRB or Nikon Eclipse E800 microscope. Images were photographed using Kodak Ektachrome 64 film.

CHAPTER 3: A SYSTEMATIC SCREEN FOR TRANSGENE INSERTIONAL MUTANTS

3.1 Introduction

3.1.1 74 lines of transgenic mice used in this study were generated by microinjection of one of eight DNA constructs into the pronuclei of fertilised mouse eggs.

The *Igf-2* and *H19* loci are closely linked on mouse chromosome 7 but are differentially expressed depending upon parental origin, *Igf-2* normally being expressed from the paternally inherited allele [83] and *H19* from the maternally inherited allele [84].

Studies were initiated to elucidate the function of five regulatory elements located in the *Igf-2/H19* region (see Fig 3.1) that might have a role in genomic imprinting and gene expression at this locus. To eliminate any cis interactions with other domains in this region it was decided to study the function of these elements in isolation from their normal genomic environment. This can be most easily achieved by using injection transgenesis to make multiple transgenic lines for each DNA construct.

Eight different constructs were used, each based on the 153bp, *Igf-2* P3 promoter region upstream of a luciferase reporter cassette; consisting of the firefly (*Photinus pyralis*) *luciferase* gene and an adjoining SV40 small t intron/polyadenylation signal, which ensures correct expression of the reporter in mammalian cells [85]. The remaining seven constructs contained various combinations of four *Igf-2/H19* regulatory regions, attached to this basic reporter construct (see Fig.3.2).

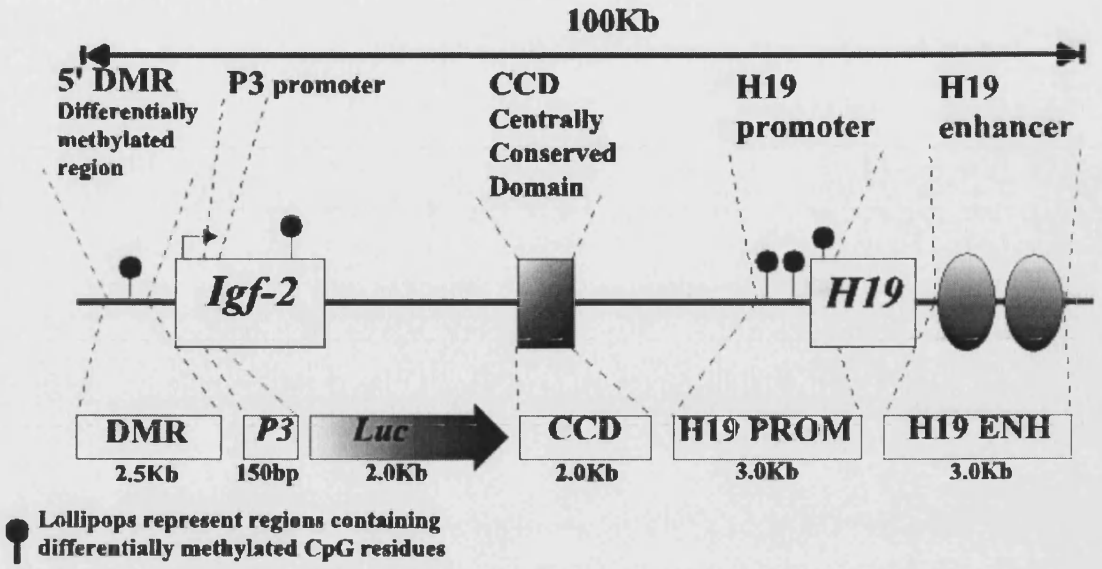

Fig. 3.1. The Igf-2 and H19 loci and regions used to make the transgene constructs.
These include the differentially methylated region (DMR), the *Igf-2* P3 promoter, the centrally conserved domain (CCD), and the *H19* promoter and enhancer (H19 PROM/H19 ENH). Each construct included a luciferase reporter gene (Luc) (figure adapted from Bennett [80]).

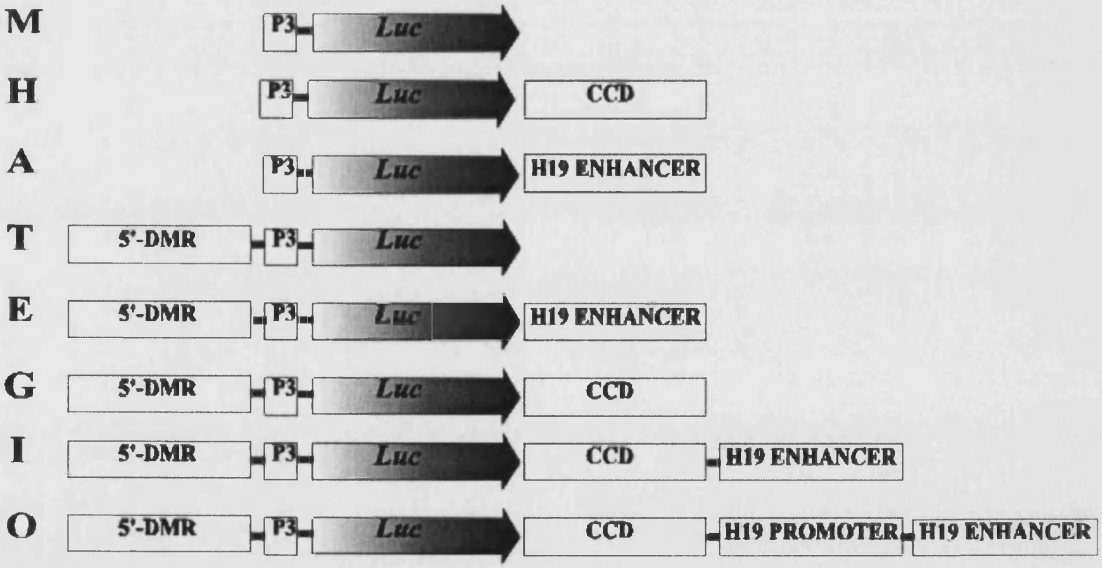

Fig. 3.2. Constructs used to make transgenic mice.
Note that the initial letter of each line corresponds to the construct used. Genomic regions used include the differentially methylated region (DMR), the centrally conserved domain (CCD) and the *H19* promoter and enhancer elements. Each construct contained the *Igf-2* P3 promoter and a luciferase reporter gene (Luc) (figure adapted from Bennett [80]).

Constructs were linearised and then microinjected into one pronucleus of a fertilised mouse egg derived by crossing a C57BL/6J male with a CBA/Ca female.

Each construct was assigned a letter of identification and used to generate multiple transgenic founders, the name of the associated line being derived from the sex of the founder and the letter of the construct used. For example, the Ann line was derived from a female founder carrying an 'A' construct transgene.

Most lines were tested for transgenicity by performing a luciferase assay on a tail biopsy. Lines that did not express detectable levels of luciferase were genotyped by Southern analysis using a transgene specific probe. Southern blotting was also employed to confirm that each transgenic line represented an integration event of one or more transgene copies at a single position in the mouse genome.

In this way 74 lines of transgenic mice were generated with multiple lines being derived from one of eight DNA constructs and each representing a unique transgene integration event.

3.1.2 A systematic screen for insertional mutants

The mouse lines used in this study were derived in Oxford and subsequently transferred to Bath. Stocks in Oxford had been exposed to a variety of common mouse viruses and in order to satisfy house rules in Bath every line was re-derived by Caesarian section prior to entering the animal facility there. Foster mothers subsequently raised litters delivered in this way. It was during this procedure that a number of developmental

abnormalities were observed which might have otherwise escaped detection due to peri-natal lethality or cannibalism by parents. It was postulated that some of these phenotypes may have arisen by transgene insertional mutagenesis. This is a well-known phenomenon, and screens for insertional mutants have previously been conducted on large series of transgenic mice [26]. In order to identify possible insertional mutant phenotypes it was decided to initiate a systematic screen on the transgenic lines generated. This study is ongoing and is based around a two-step breeding strategy.

In order to identify recessive as well as dominant mutations it was necessary to generate animals that were homozygous for the transgene by intercrossing hemizygous transgenic mice. Such a strategy also facilitated the identification of embryonic or peri-natal lethality in homozygous animals that would upset the normal 1:2:1, homozygous transgenic:hemizygous transgenic:non-transgenic ratio of offspring types expected from such a cross. Sex-linked mutations would also be identifiable in that a sex-linked phenotype will be apparent in 100% of the transgenic male offspring from such a cross but only 50% of the transgenic female offspring. Detection of sex-linked embryonic lethality was also possible through the generation of a sex-ratio distortion of transgenic offspring from such crosses.

The need for the second breeding step in this strategy becomes apparent when considering the difficulties in distinguishing hemizygous and homozygous transgenic animals. Both the luciferase and Southern blot genotyping assays allow only the discrimination of transgenic from non-transgenic mice, but not the unambiguous distinction of hemizygous from

homozygous transgenic animals. Backcrossing a known transgenic, generated by hemizygous intercrossing, against a non-transgenic F1(C57/CBA) (resulting from a C57BL/6J against CBA/Ca cross), and analysing the genotypes of the offspring, allowed the exact genotype of the transgenic parent to be determined. A hemizygous parent should produce an equal number of both transgenic and non-transgenic offspring, whereas a homozygous parent will produce offspring that are all transgenic. Animals being tested in this manner were bred until it had been determined, with statistical significance, whether they were homozygous or hemizygous. Confirmation of homozygosity required a transgenic animal, upon backcrossing against an F1(C57/CBA) partner, to produce at least 11 transgenic pups without any non-transgenics ($p<0.001$, using the χ^2 test, see section 3.2.2). The identification of at least one homozygous mouse of each sex bearing no detectable phenotype was deemed enough to eliminate this line from further testing.

Thus, the coupling of such genetic testing for homozygosity, with the intercross strategy for the detection of post-natal defects, facilitated the screening of a large number of transgenic lines for a variety of putative transgene insertional mutant phenotypes.

3.1.3 Drawbacks of such a screening strategy

By means of hemizygous intercrossing, lines producing obvious defects could be quickly ear-marked for further investigation. Genetic testing for homozygosity was required to eliminate remaining lines from the screen and in the majority of lines in which no insertional mutation was present, both male and female homozygotes were identified within the first few animals tested. A noticeable shortcoming in this screening strategy was the

difficulty encountered when a putative insertional mutation generated a phenotype other than an obvious post-natal defect such as embryonic lethality or sterility. In such cases it became necessary to subject large numbers of transgenic animals to genetic testing for homozygosity until numbers sufficient to provide statistical significance had been bred. Obviously such a strategy requires considerable effort and financial costs, meaning that further genetic testing of lines following the identification of single homozygotes of each sex, stretched beyond the scope of the study. As a result, it is possible that more subtle phenotypes may have been missed. The nature of this strategy also creates difficulties in identifying and characterising mutant phenotypes that display variable penetrance or expressivity (although at least two of the identified mutant lines are suspected to have variably penetrant phenotypes, see below). This problem was accompanied by the fact that transgenic mice were generated on a mixed genetic background that became less uniform with each additional breeding step. This could have interfered with the reproducibility of variably penetrant phenotypes, which are affected by differences in genetic background.

Finally, the generation of transgenic mice from a single founder and the inbreeding required by this screening strategy meant that the fixation of a non-transgene-related, spontaneous mutant phenotype in the mouse population was a realistic possibility. Prior to conducting further characterisation it was necessary to eliminate this as the source of mutation in putative insertional mutant lines by confirming that the transgene and phenotype were co-segregating and closely linked.

3.2 Materials And Methods

3.2.1 Intercross strategy to identify recessive mutant phenotypes

Within each line, mice previously identified as being transgenic were bred and a tail biopsy taken from all progeny at between 4 and 7 days of age and used for genotyping. Offspring were kept under observation for possible mutant phenotypes.

3.2.2 Backcross strategy to identify mice homozygous for the transgene

To determine whether transgenic mice derived from a hemizygous intercross were homozygous or hemizygous for the transgene, they were bred with a wild-type (usually F1(C57/CBA)) mouse. Offspring were culled at birth and a tail biopsy taken and genotyped. This was carried on until enough progeny had been tested to confirm whether the transgenic parent was hemizygous or homozygous. The number of progeny tested was determined by χ^2 analysis, taking the null hypothesis to be that the transgenic parent is hemizygous. In this case equal numbers of transgenic and non-transgenic progeny should be born. For a χ^2 test to have significance the expected numbers in each class must be at least 5, meaning that a minimum of 10 progeny must be tested. If 11 offspring are tested and all are found to be transgenic, performing a χ^2 test will give a P value of < 0.001, in other words there is a likelihood of less than one in a thousand that the transgenic parent is hemizygous. Thus 11 or more progeny were tested before the genotype of the transgenic parent was confirmed as homozygous. The identification of one or more non-transgenic offspring confirmed the parental genotype as hemizygous.

3.2.3 Genotyping

Progeny were genotyped in duplicate by luciferase assay on a tail biopsy sample. In the event that an assay proved inconclusive, especially in lines expressing lower levels of luciferase, genotyping was performed by Southern analysis on genomic DNA derived from biopsy material (see section 2.2.17). Southern blot probes were selected based on the criteria that they could hybridise to both the transgene and a sequence endogenous to the mouse genome. This facilitated the detection of both an endogenous band, confirming a successful assay and, in the case of a transgenic sample, a transgene specific band.

3.2.4 Caesarian rederivation

Timed matings were set up in Oxford between transgenic animals and either wild-type F1(C57/CBA) or transgenic partners. Pregnant mothers were transported to Bath and sacrificed on day 18.5 of gestation by cervical dislocation. The mother's body was dipped in 70% EtOH and the uterus carefully dissected out and rinsed in sterile PBS at 37°C. The foetuses were dissected out by a second person and passed to a third who revived the pups and transferred them to a foster mother. Mice that had given birth that day or one day previously were chosen as fosters and their own litter removed up to four hours beforehand.

3.3 Results

3.3.1 An overview of screen to date

Of the original 74 transgenic lines generated, homozygous animals in both sexes were bred in Oxford for 21 lines (see Table 3.1) 19 of which were not transferred to Bath. A further 14 lines either failed to breed in Oxford or were not successfully re-established in Bath and became extinct. During the Caesarian re-derivation of lines in Bath a number of abnormalities were discovered (see Table 3.2). The 41 transgenic lines successfully re-derived in Bath were also put through the two-step breeding strategy already described in section 3.1.2, in order to screen for recessive developmental abnormalities (see Table 3.1)

In summary (see Table 3.3), 45 lines were readily bred to homozygosity for the transgene in both sexes, allowing their elimination from the study. An additional 6 lines were bred extensively but either failed to yield breeding homozygote male or female animals, or homozygotes with manifest mutant phenotypes. Three lines have post-natal phenotypes confirmed as being associated with transgene insertion (Ann, Harry and Holly (although occasional homozygous mutants have bred for this line)) and have been further characterised [80], 2 lines have suspected embryonic lethality phenotypes (Antonio and Ingrid) and the remaining line has suspected embryonic lethality with variable penetrance such that some putative homozygotes are born and display growth retardation and subsequently die before reaching the age of sexual maturity (Gertrude). In 12 lines, either male or female homozygotes were never identified. In the 4 lines in which no female homozygotes were bred, insufficient animals were tested to allow for statistical significance and these lines displayed no evidence of

any mutant phenotype. Testing of females in one of these lines (Quark) is ongoing, but the remaining three lines are now extinct (Ian, In and Tarquin). Similarly, in 4 of the 8 lines in which no male homozygotes were identified, the number of animals tested was insufficient and no mutant phenotype was apparent. All 4 of these lines are now extinct.

In one of the remaining lines in which male homozygotes were never identified, Ob, a male infertility phenotype has been characterised (see Chapter 8). A total of 36 transgenic males were set up for genetic testing by backcross mating. Of these, only 23 animals bred, all of which were confirmed as hemizygous for the transgene. The remaining 13 animals (36% of the total set up) failed to breed. In a second line – Grace (now extinct), male infertility seemed probable. Again, a noteable proportion of transgenic males set up for genetic testing failed to breed (6 of 26, 30%) whereas female homozygotes were readily identified (4 of 14 transgenic females tested). Another line (Axe) shows evidence of embryonic or perinatal lethality. Although only one female has been tested, no homozygotes animals have been identified amongst a total of 23 transgenic animals tested (the probability of this happening by chance is <0.001, as determined by χ^2 analysis). The Titus line exhibits a post-natal lethality phenotype that affects approximately one third of offspring from transgenic intercrosses (see Table 3.4). Here again, the identification of 2 female homozygotes might reflect a variability of phenotypic penetrance.

Table 3.1. Breeding data derived from the screening program

Line	Succesfully re-established in Bath?	Abnormalities observed during Caesarian?	Mutation revealed by screen?	Numbers bred to date.			
				♂		♀	
				tg/tg	tg/+	tg/tg	tg/+
Alicia	Yes	No	No	3	8	1	10
Alison	No	No	No	2	0	2	1
Amanda	Yes	No	No	1	2	1	4
Anabella	No	No	No	0	1	0	2
Andrew	No	No	No	0	2	0	2
Ann	Yes	No	Yes	See Chapter 5			
Antonio	Yes	No	No	0	15	0	16
April	No	No	No	0	2	0	2
Archy	Yes	No	No	1	8	3	2
Arramis	No	No	No	1	0	1	1
Axe	Yes	Yes	No	0	22	0	1
Ayah	Yes	No	No	0	7	0	8
Azure	Yes	No	No	3	7	6	8
Edmond	No	No	No	0	1	1	2
Edna	No	No	No	1	0	2	0
Edy	No	No	No	1	0	1	4
Elaine	No	No	No	1	0	2	0
Eleanor	No	No	No	0	0	0	0
Ellen	No	No	No	1	1	1	1

Elly	No	No	No	2	0	2	0
Elton	No	No	No	0	1	1	1
Elvis	Yes	No	No	2	11	1	7
Erasmus	No	No	No	1	0	1	1
Eric	No	No	No	0	1	0	2
Ethel	Yes	No	No	2	2	1	6
Eva	Yes	Yes	No	1	8	2	5
Gentian	No	No	No	2	3	2	11
George	No	No	No	2	2	3	13
Gertrude	Yes	No	No	0	15	0	16
Grace	No	No	No	0	26	4	10
Graham	No	No	No	2	1	2	7
Hamish	Yes	Yes	No	3	5	2	3
Hank	No	No	No	2	0	2	2
Harold	Yes	Yes	No	1	5	8	4
Harry	Yes	No	Yes	W.R. Bennett, PhD thesis[80]			
Hector	No	No	No	1	2	2	2
Heidi	No	No	No	0	3	0	7
Helen	No	No	No	0	0	0	0
Helga	Yes	No	No	1	12	1	7
Holly	Yes	No	Yes	W.R. Bennett, PhD thesis [80]			
Homer	No	No	No	1	1	2	2
Hugo	No	No	No	0	4	3	3
Humphrey	No	No	No	2	2	1	0

Ian	Yes	Yes	No	1	3	0	0
Ibadan	Yes	No	No	1	1	1	6
Ice	Yes	Yes	No	1	0	2	2
Id	Yes	Yes	No	0	1	0	0
If	Yes	No	No	2	2	3	5
Ill	Yes	No	No	2	4	1	0
In	Yes	Yes	No	1	2	0	3
Ingrid	Yes	Yes	No	0	9	0	15
Isac	Yes	No	No	1	0	1	1
Oat	No	No	No	2	2	3	1
Ob	Yes	No	Yes	0	23	1	7
Oc	Yes	Yes	No	1	6	1	3
Odd	Yes	Yes	No	2	4	1	4
Oh	No	No	No	2	6	3	4
Oil	Yes	Yes	No	1	0	1	7
Ok	Yes	No	No	1	3	2	5
On	No	Yes	No	0	7	3	1
Ost	Yes	Yes	No	1	6	4	0
Ovid	Yes	No	No	3	9	3	4
Owl	Yes	Yes	No	1	4	1	0
Tarquin	Yes	No	No	1	0	0	1
Tessa	No	No	No	1	0	2	1
Theresa	No	No	No	2	1	1	1
Tiberius	No	No	No	0	0	0	0
Tilly	Yes	No	No	3	3	1	1

Tim	Yes	No	No	1	0	1	2
Titus	Yes	No	No	0	32	2	3
Tracy	Yes	No	No	2	0	1	4
Tutu	No	No	No	0	1	0	2
Quark	Yes	No	No	1	4	0	3
Quasar	Yes	No	No	2	14	1	19

Table 3.2. Abnormalities discovered during Caesarian sectioning

Line	Defect
Axe	1 craniofacial defect - lower jaw severely affected
Eva	2 "big-skulls" - grossly expanded crania
Hamish	2 exencephalies
Harold	1 exencephaly
Ian	1 execephaly, 2 omphalocoel, 1 "puffer"-fluid-filled thoracic region and pale appearance
Ice	1 "thalidomide" - stunted limbs
Id	1 "thalidomide"
In	1 hindleg deformity
Ingrid	1 "thalidomide"
Oc	1 hindlimb deformity - "paddle-limb"
Odd	1 hindlimb deformity - "flipper foot"
Oil	1 hunchback - possible lumbo-sacral spina bifida
On	1 "puffer"
Owl	1 "puffer"

Table 3.3. Summary of data derived from screening program

Number of lines	Breeding status	Defects
45	♂ and ♀ bred to homozygosity	None
7 (Does not include 10 lines where too few/none were tested prior to extinction).	No ♂ or ♀ homozygotes or homozygotes with manifest mutant phenotypes.	3 lines, post-natal phenotypes (Ann, Harry, Holly).
		1 line, partially penetrative, growth retardation/embryonic lethality (Gertude).
		3 lines, suspected embryonic lethality (Antonio, Ingrid, Ayah).
4	Only ♂ bred to homozygosity	Probably none (Ian, In, Tarquin – extinct, Quark – still breeding).
8	Only ♀ bred to homozygosity	1 line, ♂ infertility (Ob).
		1 line, probable ♂ infertility (Grace – extinct).
		1 line, possible ♂ embryonic lethal (Axe).
		1 line, possible partially-penetrative post-natal lethality (Titus).
		4 lines, probably none (Edmond, Elton, Hugo, On).

Table 3.4. Titus breeding data.

Sex/genotype	Total number of animals	Post natal deaths	% of total animals displaying transgene specific abnormality
♂ - transgenic	37	13	35
♂ - non-transgenic	15	2	
♀ - transgenic	35	10	29
♀ - non-transgenic	14	0	

3.4 Discussion

3.4.1 The screen has identified several lines displaying reproducible developmental abnormalities

The screen successfully identified 4 lines that display reproducible developmental abnormalities (see Table 3.5). These lines have subsequently been confirmed as *bona-fide* transgene insertional mutants and have been subjected to further investigation.

A defect in the Ann line was first observed in litters derived from hemizygous intercrosses in Oxford. A number of pups displayed progressive ataxia and tremor from around twelve days. These mice were also subject to gradual weight loss and worsening paralysis, and eventually died between 19 and 25 days old. Following successful re-derivation in Bath, it was decided to further investigate this line as a putative insertional mutant. The outcome of these investigations will be presented in Chapters 4 - 7.

In one early Harry litter generated by a hemizygous intercross in Oxford, two transgenic stillborn pups showed extreme ventral curvature, small size and highly abnormal skin texture and colour. Further hemizygous intercrosses, both in Oxford and, following successful re-derivation, in Bath, reproducibly generated "piebald" transgenic pups in which homozygous mutants display a white coat colour spotting and lethal megacolon phenotype that most likely results from a neural crest defect. This line was selected for further investigation and subsequently the mutation was confirmed as being linked to the integrated transgene at a site in mouse Chromosome 15 [80]. The position of the transgene was

mapped close to an existing coat colour mutation, *dom* (dominant megacolon), which apart from being dominant, exhibits an almost identical phenotype to that of Harry. The *dom* phenotype results from a mutation in the *sox-10* gene and represents a mouse model for the human Waardenburg-Shah syndrome [86]. Northern analysis of Harry mutant mRNA revealed no abnormalities in *sox-10* transcripts and to date it is not certain whether Harry represents a new allele of the *sox-10* gene or a novel mutant of a gene located nearby [80].

The Holly line consistently gave small litters during hemizygous intercrossing in Oxford. Furthermore, three transgenic pups re-derived by Caesarian section in Bath, despite appearing normal at birth, displayed progressively worsening corneal opacity from about two weeks of age. This line was also chosen for further investigation and the mutation was confirmed as being linked to the transgene. Through FISH and linkage mapping the integration site was identified at the proximal tip of Chromosome 1. A number of possible, but not obvious, candidates were known to map in this region and Northern analysis was used to eliminate one gene, *Eya1* before another, the *col9a1* collagenase gene was found to display aberrant expression in developing Holly mutant eyes. Holly does not represent a null mutation of the *col9a1* gene but may instead be a mutation affecting expression in some tissues [80]. With further investigation Holly was found to represent a useful mouse model for the human disease, closed angle Glaucoma.

Table 3.5. Transgene insertional mutant lines identified by screen

Line	Phenotype	Chromosome	Mapping	Gene
Ann	Cerebellar ataxia	4	See Chapter 5	*mDab1*
Harry	Neural crest defect	15	W.R.Bennett	*Sox10*
Holly	Cataracts/gluacoma	1	W.R.Bennett	*Col9a1* (*Col19*?)
Ob	Male sterility	8	See Chapter 8	unknown

Although investigations thus far have not progressed to the advanced stage reached for the three lines mentioned already, work done on the Ob line strongly suggests another recessive mutant phenotype. To date no homozygous male mice have been identified and approximately one third of male transgenic offspring generated by transgenic intercrossing failed to breed. Homozygous females were readily identified, implying a recessive male sterility phenotype in this line. Further characterisation of the Ob line will be detailed in Chapter 8.

3.4.2 A variety of abnormalities were observed during Caesarian re-derivation

As stated, breeding studies conducted in Oxford allowed the elimination of 19 transgenic lines, whilst a number of other lines failed to breed and became extinct. It was attempted to re-derive the remaining lines in Bath by Caesarian sectioning (see section 3.2.4), and in the majority of cases this proved successful. A number of abnormalities were observed in pups during sectioning (as summarised in Table 3.3).

Noticeably, a high proportion of the abnormalities observed in pups during Caesarian sectioning could all be grouped into four classes which may be interrelated. Pups from In, Ice, Ingrid, Id, Oc and Odd displayed some form of limb deformity (fused digits, stunted or absent fore-limbs) whilst abnormal Owl, Ian and On pups were termed "puffer" mutants to

describe a fluid-filled thoracic cavity. A number of Ian, Harold and Hamish pups displayed exencephaly. And finally pups from the Ian, Oil and Ost lines presented either omphalocoele or sacro-lumbar defects. All four classes of mutant could be encompassed within the sphere of Neural Tube Defects (NTDs) that result from a failure of the neural tube to close at various sites along its length. Of these, the Ian line proved difficult to maintain and became extinct, thereby curtailing follow-up studies, whilst subsequent breeding indicates that the Ingrid and Axe lines are suspected recessive embryonic lethal mutants.

A correlation has previously been shown between exencephaly, limb defects, omphalocoele and lower spinal defects and a failure of the neural tube to close but in the case of the thoracic oedema observed in a number of animals this correlation is rather more tentative. One possibility is that a failure of neural tube closure could prevent colonisation of the cardiac outflow tract by neural crest derivatives [87], although this hypothesis is rather questionable.

It is remarkable that such defects in independent transgenic lines are, in a number of cases, highly similar. Furthermore these presumptive neural tube defects arise only in lines derived from three of the eight transgene constructs, each of which have the CCD (centrally conserved domain) [88] enhancer element in common. These strands of evidence may suggest that the proposed neural tube defects are derived not from transgene insertional mutagenesis but rather from some effect associated with the CCD. It has been proposed that the CCD acts as a mesoderm-specific enhancer for the *Igf-2* gene. High expression of CCD-driven reporter genes in mesodermally derived tissues, such as the notochord, may disrupt the

development of the Neural Tube, a process which is known to be highly sensitive to interference. Alternatively, multiple copies of the CCD enhancer could affect the expression of other genes by binding high concentrations of transcription factors required for normal development of the Neural Tube.

It must be stated that these Neural Tube defects, along with a variety of other mutant phenotypes discovered during re-derivation in the Axe, Eva, Hamish and Harold lines have never been recapitulated during subsequent breeding. It is possible that a number of these phenotypes could have resulted from careless handling during sectioning. Alternatively, perturbation of normal development could have arisen sporadically and be totally unrelated to insertion of the transgene. This would be unexceptional since during any normal pregnancy a proportion of mouse embryos will not reach full term and will be resorbed at some stage during gestation.

3.4.3 Several other lines may represent additional mutant phenotypes

Although not confirmed as definite transgene insertion mutants, a number of lines did display phenotypic and/or breeding abnormalities suggestive of a mutant phenotype.

During hemizygous intercrossing in Oxford it was reported that a number of Gertrude pups, despite appearing normal at birth, typically died after 7 to 10 days by which time they weighed 30% to 40% less than their siblings. This phenotype was never reproduced during extensive breeding in Bath, although a number of pups were observed which were markedly smaller than their siblings for the first two weeks but caught up in size thereafter.

Genetic screening of this line via backcross mating was unable to identify any homozygous animals, although a large number of hemizygotes of both sexes were bred (15 males and 16 females). This data correlates with an embryonic lethality mutation, although the fact that a number of putative homozygotes were born but died shortly thereafter suggests a partially penetrant phenotype. The difficulties in studying this line were compounded by the fact that Gertrude mice were particularly poor breeders, with transgenic mice frequently failing to produce litters.

Two further lines may also represent recessive embryonic lethal mutants. In both the Antonio and Ingrid lines, no homozygous animals of either sex were ever identified. Sufficient male and female hemizygotes were bred (Antonio: 15♂, 16♀, Ingrid: 9♂, 15♀ to strongly suggest recessive embryonic lethality in both lines. In future it will be necessary to analyse intercross litters *in-utero* in order to characterise when the loss of homozygotes occurs and to determine whether there is an obvious cause of death.

Similar to the situation in the Ob line, breeding of Grace male homozygotes proved impossible, despite the identification of 20 hemizygous male animals (and both hemizygous and homozygous females (the 28% observed correlates well with the 1/3 expected)). Of the 26 male transgenic animals set up for backcross testing, 6 did not breed (30% of male transgenics). This is suggestive of recessive male sterility in this line, although further characterisation was prevented by its extinction.

Despite the identification of 22 Axe hemizygous male animals, no homozygous males were ever bred. Of two Axe females tested, one hemizygote and one homozygote were identified. Since all animals tested

bred successfully, sterility in homozygote males seems improbable. This data could therefore be explained either by a sex-linked, embryonic-lethal phenotype or by variably penetrant embryonic-lethality affecting both sexes. Further genetic testing of Axe transgenic females would be required to confirm either of these possibilities. As for the Antonio and Ingrid lines, Axe intercross litters should also be examined *in-utero*.

In the Titus line approximately one third of offspring generated by hemizygous intercrossing die at, or shortly after, birth (see Table 3.4). The identification of two female, but no male homozygotes may again reflect variable penetrance of this phenotype, although further genetic testing of transgenic females would be required to confirm this.

3.4.4 Numbers of mutants are comparable with those of similar studies

With Ann, Harry, Holly and Ob the only lines confirmed as subject to transgene insertional mutagenesis thus far, and taking into consideration that only 63 of the original 74 transgenic lines have been subjected to extensive breeding analysis, we can calculate the overall frequency of transgene insertional mutagenesis in this series of mice to be at least 6.3%. However, at this stage it may be safer to consider this as the frequency of readily detectable mutants, since a number of putative mutations of a less obvious nature (including possible embryonic-lethal phenotypes) are still awaiting confirmation. Two such previous studies reported ratios of visible mutation at 3% (in a series of 200 transgenic lines) [26] and 1.5% (139 transgenic lines) [55]. The figure for this study of at least 6.3% is higher than, but still in keeping with, those of the other studies. Overall frequencies of transgene insertional mutation, including prenatal lethal as well as visible phenotypes, have been estimated at between 5% and 10%

[55, 89, 90]. These figures suggest that identification of further insertional mutant lines in this screen is not unlikely, and indeed, if the remaining six putative insertional mutants are included in calculations, an overall figure of 16% for transgene insertional mutagenesis is reached. This is in keeping with figures obtained in the previous such studies.

3.4.5 A high proportion of mutants found in such screens have previously been identified

One noticeable facet of the screen as a whole is that a high proportion of the visible insertion mutants generated have arisen through re-mutation of classical loci. This statement is true both for the Harry line, which is probably a new allele of the *dom* locus, and, as we shall see in Chapters 4 to 7, the Ann line. These findings are not uncharacteristic with a notable review of transgene insertional mutation stating that; of 23 visible, viable, transgenic mutations described, 13 were at previously known loci [26].

Obviously the screening strategies employed contribute greatly to these findings in that they favour genes which can be mutated to produce viable animals with visible abnormalities. The high frequency of re-mutation of classical loci does suggest that a significant proportion of such genes have already been mutated. It may therefore be advisable for future mutagenesis studies to be refined so that screening for embryonic lethal mutants, or more subtle phenotypes, is more rigorous. Indeed such problems are now being addressed with the utilisation of the SHIRPA protocol for detecting subtle neurological defects in a large-scale ENU mutagenesis-screening program currently being conducted [91]. Such strategies may well be beyond the scope of studies such as ours, where transgenic experiments were initiated with a completely separate aim and

the discovery of mutations was purely serendipitous. However, such studies, despite perhaps lacking the scale and depth of specific mutational screening programmes, have led to the functional characterisation of several mouse genes.

3.4.6 Are such visible mutation rates consistent with insertional mutagenesis being completely random?

It is the widely held view that transgene integration into the mouse genome is random or at least near-random. It has however been estimated that if this was the case then the rate of visible mutation in transgenic mice should be 0.3% [26]. Our findings along with those of two similar studies suggest that this figure is somewhat less than that observed. Although limited evidence is available, non-random integration of transgenes into genes or other mutational 'hot-spots' could explain this apparent disparity.

3.4.7 Conclusion

Screening of the original cohort of luciferase transgenic mice is still incomplete, however, several putative transgene insertional mutants have been identified. Of these, four have been characterised in some detail, including confirmation of co-segregation of the phenotype with the transgene. The Harry and Holly lines have been described previously [80] whilst the Ann (Chapters 4 – 7) and Ob (Chapter 8) lines are the subject of this thesis.

CHAPTER 4: ANN - A MODEL FOR CEREBELLAR ATAXIA

4.1 Introduction

4.1.1 Identifying the physiological basis of the Ann phenotype

Ann mutant animals have a severe deficit in locomotion, but the physiological basis for this could be one of several possibilities that fall into at least three broad catagories:

The inability of mutants to walk without reeling to one side might be attributable to the wasting or weakness of skeletal muscle, which is symptomatic of a neurogenic or myopathic disorder. A neurogenic disease could be of either a motor neuron disease type, in which the nerve cell bodies of motor neurons are primarily affected, or a peripheral neuropathy, in which the motor axon is primarily affected. Myopathic disorders result from muscle fibre degeneration. Alternatively, an inability to plan or execute movements properly could be the basis of the Ann disorder and if so, might originate in one of the higher structures that exert some form of control over voluntary movements such as the motor cortex, cerebellum and upper motor neurons.

Such a broad range of possibilities presents a difficult challenge in the identification of the physiological basis of the Ann mutant phenotype. The identification of any pathological changes in Ann mutant mice would provide an invaluable handle on the exact nature of the disorder.

4.1.2 The motor unit

The term 'motor unit' was first used to define the basic unit of motor function i.e. a motor neuron and the muscle fibres it innervates (discussed in [92]). A closer examination reveals that a motor unit can be subdivided into four functional components: the motor neuron cell body, the motor

axon, the neuromuscular junction (NMJ) and the muscle fibres innervated by the motor neuron.

Motor nuclei are located in the ventral horns of the spinal cord where they synapse with both afferent neurons and neurons of descending pathways, as well as spinal interneurons. Consequently both voluntary and reflex movements are facilitated through innervation of skeletal muscle by motor neurons. Action potentials are transmitted along the myelinated motor axon to the NMJ, which is the synapse between motor neurons and individual skeletal muscle fibres. The action potential generated at the NMJ is rapidly propagated throughout the length of the fibre and facilitates its mechanical contraction.

Skeletal muscle fibres are elongated, multinucleate cells, consisting of myofibril bundles enclosed in a membrane called the sarcoplasmic reticulum. A single muscle fibre is usually innervated by only one motor axon, although a single motor neuron can innervate more than one muscle fibre.

4.1.3 Myopathic disorders

Most diseases of the motor unit are characterised by weakness and wasting of skeletal muscles. If muscle becomes dysfunctional and denervation is not the cause, then the disorder is said to be myopathic. The muscle weakness observed in most inherited myopathies arises from the degeneration of muscle fibres, although in other cases a biochemical or some other defect in muscle fibres may be responsible.

The best-characterised inherited myopathies belong to the muscular dystrophy group of diseases, and all involve the degeneration of muscle fibres. The commonest muscular dystrophy, Duchenne muscular dystrophy (DMD) is a fatal, X-linked, myopathic disease affecting 1 in 3300 boys. DMD, along with an associated disease, Becker muscular dystrophy, is caused by mutation of the large membrane-associated protein, dystrophin (reviewed in Hoffman and Kunkel, 1989) [93].

Several of the proteins involved in other muscular dystrophy types co-localise with this protein in the dystrophin associated glycoprotein complex (DAGC). This complex is thought to be important in anchoring muscle cells to the extracellular matrix and in so doing protect the sarcolemmal membrane from the mechanical stresses that develop during muscle contraction. Disruption of this linkage has been proposed as the basis of the muscle fibre degeneration common to the different forms of muscular dystrophy (see Fig. 4.1) [94, 95].

A pattern of muscle fibre degeneration and regeneration is observed in these diseases resulting in characteristic pathological features. Regenerating muscle fibres are typically of small-calibre and have centrally located nuclei. Necrotic fibres are also evident as is the accumulation of macrophages. Eventually in dystrophic muscle, myofibres are replaced by connective tissues. Additionally, elevation of serum creatine kinase levels is indicative of the breakdown of the sarcoplasmic membrane. Mouse models for a number of the muscular dystrophy types are already in existence with the gross phenotypes of several bearing strong similarities to the Ann mutant (see Table 4.1).

A mouse mutant lacking dystrophin, the *mdx* mouse, was shown to exhibit the severe muscle pathology characteristic of DMD during the first 6 weeks of life. Thereafter the muscles of *mdx* mice recovered by virtue of substantial muscle regeneration, and these mice subsequently led apparently normal lives, displaying little of the features common to DMD.

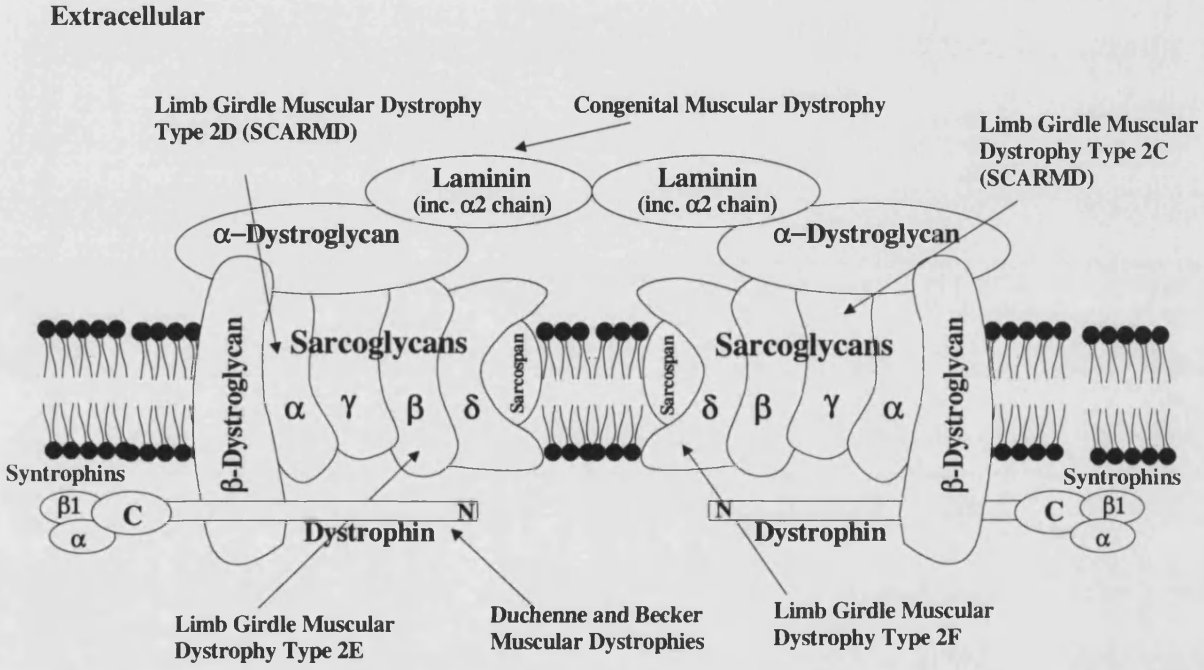

Fig. 4.1. The components of the Dystrophin-associated glycoprotein complex.
The complex provides a physical linkage between the muscle cell cytoskeleton and the extracellular matrix. Loss of a number of these proteins is associated with a variety of Muscular Dystrophy disease types, as indicated. Figure adapted from Novocastra Laboratories Ltd. Product range 2000 catalogue.

Table 4.1. Mouse models of muscular dystrophy diseases

Mouse mutant	Gene	Human syndrome	Gross Phenotype	Histopathology
Mdx [96]	*Dystrophin [97]*	Duchenne muscular dystrophy (DMD)	Tremors and mild discoordination from 12 months.	Dystrophic skeletal muscle from 2 weeks, becoming normal from 6 weeks.
mdx/utrn$^{-/-}$ [98, 99]	*Dystrophin /utrophin*	Duchenne muscular dystrophy (DMD)	Decreased activity, waddling gait, stiff limbs, thoracic kyphosis and premature death	Dystrophic skeletal muscle from 2 weeks leading to interstitial fibrosis. Cardiomyopathy.
Dystrophia muscularis (*dy*) [100]	*Laminin α2 [101, 102]*	Congenital muscular dystrophy (CMD)	Progressive weakness/paral -ysis from 3.5 weeks, death before 6 months.	Characteristic dystrophy of skeletal muscle, peripheral nerve myelination defects.
Myodystropy (*myd*) [103]	Unknown	Facioscapulohumeral dystrophy (FSHD)	Abnormal posture, small size, shuffling gait, thoracic kyphosis. Death around 4 months.	Focal dystrophic lesions of skeletal muscle.
dag1$^{-/-}$ *dag1*$^{-/-}$ chimeras [104, 105]	*α/β dystroglycan* (*dag1*)	None reported	*dag1*$^{-/-}$: embryonic lethal. dag1$^{-/-}$ chimeras: waddling gait, kyphoscoliosis from 3 months, progressively worsening.	Skeletal muscular dystrophy, increased hindlimb muscle mass.
sgca$^{-/-}$ [106]	*α-sarcoglycan* (*sgca*)	Limb girdle muscular dystrophy 2D (LGMD 2D)	Abnormalities in contractile properties of skeletal muscle.	Progressive skeletal muscular dystrophy. Increased muscle mass.
gsg$^{-/-}$ [107]	*γ-sarcoglycan* (*gsg*)	Limb girdle muscular dystrophy (LGMD2C)	Variably abnormal gait, premature death.	Dystophy of skeletal muscles, cardiomyopathy.

This has limited the effectiveness of the *mdx* mouse as a model for DMD [108]. The explanation for the phenotypic differences between *mdx* and DMD was subsequently attributed to the dystrophin related protein, utrophin. The expression of utrophin was found to be upregulated in *mdx* muscle where it functionally compensates for the dystrophin deficiency [109]. This was confirmed by the generation of *mdx:utrn*$^{-/-}$ double mutants, which displayed progressive DMD-like clinical and pathological changes, thus providing a more accurate model of DMD than the *mdx* mouse [98, 99]. Double mutants are subject to a marked reduction in size, a waddling gait, progressive dorsal-ventral curvature of the spine and eventual death. Although differing in the time course of disease progression (onset at 4 to 6 weeks, death by 20 weeks) many of these gross phenotypic features are extremely similar to those of Ann.

The superficial similarities between the Ann mutant and a number of mouse models for various muscular dystrophies suggests that the nature of the disorder in Ann mutants may be myopathic in origin, and could be of the muscular dystrophy type. An obvious way to test this suggestion would be to carry out a histological examination of Ann mutant muscles in order to look for any characteristic muscular dystrophy disease pathology.

4.1.4 Motor neuron diseases

The human motor neuron diseases are a heterogeneous group of syndromes that have the common features of progressive degeneration of motor neurons and denervation atrophy of skeletal muscle. Motor neuron diseases may be sporadic or inherited, with clinical observation alone often insufficient to distinguish the two categories. Some of the diseases may affect only spinal motor neurons (termed lower motor neurons), whereas

others may affect both lower motor neurons and neurons that originate in higher regions of the brain (termed upper motor neurons), such as the neurons of the corticospinal tract.

Muscular atrophy is a characteristic change in muscles innervated by degenerating lower motor neurons. As a result of denervation, muscle fibres are seen to shrink and eventually disappear. The axons of surviving neurons may sprout and reinnervate some of these muscle fibres but if the effect on motor neurons is progressive and affects surviving motor neurons then atrophy will be observed in groups of adjacent muscle fibres that will also take on an angular morphology

Degeneration of all motor neurons is characterised by a number of changes to neuronal morphology. The cell body of the motor neuron may swell in size with the nucleus adopting an eccentric position. Nissl substance is observed at the margin of the cell body rather than around the nucleus as in normal cells. These changes to the morphology of the cell body are termed chromatolysis, and are a diagnostic feature of motor neuron degeneration. Additionally Wallerian degeneration may be observed in which the axon terminal and its distal segment degenerates leaves behind myelin debris.

Approximately 80% of human inherited motor neuron disease is due to mutation of the SMA locus on chromosome 5. SMA (spinal muscular atrophy) affects mostly the lower motor neurons and is subdivided into three classes based on the level of severity. All three classes manifest as muscular weakness and localise to the same region of human chromosome 5, suggesting the involvement of a single gene with multiple alleles.

Neuropathological studies of SMA patients reveal a paucity of spinal motor neurons, with those surviving exhibiting chromatolysis. More subtle changes are also widespread throughout the nervous system, such as chromatolysis in sensory neurons. It has long been thought that SMA primarily involved the cell soma of motor neurons but it has been suggested that the primary abnormality originates in the distal axons (for a review see [110]).

A number of mouse motor neuron disease mutants have been identified in which the lower motor neurons are primarily affected and which might serve as useful models for SMA (see Table 4.2). Furthermore a number of these mutants such as *pmn* (progressive motor neuropathy) [111], *mnd* (motor neuron degeneration) [112] and *mnd2* (motor neuron degeneration 2) [113] exhibit features which are strongly reminiscent of those observed in Ann mutants such as small size, progressive paralysis and premature death. This could suggest that Ann represents a model for some form of lower motor neuron disease.

Undoubtedly the most well-known human motor neuron disease is Amyotrophic lateral sclerosis (ALS). This disorder can be either sporadic or inherited and involves the progressive degeneration of both upper and lower motor neurons. The weakness and paralysis observed is attributable to degeneration of lower motor neurons, whilst spasticity and hyperreflexia result from lesions of the upper motor neurons. The hereditary and sporadic forms of ALS are clinically indistinguishable, but only about 10% of cases are inherited [114]. Mutations of the Cu/Zn *superoxide dismutase 1* (*SOD1*) gene have been found as the cause of disease in approximately 20% of familial ALS (FALS) cases [115]. SOD1 is a

Table 4.2. Mouse models of motor neuron disease

Mutant	Gene	Gross phenotyope	Pathology
progressive motor neuropathy (pmn) [111]	Unknown	Progressive atrophy and paralysis, firstly of the pelvic girdle and hindlimbs, followed by forelimbs. Mutants smaller than normal. Death at 6 to 7 weeks of age.	Degeneration, mostly of lower motor neurons, originating at motor endplates and progressing proximally, causing atrophy of skeletal muscle.
motor neuron degeneration 2 (mnd2) [113]	Unknown	Unstable gait, hunched posture and loss of balance visible from between 21 and 24 days, gradual decline in mobility of mutants. Failure to gain weight and eventual death prior to 40 days.	Chromatolysis exclusively in lower motor neurons, and denervation atrophy of skeletal muscles
Altered expression in various transgenic lines [116]	*Cu/Zn superoxide dismutase 1 (SOD1)*	Progressive weakness, muscle atrophy and paralysis.	Loss of motor neurons, Wallerian degeneration and denervation atrophy.
Altered expression in various transgenic lines [117, 118]	*Neurofilament L (NF-L)* *Neurofilament H (NF-H)*	Generally motor dysfunction and weakness.	Chromatolysis and perikaryal and axonal swellings containing neurofilament bundles
Motor neuron degeneration (mnd) [112]	Unknown	Hindlimb weakness and ataxia between 5 and 11 months, progressing to severe spastic paralysis of all limbs and death by 9 to 14 months.	Degeneration of both upper and lower motor neurons.
Wobbler (wr) [119]	Unknown	Small size, fine head tremor and 'high-stepping' unsteady gait from 3 weeks. Progressive weakness from the fourth or fifth week, more severe in the forelimbs and anterior of the body. Most mutants die by 2 or 3 months.	Degeneration of motor nerve cells in the brainstem and spinal cord

member of a family of metalloenzymes that have the ability to catalyse the conversion of O_2^- to H_2O_2 and O_2. Transgenic mice expressing mutant forms of human [116] and mouse [120] *SOD1* have been generated and exhibit several clinical signs of ALS such as progressive weakness, muscle atrophy and paralysis, whereas transgenics expressing wild-type *SOD1* display no phenotype.

Several other mouse motor neuron disease mutants are known to display degeneration of both upper and lower motor neurons and thus bear similarities to ALS (see Table 4.2). A number share similar phenotypes to the Ann mutant, most notably the recessive *wobbler* (*wr*) mutant that exhibits degeneration of the motor nerve cells in the brainstem and spinal cord [119]. Homozygotes are identifiable from about 3 weeks of age, being smaller than normal littermates and exhibiting a fine tremor of the head and a 'high-stepping' unsteady gait. Progressive weakness is apparent from the fourth or fifth week and most mutants die by 2 or 3 months of age. To consider the Ann mutant as a possible motor neuron disease model it will be essential to look for the pathological changes, both in muscle and motor neurons, which characterise these diseases.

4.1.6 Ion channels and channelopathies

Present in all cells, ion channels are membrane-spanning glycoproteins that play a key role in the normal function of both nerves and muscles. Ion channels belong to one of two major classes according to the type of signals that modulate their activity. The binding of a biologically active molecule such as a hormone or neurotransmitter activates ligand-gated ion channels. This type of channel plays an important role in controlling ion flux in the postsynaptic regions of nerve and muscle cells. Regulated by changes in

membrane polarity, voltage-gated ion channels are critical to the propagation of action potentials in nerve cells.

Channels of both classes have been associated with a variety of genetic disorders, with defects in voltage-gated ion channels being especially prevalent. Neurological abnormalities are common to mutations in a number of K^+, Na^+ and Ca^{2+} ion channel genes. Weakness, ataxia, myotonia and paralysis are characteristic features of such channelopathies (for review see [121]). The genes encoding numerous ion channel subunits belonging to a variety of types have been identified and the characterisation of a number of these subunits has been aided by the availability of a myriad of spontaneous and engineered mouse mutants in the corresponding genes (see Table 4.3). Again a number of mutants of different ion channel types display phenotypic similarities to Ann mutants, including small size and gait abnormalities.

Amongst these is the recessive *weaver* (*wv*) mouse, which results from the spontaneous mutation of the inwardly rectifying K^+ channel gene, *Kcnj6 [122]. Wv* homozygotes are identifiable from 2 weeks of age by their small size, unstable gait, weakness and hypotonia [123]. In this case the ion-channel defect results in developmental abnormalities in the cerebellum (discussed in section 4.1.8).

The *leaner* (*la*) *Cacna1a*, Ca^{2+} channel mutant also exhibits cerebellar defects that are manifest as ataxia, stiffness and retarded motor activity from 8 to 10 days of age [123]. Most *la* homozygotes die at weaning. Mutations in the human homologue of the *Cacna1a* gene, CACNA1A1, result in the human hereditary ataxia spinocerebellar ataxia 6 [124].

Table 4.3. Mouse models of ion channelopathies

Mouse mutant	Gene	Channel type	Human syndrome	Gross Phenotype	Pathology
Targeted mutation [125]	*Kcna1*	K^+, shaker-like	Episodic ataxia 1 (EA1)	Frequent spontaneous seizures.	Altered axonal action potential conduction.
Kcnc1$^{-/-}$ [126]	*Kcnc1*	K^+, shaker-like	Unidentified	Reduced body weight and poor coordination of motor skills.	Defective muscle fibre contraction/relaxation and force generation.
weaver (*wv*) [123]	*Kcnj6* [122]	K^+, inward rectifier	Unidentified	Small size, unstable gait, weakness and hypotonia from 2 weeks of age, most die at weaning.	Cerebellum defects: granule cell death, abnormal Purkinje cell morphology.
muscular dysgenesis (*mdg*) [127]	*Cacn1as* [128]	Ca^{2+}, α subunit	Hypokalaemic period paralysis (Hyper PP) Malignant hyperthermia susceptibility (MHS).	Embryonic lethality.	Skeletal muscle never develops properly and totally lacks excitation-contraction coupling.
tottering (*tg*) [129] *leaner* (*la*) [123]	*Cacna1a* [130]	Ca^{2+}, α subunit	Episodic ataxia 2 (EA2) Familial hemiplegic migraine (MHP) Spinocerebellar ataxia 6 (SCA6).	*tg*: Behavioural absence seizures, stereotyped partial motor seizures and ataxic gait. *la*: ataxia, stiffness and retarded motor activity, death at weaning.	*tg*: morphologically normal CNS. *la*: cerebellum reduced in size, loss of Purkinje and Golgi cells.
lethargic (*lh*) [123]	*Cacnb4* [131]	Ca^{2+}, β subunit	Unidentified	Unstable gait, seizures and lethargic behaviour. Mutants are smaller than normal, death before 2 months of age.	No pathological changes in CNS.
motor end plate disease (*med*) [132]	*Scn8a* [133]	Na^+	Unidentified	Progressive weakness of skeletal muscle apparent from 8 to 10 days, eventual death within 2 weeks of onset.	Muscular atrophy, terminal sprouting of motor axons which also display slower than normal conduction velocities.

Multiple alleles of the *Scn8a* Na^+ voltage-gated ion-channel α subunit gene have been isolated in the mouse. *Motor end-plate disease* (*med*) is a spontaneous recessive mutation of the *Scn8a* gene [133] that is characterised by progressive weakness of skeletal muscle and is apparent from 8 to 10 days of age leading to eventual death within 2 weeks of onset. Muscular atrophy is accompanied by terminal sprouting of motor axons that also display slower than normal conduction velocities [132].

Conclusive identification of an ion channelopathy based on histopathological analysis alone is virtually impossible owing to the range of tissues and functions dependant upon different ion channel types (e.g. motor end plate through to higher brain regions). In this instance, some form of molecular data would be invaluable to conclusively prove mutation of an ion channel-encoding gene in the Ann mutant.

4.1.7 Myelination and related neuropathies

The majority of axons in the nervous system are encapsulated in a myelin sheath that acts as an insulating structure and facilitates the high-speed conduction of action potentials. The myelin sheath consists of repeated bimolecular layers of lipids interspersed between adjacent protein layers, and is derived from multiple wrappings of oligodendrocyte (in the CNS) or Schwann cell (in the PNS) processes around the axon. The majority of cytoplasm is extruded from these layers leaving a highly compacted and organised sheath structure.

The most common human neuropathies result from perturbation of myelin formation or maintenance and have the common characteristic of a reduction in nerve conduction velocity. Since both sensory and motor

axons are myelinated, myelinopathies may affect both motor and sensory functions. Loss of sensation and parasthesias may result from sensory impairment, whilst weakness and paralysis are typical signs of motor abnormalities. Most inherited myelinopathies result from mutations of the structural proteins of myelin and can lead to dysmyelination or demyelination in the PNS, CNS or both (for reviews see [134-136]).

A number of mouse mutants, both naturally occurring and engineered, are available as models for different types of myelinopathy (see Table 4.4). Again similarities with the Ann mutant, especially tremors and gait abnormalities, are notable in several of these mutants suggesting the Ann phenotype may result from a myelination defect. Amongst the myelination mutants which are outwardly similar to Ann are two mouse models of different human Charcot-Marie-Tooth-type peripheral neuropathies.

PMP-22 is a glycosylated membrane protein present in virtually all PNS myelinated fibres. The protein is expressed in Schwann cells and incorporated into the myelin sheath of PNS axons where it appears to play a structural role [137, 138]. The *pmp22* gene is also expressed in the CNS but no protein is made there [136]. The *trembler* (*Tr*) mouse is an autosomal dominant *pmp22* mutant that displays a severe peripheral neuropathy in which myelin sheaths in the PNS are thin or absent [139]. *Trembler* mutants are identifiable from 9 or 10 days of age owing to a rapid tremor. Affected animals suffer occasional seizures, a gait abnormality involving mainly the hindlimbs, and develop paralysis. Mortality is high between 3 and 4 weeks [140]. The *trembler* mouse represents a useful model for the human hereditary neuropathy Charcot-Marie-Tooth disease

Table 4.4. Mouse myelination mutants

Mutant	Gene	Human syndrome	Gross phenotype	Clinical phenotype
Shiverer (*shi*) [141]	*Myelin basic protein* (*mbp*) [142]	None identified	Tremor during locomotion from 12 days of age becoming progressively more severe, discoordination of hindlimbs, seizures, smaller than littermates by 4 weeks of age, death between 50 and 100 days.	Absence of myelin formation in the CNS, myelin sheaths, where formed, are thin and lack the MDL
Jimpy (*jp*) [143]	*Proteolipid protein* (*plp*) [144]	Pelizaeus Merzbacher disease (PMD)	Marked tremor of hindquarters when attempting movement and convulsions from 3 weeks of age, death between 20 and 40 days.	Oligodendrocyte death by apoptosis, surviving oligodendrocytes assemble myelin-like structures exhibiting reduced spacing of IPL.
trembler (*tr*) [140]	*Peripheral myelin protein, 22kDa* (*Pmp22*) [145]	Charcot-Marie-Tooth disease type 1a (CMT1a) Hereditary neuropathy with liability to pressure palsies (HNPP)	Seizures, gait abnormality (mainly of hindlimbs) from 9 days, eventual paralysis. Death between 3 and 4 weeks.	Myelin sheaths in PNS thin or absent, Schwann cells proliferate throughout life.
Mpz $^{-/-}$ [146]	*Myelin protein zero* (*Mpz*)	Charcot-Marie-Tooth disease type 1b (CMT1b) Dejerine-Sottas disease (DSS)	Abnormal gait and tremors develop between 2 and 3 weeks of age. Defects not lethal	Heterogeneous pattern of dysmyelination, axons often surrounded by abnormal myelin (due to incomplete compaction at the IPL) and many degenerate.
Quaking (*qk*) [147]	Unknown	None identified	Marked rapid tremor from 10 days of age, developing fully by 3 weeks. Seizures when mature	Myelin deficiency mostly in CNS. Myelin sheaths thinner than normal loosely wrapped around axon.
Mag $^{-/-}$ [148]	*Myelin-associated glycoprotein* (*Mag*)	None identified	Subtle behavioural changes.	Onset of myelination delayed, subtle morphological abnormalities of oligodendrocytes.

type 1a (CMT1a) in which the genetic defect in some cases has been identified as a point mutation within the *PMP22* gene [149].

Myelin protein zero (Mpz) is the most abundant protein in the myelin of the PNS [135]. It is a membrane glycoprotein that is thought to act as a homophilic adhesion molecule and is important in maintaining the IPL (Intraperiod line) of the myelin sheath. Mpz is expressed in Schwann cells at the time of myelin formation in the PNS [150]. Although no naturally occurring *Mpz* mouse mutants have been isolated, gene targeting has been used to engineer an *Mpz* null strain [146]. Knockout mice exhibit a heterogeneous pattern of dysmyelination with many axons surrounded by abnormal myelin, due to incomplete compaction at the IPL. In some Schwann cell-axon units no myelin forms at all whereas in other units, morphologically normal, compact myelin is observed. Furthermore, many axons degenerate when associated with abnormal myelin in these mice. Mutants develop an abnormal gait and tremors between 2 and 3 weeks of age, although the defect is not lethal.

Mutations in the *Mpz* gene are responsible for Charcot-Marie-Tooth disease type 1b; a demyelinating disorder of the PNS [151], and also Dejerine-Sottas disease (DSS); a more severe disorder of the same type [152]. As with a putative myopathic or motor neuron disorder, a thorough histological analysis of myelin integrity in Ann mice would be required to test the possibility of a myelin defect in this strain.

4.1.8 The cerebellum and cerebellar mutants.

The cerebellum is a highly organised, foliated structure that lies dorsal to the brain stem. It is involved in coordinating the planning, timing and patterning of muscular contractions during voluntary movements. It does this by receiving both internal feedback (from regions of the motor cortex) concerning the programming and execution of movement, and external feedback from the peripheral nervous system, allowing motor performance to be monitored. By comparing these internal and external feedbacks the cerebellum can adjust movement and posture by modulating the descending motor systems of the brain.

The cerebellum can be divided in a number of ways. It consists of an outer layer of grey matter; the cerebellar cortex, an internal layer of white matter, and three pairs of deep nuclei. The cerebellar cortex can itself be subdivided into three layers, the outermost molecular layer (ML) which contains mostly axons, the Purkinje cell layer (PCL) in which Purkinje cell bodies are arranged in a single layer, and the internal granular layer (IGL) containing mostly densely packed granule cells.

Disorders of the cerebellum lead to a number of characteristic symptoms depending upon the exact nature of the defect. The most common is ataxia, a term which encompasses a variety of abnormalities in the execution of voluntary movements including errors in the rate, regularity, range and force of movement. This is often manifest as an ataxic gait, in which the stance is wide and movement is hesitant and unsteady.

The single cell thick Purkinje cell layer is of paramount importance to normal cerebellar function in that it provides the sole output of the

cerebellar cortex, through Purkinje cell axonal projections, to the underlying white matter (see Fig. 4.2). Purkinje cells receive their major afferent input from mossy fibres through synapses with granule cells. The number of small, densely-packed, neurons in the internal granular layer exceeds the total cell number in the cerebral cortex. Granule cells make important excitatory connections with Purkinje cells via their axons that extend to the outer molecular layer, where they become parallel fibres that synapse with the Purkinje cell dendrites. Purkinje cells and granule cells constitute the two major cell populations of the cerebellar cortex and in many cerebellar disorders defects in either or both of these cell populations are apparent.

A number of mouse mutants exist which display some form of cerebellar dysfunction that often results from either the abnormal development or degeneration of one or more of the cerebellar cell populations (see Table 4.5). An ataxic gait is a characteristic feature of cerebellar dysfunction which these mutants have in common. This may be accompanied by hypotonia and a tremor that is frequently apparent at the end of movement. Of the variety of neurological and neuromuscular mutants discussed in this chapter, the Ann mutant phenotype bears the strongest similarities in terms of clinical phenotype with mouse mutants affected by some form of cerebellar dysfunction. Therefore the mutants belonging to this class deserve detailed consideration.

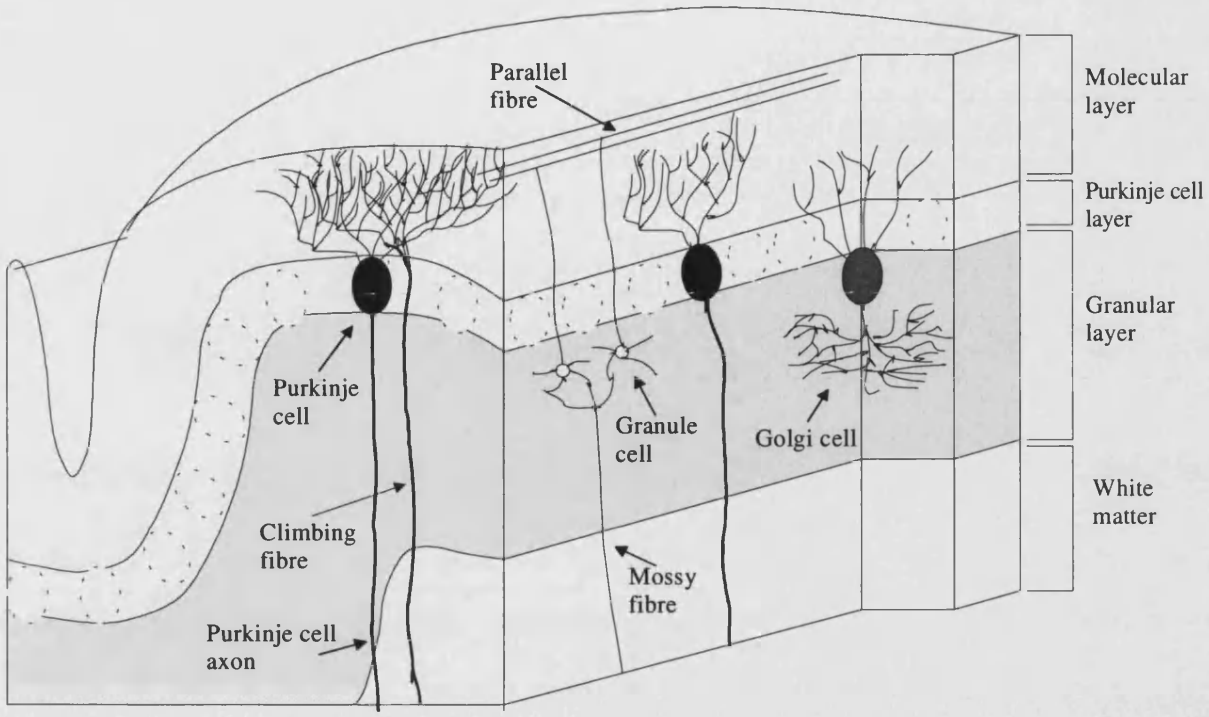

Fig. 4.2. The laminar organisation of the cerebellar cortex.
Vertical section of a single cerebellar folium showing both longitudinal and transverse planes. Figure adapted from Chapter 41 of Principles of Neural Science, [92].

Several classical cerebellar mutant strains are due to defects that intrinsically affect the Purkinje cell population leading to the degeneration of these cells. This can in turn produce effects on other cell types, most notably the granule cells, which fail to proliferate in the absence of Purkinje cells. This is true of two cerebellar mutants, the recessive *staggerer (stg)* [153] and semidominant *lurcher* (*Lc*) [154] strains. In both, intrinsic Purkinje

Table 4.5. Mouse mutants displaying cerebellar dysfunction

Mutant	Gene	Phenotype	Cause
Purkinje cell degeneration (*pcd*) [155]	Unknown	Moderate ataxia, small size, normal life span, cerebellum slightly reduced in size.	Degeneration of Purkinje cells, intrinsic to Purkinje cell population.
lurcher (*Lc*) [156]	*Grid2 [157]*	-/- : postnatal death +/-: ataxia, small size, viable.	Loss of Purkinje cells intrinsic to Purkinje cell population. Secondary loss of granule cells.
staggerer (*sg*) [158]	*Rora [159]*	Underdevelopment of cerebellar cortex, staggering gait, hypotonia, tremor and small size. Death usual during forth week.	Deficiency of 60-90% Purkinje cells, intrinsic to this population. Remaining Purkinje cells unable to differentiate properly leading to secondary loss of granule cells.
stumbler (*stu*) [160]	Unknown	Stumbling, ataxic gait from 10 days, abnormal righting reflex, smaller than normal, death before weaning. Cerebellar cortex reduced in size but retains its normal foliation.	Paucity of Purkinje and granule cells from 10 days, limited degeneration of Purkinje cells from 20 days, normal amounts of these cells types never produced.
wasted (*wst*) [161]	Eef1a2 [162]	Tremor and uncoordinated body movements from 20 days of age, progressive paralysis and failure to gain weight leading to death by 30 days of age.	Degeneration of Purkinje cells and focal demyelination in the cerebellum.
nervous(nr) [163]	Unknown	Ataxic gait and small size from 2 to 3 weeks, mutants are viable but very poor breeders.	90% loss of Purkinje cells between 23 and 50 days due to inability of granule cells to proliferate and migrate inwards from EGL.
weaver(*wv*) [123]	*Kcnj6 [122]*	See Table 4.3.	See Table 4.3.
leaner(*la*) [123]	*Cacna1a*	See Table 4.3.	See Table 4.3.
reeler (*rl*) [140]	*Reelin [164]*	Tremors and a severely ataxic gait from 2 weeks of age. Mutants are inviable on inbred but viable on an outbred background.	Grossly abnormal organisation and lamination of cerebellar cortex, Purkinje and granule cell numbers reduced. Ectopia of Purkinje cells due to defect in neuronal migration.
scrambler(*scm*) [165]	*mDab1 [166]*	As *reeler* except inviable on inbred and outbred backgrounds	As *reeler*.

cell defects result in the degeneration of this cell type and a subsequent reduction in granule cell numbers.

Alternatively, the granule cell population may not be affected by Purkinje cell loss, e.g. in the *wasted* (*wst*) mutant [161], whilst in the *stumbler* (*stu*) mutant normal numbers of both Purkinje and granule cells are never established [167]. Obviously the effects on cerebellar development are dependant on the function of the gene product that has been disrupted in these various mutants.

The development of the laminar structure of the cerebellum is dependant on highly choreographed neuronal migrations. Several mouse mutants have been identified in which defects in neuronal migration result in cerebella lacking the normal laminar structure. In the *weaver* (*wv*) and *nervous* (*nr*) mutants granule cell death and subsequent migration defects adversely affect the Purkinje cell population [168].

Alternatively in *reeler* (*rl*) and *scrambler* (*scm*), which are defective in a common signalling pathway [169], severe lamination defects result from abnormal Purkinje cell migration during cerebellar development [170-172].

Again, histopathological analysis of the morphology of the cerebellum and its associated cell types presents the most logical approach to investigating whether a cerebellar defect is the cause of the Ann mutant phenotype.

4.2 Materials And Methods

4.2.1 Fixation of mouse tissues by perfusion

Perfusion fixation was performed with the assistance of Dr. J. Smith, (University of Birmingham). Mice were terminally anaesthetised by intraperitoneal injection with 1μg of Sagatal per gram of bodyweight. The abdominal cavity was cut open and the diaphragm cut away from the rib cage, the rib cage was then cut up either side and lifted to expose the heart. A cannula was then inserted through the base of the heart and manoeuvred into the aorta. Using fine plastic tubing the cannula was connected to a 50ml syringe barrel and, by applying light pressure to the syringe plunger, the specimen was perfused firstly with approximately 30ml of sterile PBS containing 0.3ml of heparin (at a concentration of 5000 units/ml). The PBS was then substituted for 4% paraformaldehyde in PBS and approximately 50ml of this solution was used to further perfuse the specimen until the upper limbs had visibly stiffened as a result of fixation. The mouse was then decapitated and the brain dissected into 4% paraformaldehyde in PBS, the upper spinal cord was also dissected into this fixative. Samples were postfixed for a further 12 hours prior to continuation of tissue processing.

4.2.2 Preparing Alcian blue/Alizaran red stained skeletons

Mice were killed by asphyxiation with CO_2, skinned, eviscerated and as much fat and muscle tissue removed as possible. Carcasses were fixed in 100% ethanol for 5 days, rinsed in dH_2O for a few minutes and then transferred to the staining solution (1 volume 0.3% alcian blue (Gurr) dissolved in 70% EtOH, 1 volume 0.1% alizaran red (Raymond Lamb) dissolved in 95% EtOH, 1 volume glacial acetic acid, 17 volumes 70% EtOH) for 4 days. Following staining, specimens were washed in dH_2O for a few minutes and then cleared in 20% glycerol/1% KOH until the bones

became visible (over several weeks). Skeletons were transferred to 50% glycerol for 2 days and then stored in 100% glycerol indefinitely.

4.2.3 Cresyl violet staining of spinal cord sections

This was performed according to a standard protocol [82]. Slides prepared as described (section 2.2.23), were dewaxed in two 2 minute changes of Histoclear (National Diagnostics) then rehydrated by passing through 100%, 100%, 95%, 90%, 70% and 50% EtOH for 2 minutes in each solution, followed by 1 minute in dH_2O. After covering in 1% cresyl violet solution (acidified with 0.25% glacial acetic acid) for 30 minutes, slides were rinsed in dH_2O. Slides were then passed through 96% EtOH (1minute) and rinsed in 100% EtOH for 2 minutes. Following a rinse in histoclear, slides were mounted under coverslips with DPX mountant.

4.3 Results

4.3.1 Gross features of the Ann phenotype

Ann mutants were identifiable at around 12 days of age by a fine whole-body tremor. This persisted for a further 2 to 3 days before disappearing. From 13/14 days onwards mutants displayed difficulties with normal locomotion. Affected animals were unable to walk forward for more than 2 or 3 paces without keeling over to one side. Once on their side mutants would frantically kick their legs until they managed to right themselves. By 16/17 days mutants would attempt to walk only infrequently and spent most of their time sitting still with a hunched posture (due to dorsal-ventral curvature of the spine).

Mutants did not increase in size from 12/13 days and became smaller than their littermates (see Fig. 4.3). By 17/18 days of age they had an emaciated appearance. Mutants died at around 21 days of age although some died as early as 19 days, whilst others survived to 24 days. None ever survived weaning for more than one day.

Mutants responded to visual, auditory and pain (tail pinch) stimuli, suggesting their sensory systems were functioning normally. When lifted by the tail, mutants did not clasp their rear paws, a behaviour that is common to several neurological mutants. The phenotype of mutants on both mixed C57BL/6J x CBA/Ca and inbred C57BL/6J genetic backgrounds were indistinguishable.

Fig. 4.3. Photograph of the Ann mutant.
Comparison of 21 day old Ann mutant (right) and wild-type (left) siblings. Note the small size and hunched posture of the mutant animal.

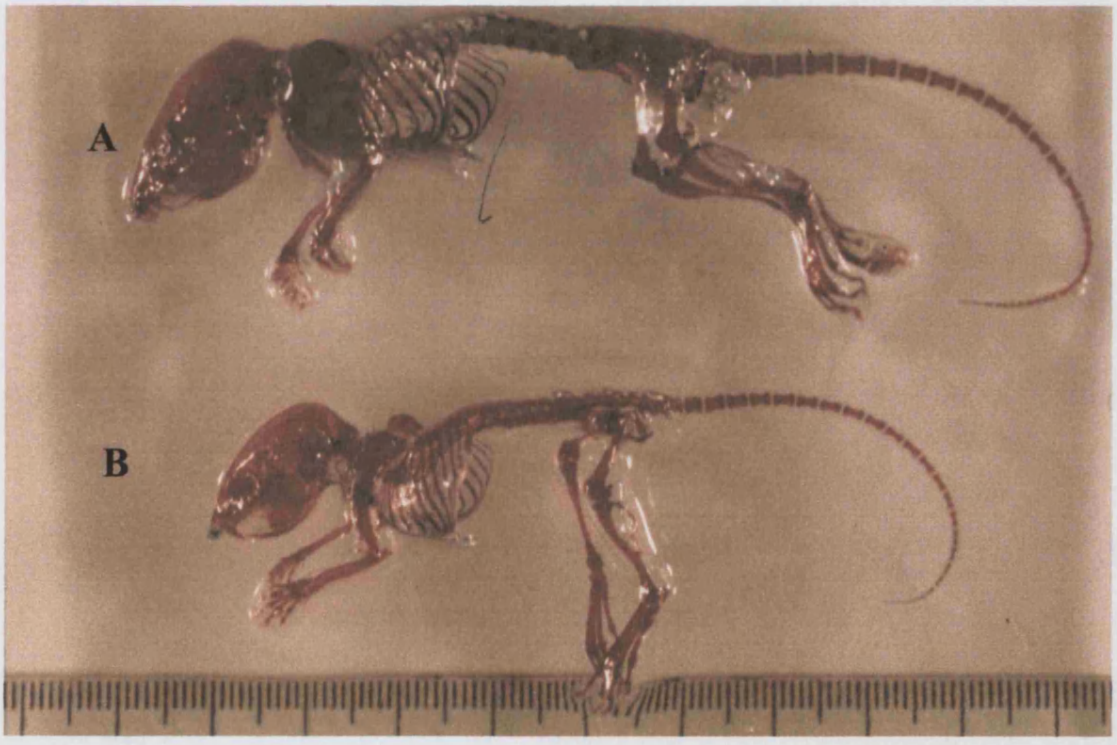

Fig. 4.4. Ann skeletal preparations.
Alcian blue/alizarin red stained skeletal preparations from 21 day old wild-type (above) and Ann mutant (below) siblings. Other than the obvious size differences, no gross skeletal abnormalities are apparent.

4.3.2 Examination of Ann skeletons

To investigate the possibility of skeletal defects that might contribute to the Ann mutant phenotype, skeletons were prepared from 19 day old Ann wild-type and mutant animals. Skeletons were stained with Alcian red (stains bone) and Alizaran blue (stains cartilage) dyes. Comparison of both preparations confirms that, except for the obvious reduction in size, the skeleton of the Ann mutant bears no abnormalities (see Fig. 4.4).

4.3.3 Measurement of Ann mass over time

For a number of litters derived from Ann hemizygous intercrosses, pups were weighed daily from 8.5 days post partum (when individuals could be marked by toe clipping) until 20.5 days (when mutants were normally killed). Mean wild-type and mutant mouse body mass values were plotted against age (measured as days post partum see Fig. 4.5). Both wild-type and mutant mice gain mass steadily from 8.5 days, but whilst this increase continues in wild-type mice through to 20.5 days, in mutants body weight levels peak at 14.5 days and decrease thereafter. A significant difference in body mass between mutant and wild-type animals is apparent from 17.5 days onwards (as indicated by standard deviations see Fig 4.5.).

This failure to increase body mass beyond a certain level could result from an inability in mutants to compete with siblings for maternal nourishment. This would certainly be consistent with the locomotor abnormalities and emaciated appearance displayed by Ann mutants. An alternative possibility may be that a defect in the gastrointestinal tract of these mice may prevent them from obtaining sufficient nutrition. Both possibilities remain to be investigated.

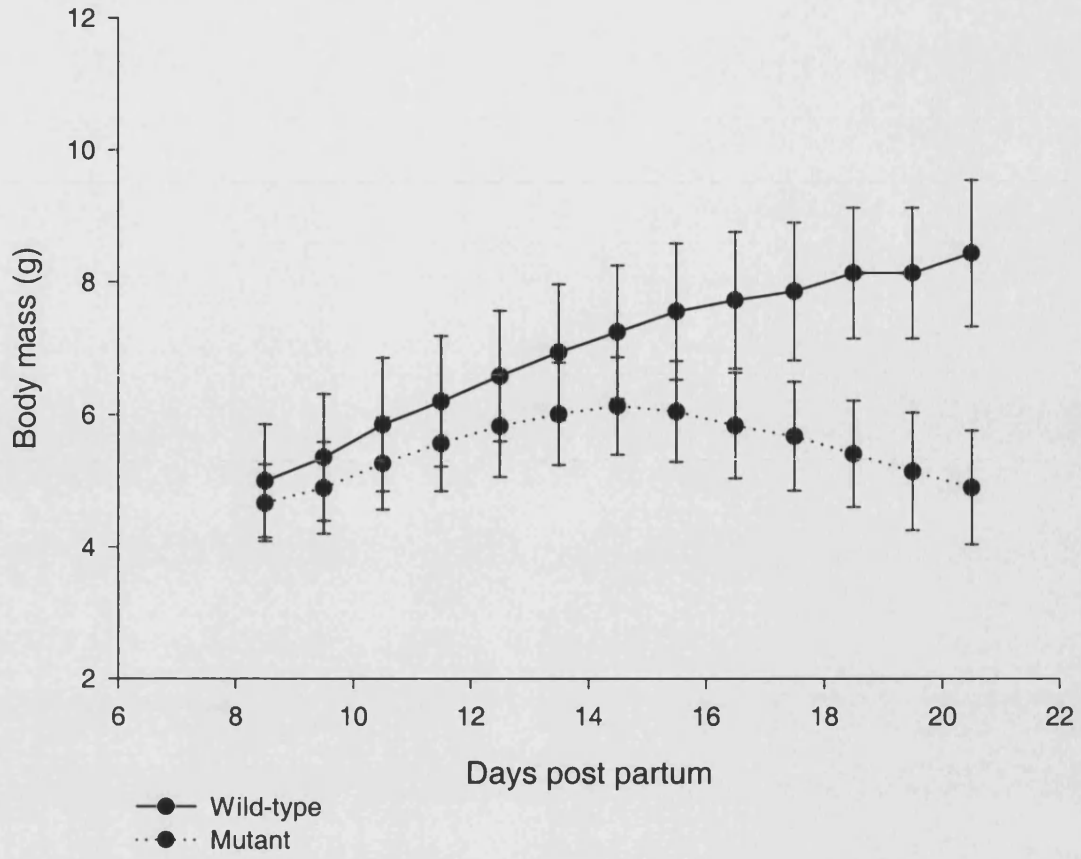

Fig. 4.5. Ann vs wild-type growth curve.
Growth curves showing wild-type and mutant mouse body mass against days post partum. Data points represent mean body mass values for 38 (wild-type) and 19 (mutant) individuals

In addition to whole body mass measurements, at 20.5 days post partum, the mass of a variety of organs and tissues was measured to allow comparison between mutant and wild-type animals. The mean masses of a variety of organs from both wild-type and mutant mice are plotted in Fig.4.6.

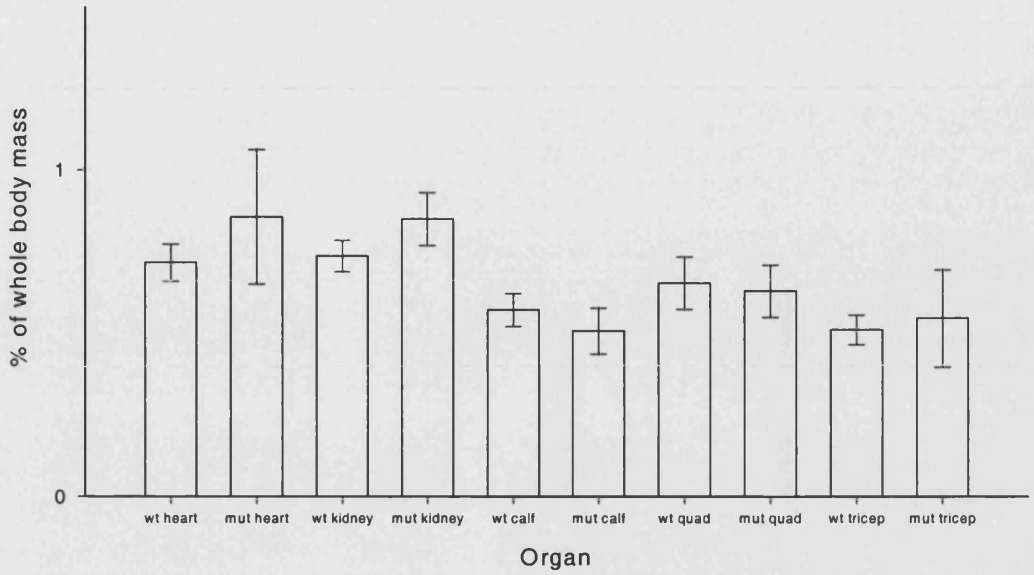

Fig. 4.6. Relative organ mass.
Plot showing mean organ mass as a percentage of mean body mass for both wild-type (wt) and mutant (mut) animals. Organs were heart, kidney and three different skeletal muscles: calf, quadricep (quad) and *triceps brachii* (tricep). Mean values obtained from 38 wild-type and 19 mutant animals at 21 days post partum. Standard deviations are represented by error bars.

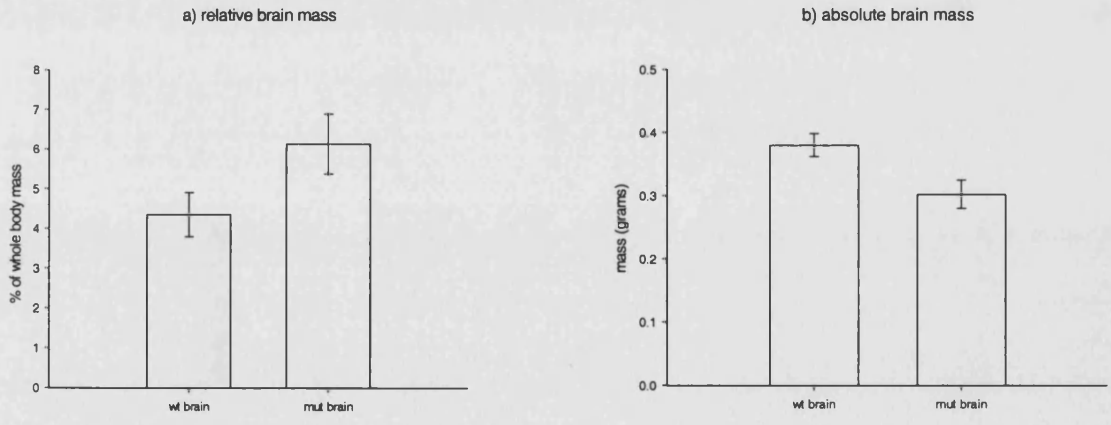

Fig. 4.7. Relative and absolute brain mass.
Plots showing a) mean brain mass as a percentage of mean body mass and b) mean brain mass as an absolute value (in grams), for both wild-type (wt) and mutant (mut) animals. Mean values obtained from 38 wild-type and 19 mutant animals at 21 days post partum. Standard deviations are represented by error bars.

With the exception of the brain, all organs weighed showed no significant differences in mass between mutant and wild-type animals when represented as a percentage of total body mass (as indicated by standard deviations in Fig. 4.6.). Average absolute brain mass was found to be greater in wild-type versus mutant mice but this trend was reversed when the average brain mass was calculated as a percentage of total body mass (see Fig. 4.7). Studies conducted on human sufferers of starvation have shown brain wastage to be much less dramatic than other organs. This is in keeping with our findings and reinforces the possibility that a failure to feed may be the cause of death in mutants.

4.3.4 Histological analysis of Ann muscle

To investigate the possibility of a myopathic disorder in Ann mutant mice a variety of muscle types were examined histologically. Transverse sections of *biceps femoris* and *triceps brachii* muscles from 19 day old wild-type and mutant mice were cut and stained with haematoxylin and eosin. As can be seen (Fig. 4.8) wild-type and mutant muscles displayed no obvious differences, with muscle fibres from both types of animal being regular in shape and size, and nuclei located at the periphery of each cell.

None of the pathological signs of muscular dystrophy diseases, such as centrally located nuclei and muscle fibre necrosis (see Fig. 4.8[E]), were observed in mutant muscle. Signs of musclar atrophy e.g. clusters of small, angular muscle fibres (see Fig. 4.8[F]), were also not apparent in mutant muscle sections.

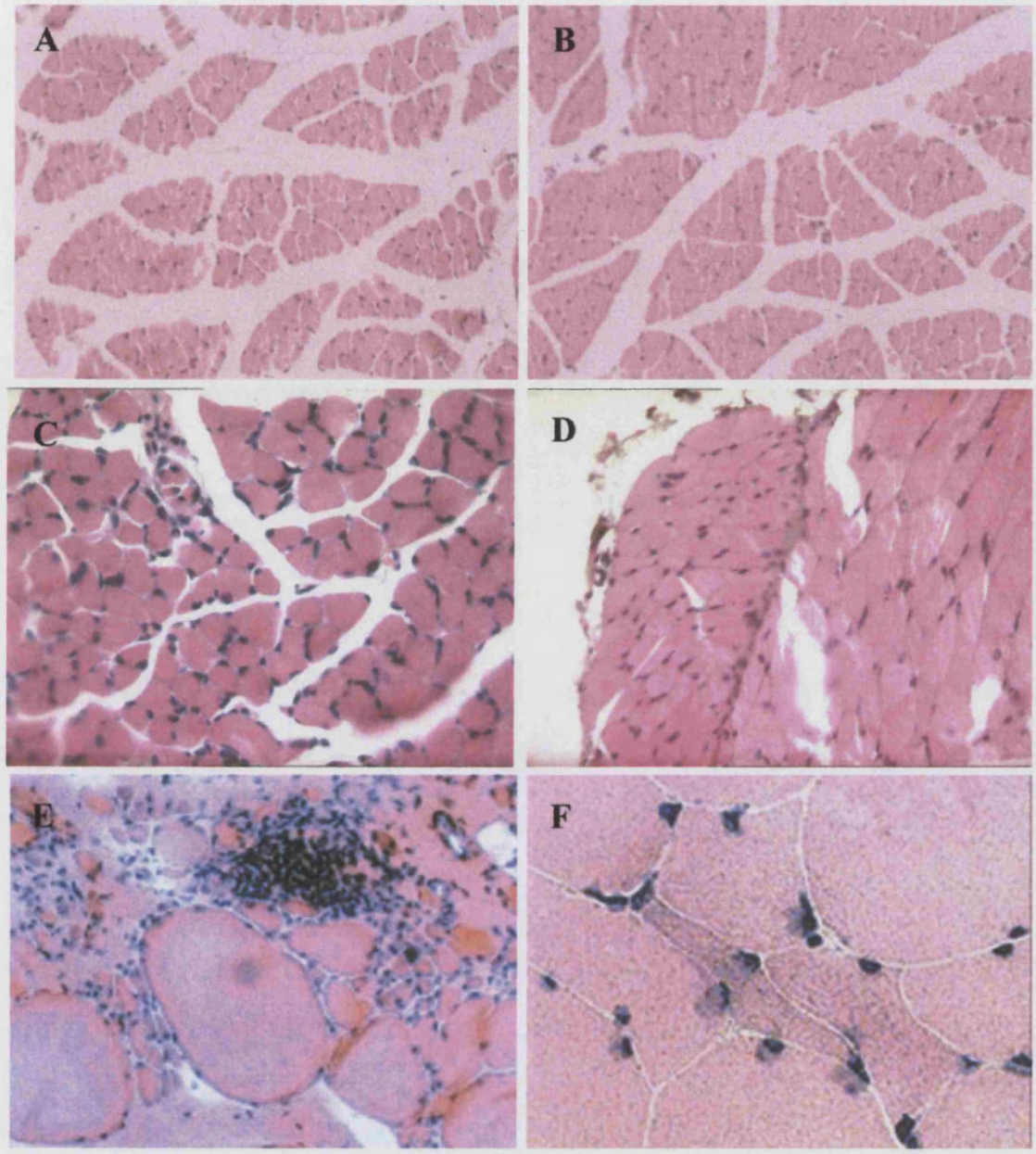

Fig. 4.8. Ann vs wild-type muscle.
Comparison of muscle morphology of 21-day-old wild-type and Ann mutant mice. Haematoxylin and eosin stained, transverse sections from wild-type *biceps femoris* (A) and *triceps brachii* (C) muscles showed no morphological differences from Ann mutant *biceps femoris* (B) and tric*eps brachii* (D). No abnormalities, such as those common to Muscular Dystrophy (E) or Muscular atrophy (F) type diseases were visible in mutant muscle sections. (E) and (F) obtained from [173]

4.3.5 Histopathology of Ann brains

The possibility of central nervous system abnormalities in Ann mutants meant that examination of mutant brains was required. In addition to the overall reduction in brain size, it was apparent from visual examination that the cerebella of Ann mutants were much smaller than those of wild-type controls (see Fig. 4.9[A]). Histological analysis provided a further insight into the nature of the defect in these mice.

Most noticeable was the complete lack of foliation apparent in the wild-type cerebellum (see Figs. 4.9 and 4.10). Furthermore, the characteristic pattern of cerebellar lamination appeared to be disrupted. The relatively cell-free outer molecular layer was discernable despite being somewhat reduced in thickness, whereas the Purkinje cell layer was completely absent. Instead of being aligned in a single-cell thick row at the superficial aspect of the granule cell layer, Purkinje cells were scattered throughout and beneath a granule cell layer which was itself markedly reduced in size. Purkinje cells were also found together in clusters beneath the granule cell layer (see Fig. 4.10).

Examination of the cerebral cortex also revealed disruption to the normally laminated structure of this brain region. A co-ordinated 'inside-out' pattern of neuronal migration during cortical development generates a characteristic six-layered structure in the mammalian cerebral cortex. This classic pattern of lamination seems to be disrupted in Ann mice with large pyramidal cells and small granule cells being interspersed rather than segregated into disparate layers (see Fig. 4.11). This is most apparent in the marginal zone (layer I), which is located under the pial surface. Normally almost devoid of cell nuclei, in mutant brains this layer appears to have been infiltrated by neurons and as such becomes indistinguishable from the other layers.

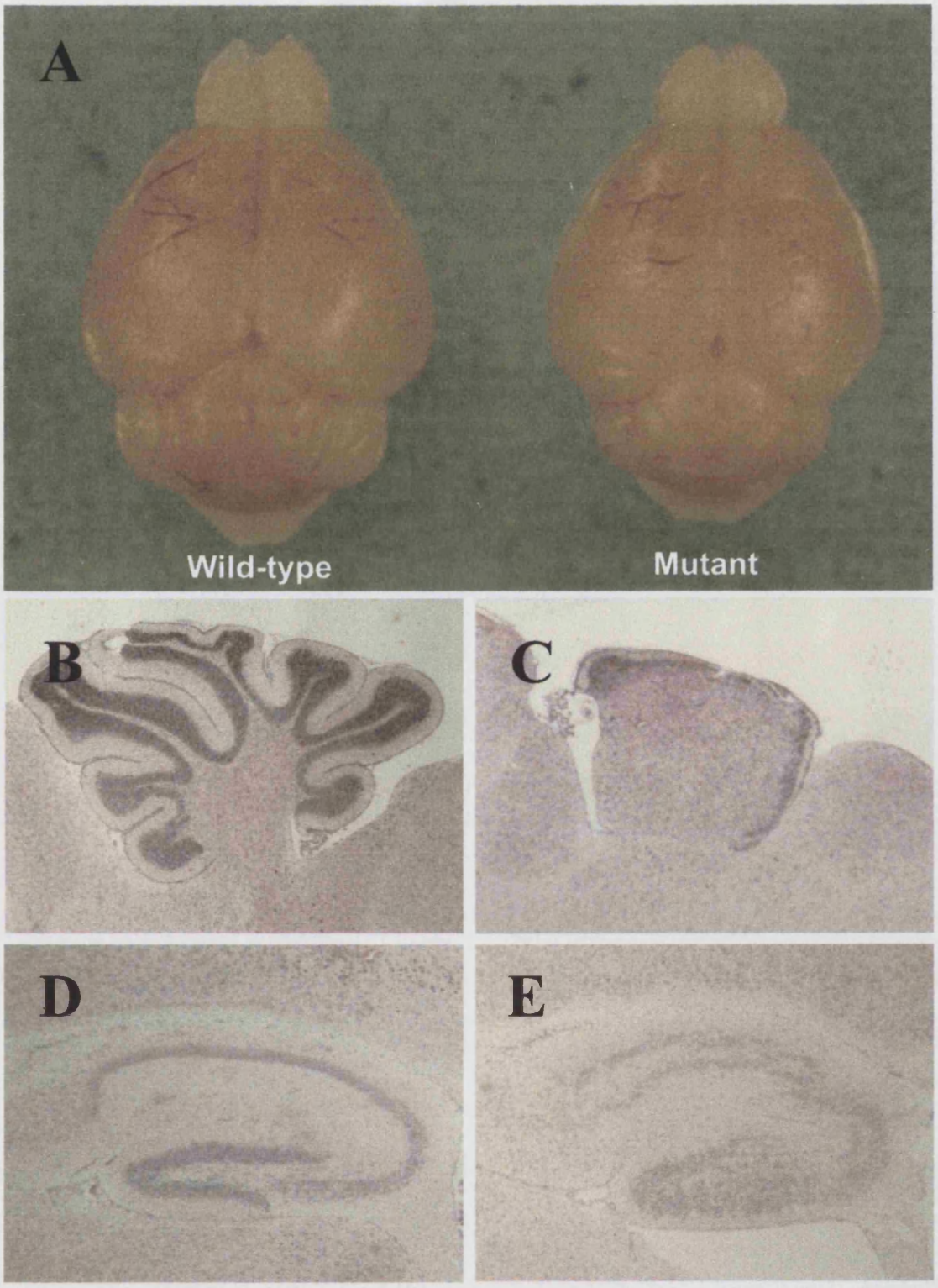

Fig. 4.9. Ann vs wild-type brains.
Analysis of brains from 21 day old wild-type and Ann mutant littermates. A) Comparison of whole brains reveals a marked reduction in the size of the mutant cerebellum. These differences are even more apparent in Haematoxylin and eosin stained 7μm transverse sections taken from the midline of B) wild-type and C) mutant cerebella. Comparison of Haematoxylin and eosin stained 7μm transverse sections taken from D) wild-type and E) mutant hippocampi.

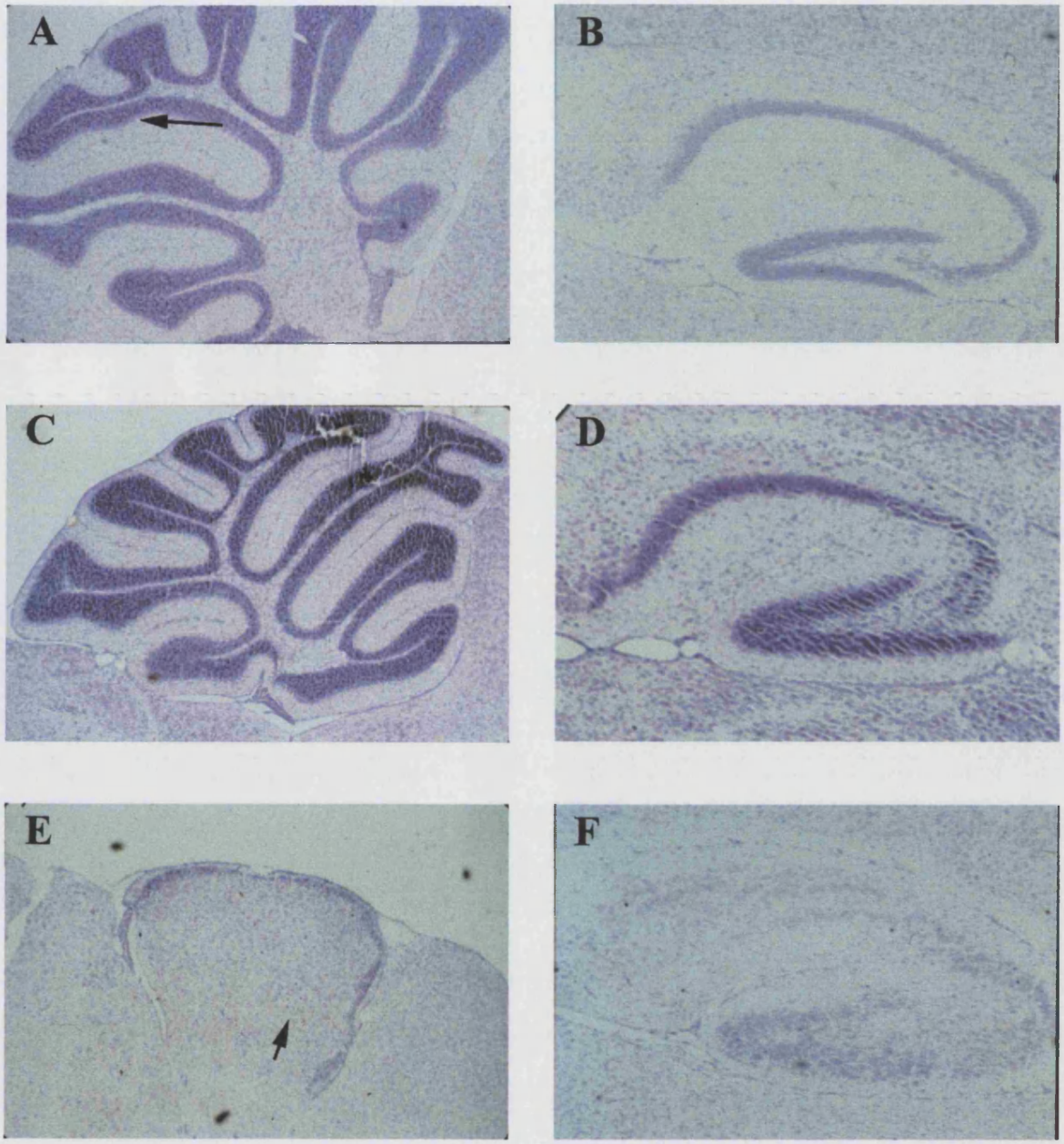

Fig. 4.10. Ann vs wild-type cerebellum/hippocampus.
Comparison of cerebella and hippocampi of wild-type (A and B), hemizygous transgenic (C and D) and homozygous mutant (E and F) littermates. Cresyl violet staining was performed on 7μm thick sections taken from the midline of 21 day old mouse brains. The arrow in A) denotes the single cell thick Purkinje cell layer whilst the arrow in E) denotes ectopic clustering of Purkinje cells beneath the granule cell layer.

Abnormalities in the neuronal organisation of the hippocampus were also discovered. In the wild-type hippocampus the pyramidal neurons of the CA1 and CA3 regions, as well as the dentate gyrus, are arranged in clearly distinguishable, discrete rows. The mutant hippocampus lacks this organisation, with the pyramidal cells of these regions being almost randomly dispersed (see Fig. 4.8. and Fig. 4.10). Furthermore, the granule cells of the mutant Dentate Gyrus are also found to be scattered almost randomly.

4.3.6 Histological analysis of Ann spinal motor neurons

From an examination of transverse sections, it was apparent that the spinal cord as a whole exhibited no obvious differences to that of wild-type controls. Since this region has been implicated in a number of mouse mutants bearing phenotypic similarities to Ann, it was decided to examine the spinal motor neurons of mutants more closely. At higher magnification, individual motor neurons could be observed. Upon comparison with wild-type samples, no obvious abnormalities in the general morphology of these cells were discernable with both wild-type and mutant neurons exhibited the same general size, shape and staining intensities (see Fig. 4.11).

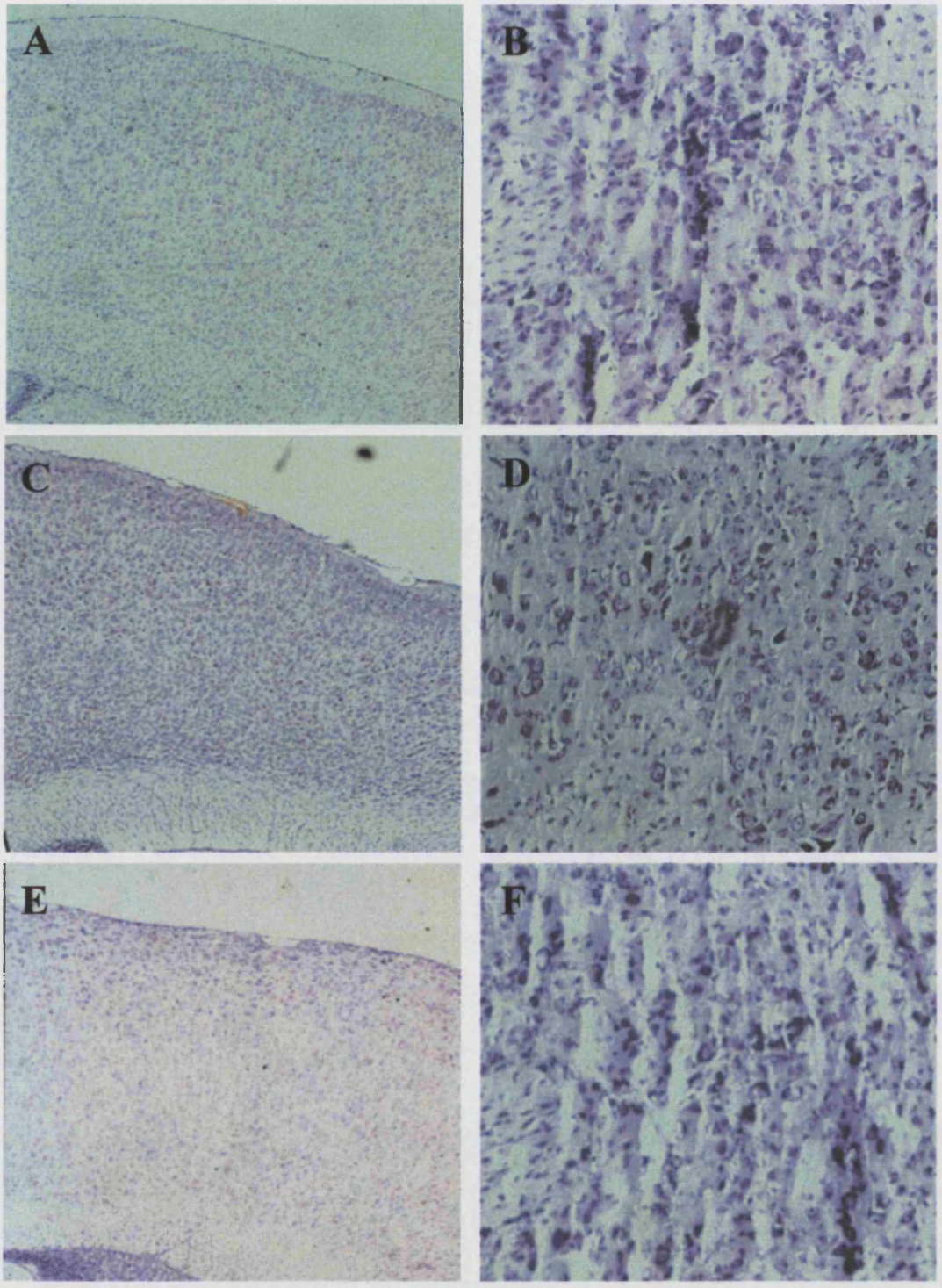

Fig. 4.11. Ann vs wild-type cerebral cortex/spinal motor neurons.
Comparison of cerebral cortex and spinal motor neurons of wild-type (A and B), hemizygous transgenic (C and D) and homozygous mutant (E and F) littermates. Cresyl violet staining was performed on 7μm thick sections taken from either the midline of the brain (A, C, E) or C2-C3 region of the spinal cord (B, D, F).

4.4 Discussion

4.4.1 Ann mutants do not have a myopathic disorder

Although differences are apparent, Ann mutants do exhibit some notable similarities to a number of the muscular dystrophy mouse mutants. For example, the abnormal gait, reduced size and dorso-ventral curvature of the spine observed in the *mdx/utrn*$^{-/-}$ mouse are all features that are apparent in Ann mutants [98] [99].

To investigate the possibility of a myopathic disorder in Ann mutant mice, a variety of muscle types were examined histologically. As can be seen in figure 4.6, transverse sections of mutant *biceps femoris* and *triceps brachii* muscles exhibited no obvious differences to those of wild-type littermates. Both wild-type and mutant muscle fibres were regular in shape and size and their nuclei were located at the periphery of the cell. Certainly none of the characteristic features of dystrophic muscle i.e. variations in fibre size, centrally located nuclei, necrotic fibres and infiltration by mononuclear cells [174], were observed. The absence of pathological features in Ann mutant muscle sections indicates clearly that the Ann phenotype is not that of a muscular dystrophy disease.

Atrophy of muscle fibres is most often caused by the loss of motor innervation and is characterised by a reduction in size and an angular morphology of groups of adjacent muscle fibres (see Fig. 4.8[F]). No atrophic regions were observed in Ann muscle sections, suggesting that innervation of skeletal muscle is normal. We could therefore tentatively conclude that the defect in Ann mutants does not involve the basic motor unit, and that skeletal muscle, the neuromuscular junction, and lower

motor neurons are all functionally intact. As such it is improbable that the Ann mutant could serve as a model for the two commonest forms of motor neuron disease since lower motor neurons are affected in both ALS and SMA, and muscular atrophy is evident in both syndromes.

It should be stated that in a number of diseases affecting the lower motor neurons, denervation atrophy of skeletal muscles accompanies changes in these neurons. Such changes are absent though in diseases exclusively affecting the upper motor neurons. Thus the possibility that the Ann phenotype reflects an upper motor neuron defect or alternatively a myelination or ion channel disorder could not be negated at this stage. A study of neuronal morphology in the spinal cord revealed no gross abnormalities but more subtle changes (i.e. at the sub light microscopic level) may well have gone undetected.

4.4.2 Ann mutants display gross abnormalities of the cerebellum

The chance that a defect in some region of the CNS is responsible for the gross Ann phenotype necessitated an examination of the brain and spinal cord of mutants. A brief visual comparison of the brains of wild-type and mutant littermates immediately yielded insight into the possible cause of the Ann phenotype. Disregarding the overall size reduction of mutant brains, it was obvious that the cerebellum of mutants is disproportionately smaller than in wild-type mice. This size disparity was clearly visible in sagittal brain sections from 21 day old mice. The mutant cerebellum is severely hypoplastic, in addition the normal foliated structure of the cerebellar cortex is completely absent and the discrete cellular layers observed in the wild-type cerebellum are disrupted.

The cerebellar cortex normally consists of three discrete layers: the outer molecular layer (OML), the Purkinje cell layer (PCL) and the internal granular layer (IGL). An IGL is present in Ann mutant brains but numbers of granule cells appear to be greatly reduced in comparison to wild-type. A cell-free OML is still located at the outside of the cerebellum but the Purkinje cell layer, normally found beneath, is almost completely absent. On closer inspection, clusters of large, darkly staining cells, which are most probably ectopically located Purkinje cells, can be found in locations beneath the IGL.

Development of the cerebellum (reviewed in D'arcangelo and Curran, 1998 [175]) begins at embryonic day 11 in the mouse with tangential migration of granule cell precursors from the fourth ventricle to form the external germinal layer (EGL). Purkinje cell precursors are subsequently born at the ventricular surface and migrate outward along radial glial fibres, eventually forming the Purkinje cell layer just below the EGL. Granule cell precursors in the EGL then proliferate rapidly and, upon exit from the cell cycle, migrate inwards, again along radial fibres [176]. These cells cross the OML and PCL, to form the broad internal granule layer (see Fig. 4.2).

Although features of the Ann mutant cerebellum bear similarities with a number of the cerebellar mutants (discussed in the introduction to this chapter), the morphology observed is most highly reminiscent of that found in the *reeler* and *scrambler* classical mouse mutants (see Table 4.5.). *Reeler* and *scrambler* mutant cerebella are grossly abnormal, being much reduced in size and displaying an almost complete lack of foliation. As a result of a failure to migrate, the Purkinje cell layer is completely missing, with the majority of cells of this type found in deep clusters [170, 172].

Granule cells are much reduced in number and remain superficial to any Purkinje cells. The absence of Purkinje cells next to the EGL is thought to reduce the proliferation of granule cells, possibly due to the lack of a secreted mitogenic factor. In *rl* and *scm*, granule cells still migrate inward forming a much reduced granule cell layer and allowing the molecular layer to form. It is the paucity of granule cell numbers that results in the reduced size and lack of foliation of *rl/scm* cerebella.

The molecular basis of these mutants is known to lie in a common signalling pathway that is essential to normal Purkinje cell migration. The cloning of the gene mutated in *reeler* mice; *reelin*, was facilitated by generation of another *reeler* allele (rl^{ts}) by transgene insertional mutagenesis [177]. The *reelin* gene product is a large extracellular protein secreted by granule cells in the outer molecular layer (OML) and the EGL of the developing cerebellum (see Fig. 4.12.) [178]. Secreted reelin was proposed to facilitate normal migration of Purkinje cells from the ventricular zone to their normal positions beneath the OML [175]. When the reelin signal is abolished, such as in *rl* mice, Purkinje cells do not migrate correctly and remain in deep, subcortical locations [172]. The reduction in granule cell numbers is secondary to the abnormal migration of Purkinje cells. *Reeler* homozygotes display tremors and a severely ataxic gait from around 2 weeks of age [140]. Mutants are non-viable on inbred genetic backgrounds but may survive and breed on an outbred genetic background despite no apparent difference in cerebellar histopathology [179].

Abnormal expression of the *mouse disabled 1* (*mdab1*) gene is responsible for *scm* [166, 180]. *mdab1* is an intracellular tyrosine kinase signalling adaptor molecule which functions downstream of reelin in the same pathway.

High levels of mDab1 protein are expressed by the Purkinje cell precursors that migrate from the fourth ventricle to positions directly beneath the EGL (see Fig. 4.12) [166, 169, 171]. Interaction of reelin with these Purkinje cell precursors is essential for their appropriate migration. The reelin signalling pathway is therefore required for the formation of the Purkinje cell layer. Exactly how reelin signalling achieves this outcome remains the subject of much speculation [181].

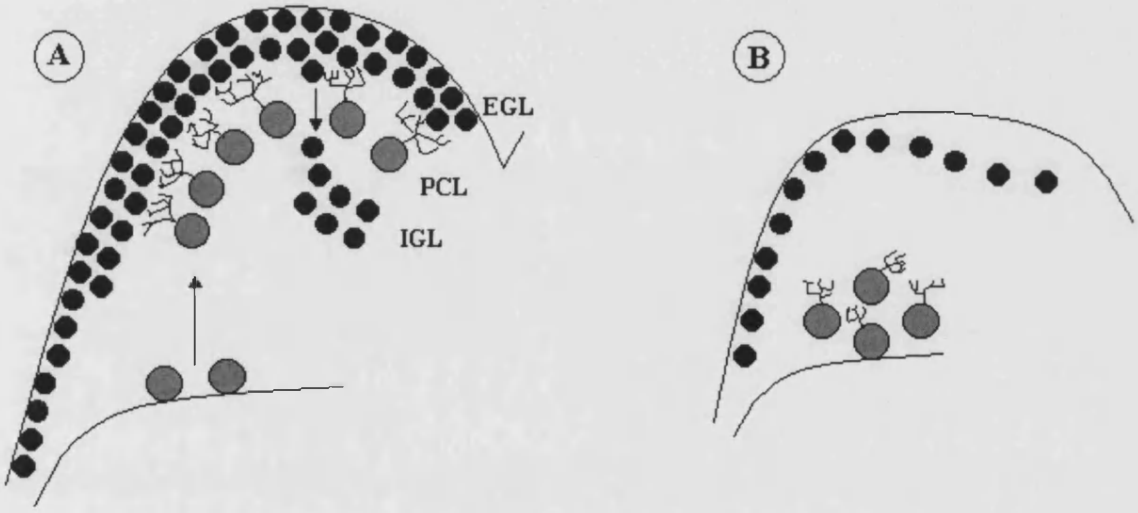

Fig. 4.12. Development of the cerebellum in wild-type and *rl/scm* mice.
Cerebellar development in wild-type (A) and *rl/scm* mutants (B). Beginning at around embryonic day 11, granule cells (represented by filled circles) migrate outwards from the fourth ventricle to form the EGL. Migration of mDab1 expressing Purkinje cells (shown as shaded circles with dendritic projections) to form the PCL (beside the Reelin expressing EGL) is followed by inward migration of granule cells to form the IGL (postnatal days 0 to 14). In *rl/scm*, Purkinje cells do not migrate outwards and remain in deep sub-cortical locations with a resulting reduction in granule cell numbers. The cerebellum is therefore much smaller than normal as well as being structurally disorganised (figure adapted from D'Arcangelo and Curran, 1998 [175]).

The almost identical morphological defects of the Ann and *rl/scm* cerebella suggests that the mutation in Ann may affect some component of the reelin signalling pathway. Alternatively the molecule disrupted in Ann may function independently of this pathway to influence Purkinje cell migration. Only the identification of the molecule disrupted in Ann will resolve these possibilities.

It seems reasonable to assume that the Ann ataxic phenotype could originate solely from the cerebellar abnormalities observed since in a number of mouse mutants displaying highly similar phenotypes only the cerebellum is affected (see Table 4.5.). As such, the Ann line could serve as a useful model of cerebellar ataxia in humans. How does Ann compare with these diseases? The human hereditary ataxias result from degeneration of the cerebellum and its efferent and afferent connections. Both autosomal dominant and autosomal recessive diseases are known and both types are often associated with trinucleotide repeat expansion at a specific locus.

Friedreich's ataxia (FA) is the most common form of autosomal recessive ataxia. Caused by trinucleotide repeat expansion of the Frataxin gene [182], this disease is characterised by progressive ataxia from puberty and can be associated with cardiomyopathy. Neuropathologically, the cerebellar cortex is generally unaffected and degeneration of the spinocerebellar, posterior column and pyramidal tracts of the spinal cord are the predominant features [183].

Classification of the autosomal dominant ataxias on a neuropathological basis is complicated by extensive heterogeneity. As a result these diseases,

including olivopontocerebellar atrophy (OPCA), familial cortical cerebellar atrophy (FCCA) and Machado Joseph disease (MJD) have been reclassified as the spinocerebellar ataxias numbers 1 to 7 (SCA1 – SCA7), according to the genetic loci involved [184].

Olivopontocerebellar atrophy results from trinucleotide repeat expansion of either the ataxin 1 (SCA1) [185] or ataxin 2 (SCA2) [186] genes. Neuropathologically, OPCA exhibits severe atrophy of the cerebellum and basis pontis [183]. Cerebellar abnormalities are characterised by a loss of Purkinje cells and a reduction in the thickness of the molecular layer. Both the foliation and laminar structure of the cerebellum appear intact.

Machado Joseph disease (SCA3) is caused again by trinucleotide repeat expansion, this time in the ataxin 3 gene [185, 187]. In this form of hereditary ataxia the overall size of the cerebellum is reduced but the cerebellar cortex remains intact. Degeneration of the dentate nucleus and the dorsal columns of the spinal cord are responsible for the SCA3 phenotype [183].

Finally, familial cortical cerebellar atrophy (SCA6) is also caused by an expansion of trinucleotide repeats, except that in this case a voltage gated Ca^{2+} channel gene, CACNA1A, is involved [124]. Purkinje cells in the cerebellum are reduced in number and have an abnormal morphology. As in OPCA, both the foliation and laminar structure of the cerebellum appear intact [183]. As mentioned previously, the *tottering and leaner* mice, in which the *cacna1a* gene is mutated [130], represents a model for SCA6 and also presents a highly similar phenotype to that of the Ann mutant (see Table 4.3).

4.4.3 The cerebral cortex of Ann mutants shows histopathological defects

Histological examination of the cerebral cortex in Ann mutants revealed a disruption to the normal laminar arrangement of this structure. The cerebral cortex is normally arranged in six well-defined layers based on the differing amounts of large pyramidal, small pyramidal and nonpyramidal cells in that region. Pyramidal cells are responsible for the transmission of efferent output from the cortex, whereas non-pyramidal cells primarily receive afferent inputs. The cortical layers are numbered sequentially from the surface next to the pia mater to the underlying white matter. Layer I is composed largely of axons and contains few cell bodies. Layers II, III, V and VI contain mostly pyramidal cells which provide the output from the cortex. Layer IV consists primarily of non-pyramidal cells and receives afferent input from the thalamus.

The increase in cell density of the region just beneath the pial surface provides the most obvious indication of the defects in the laminar structure of the mutant cerebral cortex. As a result, a clearly defined layer I is absent in the cerebral cortex of mutants. Rather than consisting of obvious layers in which one cell type predominates, in the remainder of the mutant cerebral cortex large pyramidal cells are scattered throughout and lamination is virtually undetectable. This is identical to the situation in the cerebral cortex of *rl* [188] and *scm [169, 189]* mutants in which a defect in neuronal migration during cerebral development results in an absence of lamination.

In the first stage of cortical development a pre-plate (also known as the primordial plexiform layer (PPL)), containing Cajal-Retzius and subplate neurons, forms just below the pial surface (see Fig. 4.13). Development

proceeds with a series of neuronal migrations in which neurons at the ventricular zone stop dividing and migrate outwards along radial glial fibres [190]. These neurons must invade the preplate to reach their final destination where they displace subplate neurons and form the cortical plate (CP). Each neuronal migration goes beyond those that have previously taken place, in a classic 'inside-out' pattern. Therefore, cortical plate neurons which are 'born' (i.e. stop dividing and begin migrating) later, will end up in a more superficial location than those 'born' earlier. This generates the laminar structure of the mature cortex that consists of six discrete neuronal layers in which the cortical plate neurons (layers II - VI) lie between the Cajal-Retzius containing marginal zone (MZ), and the subplate (SP) [190].

In *rl* and *scm* mutant mice, migrating cortical plate neurons fail to invade the preplate, which itself forms normally [169, 188, 189]. Additional migrating neurons are unable to bypass their predecessors and thus accumulate under the pre-plate in a disorganised fashion. As a result, the laminar structure of the normal cortex never forms (see Fig. 4.13). Furthermore, the failure of the preplate to split into the marginal zone and the subplate results in Cajal-Retzius and subplate cells remaining superficial to the cortical plate in a structure known as the superplate (SPP) [181].

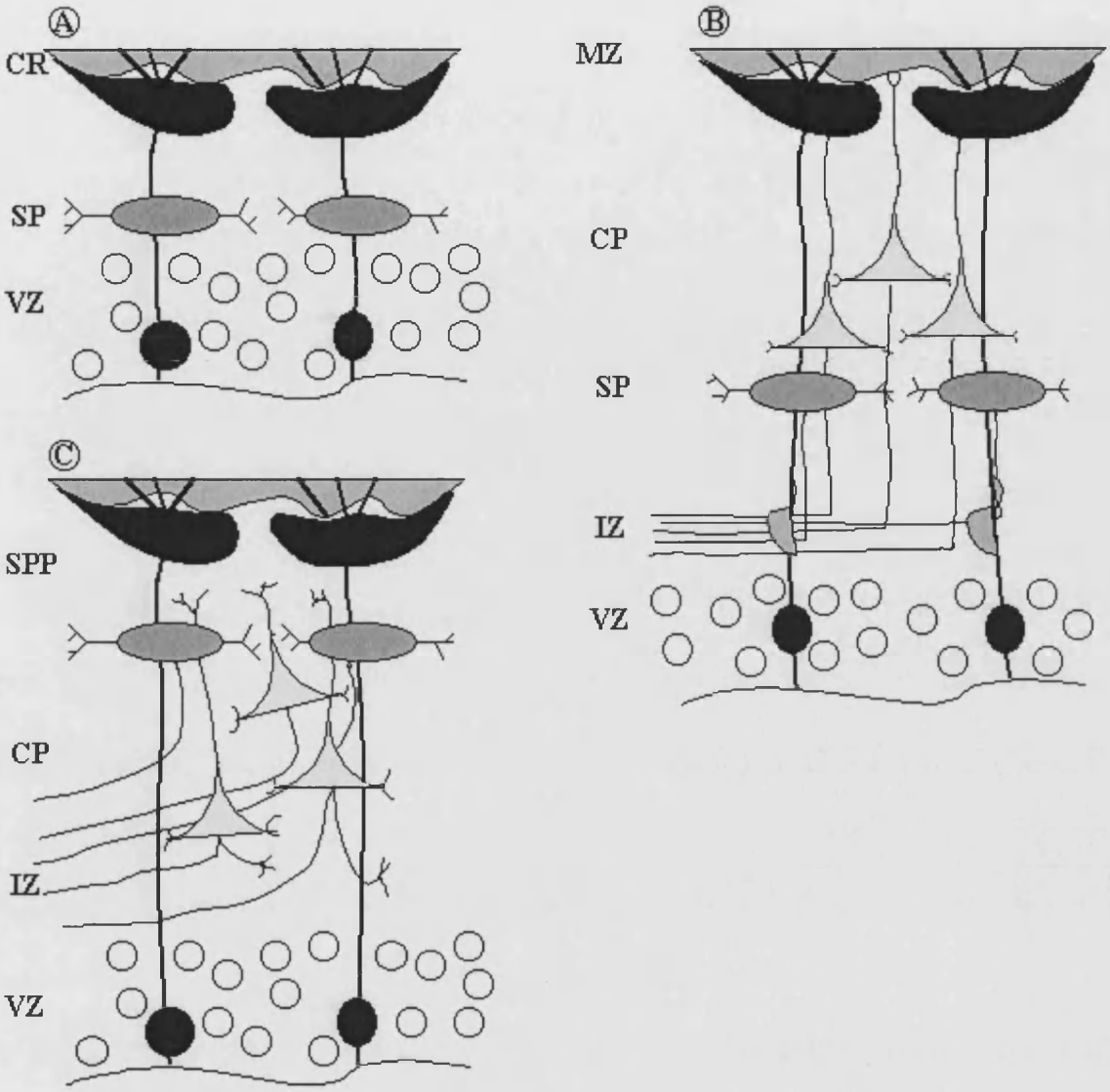

Fig. 4.13. Development of the cerebral cortex in wild-type and rl/scm mice.

Development of the cerebral cortex in wild type (A&B) and rl/scm mutants (A&C). The PPL, which contains reelin expressing Cajal-Retzius cells as well as subplate cells, is invaded by migrating neurons which express mdab1, splitting the PPL into the MZ and SP. These neurons travel from the fourth ventricle along radial glial fibres and stop migrating between the MZ and SP, forming the CP. The 'outside-in' pattern of neuronal migration generates the laminar structure of the cerebral cortex. In *rl/scm* mutants, migrating neurons fail to split the PPL resulting in a disorganised cortical plate located beneath the resulting SPP (figure adapted from Rice and Curran, 1999 [181])

During normal cortical development reelin is secreted by Cajal-Retzius neurons in the marginal zone [164, 178]. Migrating cortical plate neurons that bypass older cortical plate neurons and insert beneath the marginal zone express mDab1 [169]. As in the developing cerebellum, reelin secreting cells are closely apposed to cells expressing mDab1, indicating that reelin signalling is important for appropriate neuronal migration. The exact role of reelin signalling in this process remains undefined. One possibility is that the reelin signal facilitates the penetration of the preplate by migrating cortical plate neurons, possibly through the modification of cell-cell interactions [191]. Another possibility is that reelin binding to cortical neurons could generate a signal for these cells to stop migrating, this however would not explain the failure of migrating cortical plate neurons to penetrate the preplate. Finally, reelin signalling could affect neuronal migration by modifying the interaction between migrating cortical plate neurons and radial glial fibres.

Essentially identical changes in the development of both the cerebellar cortex and the cerebral cortex in Ann mutant and *rl/scm* mice provides strong evidence that the basis of the Ann phenotype rests with a defect in *reelin* signalling. Again, without having isolated the molecular basis of the Ann mutation one cannot progress beyond mere speculation as to the likelihood of this. Furthermore, it is not inconceivable that a molecule functioning outwith this signalling pathway could be involved in neuronal migration during the development of both the cerebellum and the cerebral cortex and that a defect in this molecule could result in a phenotype that is difficult to distinguish from that of *rl/scm* mice.

The contribution of these cerebral defects to the overall Ann phenotype is difficult to discern since the cerebral cortex is involved in a variety of higher brain functions. These include somatic sensation, learning and memory as well as the control of movement [92]. The defects observed in the cerebellum could alone account for the Ann phenotype although it is possible that abnormal functioning of the motor cortex could in some way contribute to the movement disorder observed in mutants. Sensory defects resulting from abnormalities in the sensory cortex cannot be ruled out although touch, hearing and vision appear to function normally, as determined by admittedly rudimentary tests, in Ann mutants. In order to ascertain if mutant mice exhibit defects in learning and memory it would have been necessary to carry out a variety of behavioural tests. Considering the extreme locomotor disorder and short life span of mutants it is doubtful whether such tests would have provided any meaningful indication as to the presence of learning and memory defects in mutant mice.

Several human neuronal migration disorders exist in which the abnormal development of the cerebral cortex resembles that seen in the Ann mutant. Lissencephaly (meaning smooth brain) is a condition in which deficient neuronal migration results in either the absence of (agyria) or reduction in (pachygyria) of the surface convolutions, or gyri, of the cerebral hemispheres [192]. Additionally, the cortex is disorganised and lacks normal lamination. Lissencephaly results in profound mental retardation, intractable seizures, feeding problems and a shortened life-span [193]. Double cortex is a closely related abnormality in which defective neuronal migration results in the formation of an abnormal heterotopic band of neurons in the white matter, underlying what appears a normal cortex.

The clinical manifestations of such an abnormality include epilepsy and mental retardation [194].

That cases of an X-linked form of lissencephaly and double cortex have been found within the same pedigree, suggested that some forms of these diseases could have a common, X-linked, genetic basis [195]. This was confirmed with the isolation of the *doublecortin* gene on the human X-chromosome [196]. The function of doublecortin is unknown but the protein does contain potential phosphorylation sites for a variety of kinases including the Abl tyrosine kinase [196]. This is interesting given that the mDab1 protein is known to interact with Abl during neuronal development in the mouse brain [197] (see section 6.4.2), suggesting a possible interaction between the mDab1/reelin signalling pathway and doublecortin.

An autosomal gene involved in lissencephaly has also been isolated. The *Lis1* gene is located on chromosome 17 and encodes the platelet activating factor acetylhydrolase β1 subunit (PAFAH1B) [198, 199]. This protein contains eight WD40 subunits that have homology to β-subunits of heterotetrameric G-proteins. The fact that non-receptor tyrosine kinases, such as Abl, are known to phosphorylate the α-subunit of several such G-proteins, again presents a possible link between this protein and the mDab1/reelin pathway [200].

Mutations in mouse *Pafah1b* have been generated with graded reductions in gene activity resulting in neuronal migration defects [201]. Furthermore, strong similarities in the overall lissencephaly phenotype of patients with X-linked lissencephaly and those in which the *LIS1* gene is mutated

suggests that doublecortin and Pafah1b may be involved in a common pathway controlling neuronal migration [202]. The possible involvement of such a pathway with mDab1/reelin signalling must be resolved.

To date no human mutations in mDab or reelin have been identified. This coupled with the fact that Ann mutants exhibit none of the seizures associated with lissencephaly suggests that the Ann mouse may be of limited use as a possible model for human syndromes involving defective neuronal migration in the developing cerebral cortex.

4.4.4 Histopathology of the Ann Hippocampus suggests learning and memory defects

Given the identical pathologies of Ann and *rl/scm* cerebellar and cerebral cortices an investigation into the possibility of additional similarities was deemed appropriate. A further region of the brain that is severely affected in *rl/scm* mice is the hippocampus [189, 203, 204].

The hippocampus is a component of the limbic system and is involved in learning and memory functions. Like both the cerebellum and cerebral cortex, the hippocampus has a laminar organisation [175]. Development of one such laminar region in the hippocampus, the stratum pyramidale (SP), is reminiscent of that of the cerebral cortex, with hippocampal pyramidal cells migrating along radial fibres in an 'inside-out' manner forming a compact layer. Conversely, during the development of the compact layers of the dentate gyrus (DG), granule cells migrate in an 'outside in' fashion (see Fig. 4.14) [175].

It is interesting to note the presence of reelin expressing Cajal-Retzius like cells in the outer marginal layer (OML) that separates the stratum pyramidale from the dentate gyrus [175, 205]. These cells are known to be important for correct neuronal migration during SP and DG development. Unsurprisingly, pyramidal cells express mDab1 as they migrate in the direction of the OML [169]. This is also true of migrating granule cells that express mDab1 as they themselves move toward reelin expressing cells.

In *rl/scm* mutant mice, rather than forming a discrete structure, the pyramidal neurons of the stratum pyramidale are split into two layers [165, 189]. Similarly, the granule cells of the dentate gyrus are scattered randomly rather than being tightly packed as normal. Considering the respective expression patterns of rln and mDab1, abnormalities in neuronal migration, akin to the situation in both the cerebellar and cerebral cortices, provides the likely explanation for such defects.

Given the role of the hippocampus, there is a strong possibility that the hippocampal pathology observed affects learning and memory functions in Ann mice. Again it would have been necessary to carry out a variety of behavioural tests in order to confirm this.

4.4.5 Ann mutants display no abnormalities of spinal motor neurons

It is reasonable to propose that an ion-channel or myelination defect could affect both the brain and the motor neurons. Furthermore, the phenotypes of several ion-channelopathy and myelinopathy mouse mutants, as well as those described as motor neuron disease mutants, bear a striking resemblance to Ann in a number of ways (see Table 4.2.). With this in mind, a superficial histological investigation of spinal motor neurons in the Ann

mutants was conducted in order to determine if any gross morphological abnormalities were apparent.

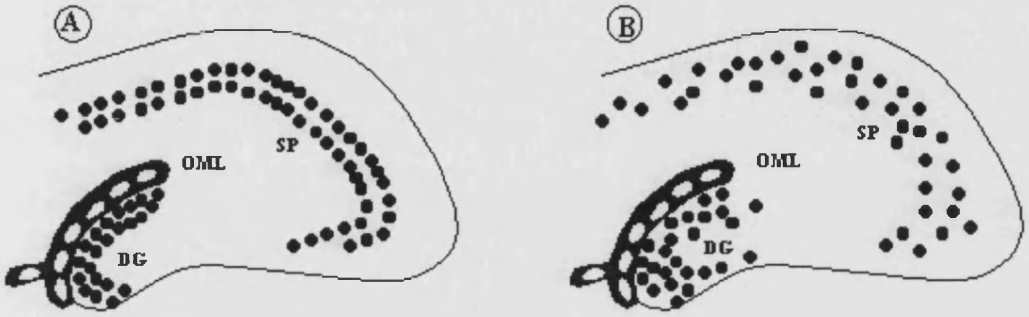

Fig. 4.14. Development of the hippocampus in wild-type and *rl/scm* mice.
Development of the hippocampus in (A) wild-type and (B) *rl/scm* mutants. The SP forms by migration of mDab1 expressing, hippocampal pyramidal cells in an 'inside-out' fashion, whilst the DG forms by 'outside-in' migration of mDab1 expressing, granule cells. The OML contains reelin-secreting, Cajal-Retzius-like cells. In *rl/scm* mutants, migrating neurons do not form compact layers and cells of both the SP and DG become scattered. (Figure adapted from D'Arcangelo and Curran, 1998 [175])

Comparison with sections from age-matched control mice revealed no obvious morphological differences in spinal motor neurons in the ventral horns of the mutant spinal cord. Although only superficial in nature, these observations are suggestive that the Ann phenotype is derived solely from the brain defects identified. In order to state conclusively that mutant spinal motor neurons are morphologically normal an ultrastructural examination of these cells would be necessary. Furthermore it would also be desirable to investigate the neurons of the peripheral nervous system to eliminate their involvement.

CHAPTER 5: MAPPING THE SITE OF TRANSGENE INTEGRATION

5.1 Introduction

5.1.1 the need for a map position

In the modern era of molecular genetics the ability to define the position of a locus on a genetic map of one form or another provides an invaluable tool for use in both biological and medical research. Gene mapping can be utilised to advance from a genetic disease to the molecular cloning of the disease-causing gene. Conversely, mapping can be used to associate a genetic disease with a DNA clone of unknown function. With the human and mouse genome sequences soon to be realised, a high-resolution map position will potentially enable testing of all putative genes within the vicinity of a mutant lesion such as a transgene insertion. By providing a molecular handle on a genetic disease, gene mapping can contribute to the diagnosis, understanding and eventual treatment of the disease.

5.1.2 Linkage mapping

Genetic maps exist in a number of forms dependant upon the type of information contained within. Linkage mapping is a direct descendant of the classical genetics performed by Mendel and involves the analysis of transmission of genotypes and phenotypes from parents to offspring. Genes that are linked will only be separated by recombination during meiosis. Roughly speaking, recombination occurs at random sites and it thus follows that the farther apart two linked genes are from each other the more likely they are to be separated by meiotic recombination. A relative value of genetic distance can therefore be provided by the frequency of recombination between two loci. Genetic distance is measured in centimorgans (cM), with 1cM equalling a recombination frequency between two loci of 1%.

Studying the segregation of gametes in mice requires the experimental breeding of animals that are genetically or molecularly defined at the loci of interest, and the analysis of offspring generated by such crosses. Additionally, linkage mapping can only be performed on loci that are polymorphic, with two or more alleles. Originally genes were mapped by following the segregation of mutations that generated an easily identifiable phenotypic change e.g. coat colour mutations. This meant that only genes *per se*, and not other non-phenotype determining genomic regions could be mapped. This situation changed with the dawn of the recombinant DNA era, which allowed the identification of polymorphisms at the nucleotide level. Now nucleic acid variations, from RFLPs (restriction fragment length polymorphisms) to SNPs (single nucleotide polymorphisms) are amongst the polymorphic markers whose segregation can be followed and can thus be linkage mapped. Of the wide variety of polymorphic genomic elements that have been identified and used in linkage mapping, the most useful to date has undoubtedly been the simple sequence length polymorphism (SSLP), or microsatellite. These can be either mono-, di-, tri, or tetrameric sequences repeated (several times) in tandem [206].

Any linkage mapping exercise requires the use of a panel of samples in which the segregation of the locus of interest can be followed. If this locus is defined only as a phenotypic mutation then the generation of such a panel will require the breeding of animals in which this phenotype can be tracked prior to DNA preparation for marker typing. Two breeding strategies can be utilised in order to generate such a panel and the use of either requires the existence of at least two alleles at the locus of interest and the ability to distinguish these alleles.

The first stage of the outcross-backcross mapping protocol is the generation of an F1 heterozygote. This is achieved by the so-called 'outcross' in which one animal, homozygous for the wild-type allele of the gene of interest, is crossed with another animal, homozygous for the mutant allele. Animals of the F1 generation, which will all be heterozygous, are then bred against animals that are homozygous for the mutant allele, allowing the segregation of the wild-type allele to be followed easily in the N2 generation (see Fig. 5.1). The advantage of such a strategy is that the backcross stage generates animals of only two genotypes (+/m and m/m) in which recessive mutations can be differentiated phenotypically. The disadvantage is that since only one of the backcross parents is heterozygous, only meiotic recombination events in a single parent are informative.

The outcross-intercross strategy again involves an initial outcross step designed to generate F1 heterozygote animals. The subsequent breeding step in this case involves the crossing of these F1 animals against each other, thus creating an F2 generation with three possible genotypes (see Fig. 5.2.). This is the source of a major drawback in the use of such a strategy. When studying a recessive mutation it is impossible to distinguish +/+ from +/m animals by phenotype alone and as a result these animals cannot be included in segregation analysis, meaning only 25% of offspring will be scored. Unlike the outcross-backcross strategy, since both parents at the second breeding step are of the heterozygous F1 type, meiotic recombination events occurring in both will be informative.

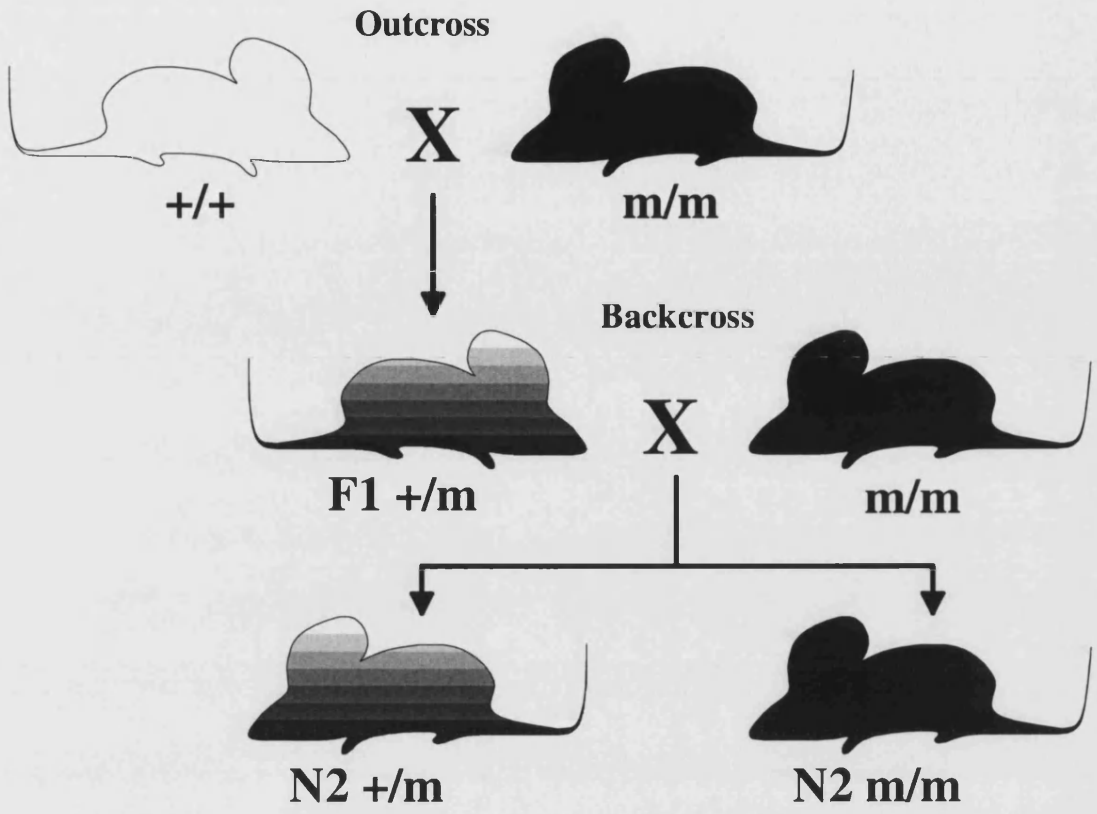

Fig. 5.1. The outcross-backcross mapping protocol.
+/+ animals (white) are homozygous for the wild-type allele at the locus of interest, m/m animals (black) are homozygous for the recessive mutant allele, which does not effect viability or fertility, at this locus and +/- animals (grey) are heterozygous. As a result of crossing F1 animals against animals of the m/m parental genotype N2 animals can be only one of two possible genotypes (+/m or m/m) which can be distinguished phenotypically. Figure adapted from [1].

The breeding strategy used to map a phenotypically defined mutation depends greatly upon the nature of the mutation being studied. For example, if the mutation is recessive and deleterious then the backcross strategy will be unsuitable because the second breeding stage involves the

crossing of an F1 heterozygote against a homozygous mutant. In this case it would be necessary to utilise the intercross breeding strategy. Given the fact that, unlike the intercross regime, all N2 progeny derived from a backcross are informative, for non-deleterious recessive phenotypes the backcross represents the method of choice.

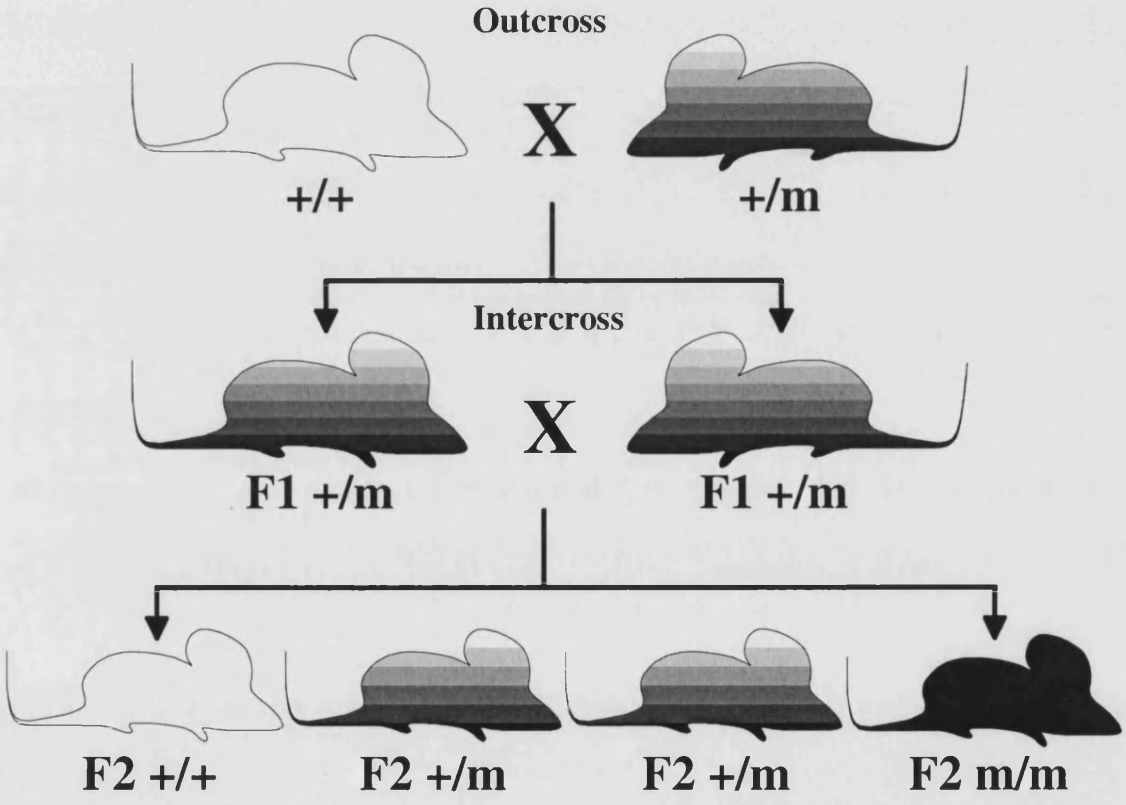

Fig. 5.2. The outcross-intercross mapping protocol.
+/+ animals (white) are homozygous for the wild-type allele at the locus of interest, m/m animals (black) are homozygous for the recessive mutant allele at this locus and +/- animals (grey) are heterozygous. In the F2 generation +/+ and +/m animals cannot be distinguished phenotypically thus allowing only m/m homozygous mutant animals to be used for linkage analysis. Figure adapted from [1].

If the locus of interest can be defined on purely a molecular basis, then the need for mouse breeding may be superfluous. In this case it is possible to carry out the mapping exercise using a pre-existing panel of DNA samples derived from a prior breeding exercise.

A wide variety of mapping panels exist and all have associated advantages. Before microsatellite markers were available, the mapping panel of choice was one of those derived from the offspring of an interspecific backcross between two species, *M. musculus* and *M. spretus* [207]. A greater degree of evolutionary divergence meant that a larger number of RFLPs (which were the most polymorphic markers known at this stage) existed between these two species than between the inbred strains of laboratory mouse. With the discovery of microsatellite markers, other mapping panel types have largely superseded interspecific mapping panels. The high degree of polymorphism between microsatellites within inbred strains of laboratory mouse has facilitated the use of panels based on intercrosses between F1 animals derived by outcrossing two different inbred strains [38]. Another resource which, despite having existed for a while, has found increased usage due to the discovery of microsatellites, is the recombinant inbred (RI) mouse strains. These are generated by an initial outcross between two inbred strains, followed by at least twenty generations of inbreeding [208]. Through the application of microsatellite markers it has been possible to utilise these strains in a large number of linkage mapping exercises [38].

5.1.3 Chromosomal mapping

Whilst linkage mapping involves the ordering of loci through recombinational distance, chromosome mapping is based around the assignment of a locus to a specific chromosome or chromosomal segment

that makes up part of the organisms karyotype. This is made possible by the fact that individual chromosomes can be defined cytogenetically according to their size and discrete banding properties when stained with agents such as Giemsa [209].

When a locus-specific nucleic acid probe is available, then *in-situ* hybridisation (ISH) is often the method of choice for defining its chromosomal location. Chromosome preparations on microscope slides can be denatured, allowing sequence-specific hybridisation of the labelled probe to its target [210, 211]. Initially probes were labelled with radioisotopes, facilitating visualisation of target-specific hybridisation through autoradiography. This methodology has been largely superseded by fluorescence *in situ* hybridisation (FISH) which uses probes labelled with fluorescent tags, providing greater resolution and ease of use [40].

The generation of somatic cell hybrid lines in culture provided a further means for assigning chromosomal locations to genes. These hybrid cells contain only a portion of a single mouse chromosome in combination with a complete human or hamster 'host' karyotype. Fully characterised panels of somatic cell hybrid lines, in which each line contains a different region of the mouse karyotype, can be used to assign chromosomal locations by correlating the presence or expression of a gene with a specific mouse chromosome or sub-chromosomal region [212].

Using somatic cell hybrids as starting material, radiation hybrid panels provide another gene mapping methodology that is as highly resolving as linkage mapping, without the requirement for mouse breeding [42]. Through X-ray irradiation of a somatic cell hybrid containing a single

chromosome, followed by fusion of this line with a suitable host (commonly a hamster cell line), approximately 100 new hybrid clones can be generated, each containing a fragment of the mouse chromosome from the original hybrid line. Relying on the premise that DNA markers located close together are less likely to be separated by chromosome fragmentation, analysis of radiation hybrid cells can be used to generate a highly resolving genetic map based on physical rather than recombinational distance.

5.1.4 Physical mapping

Physical mapping bridges the gap between the linkage or chromosomal assignment of a marker and its actual molecular constitution. This is achieved by assigning a genetic marker to a genomic clone or DNA sequence. A much higher degree of mapping resolution is therefore attainable through physical mapping than the other mapping methodologies already discussed. Indeed, the nucleotide sequence of a genomic region could be considered as the form of map that provides the highest level of mapping resolution achievable. Physical maps are more often found as a contiguous series of overlapping DNA clones, known as a contig. Each clone can contain inserts as large as several hundred kilobases owing to the YAC (yeast artificial chromosome) [43], and more recently, BAC (bacterial artificial chromosome) and PAC (P1 artificial chromosome) cloning vectors that are available [44].

Contigs can be generated by the end sequencing of individual clones and using the sequence generated to isolate overlapping clones from a genomic library [213-215]. By this means one can 'chromosome walk' from a clone identified as containing a marker of interest to further clones that may

contain the gene shown to be linked to that marker. In this way it is possible to progress from the linkage mapping of a disease to its molecular basis. A number of methodologies exist for the identification of a gene from a large DNA clone (YAC, BAC or PAC). These include exon trapping [47], identification of CpG islands [48] and cross-species hybridisation of sequences [216]. Although laborious, such positional cloning exercises have yielded valuable successes e.g. the cloning of the gene mutated in Duchene Muscular Dystrophy; *dystrophin* [217].

5.1.5 Strategies for mapping an inserted transgene

A variety of strategies can be employed in order to map a transgene inserted into the genome randomly at a single location. Having only the transgene itself as a probe prevents the use of existing mapping panels since they will not contain the inserted transgene. This problem can be circumvented if the transgene is used as a handle in the cloning of genomic sequence flanking the site of transgene insertion. This endogenous sequence can then be applied to a mapping panel in the usual manner and a map location derived. Such a methodology may however be complicated by the initial cloning of flanking sequence, which can be difficult owing to the often unpredictable nature of transgene insertion site (see Chapter 7).

Mapping by ISH or FISH obviates the need for a cloning exercise since the transgene itself can be used as a probe. The level of mapping resolution attainable through such methodologies is less than that from linkage mapping and generally one cannot proceed directly from an ISH or FISH location to a positional cloning exercise. Such an assignment can still prove useful by facilitating a search of existing mutants with similar phenotypes that have a similar chromosomal location. In this way possible alleles of a

transgene insertion mutant can often be identified. The recent development of novel *in-situ* protocols (e.g. fibre *FISH* [218]) does mean that much higher levels of mapping resolution can now be achieved.

A further strategy that does not necessitate the cloning of flanking genomic sequence is the generation of an intercross or backcross panel specific to the transgenic strain in question. This methodology does though involve the breeding of large numbers of animals, which can be both time-consuming and expensive, especially when full genome coverage is required.

5.1.6 Mapping the Ann transgene

In an effort to elucidate more about the molecular nature of the transgene insertional mutation in the Ann line it was decided to proceed with mapping of the transgene in this line.

Prior to commencing a mapping exercise it was deemed necessary to prove that the transgene and the mutant phenotype were associated allowing the inference to be made that the transgene insertion was causative of the phenotype.

Fluoresence *in situ* hybridisation of Ann metaphase chromosome spreads was used as a starting point in the mapping exercise since expertise in this technique was already available in the laboratory. This would allow a tentative chromosomal assignment that could then be confirmed with a small-scale linkage mapping exercise using microsatellite markers. At this stage possible candidate genes and mutation would become apparent and could be tested if possible. Further linkage mapping could also be carried

out if required in order to gain a more detailed map position for the site of transgene insertion.

5.2 Materials And Methods

5.2.1 Microsatellite primers

Using information from the mouse genome informatics (Jackson labs.) [219] and Whitehead Institute/MIT Centre for Genome Reasearch [79] databases, microsatellite primer pairs were selected based on a number of criteria. Primers were chosen for intercross mapping analysis based on their proximity to the site of transgene integration, such that the locations of the primers spanned the appropriate region as determined by FISH studies. Primers were selected from four candidate mouse chromosomes (Chromosomes 4, 6, 8 and 12) following FISH analysis (see section 5.3.2). For backcross mapping analysis, primers positioned at regular intervals flanking D4Mit155 were selected. As these studies progressed, further primers were selected according to their proximity to the putative location of the transgene insertion determined by this mapping analysis.

For all mapping studies the existence of size polymorphism between the C57BL/6J and CBA/Ca inbred mouse strains was essential. Unfortunately the mouse genome informatics (Jackson labs.) and Whitehead Institute/MIT Centre for Genome Reasearch databases contained no information on the CBA/Ca strain, thus primers were selected based on a comparison of C57BL/6J information with that of the C3H inbred mouse strain that is closely related to CBA/Ca. The actual existence of a size polymorphism between strains was then determined by testing inbred C57BL/6J and CBA/Ca samples by PCR and product visualisation (described below) for each set of primers purchased.

Chromosome	Marker	C57 size (bp)	C3H size (bp)	C57/CBA polymorphism?
4	D4Mit15	279	329	No
	D4mit155	205	189	Yes
6	D6Mit16	152	145	Yes
	D6Mit69	164	168	Yes
8	D8Mit73	172	166	Yes
	D8Mit74	126	120	Yes
12	D12Mit14	130	146	Yes
	D12Mit34	174	166	Yes
	D12Mit118	134	124	No

Table 5.1. Microsatellite primers selected for intercross mapping.

Using the criteria detailed, for intercross mapping nine suitable primer pairs were purchased (Research Genetics inc. see Table 5.1.). Based upon the results of intercross and backcross mapping analysis a further eleven (chromosome 4 specific) microsatellite primer pairs were purchased. Microsatellite PCR reactions were performed as detailed in section 2.2.16.

Marker	cM Position	C57 size (bp)	C3H size (bp)	C57/CBA polymorphism?
D4Mit153	45.50	122	112	No
D4Mit176	46.50	140	146	No
D4Mit155	49.60	205	189	Yes
D4Mit168	50.80	125	125	No
D4Mit331	50.80	124	118	Yes
D4Mit29	51.00	No info.	No info.	No
D4Mit31	51.30	122	112	Yes
D4Mit43	51.40	114	110	Yes
D4Mit332	53.60	138	152	Yes
D4Mit334	57.00	126	108	Yes
D4Mit203	60.00	144	124	Yes

Table 5.2. Microsatellite primers selected for backcross mapping.

5.2.2 Small scale polyacrylamide gel electrophoresis

Non-denaturing 8% polyacrylamide gels were made using the Mini-Protean II (Bio-rad) system according to the manufacturers instructions. Gels were run for 2-3 hours, according to expected product size, at 100V constant voltage with 1x TBE (made from 5x stock, 2.2M Tris base, 2.2M boric acid, 10mM EDTA pH8.0) in the upper buffer chamber and 0.5x TBE in the lower chamber. For the silver staining procedure used to visualise the PCR products (section 5.2.4), glass plates were carefully separated and the gel removed into a glass trough.

5.2.3 Large scale polyacrylamide gel electrophoresis

Glass sequencing plates were prepared by firstly cleaning with soap and water and then with xylene. The notched plate was then treated with a 1ml coating of repel-silane (Sigma) followed by wiping the surface of the plate with IMS. The flat plate was similarly treated with a coating of bind silane (3µl bind silane (Sigma), 1ml IMS, 0.5% glacial acetic acid) followed by IMS. The plates were assembled using sequencing tape (Gibco) with spacers between. 50ml of a 6% acrylamide-urea gel mix was prepared using 21g of urea, 5ml 10x TBE, 10ml 30% acrylamide:bis-acrylamide (19:1) and 20ml H_2O). The urea was dissolved under the hot tap and then allowed to cool to room temperature. Following the addition of 250µl of 10% Ammonium Persulphate (Sigma) and 25µl TEMED (Sigma) the mixture was mixed and quickly poured using a 50ml syringe. After allowing to set for at least 2 hours, the gel was inserted into the gel tank, both buffer chambers filled with 1x TBE and a 24 well shark-toothed comb inserted. The gel was then pre-run for at least 30 minutes with the power pack set at a constant power of 50 watts and constant temperature of 50°C. Following the addition of 3x STR formamide loading buffer (10mM NAOH, 95% formamide, 0.05% bromophenol blue, 0.05% xylene cyanol), 5µl of each PCR reaction was denatured at 95°C for 2 minutes prior to loading. Samples were run at a constant power of 50 watts and constant temperature of 50°C for at least 2 hours (depending on product size). Further samples could be loaded at 10-30 minute intervals (again dependant upon product size). After a suitable running time, gels were removed from the apparatus and glass plates prized apart using a razor blade. The gel was then subjected to the silver-staining procedure in a plastic trough whilst still attached to the flat sequencing plate.

5.2.4 Visualisation of PCR products by silver staining

After electrophoresis, gels were fixed in 40% methanol for at least 30 minutes. Two 10 minute washes in 10% IMS, were followed by 5 minutes in 1x silver stain oxidiser concentrate (Bio-rad). Gels were then washed, usually for 3x 5minutes in dH_2O, until the yellow colouration had been removed. Following a 20-minute wash in 0.1% $AgNO_3$ and a short rinse in dH_2O, gels bands were developed by washing in developing solution (2% Na_2CO_3/0.01% formaldehyde (both Sigma)). On appearance of a brown precipitate, developer was changed, until bands were clearly visible. Prior to analysis, gels were washed in dH_2O and in the case of the small gels, dried down under vacuum, on 3mm paper (Whatman).

5.2.5 Analysis of backcross mapping data

Data obtained from backcross linkage analysis was processed using the Gene-link program [220]. For both backcrosses performed, databases were created in which genotyping information for every animal tested could be entered. The program was then able to automatically order loci (this is done by maximum likelihood order analysis) and calculate linkage distances and the associated 95% confidence interval.

5.3 Results

5.3.1 The transgene and phenotype are linked

Prior to embarking upon a detailed study of a mutant phenotype caused by transgene insertion, it is essential to demonstrate that the transgene is indeed the causative agent of the mutation. With a lack of conclusive molecular evidence, statistical analysis was used to establish that the mutant phenotype resulted from transgene insertion. A null hypothesis was proposed that there was no linkage association between the transgene and the mutant phenotype i.e. that these two traits segregate independently from one another, and the transgene was assigned as a dominant trait (i.e. both hemizygotes and homozygotes are identifiable as transgenic) and the phenotype as recessive (i.e. only homozygotes are affected and identifiable) then, using Mendelian genetics, and if there is no linkage, the following was expected: 9/16 wild-type and transgenic; 3/16 Ann mutant and transgenic; 3/16 wild-type and non-transgenic and 1/16 Ann mutant and non-transgenic. The data for 16 Ann litters (129 pups) can be summarised in tabular form (see Table 5.3.).

	wild-type	**Ann mutant**
Transgenic	71 (72.6)	31 (24.2)
Non-transgenic	27 (24.2)	0 (14.3)

Table 5.3. Ann intercross breeding data
Expected and observed numbers from a total of 129 mice (16 litters). The values in the table are those observed and those in brackets are expected.

Using these values, a χ^2 test was performed using the following formula:

$$\chi^2 = \sum \frac{(O-E)^2}{E}$$

Where O is the observed value, E is the expected value and (O-E) is the absolute value of the difference between O and E.

$\chi^2 = 16.6$

- for 3 degree of freedom this gives $p<0.001$

As the probability of the null hypothesis being correct is <0.05 this hypothesis can be rejected and it can be stated that there is a statistically significant likelihood that the two traits, the transgene and the Ann mutant phenotype, are linked (there is a chance of less than 1 in 1,000 that this assumption is incorrect). This strongly suggests that the insertion of the transgene is responsible for the Ann mutant phenotype.

5.3.2 Mapping the site of transgene insertion by FISH and G-banding

Having confirmed that the Ann phenotype and the inserted transgene were linked, it was decided to initiate studies to obtain a map position for the transgene to facilitate a search for possible candidate genes or provide a starting point for the cloning of the gene responsible for the Ann phenotype.

That the transgene itself was the only probe available at this stage limited the strategies that could be employed in mapping the site of transgene insertion. Chromosomal mapping by FISH, using the transgene as a probe, would provide a useful handle on the map position of insertion site and

allow the identification of possible candidate genes. FISH was therefore selected as the method of choice for initial mapping studies. A methodology was employed whereby hybridisation of a biotinylated transgene probe to Ann metaphase chromosome spreads could be visualised using anti-biotin fluorescent antibodies. Prior G-banding of these spreads with Giemsa dye facilitated the identification of the transgene-specific chromosome by comparison with existing mouse karyotypes.

Metaphase Ann chromosome spreads subjected to FISH and G-banding are shown in Fig. 5.3. These images show that the integrated transgene (identifiable by red spots in the FISH images) has an approximate mid to distal location on a medium to large sized chromosome. Comparison with existing mouse G-banded karyotypes provides further insight as to the possible identity of the transgene-specific chromosome (see Fig. 5.4.). Due to their acrocentric nature and, in many cases, similar banding patterns, it can be difficult to make a chromosome assignment unequivocally through G-banding. Chromosomes 4, 6, 8 and 12 were suggested as strong candidates owing to their size and banding patterns. Of these, Chromosome 4 was suggested as the most likely candidate by a mouse karyotyping expert (M. Lee personal communication).

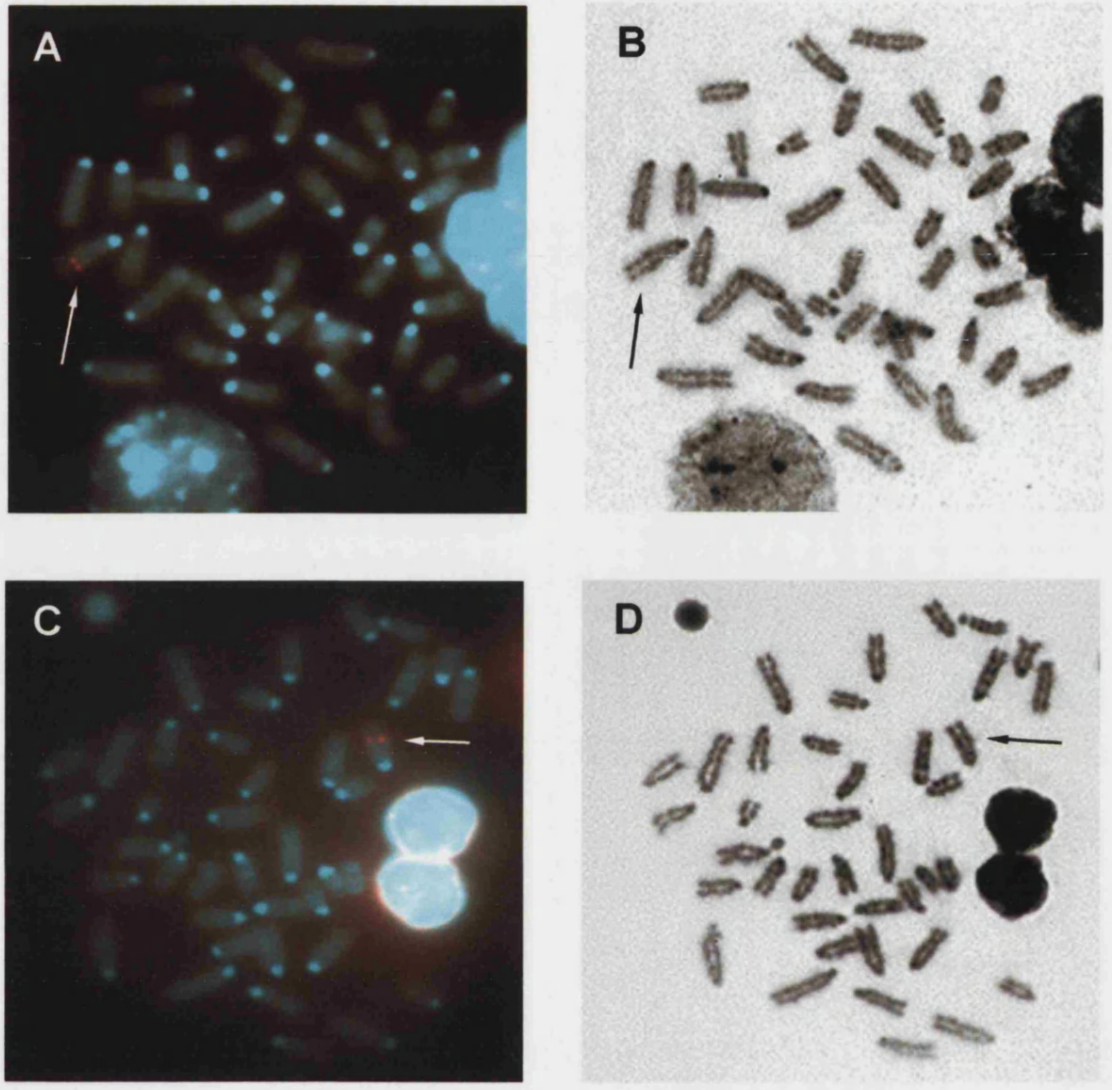

Fig. 5.3. Ann FISH and G-banding.

Chromosomal mapping of the transgene insertion by FISH and G-banding of Ann metaphase chromosome spreads. Fluorescence *in situ* hybridisation of Ann metaphase chromosome spreads using a transgene specific probe fragment, (A) and (C). The site of transgene insertion is identified by a fluorescent spot on sister chromatids of the same chromosome (indicated by arrow). G-banding of the same spreads is shown in (B) and (D), again the site of transgene insertion is indicated.

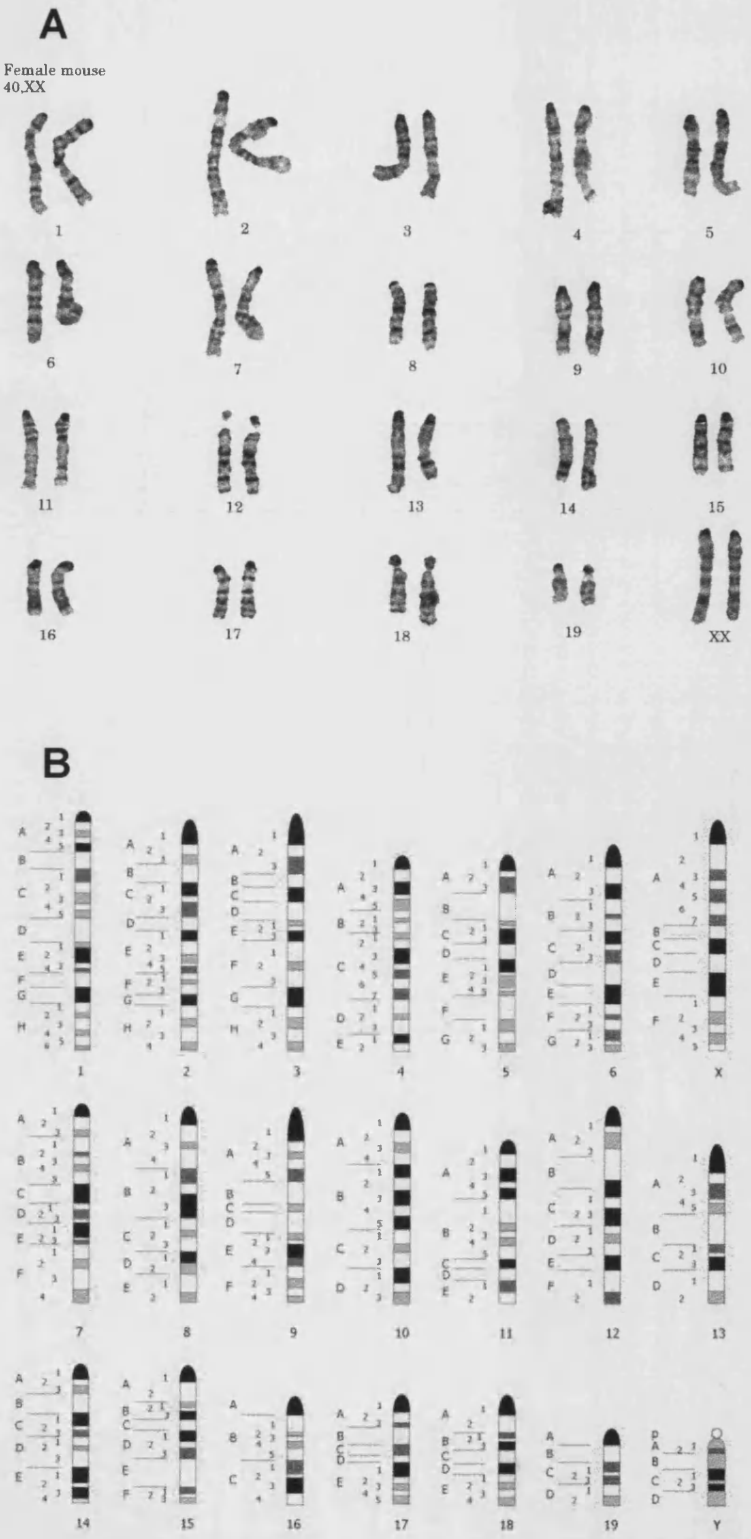

Fig. 5.4. Standard mouse karyotypes.

These were used for comparison with Ann G-banding results. G-banded mouse chromosomes (A) and an iodiogram illustrating G-banding patterns (B) were used to narrow down the chromosome of interest to one of four possibilities (Chromsome 4, 6, 8 or 12). Karyotypes obtained from the University of Washington, School of Pathology web site.

5.3.3 Confirming the chromosomal location by small-scale intercross mapping

FISH and G-banding analysis on metaphase chromosome spreads from Ann hemizygous mice had suggested that chromosome 4, 6, 8 or 12 might harbour the transgene array. It was decided to utilise microsatellite markers in a linkage mapping exercise in order to confirm/eliminate these possibilities.

Transgenic founders had been generated using F1 embryos derived from crossing C57BL/6J and CBA/Ca mice. Interbreeding of subsequent generations meant that all available transgenic mice had genetic backgrounds of a mixed C57 and CBA constitution. To be informative for possible intercross mapping analysis, it was essential for breeding mice to have suitable haplotypes for the microsatellite markers being tested. In order to identify suitable breeding mice, haplotype analysis of selected microsatellite markers from the four candidate chromosomes was initiated. Two male and two female mice of breeding age were tested for microsatellite markers on chromosome 6 (D6Mit16), 8 (D8Mit73) and 12 (D12Mit34) (see Table 5.4.). According to the fragments amplified, mice were typed as being of C57 type, CBA type or F1 type (both C57-specific and CBA-specific fragments).

Based on the FISH and G-banding data generated, microsatellite markers were likely to be positioned close to the inserted transgene array. Thus, excepting the possibility of recombination events, one would expect a marker from the correct chromosome to segregate with the transgene. Since the embryos used to generate founder transgenic mice were of F1(C57BL/6J, CBA/Ca) it was reasonable to suggest that the transgene was integrated on either a C57 or CBA chromosome. Therefore typing of a

5.3.3 Confirming the chromosomal location by small-scale intercross mapping

FISH and G-banding analysis on metaphase chromosome spreads from Ann hemizygous mice had suggested that Chromosome 4, 6, 8 or 12 might harbour the transgene array. It was decided to utilise microsatellite markers in a linkage mapping exercise in order to confirm/eliminate these possibilities.

Transgenic founders had been generated using F1 embryos derived from crossing C57BL6/J and CBA/Ca mice. Interbreeding of subsequent generations meant that all available transgenic mice had genetic backgrounds of a mixed C57 and CBA constitution. To be informative for possible intercross mapping analysis, it was essential for breeding mice to have suitable haplotypes for the microsatellite markers being tested. In order to identify suitable breeding mice, haplotype analysis of selected microsatellite markers from the four candidate chromosomes was initiated. Two male and two female mice of breeding age were tested for microsatellite markers on Chromosome 6 (D6Mit16), 8 (D8Mit73) and 12 (D12Mit34) (see Table 5.4.). According to the fragments amplified, mice were typed as being of C57 type, CBA type or F1 type (both C57-specific and CBA-specific fragments).

Based on the FISH and G-banding data generated, microsatellite markers were likely to be positioned close to the inserted transgene array. Thus, excepting the possibility of recombination events, one would expect a marker from the correct chromosome to segregate with the transgene. Since the embryos used to generate founder transgenic mice were of F1(C57BL6/J, CBA/Ca) it was reasonable to suggest that the transgene was integrated on either a C57 or CBA chromosome. Therefore typing of a

marker linked to the transgene should generate an F1 pattern for hemizygous transgenic mice and C57 or CBA specific patterns for non-transgenic wild-type or homozygous-transgenic mutant mice, dependant upon into which chromosome the transgene has integrated.

	3♂	7♀	6♂	9♀
D6Mit16	CBA	C57	CBA	CBA
D6Mit69	CBA	CBA	CBA	CBA
D8Mit73	F1	C57	F1	C57
D8Mit74	F1	C57	C57	C57
D12Mit14	CBA	CBA	CBA	CBA
D12Mit34	CBA	CBA	CBA	CBA

Table 5.4. Microsatellite typing of breeding animals.
Genotyping of breeding animals using microsatellite markers specific to chromosomes 6, 8 and 12.

The results of markers for chromosomes 6 and 8 shown in Table 5.4. yield immediate insight into the possible identity of the transgene-specific chromosome. Since the mice typed were all hemizygous transgenic, and none of the markers analysed displayed an F1 banding pattern for every mouse, it seems unlikely that any of these microsatellite markers are linked to the transgene array. The possibility of recombination events distorting segregation patterns in such numbers seems unlikely given the expected proximity between the markers selected and the transgene (based upon the relative position of the transgene along the chromosome as determined by FISH).

To strengthen these suggestions it was decided to cross the mice that had been tested and type the offspring with microsatellites in order to investigate possible correlations between transgene and microsatellite segregation. The results confirm that the segregation of markers D6Mit16 and D8Mit73 bears no relationship with that of the transgene, allowing Chromosomes 6 and 8 to be eliminated from further investigation (see table 5.5.)

Both Chromosome 12 markers yielded the same banding pattern (CBA/Ca) for all four breeding mice, meaning that testing of intercross litters with these markers would be uninformative. To overcome this, mouse 3♂ was mated with a C57BL6/J inbred female, producing offspring that were all confirmed as being of the F1 type for the D12Mit14 and D12Mit 34 microsatellite markers. Two sibling breeding pairs were set up from this outcross. Mice selected for breeding were also found to carry the F1 haplotype for the more recently obtained Chromosome 4 marker D4Mit155.

Intercross litters were generated and typed, firstly with D4Mit155. Typing of the first two litters (15 mice) with this marker revealed a definite trend suggesting its co-segregation with the transgene. Typing of four further intercross litters was used to test wether the transgene and marker D4Mit155 were indeed linked. Again, χ^2 analysis was performed using the results shown in Table 5.6. A probability of >0.0001 was calculated for the null hypothesis, that the two loci were unlinked, being correct. This was done using the special χ^2 equation for intercrossing outlined in the book *Mouse Genetics* [1]. Given this result, further testing of the Chromosome 12 markers (D12Mit14 and D12Mit34), was deemed to be unnecessary.

	Parents		Litter								
Mouse no.	3♂	7♀	1♂	2♂	3♂	4♂	5♂	6♂	7♂	8♀	9♀
Transgene	T/wt	T/wt	T/wt	wt/wt	T/wt	T/T	T/wt	T/T	T/wt	wt/wt	wt/wt
D6Mit16	CBA	C57	F1	F1	F1	F1	F1	F1	F1	F1	F1
D8Mit73	F1	C57	C57	C57	C57	F1	C57	C57	F1	C57	C57

	Parents		Litter							
Mouse no.	6♂	9♀	1♂	2♀	3♀	4♀	5♀	6♀	7♀	8♀
Transgene	T/wt	T/wt	T/wt	wt/wt	T/T	T/T	wt/T	wt/T	wt/T	wt/T
D6Mit16	CBA	CBA	CBA	CBA	CBA	CBA	CBA	CBA	CBA	CBA
D8Mit73	F1	C57	F1	C57	F1	F1	F1	F1	C57	C57

Table 5.5. Genotyping of parents and offspring for two microsatellite markers.
Genotyping of parents and offspring for two microsatellite markers (D6Mit16 and D8Mit73) reveals no correlation with the segregation of the transgene, allowing elimination of Chromosomes 6 and 8 as possible candidates.

Transgene status	No. offspring	D4Mit155		
		C57	F1	CBA
wt/wt	21	21	0	0
T/wt	23	1	21	1
T/T	6	0	0	6

Table 5.6. Small scale intercross analysis.
Small scale intercross analysis shows possible co-segregation of the transgene and the Chromosome 4 microsatellite marker D4Mit155.

5.3.4 Fine mapping using a backcross strategy

Having obtained a chromosomal assignment and a tentative map position through a small scale intercross study, it became possible to search the Mouse Genome Database for possible candidate genes and mutations located around the same region of mouse chromosome 4. Three good candidate genes were identified in this way allowing molecular studies on these genes to be initiated (see Chapter 6).

It was decided that the pursuit of a more exact map position would provide a stronger indication as to likely candidate genes located in this region. To do this a backcross mapping strategy was employed whereby four breeding harems were set up, each containing a single hemizygous transgenic male (confirmed as being of the F1 haplotype for the microsatellite marker D4Mit155) and four C57BL/6J inbred females. This was thought to be the best way to generate a useful amount of data in as short a period as possible. Each F2 pup born (representative of a single meiotic event) was typed with a number of microsatellite markers located near to D4Mit155, as well as being tested for transgenicity by luciferase assay. Large numbers of animals could be quickly typed by running up to 96 microsatellite PCR reactions on a single polyacrylamide gel (a typical example is shown in Fig. 5.5). All breeding males were tested for each new marker used to confirm an F1 haplotype. As the analysis progressed and preliminary mapping data was generated further microsatellite markers were obtained for use in the study.

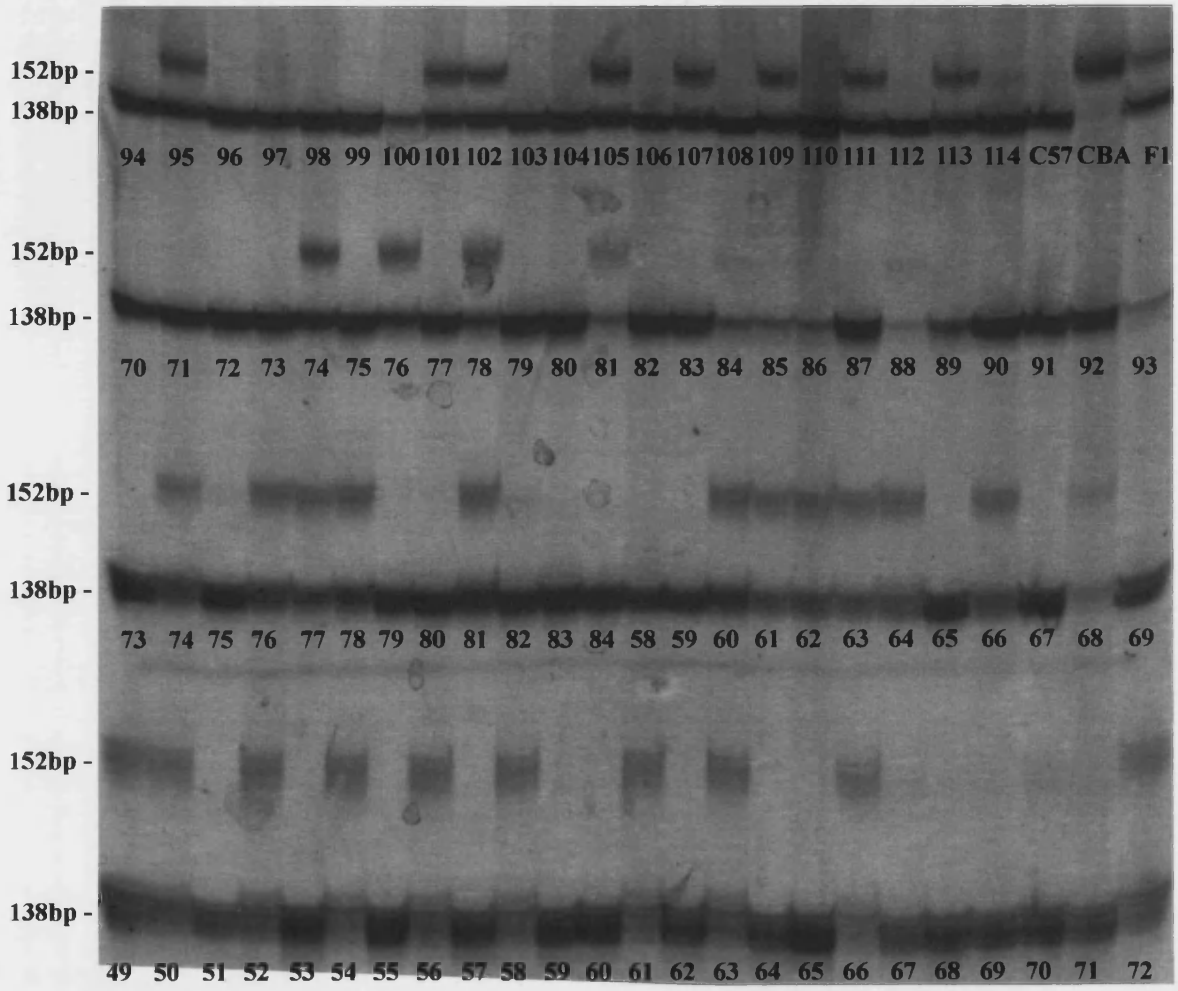

Fig. 5.5. Microsatellite marker typing of backcross DNA samples.
A typical example of a large-scale polyacrylamide gel following electrophoresis of microsatellite PCR products (in this case D4Mit332 which gives a C57-specific product of 138bp and a CBA-specific product of 152 base pairs) and visualisation of products by silver staining. By having multiple loadings a large number of samples can be tested on a single gel (in this case 96: backcross samples 49-84 from one cross and 58–114 from another as well as C57, CBA and F1 controls).

Similar to the situation described in section 5.3.3, segregation of a linked microsatellite marker with the transgene in these crosses would be expected to result in non-transgenic offspring of the C57BL/6J haplotype for this marker, whilst transgenic hemizygotes would be of the F1 haplotype. Any deviations must result from a meiotic recombination event taking place between the marker and the transgene in the paternal gametes.

Data was entered into a Gene-link 2.0 database that had been set up for this study. The haplotypes of each of the 237 F2 offspring for 7 microsatellite markers is shown in Fig. 5.6. (it should be noted that the markers D4Mit31 and D4Mit43 gave identical results). Using this data, the Gene-link software was able to order the microsatellite markers in relation to each other and the transgene array. In addition, this program calculated linkage distances between markers, including 95% confidence intervals (see Fig. 5.7.). This data shows that the transgene is positioned between the markers D4Mit155 and D4Mit331. Further typing using Mit microsatellite markers located between D4Mit155 and D4Mit331 was prevented due to the absence of C57/CBA size polymorphism for all markers located in this region.

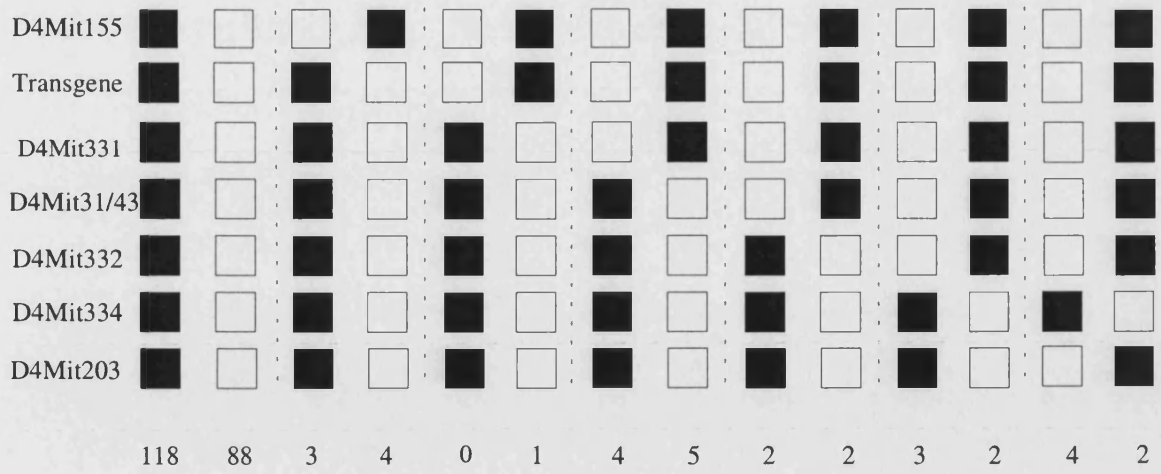

Fig. 5.6. Backcross linkage mapping haplotype diagram.
Backcross linkage mapping of the transgene against a number of chromosome 4 microsatellite markers. The backcross involved the breeding of hemizygous transgenic male mice of the C57/CBA background at each of the markers with C57 females. The results of the 237 informative meioses analysed are shown for each marker, black squares represent a CBA genotype whilst white squares represent a C57 genotype.

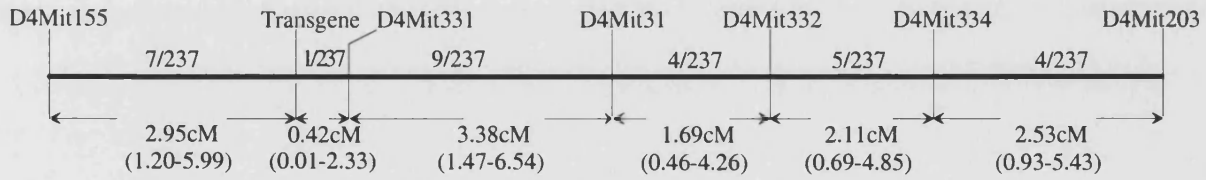

Fig. 5.7. A genetic map of the region surrounding the transgene insertion.
Numbers of recombinants beween the markers analysed are detailed. Using the information shown in Fig. 5.6. markers were ordered and map distances (in cM) with corresponding 95% confidence intervals (shown in brackets) calculated using the Genelink 2.0 program.

5.3.5 Differences from published recombination frequencies are strain specific

Comparison of the mapping data generated from our backcross analysis and the Chromosome 4 consensus map revealed marked differences in the linkage distances between markers located around the transgene integration site (see Fig. 5.8.). Linkage distances derived from the backcross analysis are much elevated between the markers D4Mit155 and D4Mit331 and between D4Mit331 and D4Mit31, as compared to the consensus map.

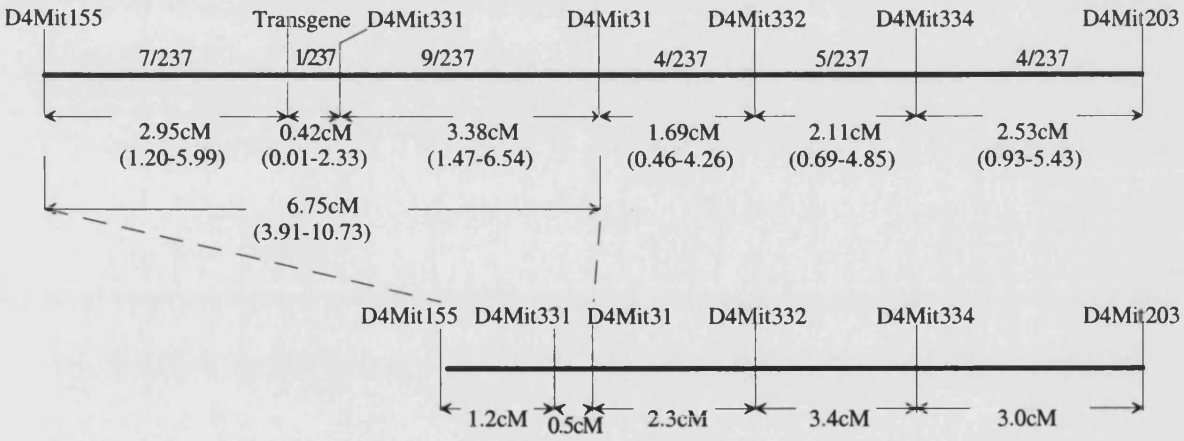

Fig. 5.8. Comparison of Ann and Chromosome 4 linkage maps.
Comparison of the linkage map constructed using the 237 meiosis backcross analysis (above, as Fig. 5.7.) with the Chromosome 4 committee consensus map (below). Striking differences in map distances are apparent between the markers D4Mit155, D4Mit331 and D4Mit 31.

To investigate the possibility that the transgene array was interfering with recombination in the surrounding genomic region, a backcross was set up between wild-type F1(C57/CBA) males and C57 inbred females. This cross mimics that used in previous backcross study except for the absence of the transgene in the breeding males. A total of sixty-seven F2 pups were genotyped for the transgene and the microsatellite markers D4Mit155, D4Mit331 and D4Mit31. The haplotypes of these pups are shown in Fig. 5.9.

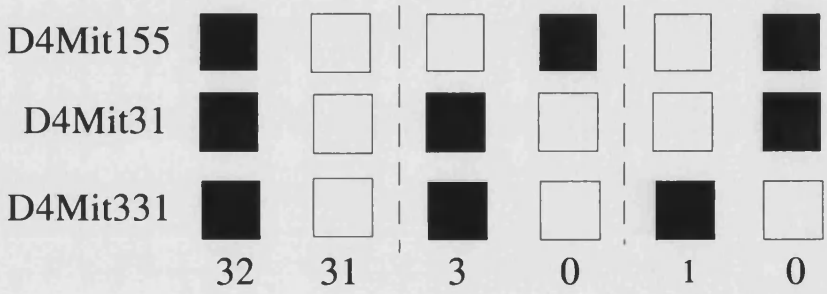

Fig. 5.9. Test backcross results.
Results of a test backcross between F1(C57/CBA) male and C57 females. Offspring were typed using the chromosome 4 microsatellite markers D4Mit155, D4Mit31 and D4Mit331. The results of the 65 informative meioses analysed are shown for each marker, black squares represent a CBA genotype whilst white squares represent a C57 genotype.

Again, this data was entered into a Gene-link 2.0 database and linkage distances calculated. Comparison of linkage distances derived from both backcross experiments suggests that the transgene insertion has no significant effects upon recombination levels in the surrounding genomic

region (see Fig. 5.10). Instead, differences observed in comparison with the Chromosome 4 committee consensus map are likely to be strain-specific.

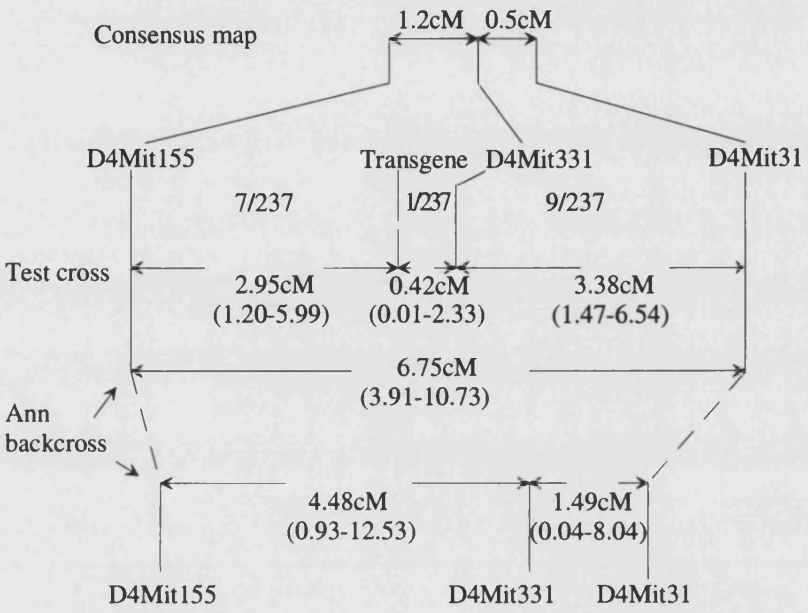

Fig. 5.10. Comparison of Ann and test backcross linkage maps.

Comparison of the linkage map constructed using the 65 meiosis test backcross (middle) with that for the 237 meosis Ann backcross (below). Map distances between microsatellite markers are comparable with 95% confidence intervals (shown in brackets) clearly overlapping. The Chromosome 4 consensus map distances between the same markers are shown (above) for comparison.

5.4 Discussion

5.4.1 The transgene maps close to the *scrambler* mutation on mouse chromosome 4

Through a combination of *FISH* and linkage mapping analysis the site of transgene integration was located on Chromosome 4 between the closely spaced microsatellite markers D4Mit155 and D4Mit331. Examination of the Chromosome 4 committee consensus map reveals a number of genes and mutations known to map near to these microsatellite markers. Of these, one mutation that is located on the consensus map in a very similar position to the transgene (i.e. between D4Mit 155 and D4Mit331) is the *scrambler* (*scm*) classical mouse mutation[221] (see Fig. 5.11), which is described in detail in Chapter 6.

Two previous linkage-mapping studies have been conducted on *scm*. The first culminated in an intraspecific intercross (between strains of a mixed DC/Le, C3HeB/FeJ background and BALB/cByJ) from which 118 meiotic events were typed for three Chromosome 4 microsatellite markers including D4Mit176. No recombinants were observed between this particular marker and the *scm* mutation [221]. The second study was conducted on a larger mapping panel comprising 492 meiotic events (between the C57BL/KsJ-$m^{+/+}$db and MA/MyJ strains) [180]. In this case the samples were ultimately typed for a number of microsatellite markers situated between D4Mit176 and D4Mit31. No recombination was observed in this case between *scm* and the D4Mit29 microsatellite, which lies close to D4Mit331. The occurrence of a single recombination event between the transgene and the closest microsatellite marker typed, D4Mit331, in the Ann backcross panel, may be attributable to strain specific differences in

recombination between the Ann C57/CBA background and those detailed above.

The map positions of the *scrambler* mutation derived from both studies are found to be consistent when the 95% confidence intervals for these map positions are considered. This is also the case when considering the map position of the Ann transgene insertion (as derived from our study) compared to the map positions of the *scrambler* mutation (derived from the studies mentioned).

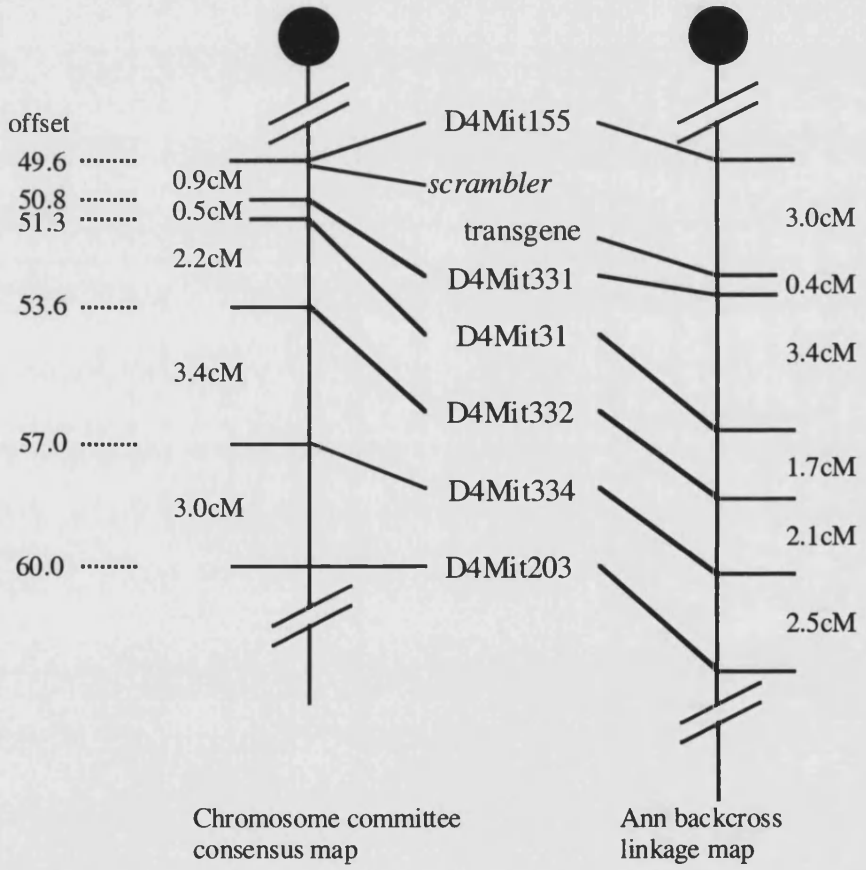

Fig. 5.11. Comparing the map positions of the scm locus and the transgene.
Comparison of the chromosome 4 committee consensus map and the Ann linkage map derived from a 237 meoisis backcross analysis. The transgene is located between the microsatellite markers D4Mit155 and D4Mit331 (as shown in the Ann linkage map) as is the *scrambler* mutation (at offset 49.7, as shown in the consensus map).

The gene mutated in *scrambler* was identified as the mouse *disabled* homologue, *mdab1*. In a separate study the chromosomal location of *mdab1* was mapped on mouse Chromosome 4 at offset 52.7 [197]. This map position differs somewhat from those of the *scm* mutation. In this case a Jax (Jackson Labs.) interspecific backcross-mapping panel (C57BL/6J x *Mus spretus*) F1 x C57BL/6J)was analysed using a small number of markers.

These discrepancies highlight the difficulties encountered when comparing linkage maps compiled from separate studies. The validity of such comparisons depends largely on the number of meiotic events analysed (which dictates the confidence intervals for mapping distances) and the markers used. To gauge the map distance between two markers using information from separate studies, the presence of a marker common to both studies is imperative. This allows a valid comparison of map positions to be made. From our study it is also clear that strain-specific recombination differences influence map distances derived from different studies (see section 5.4.3).

Bearing in mind possible differences in map locations it appeared pragmatic to examine the various linkage maps for other possible candidate genes located in the area of the transgene insertion on chromosome 4. Two other possible candidates were discovered, based upon a combination of their function and respective map positions. Both *Glyt1* and *faah* map in the vicinity of the transgene insertion [222, 223], are expressed in the brain [224-226] and are known to play important roles in the normal function of the nervous system [227, 228]. In addition the *clasper* mouse mutant also maps nearby and exhibits a phenotype that, although not identical to Ann, is similar [229]. Despite this, owing to its

map position and mutant phenotype (see chapter 4), *mdab1/scm* still represents the most attractive candidate. Efforts to confirm or eliminate *mdab1*, *Glyt1* and *faah* as candidate genes are presented in Chapter 6.

5.4.2 *mdab1* represents an attractive candidate for the Ann mutation

There are various reasons why the *scrambler* mutant represents an extremely promising candidate for the mutation in Ann. Firstly, as discussed, the map positions of both *scm* and the integrated transgene exhibit a strong correlation, more so than the other candidates mentioned (see Chapter 6, Fig 6.1.). Secondly, as outlined in Chapter 4, both the Ann and *scrambler* phenotypes show a marked resemblance in terms of clinical phenotype and brain histopathology. For these reasons, the molecular analysis of the *mdab1* gene in Ann mutants is of paramount importance.

5.4.3 Differences in recombination frequencies are strain specific and do not arise through chromosomal rearrangement

Comparison of the data generated from the Ann backcross mapping study with the Chromosome 4 committee consensus map reveals a disparity in the linkage distances separating three of the microsatellite markers flanking the integrated transgene in the Ann mouse

The map distance between markers D4Mit155 and D4Mit31, as presented in the consensus map (i.e. 1.7cM), falls beneath the 95% confidence interval for the distance between the same markers, as found in the Ann backcross mapping study (i.e. 6.75 (3.91 – 10.37))

Two explanations for this phenomenon seemed plausible. The first of these being that the presence of the integrated transgene array was somehow interfering with normal levels of recombination in this surrounding region.

Effects on genomic structure and chromatin stability around sites of transgene integration are well-documented (see Chapter 1) and alterations in map distances resulting form transgene-specific chromosomal changes have been seen. An increase in linkage distances between markers would though require the promotion of recombination events and no precedent for such a phenomenon exists. It is not though outwith the realms of possibility that the insertion of exogenous DNA at a site in the genome could somehow create a 'hot-spot' for recombination at that site.

Alternatively, differences in recombination frequency between inbred strains of laboratory mouse are also well known. Any discrepancies between our data and that used to generate the chromosome committee map could therefore rest with strain-specific differences in recombination for the mice used. Since the information used to generate the consensus map is derived from a variety of sources, including crosses involving different mouse strains, this seems a valid possibility.

The results of a test backcross involving identical strains to those used in the Ann backcross, except for the absence of the transgene, indicate that any differences from the consensus map are most probably due to strain-specific differences in recombination rates, and these are not significantly affected by the transgene insertion.

CHAPTER 6: IDENTIFYING THE MOLECULAR BASIS OF THE ANN PHENOTYPE

6.1 Introduction

6.1.1 The molecular basis of the Ann phenotype

In order to find a gene disrupted by transgene insertion it is invaluable to obtain genomic sequence flanking the transgene. The availability of such sequence allows the investigator to isolate nearby genes by providing a molecular probe for screening wild-type mouse genomic DNA libraries. A number of methods can then be employed to identify possible exons in the region, such as direct sequencing, zoo blots and exon trapping. Indeed such methodologies have been successfully applied to the cloning of novel genes mutated by transgene insertion including *legless* [230] and *limb deformity* [231].

Such a procedure would appear, in principle, to be straightforward but problems can arise for a number of reasons. For example, the cloning of genomic sequence can be complicated by the structure of the inserted transgene itself (see Chapter 7).

6.1.2 The candidate gene approach

When embarking upon such a study, possibility of allelism with an existing locus should be investigated. Such a statement becomes all the more pertinent when considering the number of insertional mutations that have been found to be allelic with existing genes or mutations.

In one previous systematic screen for visible insertional mutants in a large series of transgenic mice, amongst five lines identified as carrying visible mutations three were found to represent re-mutation of pre-existing classical loci [26]. Indeed these findings agree with the global figures for

visible insertional mutants for which just over 50% of mutants identified have been found to be allelic with existing mutations.

Obviously the efficiency in testing an insertional mutant for allelism with a candidate locus increases with the availability of good mapping data both for the candidate and for the transgene insertion. With reasonable mapping data in hand, and an ever expanding database of mouse mutant phenotypes and map positions, not to mention genomic DNA sequence, candidate loci can rapidly be tested for disruption in a new insertional mutant line.

The simplest way to perform such a test is by analysing expression of either the mRNA or protein of the candidate in homozygous mutant mice. Loss or reduction of expression of the candidate may well confirm this as the affected gene. Such results must be interpreted with caution. For example, reduction of gene expression in an anatomical structure could result as a consequence of loss of the structure concerned. In order to unequivocally test whether a mutation is allelic or not, a complementation test must be performed with an existing mutant. Unfortunately such tests can become cumbersome when mutant mice must be located and imported prior to breeding.

6.1.3 Finding and testing candidates for the Ann mutation

Successful FISH and intercross linkage mapping experiments confirmed that the transgene array in the Ann line had integrated in the mid-to-distal region of mouse chromosome 4 (see Chapter 5). Whilst fine backcross mapping of the transgene was in progress, it was decided to investigate the

possibility of candidate genes for the Ann mutation localising to this region.

Analysis of the chromosome committee map for mouse chromosome 4 in the area harbouring the transgene reveals the presence of a number of known genes and mutations that could be considered as candidates (see Fig. 6.1).

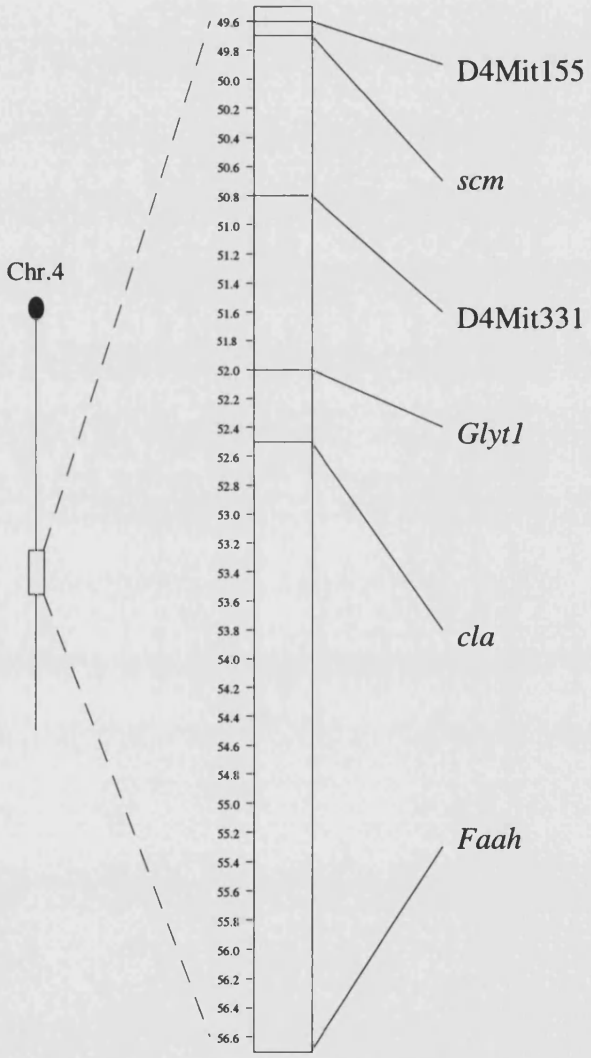

Fig. 6.1. Candidate genes on Chromosome 4.
Chromosome 4 linkage map showing Ann candidate genes located in the vicinity of the Ann transgene. The transgene was mapped between the microsatellite markers D4Mit155 and D4Mit331.

For each candidate gene (*mdab1*, *Faah* and *Glyt1*) a cDNA clone was obtained from which a probe fragment specific for the gene of interest could be derived. These probes were utilised in the investigation of both structural integrity and expression levels of the gene in wild-type, hemizygous transgenic and homozygous transgenic mice in order to elucidate any possible involvement in the Ann mutant phenotype.

6.1.4 The glycine transporter type 1 (*Glyt1*) gene as a candidate

The *glycine transporter type 1* gene, *Glyt1*, had previously been mapped to the central region of mouse chromosome 4 (chromosome committee map, offset 52.0, see Fig 6.1) [222]. Neurotransmitter transporters such as GlyT1 are essential for the re-uptake of neurotransmitters at the presynaptic membrane and on surrounding glial cells. Termination of synaptic transmission and the replenishment of transmitter pools in the presynaptic nerve terminal is dependent upon such re-uptake [228].

In keeping with such a role, the two isoforms of GlyT1 (GlyT1a and GlyT1b) have been shown to be expressed in the central nervous system of developing rat embryos, and in several regions of the adult rat and mouse CNS including the Purkinje cell layer of the cerebellum [224, 225]. *In situ* hybridisation studies on adult rat sections have shown this CNS specific expression to be of glial cell origin [232].

Glycine transporters work in tandem with glycine receptors. These receptors have been implicated in the pathogenesis of spacticity [233, 234] and the loss of motor control [235, 236] associated with the human diseases Amyotrophic Lateral Sclerosis and Parkinson's disease. The suggestion that perturbation of glycine signalling at the synaptic cleft could be

involved in such a diseases, coupled with an appropriate map location, presents the *Glyt1* gene as a good candidate for that disrupted in Ann mutant mice. As such, it was decided to look for any abnormalities in the expression of the *Glyt1* gene in Ann transgenic mice.

6.1.5 The fatty acid amide hydrolase (*Faah*) gene as a candidate

Another reasonable candidate for the Ann mutation is the *fatty-acid amide hydrolase* (*Faah*) gene. This had been mapped to the centro-distal region of chromosome 4, concordant with the Mpl gene (at offset 56.5 of the chromosome committee map, see Fig. 6.1) [223]. Faah is a membrane bound enzyme involved in the degradation of fatty acid amides, including the neuromodulatory signalling molecules oleamide and anandamide [237, 238].

Widespread distribution of *Faah* mRNA in neuronal cells in the rat CNS was demonstrated by *in situ* hybridisation [226]. Furthermore, anandamide has been shown to induce motor deficits in mice [227]. This has led to speculation that defects in Faah activity could potentially cause inheritable neurological disorders in humans.

Indeed such speculation prompted one study in which *Faah* was evaluated as a candidate for the classical neurological mouse mutation *clasper* [223], which itself maps to the mid-region of chromosome 4 [229]. *Clasper* mice exhibit an abnormal gait and whole-body tremor and are found to clasp both forefeet and hindfeet on suspension by the tail. Whilst *Faah* was eliminated as the genetic basis of the *clasper* mutation it still represents an attractive candidate gene for the Ann mutation.

6.1.6 The *disabled-1* (*mdab1*) gene/*scrambler* mutant as a candidate

As demonstrated in Chapter 5, the employment of a larger scale backcross mapping study provided a more precise map location for the transgene. Comparison of this more accurate map position with the chromosome committee consensus map revealed that *scrambler* maps extremely close to the site of transgene insertion (between microsatellite markers D4Mit155 and D4Mit331, see Fig. 6.1). This, coupled with the strong phenotypic correlation between the Ann and *scrambler* mutant phenotypes makes *scrambler* the strongest candidate of those considered. As such, the structure and expression of the *mdab1* gene responsible for the *scrambler* mutation was investigated for anomalies in Ann mutant mice.

6.2 Materials And Methods

6.2.4 cDNA probes

All probe fragments were digested with the suitable restriction endonucleases and gel purified following electrophoresis on a 1% agarose gel (see section 2.2.9).

A construct representing 1.7kb of the *Faah* cDNA cloned into the pcDNA3 vector (Invitrogen) was obtained [239]. The probe fragment was isolated by restriction endonuclease digestion with *Eco*RI and *Not*I

A *Glyt1* I.M.A.G.E Consortium clone (ref no. 420070) was obtained consisting of 1.3kb of the *Glyt1* cDNA sequence cloned into the pT7T3D-Pac vector (Amersham pharmacia). The probe fragment was isolated by endonuclease digestion with *Not*I and *Xho*I.

The *mdab1* 555 cDNA clone consists of 1.7kb of sequence that encodes the mDab1 555 protein isoform cloned in the pBS (Stratagene) vector[197]. The probe fragment was isolated by restriction endonuclease digestion with *Eco*RI.

6.2.5 Reverse transcriptase PCR

Reagents used were all obtained from the Promega reverse transcriptase kit (Promega). 1µg of RNA sample was added to 500ng of random hexamer primers and the volume made up to 10µl with DEPC-treated H_2O. This was incubated at 75°C for 10 minutes and then allowed to cool at room temperature for a further 10 minutes. The tube was spun briefly to collect the sample at the bottom and then 4µl of 5x reaction buffer, 2µl of 100mM DTT, 2µl of 5mM dNTPs (GATC) and 200 units of reverse transcriptase

added. The tube was mixed and spun briefly and then incubated at room temperature for 5 minutes prior to 60min at 37°C. Following incubation, 1µl of reaction mixture was added to a 20µl PCR reaction (as described in section 2.2.16). With the *Sox10* control primers the PCR mixture was the same as for all other PCR reactions but thermocycling conditions differed. *Sox10* reactions were denatured at 94°C for 2 minutes, followed by 40 cycles each comprising of 40 seconds at 94°C, 30 seconds at 55°C and 2 minutes at 68°C, followed by a final extension for 7 minutes at 68°C and cooling to 4°C. PCR products were analysed by electrophoresis of 5µl of the reaction mixture on a 1.5% agarose gel .

6.2.6 Primers

For reverse transcriptase PCR reactions either *mdab1* or *Sox10* control primers were used. The *mdab1* primers had been used in a previous study [180] and were 20-mers specific to positions 177-196 (mdab1.1) and 626-607 (mdab1.2) of the *mdab1* 555 published cDNA sequence:

mdab1.1 5′-AGGGAGGAGCCTTTCTCTTG-3′

mdab1.2 5′-TGTGATGTCCTTCGCAATGT-3′

For PCR reactions with this primer pair an annealing temperature of 60°C was used and the Mg^{2+} concentration of the reaction mixture was 3.0mM.

The *Sox10* control primers (Sox10-96 and Sox10-97) were both 24-mers with the following sequences:

Sox10-96 5′-AGGTCAAGAAGGAACAGCAGGACG-3′

Sox10-97 5′-GCAGGTATTGGTCCAGCTCAGTCA-3′

For PCR reactions with this primer pair an annealing temperature of 55°C was used and the Mg^{2+} concentration of the reaction mixture was 3.0mM.

6.3 Results

6.3.1 Analysis of *Glyt1* and *Faah* genomic structure

Genomic DNA from wild-type and Ann mutant mice on an inbred C57BL/6J genetic background (resulting from 10 generations of brother/sister mating) was digested with a variety of restriction endonucleases and separated by electrophoresis. Following Southern blotting, hybridisation of the filter to radiolabelled cDNA probes was carried out.

A 1.3kb *Glyt1* cDNA fragment was used to compare the structure of this gene in wild-type and mutant animals. The identical restriction patterns of both types indicated that the transgene had not detectably interrupted the *Glyt1* genomic region covered by the cDNA probe (see Fig. 6.2). This in itself does not eliminate *Glyt1* as a candidate since the expression of the gene may still be compromised without any detectable disruption of the structural gene itself. For example, disruption of a regulatory region may affect *Glyt1* expression without being detectable using a cDNA probe on a genomic Southern blot. It was therefore decided to further investigate *Glyt1* as a candidate by examining its expression in wild-type, hemizygous transgenic and homozygous mutant transgenic mice (see section 6.3.2).

The same genomic DNA filter was stripped and re-probed with a 1.7kb *Faah* cDNA probe. Again no difference in restriction pattern between wild-type and mutant samples was detected, indicating no disruption to the region of the *Faah* genomic region covered by this probe (see Fig. 6.3). Again it was decided to further investigate the expression of this gene in

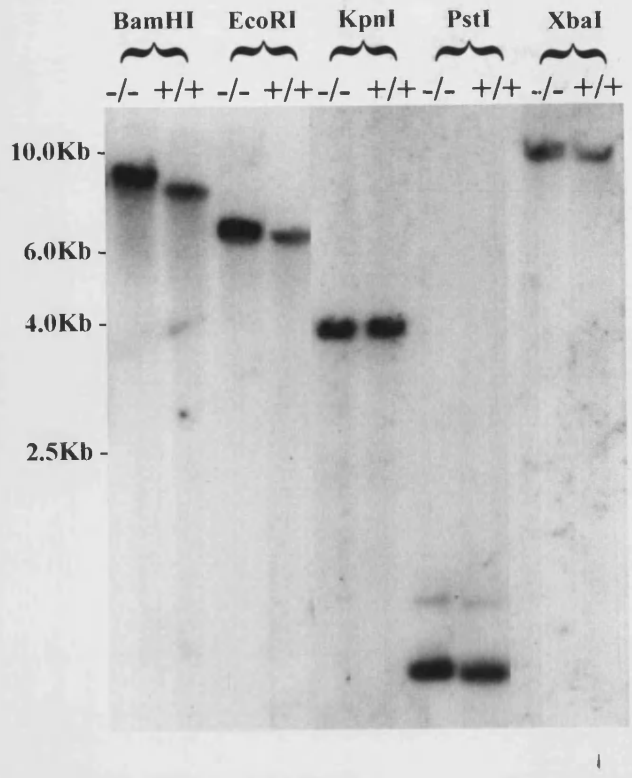

Fig. 6.2. Southern blot probed with *Glyt1*.
Southern blot of C57BL6/J Ann homozygous mutant and wild-type DNA digested with a variety of restriction endonucleases and hybridised with a 1.3Kb *Glyt1* cDNA probe.

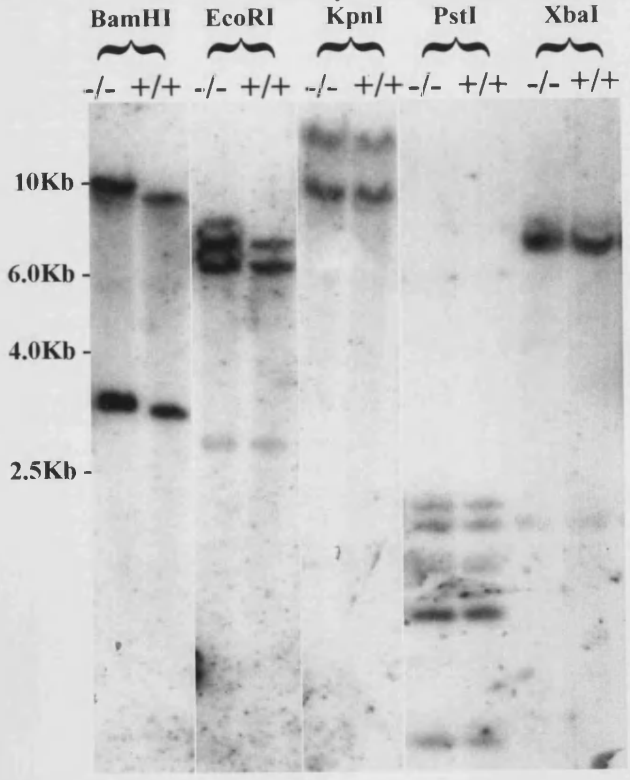

Fig. 6.3. Southern blot probed with *Faah*.
Southern blot of C57BL6/J Ann homozygous mutant and wild-type DNA digested with various restriction endonucleases and hybridised with a 1.7Kb *Faah* cDNA probe.

wild-type, hemizygous transgenic and homozygous mutant transgenic mice (see section 6.3.2).

6.3.2 Analysis of *Glyt1* and *Faah* expression

Total brain RNA was extracted from 17.5 day old mice derived from an Ann hemizygous intercross. All offspring had previously been genotyped by luciferase assay. RNA was quantified and concentration-matched duplicate samples from wild-type, hemizygous transgenic and homozygous mutant mice electrophoresed. Following Northern blotting, hybridisation to filters of radiolabelled cDNA probes was undertaken.

The *Glyt1* cDNA fragment was used to investigate the levels of *Glyt1* expression in brains of the three mouse types. Strong expression of a 3.2kb *Glyt1* transcript had previously been described in a variety of regions in the adult mouse brain [225].

Expression of this 3.2kb *Glyt1* transcript was detectable in the brains of Ann homozygous mutants as well as in hemizygous and non-transgenic mice (see Fig. 6.4). Closer inspection revealed quantitative differences between transcripts in mutant mice and those of the other two classes. This feature will be discussed in section 6.4.1.

The same filter was stripped of radionucleotide and re-hybridised with the *Faah* cDNA fragment probe. Strong *Faah* expression had previously been demonstrated in both human [239] and adult rat [238] brains. A transcript of approximately 2.5kb was detectable at comparable levels in all three mouse types (see Fig. 6.4).

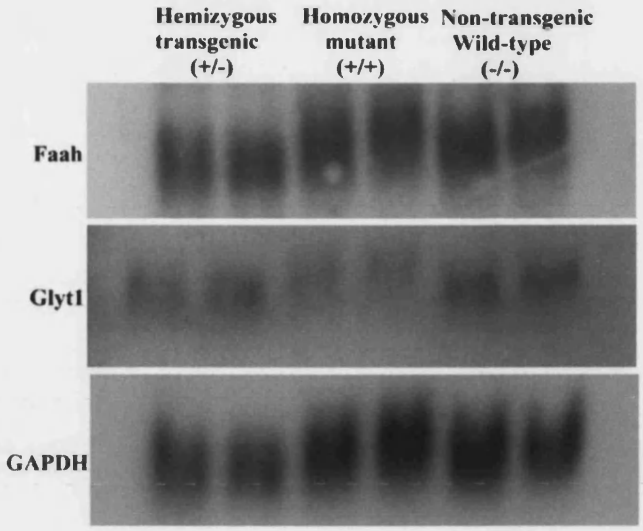

Fig. 6.4. Northern blot probed with *Glyt1* and *Faah*.
Northern blot of total brain RNA from 17.5 day old C57BL/6J Ann hemizygous transgenic, homozygous mutant and non-transgenic wild-type whole brains. The blot was hybridised with an *mGap* cDNA probe to control for loading of RNA, stripped and probed with a 1.3kb *Glyt1* cDNA probe and then stripped again prior to re-probing with a 1.7kb *Faah* cDNA probe. Autoradiographs were exposed overnight for each probe.

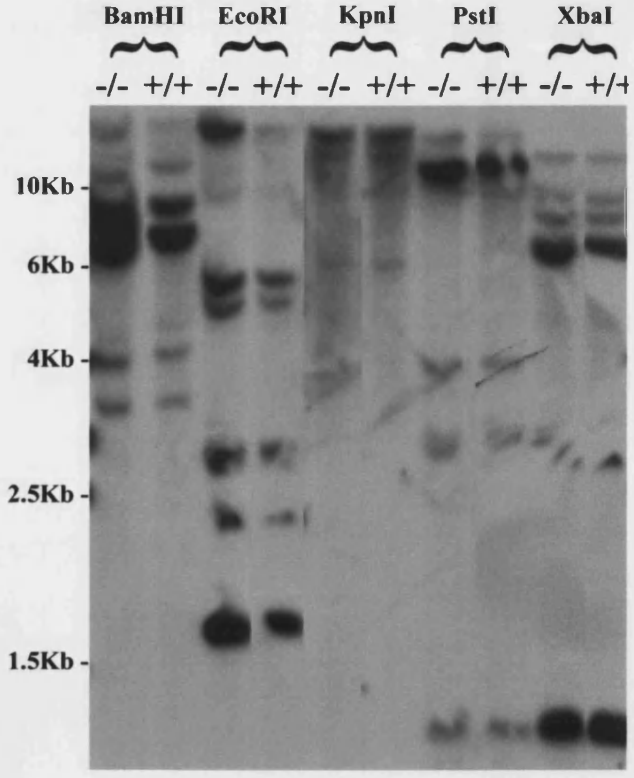

Fig. 6.5. Southern blot probed with *mdab1*.
Southern blot of C57BL/6J Ann homozygous mutant and wild-type genomic DNA digested with a variety of restriction endonucleases. The blot was hybridised with a 1.7kb *mdab1* 555 cDNA probe and the autoradiograph exposed overnight.

6.3.3 Lack of polymorphism in a large section of the *mdab1* coding region

In order to investigate the possibility of transgene insertion at the *mdab1* locus the Southern blot filter used previously was stripped and re-hybridised with the *mdab1* 555 cDNA probe. No readily detectable differences in banding patterns between mutant and wild-type genomic DNA were identifiable (see Fig. 6.5), appearing to eliminate a large section of the *mdab1* coding region from harbouring the inserted transgene. This, though, does not exclude the possibility that transgene insertion is affecting the expression of *mdab1* (discussed in section 6.4.1).

6.3.4 Analysis of *mdab1* transcript reveals loss of expression in Ann mutant mice

The presence of a 5.5kb transcript in total brain RNA extracts had been reported in adult mice. Two smaller transcripts (4.0kb and 1.8kb) had also been detected, but only in poly A-selected RNA samples [180, 240].

A further Northern blot was hybridised with a radiolabelled *mdab1* 555 cDNA fragment. Strong expression of the 5.5kb *mdab1* species was observed in the non-transgenic samples (see Fig. 6.6). This same band appeared to be completely absent in mutant samples, indicating that expression of the *mdab1* 5.5kb species was ablated in Ann mutant mice. Samples from Ann hemizygote mice showed levels of the same transcript at approximately half that observed in wild-type mice. A longer exposure of this filter revealed a weak band of around 5.5kb in size in the mutant samples (see Fig. 6.6). This band could represent a residual level of *mdab1* expression in mutant mice, or may be derived from another source.

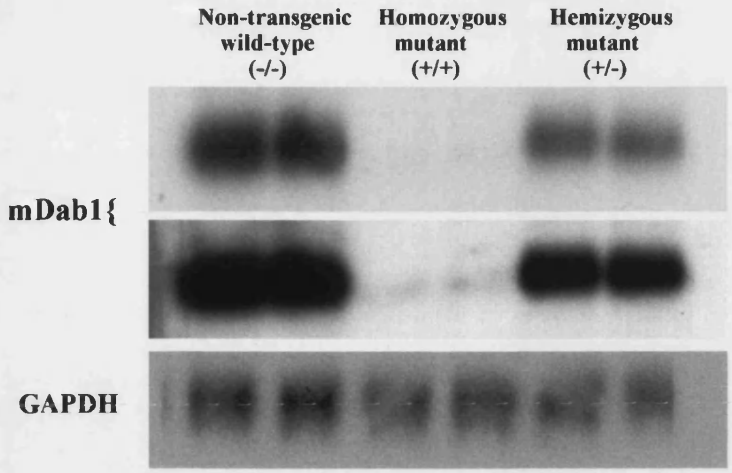

Fig. 6.6. Northern blot probed with *mdab1*.
Northern blot of total brain RNA from 17.5 day old C57BL/6J Ann non-transgenic wild-type, homozygous mutant and hemizygous transgenic whole brains. The blot was hybridised with an *mGap* cDNA probe to control for loading of RNA (bottom panel), stripped and probed with a 1.7kb *mdab1* 555 cDNA probe and the autoradiograph exposed both overnight (top) and for 48 hours (middle).

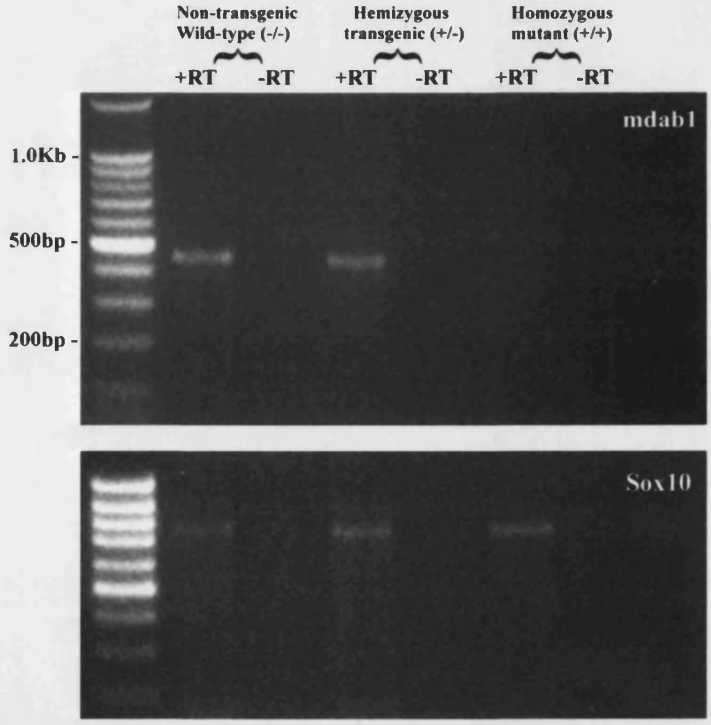

Fig. 6.7. *mdab1* RT-PCR.
RT-PCR products from total RNA extracted from 17.5 day old C57BL/6J Ann non-transgenic wild-type, hemizygous transgenic and homozygous mutant whole brains. Primers complementary to positions 177-196 and 626-607 of the *mdab1* 555 published cDNA sequence were used to generate the *mdab1* products, whilst primers specific to the mouse *Sox10* gene were used to confirm the success of each reverse transcriptase reaction.

The two smaller *mdab1* transcripts identified in other studies were visible at low levels in wild-type and hemizygous samples, but not in mutant (result not shown).

6.3.5 Reverse transcriptase PCR reveals no abnormally sized transcripts

Despite the lack of a polymorphism in a large section of the *mdab1* coding region, several possibilities remain whereby expression of the *mdab1* gene could be (almost completely) ablated by transgene insertional mutation.

Both the *scrambler* and *yotari* classical mutants result from alteration in *mdab1* 555 transcript at nucleotide position 570 [240, 241]. These abnormal RNA species are incapable of allowing production of sufficient (*scrambler*), or any (*yotari*), functional mDab1 protein. The existence of two independent mutants of this nature suggests this nucleotide position might be a highly mutable site in the *mdab1* gene. A similar type of mutation at this position in the Ann line therefore presented one possibility that required consideration.

As demonstrated, a faint band was detectable at around 5.5kb following long term exposure of *mdab1* Northern blots. Although no large scale size difference was noticeable, this band could represent low levels of an aberrant transcript. Abnormalities in this mRNA species at nucleotide 570 were investigated by means of reverse transcriptase PCR (RT-PCR) using *mdab1* specific primers flanking this position. A transcript detectable on a Northern blot should be readily amplified by the more sensitive RT-PCR technique and any abnormally sized bands produced in transgenic samples would indicate an aberrant *mdab1* transcript.

Primers used to amplify across this region in a previous study were obtained and utilised in RT-PCR experiments on wild-type, hemizygous transgenic and homozygous mutant brain, total RNA samples. Bands of the expected size (430bp) were generated from both wild-type and hemizygote samples, but no band was observed in mutant (see Fig. 6.7). Successful amplification from the same reverse transcriptase reactions with *Sox10* control primers demonstrated the viability of the samples and indicated the lack of RT-PCR-detectable *mdab1* transcript in Ann mutants. The mouse *Sox10* gene encodes a transcription factor that is known to be expressed in adult mouse brain and thus represented a suitable control for these experiments.

6.4 Discussion

6.4.1 The Ann mutant is a likely allele of *mdab1/scrambler*

Three candidate genes were investigated as the source of the Ann mutant phenotype by comparing their expression levels in wild-type, hemizygous transgenic and homozygous mutant animals, at 17.5 days post partum when the ataxic phenotype in mutants is approaching its most profound. It must be noted that a failure to detect abnormal gene expression in mutant animals does not necessarily eliminate a candidate, since post-translational defects remain a possibility as the cause of the mutation. It is though unlikely that the integration of a large, multicopy transgene array into the genome would cause a subtle mutation in which a normal sized transcript is still detectable. Therefore it seems rational to look for a dramatic effect on gene expression, at least as a starting point in the analysis of candidates.

On Northern blots, complete, or almost complete, ablation of *mdab1* message was apparent. A longer exposure of the Northern blot did reveal a faint band of about the correct size for the *mdab1* mRNA and the source of this remains unclear (see below).

Again it must be stated that even this dramatic effect does not absolutely confirm *mdab1* as the source of the Ann mutation. To prove this beyond doubt a transgene rescue experiment or complementation test using an existing *mdab1* mutant, would have to be performed. With the weight of evidence provided from the expression analysis, linkage mapping and phenotypic data, we can say within a reasonable degree of certainty that the Ann mutation did result from an anomaly in the *mdab1* gene.

No quantitative differences in *Faah* mRNA levels were observed between the three mouse types, making it the least likely candidate gene at this stage.

The situation with *Glyt1* was rather more complex given the reduction in expression levels in homozygous transgenic as compared with hemizygous transgenic and wild-type mice. This gene is known to be heavily expressed in the cerebellum of adult mice, and as we have seen (Chapter 4), this brain structure is dramatically reduced in size in mutant mice. With this in mind it was reasoned that the small reductions in *Glyt1* expression observed in mutants could be due to the hypoplasia of the cerebellum rather than through a direct affect on the *Glyt1* gene. Furthermore, if the transgene was affecting *Glyt1* expression, it was reasoned that a more dramatic effect would be expected. That a much smaller number of mouse phenotypic mutants result from haploinsufficiency as compared to complete loss of gene expression would appear to support this rationale.

To identify the physical basis of the *mdab1* defect, Southern blotting was performed to look for polymorphisms in the gene. Hybridisation with the *mdab1* 555 cDNA probe fragment will reveal polymorphisms in a region of the *mdab1* coding region and in the 3′ or 5′ untranslated regions, dependant upon the positions of endonuclease restriction sites relative to the probe. No novel restriction fragments were visible in samples digested with a variety of restriction endonucleases suggesting that the transgene array has not integrated into the region of *mdab1* spanned by the probe that was used.

Another possible source of perturbation to the expression of *mdab1* is the highly mutable region affected in both the *scrambler* and *yotari* classical *mdab1* mutants. Separate defects at nucleotide position 570 of the *mdab1* coding region are the basis for both of these mutants, and as such it was deemed prudent to exclude this site as the basis for the mutation in Ann. RT-PCR reactions, using primers spanning this position, generated normal sized products from both wild-type and hemizygous transgenic brain total RNA samples, but no product from mutants. This eliminates the existence of an abnormal *mdab1* transcript, similar to those found in *scrambler* and *yotari*, although smaller size differences may have been undetectable. The source of the faint band detectable on longer exposure of the *mdab1* Nothern blot may be explained by this result. A residual level of *mdab1* transcript detectable by Northern blot should also be picked-up by the more sensitive RT-PCR technique. That it is not questions the authenticity of this band as representing a true *mdab1* transcript. Alternative explanations exist, such as contamination of the mutant RNA samples used for the Northern blot with wild-type RNA, or even hybridisation of the probe to an *mdab1*-like transcript. Indeed an *mdab1* related gene, *mdab2*, has been identified [242].

6.4.2 Mouse *disabled 1* is a cytoplasmic adaptor protein

A yeast two-hybrid screen for proteins interacting with the Src nonreceptor protein tyrosine kinase (PTK) revealed the existence of a mouse homologue of the *Drosophila dab* (*disabled*) gene [197]. The *dab* gene was itself originally identified in *Drosophila* via its interaction with another nonreceptor PTK, *dAbl* [243]. Mutation of *dab* was found to exacerbate the $dAbl^{-/-}$ phenotype and as such belonged to a group of genes termed HDA (haploinsufficient, dependent upon *dAbl*).

The *mdab1* gene encodes a cytosolic protein and is alternatively spliced to generate at least three different mRNAs encoding protein isoforms of 555, 271 and 217 amino acid residues [197]. These isoforms have a common amino terminus which contains a protein interaction/phosphotyrosine binding (PI/PTB) domain known to bind the tetra-peptide; Asn-Pro-x-Tyr (NPxY) motif [244]. Proteins with PI/PTB domains can bind to NPxY motifs in either a phosphotyrosine dependent (e.g. Shc binding of IRS1 [245]) or independent (e.g. Fe65 binding of APP [246]) manner. The PTB domain has been shown to mediate docking functions in a number of cytoplasmic adaptor proteins including mDab1 [247].

A second mechanism by which mDab1 can interact with other proteins is through binding to the SH2 domains of the nonreceptor PTKs Src, Fyn and Abl [197]. These interactions are facilitated by tyrosine phosphorylation of mDab1 protein, and suggest a role for mDab1 in intracellular signalling cascades. mDab1 has been shown to be expressed in the developing CNS of mouse embryos and furthermore, was determined as being tyrosine phosphorylated during this period. Thus mDab1 was postulated to be involved in the development of the mammalian CNS, probably through some involvement in signal transduction cascades.

6.4.3 The *mdab1* knockout is an ataxic mutant

The exact role of mDab1 in mouse CNS development became more apparent upon the generation of *mdab1* null mutants by gene targeting [240]. Mice homozygous for a disruption of the first 47 codons of the PI/PTB domain exhibited a severe ataxic phenotype. Clearly identifiable by 15 days; mutants have an unstable gait, whole body tremor and are smaller than their siblings. They generally die between 20 and 30 days old.

The brains of *mdab1* knockout mice have severe defects in a number of regions.

6.4.4 Mutations in *mdab1* are responsible for *scrambler* and *yotari*

Generation of the *mdab1* knockout mouse facilitated the elucidation of the molecular basis of two existing classical mutants. *Scrambler* and *yotari*, both of which exhibit almost identical phenotypes to the *mdab1* knockout, were identified as arising from mutations in the *mdab1* gene [180, 241].

The *scrambler* mutant arose spontaneously in the dancer (DC/Le) mouse strain and displays a similar, if less severe phenotype to the *mdab1* knockout, having a normal lifespan (thought to result through differences in genetic background) [229]. The mutation was mapped to Chromosome 4, close to the *mdab1* map position. The appearance of the *mdab1* knockout allowed investigators attempting to positionally clone the gene responsible for *scrambler* to focus on *mdab1* and look for mutations in this gene in *scrambler* mice [241].

With a phenotype identical to *scrambler*, the *yotari* mutant arose during the targeted disruption of the inositol 1,4,5 trisphosphate gene [248]. This mutant was mapped to the same site as *scrambler*. Analysis of *mdab1* expression revealed anomalies in both mutant strains. In *scrambler*, levels of the normal 5.5kb *mdab1* transcript were greatly reduced, accompanied by the appearance of an abnormal transcript of approximately 7kb. *Yotari* mice expressed only a shorter (approximately 5.2kb) transcript at wild-type levels. Further investigation revealed that both strains, somewhat incredibly, expressed abnormal *mdab1* transcripts that were mutated at exactly the same nucleotide position. The abnormally large transcript

detected in *scrambler* was generated by the aberrant splicing of a mouse intracisternal-A particle (IAP) element to nucleotide 570 of the *mdab1* mRNA. Present at around 1000 copies per haploid mouse genome [249, 250], IAPs are retrovirus related transposable elements and have been identified as causing insertional mutations in a number of other cases in the mouse(e.g. the Albany allele of *reeler* $Reln^{rlAlb2}$)[251].

Insertion of the IAP in the *mdab1* transcript in *scrambler* creates a severely truncated form of the protein that is undetectable on Western blots, and therefore must be rapidly degraded. Only a trace level of normal protein is detectable in *scrambler*, probably originating from the residual level of normal sized message expressed in mutants.

The lesion in the *yotari* strain was found to be a deletion of 375 bases of *mdab1* coding sequence, again originating at nucleotide 570. The open reading frame is maintained in this mutant transcript, but again no normal protein is detectable, and any polypeptide generated must be unstable.

6.4.5 *mdab1* mutant mice have defects in cerebellar, cerebral and hippocampal development

As discussed in Chapter 4, neuropathological studies of *scm* mice indicated that loss of mDab1 activity during development leads to severe abnormalities in a variety of different brain regions. In the cerebellar cortex, defective migration of Purkinje cells results in the almost total loss of the Purkinje cell layer and a subsequent reduction in number of granule cells in the internal granule cell layer. As a result, the cerebellum is much reduced in size and completely lacks foliation [240, 252]. In the developing

cerebral cortex, the classic 'inside-out' pattern of neuronal migration, which generates a characteristic layered structure, is disrupted and migrating neurons are unable to bypass their predecessors and reach their appropriate locations. Hence, the normal layering is abolished and different cell types are largely intermingled [189, 240, 253]. Finally, in the hippocampal formation, the pyramidal neurons of the hippocampus and the granule cells of the dentate gyrus are randomly scattered rather than forming discrete structures. Again, defective neuronal migration is responsible for these abnormalities [206, 242].

6.4.6 mDab1 is a key component in reelin signalling during brain development

First described in 1951 [254], *reeler* is another classical mouse mutant that displays an almost identical phenotype to the *mdab1* mutants. *Reeler* mice are ataxic, their cerebellums are hypoplastic and lack foliation, and furthermore, laminated brain structures such as the cerebral cortex and hippocampal formation exibit neuronal ectopia.

The generation of a *reeler* allele rl^{ts} by transgene insertion [255], facilitated the cloning of the *reeler* gene [164], which was named *reelin* (*reln*). It was found to be a large secreted protein of 3,461 amino-acid residues and was proposed to be involved in neuronal migration in various tissues of the developing brain, probably by acting as an extracellular signalling molecule.

The almost identical phenotypes of $reln^{-/-}$ and $mdab1^{-/-}$ mice immediately suggested that these molecules were part of a common signalling pathway. This idea was strengthened by the observation that levels of mDab1 protein are increased in *reeler* brains [253], demonstrating the existence of a

biochemical link between Reln and mDab1. Furthermore, application of Reln protein to neuronal cultures causes an increase in tyrosine phosphorylation of mDab1, this phosphorylation decreased in developing brains of *reeler* mutants as compared with normal mice [256].

Additional support for a common signalling pathway comes from the expression patterns of these proteins being spatially and temporally juxtaposed in the brain structures affected in both mutants [253]. In the developing cerebral cortex Reln is secreted by the Cajal-Retzius neurons of the preplate, whilst migrating cortical plate neurons are found to express mDab1 at the time they invade this structure.

A similar pattern is observed in the developing cerebellum in which granule cell precursors in the EGL express Reln and purkinje cell precursors, which migrate from the ventricular zone towards this region, express high levels of mDab1. Migrating pyramidal cells in the developing stratum pyramidale of the hippocampus express mDab1 as they migrate toward the Reln-expressing, Cajal-Retzius-like cells in the outer molecular layer. Similarly, during neuronal positioning to form a compact layer in the dentate gyrus, mDab1 expressing granule cells migrate toward Reln secreting cells.

6.4.7 Members of the LDL receptor family transmit the Reelin signal to mDab1

The mechanisms of Reln signalling were further elucidated with the identification of Reelin binding, transmembrane receptor molecules that could transmit a signal to mDab1.

The interaction of the mDab1 PI/PTB domain with NPxY motifs has been discussed (see 6.4.2). Such motifs are present in the cytoplasmic tails of proteins belonging to the low density lipoprotein (LDL) receptor family [257] of which there are five known members. The LDL receptor (LDLR), LDL receptor-related protein (LRP), Megalin, very low density receptor (VLDLR) and apolipoprotein E receptor 2 (ApoER2) are structurally related, multifunctional cell-surface receptors that mediate endocytosis of extracellular ligands [258].

The mDab1 protein was shown to interact with several neuronally expressed transmembrane proteins, including several members of this gene family [247]. Generation of *vldlr*$^{-/-}$/*apoER2*$^{-/-}$ double mutants produced mice that displayed behavioural and neuroanatomical defects almost identical to those found in both *reln*$^{-/-}$ and *mdab1*$^{-/-}$ mice [259]. Again cerebellar, cerebral cortex and hippocampal abnormalities, suggestive of abnormal neuronal migration, were observed. Disruption of either gene alone produced more subtle phenotypes, suggesting a level of redundancy between the two receptors.

Expression of both VLDLR and ApoER2 is high in the same subset of neuronal cells that express mDab1 during brain development, namely the cortical plate neuron precursors in the cerebral cortex, purkinje cell precursors in the cerebellum, and the granule and pyramidal cells of the hippocampal formation. This is indicative of a role for these receptors in transmitting the Reln signal to intracellular mDab1. An upregulation of mDab1 levels in *apoER2*$^{-/-}$/*vldlr*$^{-/-}$ brains, just as in the *reln*$^{-/-}$ mutant, further alludes to this hypothesis. The establishment of Reln as a ligand for both

ApoER2 and VLDLR places, Reln, VLDLR, ApoER2 and mDab1 on a common signalling pathway (see Fig. 6.8) [175, 260].

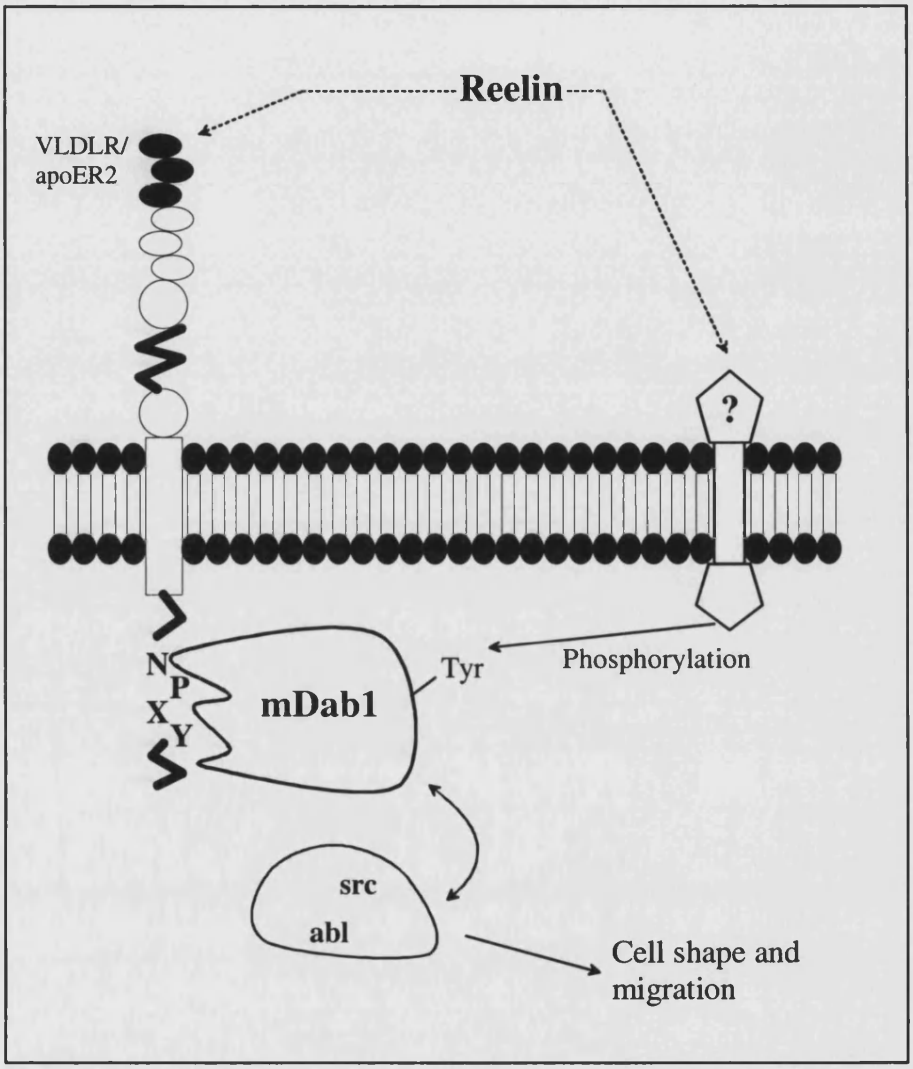

Fig. 6.8. The postulated Reelin signalling pathway.
Either direct or indirect interaction of Reelin with VLDLR or ApoER2 results in binding of mDab1 to the cytoplasmic NpxY motif of these receptors and its subsequent phosphorylation, possibly through a Reelin activated membrane tyrosine kinase. The signal is further propagated via the binding and activation by mDab1 of non-receptor tyrosine kinases, and may ultimately lead to changes in cell shape and migration.

Since mDab1 becomes phosphorylated during Reelin signalling, but the lipoprotein receptors posses no inherent tyrosine kinase activity, it is probable that mDab1 phosphorylation is affected by association of the protein with tyrosine kinases upon receptor binding of Reln. Phosphorylated mDab1 could then recruit intracellular signalling molecules containing SH2 domains, setting up signalling cascades that could alter gene expression to bring about changes in cell shape and migration. Changes to cytoskeletal organisation could also be affected by such signalling, and indeed mutants in *p35* and *Cdk5*, two molecules known to regulate cytoskeletal proteins, exhibit similarities to the *reln*$^{-/-}$, *mdab1*$^{-/-}$ and *vldlr*$^{-/-}$/*apoER2*$^{-/-}$ mutants [261, 262].

The overall effects of Reln signalling on neuronal migration still remain unclear. One possibility is that Reln acts as a stop signal for migrating neurons, thus facilitating migration to the correct positions. In the absence of this signalling (as in *reln*$^{-/-}$, *mdab1*$^{-/-}$ and *vldlr*$^{-/-}$/*apoER2*$^{-/-}$ mutants) neurons will not receive the correct positional cues and will thus migrate to ectopic sites. A second hypothesis is that Reln could be present in a concentration gradient that would induce neurons to migrate past those born at an earlier stage. Again defects in this signalling pathway would result in ectopic neuronal positioning. Alternatively, Reln signalling could act in the developing cerebral cortex to split the cortical preplate, allowing invasion of migrating cortical neurons. Failure of the preplate to split would prevent this invasion resulting in ectopic positioning of neurons beneath the preplate.

6.4.8 The Ann mutant contributes to an existing allelic series

Resulting from a deficiency in gene expression, the Ann mutant is not the first *mdab1* allele to be discovered. As we have seen, three alleles of this gene are already in existence. *Scrambler* results from the aberrant splicing of *mdab1* mRNA, whilst in *yotari* 375 nucleotides are deleted from the *mdab1* coding sequence, with the lesion occurring at the same position as in *scrambler*. An m*dab1* knockout mouse was also generated by the deletion of the first 47 codons of the PI/PTB domain.

Although the precise nature of the molecular lesion in Ann mutants has not been determined, a large section of the *mdab1* coding region seems not to have been disrupted by the inserted transgene. Furthermore, abnormalities at the nucleotide position disrupted in both *scrambler* and *yotari* are undetectable by RT-PCR in Ann.

Amongst the possibilities remaining as to the nature of the Ann mutation, disruption to either the *mdab1* 5′ or 3′ untranslated regions, or to an *mdab1* regulatory region represent the most likely explanations. If any of these possibilities turns out to be correct, the value of the Ann mouse to further studies on *mdab1* regulation and function should not be underestimated. The generation of allelic series in the mouse, usually by gene targeting or chemical mutagenesis strategies has become an essential tool in the accurate dissection of domains important in protein function [263] (e.g. *dilute* [264, 265]), or elements involved in regulating gene expression (e.g. *short ear* [266]). As a novel allele of *mdab1*, the Ann mutant contributes to an existing allelic series and therefore has the potential for use in the future analysis of *mdab*1 gene expression and the regulatory elements involved.

CHAPTER 7: MOLECULAR ANALYSIS OF TRANSGENE INTEGRATION IN THE ANN MUTANT

7.1 Introduction

7.1.1 Transgenes insert into the genome at a single site, often in multiple copies

Disruption of the function of an endogenous gene by transgene insertion often prompts further investigation of the nature of the mutation in molecular, as well as phenotypic, terms. The presence of known transgene sequence incorporated into the genome provides a useful handle for molecular studies of transgene integration. Normally this involves the cloning of genomic sequence flanking the integrated transgene. This sequence can then be used in efforts to isolate the gene mutated by the transgene insertion.

The isolation of flanking sequence can be complicated by several features of microinjected transgene DNA integration into the host genome. Firstly, as stated in Chapter 1, transgenes often integrate as multiple copy arrays. Within such arrays, single transgene copies are usually orientated in a 'head-to-tail' fashion [58, 59] although 'head-to-head' and 'tail-to-tail' orientations have been reported. Elucidation of the transgene array structure is often a pre-requisite for the cloning of sequences flanking multiple copy arrays. The convoluted nature of many transgene arrays can make this extremely difficult, often creating a considerable impediment to the development of a suitable cloning strategy.

In addition, cloning flanking sequence using a PCR-based method often involves amplifying outwards from a transgene sequence known, or at least assumed, to be in juxtaposition to the surrounding genome. The arrangement of transgene copies within an array in 'head-to-head' or 'tail-

to-tail' orientations could conceivably result in the preferential amplification of sequences internal to the array, at the junction of the transgene copies arranged in this manner.

Chromosomal rearrangements, which are often found at the site of transgene insertion (see Chapter 1) [62-64], whilst not interfering with efforts to clone flanking sequence, can create difficulties in isolating the mutated gene. For example, a genomic rearrangement near the site of integration could result in the displacement of the gene of interest from its normal position to a position either closer to, or further away from, the inserted transgene. Either scenario would be likely to create confusion when cloned flanking sequence is used as a probe to isolate clones from a wild-type genomic DNA library, as is often the approach in such studies.

7.1.2 Cloning genomic sequence flanking the transgene

When investigating a mutant phenotype caused by the effects of transgene integration upon an endogenous gene, isolation of the flanking sequence can facilitate the identification of the disrupted gene in a number of ways.

Flanking sequence provides a useful tool for linkage mapping the site of transgene integration into the genome. Obtaining endogenous sequence allows the use of an existing mapping panel for linkage mapping studies and circumvents the need to generate a panel that is specific to the transgenic line being studied. As discussed in Chapter 5, knowing the map position of the transgene facilitates a search for possible candidate genes. This, in turn, may obviate the need to isolate the affected gene by molecular means.

The requirement for flanking sequence is especially great in cases where the endogenous gene is one that has not previously been isolated. In this situation a candidate approach cannot be utilised to identify the gene. Instead it is necessary to progress from the transgene insertion site to the molecular cloning of the gene itself. To do this, the cloning of sequence flanking the transgene is essential. This sequence provides the starting point for a chromosome walk from the transgene to the affected gene. If the transgene has disrupted the function of a gene by integrating within the gene itself then such a walk could be relatively facile. Alternatively, the transgene integration could provoke an effect by disrupting an enhancer element of the gene. In this case the transgene could be located 100's of kilobases upstream of the gene, making a chromosome walk much less trivial.

It should be noted that the majority of transgene insertional mutagenesis studies originate by chance from transgenesis exercises instigated for a completely separate reason. In addition to facilitating the isolation of novel genes or new alleles of previously identified genes, transgenic mice can be used to elucidate the mechanisms by which foreign DNA integrates into the mouse genome [267]. In this instance, flanking sequence can provide a useful tool for investigating the nature of the genomic region into which the transgene has integrated and the effects that integration has on the constitution of this region.

The means of cloning transgene flanking sequence can often depend upon the nature of the transgene array and the insertion event itself. As mentioned, the often complex nature of many transgenic insertions can complicate the isolation of endogenous sequence and necessitate the use of

cloning strategies that can be highly inventive. Regardless of complexity, such cloning exercises are generally either library or PCR based.

7.1.3 Cloning flanking sequence by PCR

A major limitation of conventional PCR technology is its ability to allow only the amplification of DNA fragments between two regions of known sequence. Isolation of transgene flanking regions by PCR does though depend upon the amplification of unknown sequence. Furthermore, in this case only transgene-specific primers are available. A panopoly of strategies have been developed to allow PCR amplification of unknown sequence adjacent to a known region. In general these methods can be divided into those that involve a prior ligation step and those that utilise non-specific or unknown sequence.

One PCR technique involving a prior ligation step is Inverse PCR (I-PCR) [268]. In this case, primers are used that are specific to the known sequence (i.e. the inserted transgene) but which prime DNA synthesis in opposite directions. These primers are able to successfully amplify flanking sequence through the inversion of the known sequence in the region between the primers. This is achieved by restriction endonuclease digestion at suitable sites (at least one of which must be in the flanking region) and subsequent ligation, followed by digestion in the known region between the primers. Prior knowledge of the transgene array structure is essential for the selection of suitable restriction sites.

A number of other PCR strategies involve the ligation of linker oligonucleotides to the termini of junction fragments generated by

restriction enzyme digestion. These linkers provide sites for primer annealing, thus facilitating the amplification of unkown flanking sequence. Specificity to sequence flanking the known region is maintained through the use of primers that amplify out from this region (multiple amplifications with nested primers are often used). One such method is Capture PCR [269], which involves restriction digestion and ligation of a primer-specific double-stranded oligonucleotide linker prior to PCR amplification.

A similar, but more advanced method is Vectorette PCR [270]. This technique involves the ligation of linkers to restriction digested DNA to generate a 'Vectorette-library'. The duplex Vectorette linker contains a non-homologous central region. Amplification from a vectorette primer, specific to this region, can only proceed after the synthesis of a complimentary strand originating from the known (i.e. transgene-specific) sequence. Vectorette PCR has successfully been used to isolate transgene flanking sequence [271]. Like I-PCR, the success of a linker-based PCR technique may depend on knowledge of the transgene array structure in order to select suitable sites for restriction digestion prior to linker ligation.

Circumventing the requirement for restriction digestion/ligation prior to amplification, are a variety of techniques based upon the use of primers that can amplify directly from the unkown flanking sequence. In perhaps the most straightforward case, essentially aribitrary primers have been used to successfully prime DNA synthesis of unknown sequence flanking a known region. This technique, termed 'targeted gene walking' [270] is based upon the observation that even primers containing large numbers of mismatches (as much as 60%) can facilitate amplification as long as partial

homology at the 3′ end of the primer exists, and there is correct base pairing of the last two nucleotides at this end. A drawback of this technique is that such arbitrary priming generates non-target molecules that can constitute the bulk of the final product.

Thermal Asymmetric Interlaced PCR (TAIL PCR) [272] addresses this problem through the use of primers of different lengths in conjunction with advanced PCR cycling conditions. High annealing temperatures are known to favour primers of longer length, whilst lower temperatures allow both long and short primers to function almost equivalently. By using long primers specific to the known sequence and a short, degenerate primer to amplify from the unknown sequence, in combination with interspersed PCR cycles of high and low stringency, amplification of products flanking the region of known sequence is favoured. Use of sequence-specific, nested primers in further PCR cycles can eliminate virtually all products that are not specific to the flanking sequence.

A number of other PCR protocols exist that do not rely on a prior restriction/ligation step, but also are not dependant on random or near-random priming from unknown flanking sequence. Instead these protocols are dependant upon the fact that well characterised genomic regions may be positioned close to the region of known sequence, allowing amplification of the intervening region. One such method is Restriction Site PCR (RS PCR) [273]. This technique uses primers specific to restriction enzyme recognition sequences (RSOs) in conjunction with primers specific to the known sequence, to facilitate the amplification of flanking regions. Such a technique is based upon the assumption that at least one RSO specific to the primers being used, will be positioned close enough to the

known sequence to allow successful amplification. To increase the chances of this, it is therefore desirable to use primers specific to a number of RSOs.

Other techniques have been developed which utilise repetitive genomic sequences, rather than RSOs, to provide a site for primer annealing. A variety of repeat sequences are dispersed throughout the mouse genome such as Alu repeats, which have successfully been used in such PCR methodologies [274].

7.1.4 Cloning flanking sequence by library based methods

The majority of PCR-based techniques described depend heavily upon some prior knowledge of the structure of the transgene array. With this in mind, insertion of a completely intact transgene copy into the genome without any accompanying genomic rearrangements provides the most straightforward scenario for the cloning of transgene-flanking sequence by a PCR method. This is also true for the cloning of flanking sequence by library-based methods. Cloning flanking sequence using a library-based approach could simply involve digestion of genomic DNA with a suitable restriction endonuclease that does not cut within the transgene but does cut closely enough in the flanking regions to allow the cloning of a fragment containing the complete transgene and both 5′ and 3′ flanking sequence in a plasmid or phagemid vector (depending upon the size of the fragment). A genomic library could be generated and the desired clone isolated by screening with a transgene-specific probe. Cloning of both 5′ and 3′ flanking sequence is often desirable since it allows the identification of any genomic rearrangements at the site of insertion and facilitates a possible chromosome walk both upstream and downstream from the transgene.

In at least one case, cloning of genomic sequence flanking a single copy transgene insertion was facilitated by the fact that the transgene itself contained a complete plasmid vector sequence [275]. This negated the requirement for the generation and screening of a genomic library, since any successfully transformed clones were obviously derived from the transgene.

If the transgene is found in a multi-copy array, cloning of the complete array could still be suitable depending upon the size of the DNA fragment in question. The development of BAC (Bacterial Artificial Chromosome), PAC (P1 Artificial Chromosome) and YAC (Yeast Artificial Chromosome) vectors mean that DNA fragments of 10's and 100's of kilobases can now be cloned [43, 44]. Unfortunately the ease of handling libraries generated with such vectors can often be much less than plasmid or phagemid libraries.

If one is not attempting to clone the entire transgene array then generation of a genomic library must involve restriction endonuclease digestion of genomic DNA with an enzyme that cuts within the transgene. In a multiple copy transgene array this will generate fragments consisting of only transgene sequence, as well as those that include flanking sequence. Generation of a library from genomic DNA digested with such an endonuclease, followed by screening with a transgene-specific probe, will isolate clones carrying transgene sequence with or without accompanying flanking sequence.

Methods can be employed to prevent cloning and screening of transgene-only clones. If the sizes of the various transgene-containing fragments are known then a size-restricted library can be generated using genomic

fragments of a certain size that will include those in which the transgene sequence is accompanied by flanking sequence but not those containing only transgene sequence. Size separation of genomic fragments can be achieved in a variety of ways, e.g. sucrose gradient, gel electrophoresis/fragment purification. Transgene-positive clones isolated from a library constructed in this manner are much more likely to contain flanking sequence. The feasibility of such a cloning strategy is dependant upon whether fragments containing flanking sequence can be distinguished and subsequently size-separated from those that do not. Thus, the elucidation of the transgene array structure is essential prior to attempting such a cloning exercise.

7.2 Materials and Methods

7.2.1 Producing a restricted genomic library from Ann DNA

Ann genomic DNA was purified as in section 2.2.5 and four aliquots of approximately 10µg each digested, overnight at 37°C, with 10 units of *Kpn*I restriction endonuclease. Digested DNA was separated by electrophoresis on a 1% agarose gel and the gel section containing fragments of the 3 to 5 kb size range, excised. DNA was purified from the gel section using the QIAquick Gel Extraction Kit (Qiagen), according to the manufacturers instructions, and pooled. One seventh of the purified DNA was retained for use in Southern blot analysis, whilst the remainder was split into three equal parts that were subsequently digested each with 10 units of either *Apa*I, *Bam*HI or *Hin*dIII restriction endonuclease (Promega), overnight at 37°C. The following day, reactions were heat inactivated at 65°C for 10 minutes. Half of each digested sample was separated by electrophoresis on a 1% agarose gel and Southern blotting performed (as in section 2.2.10). The blotted membrane was hybridised with a α^{32}P-dCTP-labelled *H19* 5′ probe fragment with the analysis of the resulting autoradiograph prompting the use of the *Apa*I/*Kpn*I digested aliquot of genomic DNA in the construction of a plasmid library. 1µg of pBluescript KS II+ (pBSKSII+) plasmid DNA (Stratagene) was digested overnight with 10 units of both *Apa*I and *Kpn*I restriction endonucleases and fragments separated by electrophoresis on a 1% agarose gel. The section of gel containing the DNA fragment of approximately 3kb in length (corresponding to the linearised plasmid) was excised and DNA purified again using the QIAquick Gel Extraction Kit. Ligation reactions containing 10ng of linearised pBSKSII+ DNA and either 10ng of the ApaI/KpnI digested sample, or an equivalent volume of dH_2O, were set up. Reactions also contained 1 unit of DNA

ligase (Promega) and an appropriate volume of DNA ligase buffer (Promega). Ligation reactions were incubated overnight at room temperature and the following day 1µl was used to transform electrocompetent DH5α *E. coli* (as described in sections 2.2.1 and 2.2.2). Cells were plated on 10cm diameter, LB agar (containing 20µg/ml ampicillin with IPTG (20µg/ml LB agar)/X-gal (15µg/ml LB agar)) plates, and cultured overnight at 37°C. Numbers of blue and white colonies were counted the following day. The remainder of the ligation reaction, containing insert, was then transformed into electrocompetent DH5α *E. coli*, in 1µl aliquots. All of the transformed cells were plated together on two 22cmx 22cm square, LB agar (20µg/ml ampicillin) plates and grown overnight at 37°C. The next day, the number of colonies on each plate was counted and the plates incubated at 4°C until required.

7.2.2 Library screening

Hybond-N (Amersham) membranes were prepared for hybridisation with the *H19* 5′ probe fragment by performing colony lifts on each of the two bacterial library plates essentially as described in the Hybond-N protocols booklet. Briefly, Hybond-N membranes were cut to fit neatly on the surface of the 22x 22cm plates. Membranes were carefully lowered onto the surface of the plate and removed 60 seconds later, using forceps, onto a sheet of 3MM paper (Whatman) soaked in 10% (w/v) SDS (colony side up). After 3 minutes, membranes were transferred to 3MM paper soaked in denaturation buffer (1.5M NaCl/0.5N NaOH) for 5 minutes. Membranes were then placed on 3MM paper soaked in neutralisation buffer (1.5M NaCl/1.5M Tris(pH 7.4)) for two periods of 3 minutes each. Following vigorous washing in 2x SSC (on a shaking platform), membranes were allowed to air dry on 3MM paper prior to crosslinking (see section 2.2.10).

Membranes were then suitable for hybridisation with radiolabelled DNA probes (as sections 2.2.14 and 2.2.15).

Following incubation of agar plates for approximately 4 hours at 37°C, positive colonies were picked by excising the surrounding area of agar using the wide end of a 1ml pipette tip and placing the agar plug in an 1.5ml polypropylene tube (Sarstedt) containing 1ml of LB medium. After brief agitation, 100µl of medium was plated on a 10cm diameter LB agar/Amp plate that was then incubated overnight.

Colony lifts were performed on 10cm diameter petri dishes, for secondary screening, as described for 22cmx22cm square plates.

7.2.3 Analysis of genomic clones

Small-scale purification of plasmid DNA was performed on colonies as described (section 2.2.3). Clones were analysed by restriction endonuclease digestion of plasmid DNA using *Apa*I/*Kpn*I restriction enzymes (section 2.2.8) followed by electrophoresis on a 1% agarose gel.

Selected clones were sent for automated sequencing using the pBSKSII+ -specific M13 –40 or Reverse primers. Automated sequencing was performed using the Perkin Elmer automated sequencer according to manufacturers instructions. Sequence data was analysed using the GCG Wisconsin package.

7.2.4 DNA probes

The Lux 5′ probe was prepared by *Hin*dIII/*Eco*RI endonuclease digestion of plasmid p147a14 and gel purification (see section 2.2.9) of the 0.6kb

fragment. The Lux 3′ probe was purified from the same reaction by gel purifcation of the 1.2kb fragment generated.

The *H19* 5′ probe was purified by digestion of plasmid p1766a2 with *Xba*I and gel purification of the 1.0kb fragment produced. The *H19* 3′ probe was purified by digestion of the same plasmid with *Pst*I, again a 1.0kb fragment was gel purified for radio-labelling (as described in section 2.2.14).

7.3 Results

7.3.1 Elucidation of the Ann transgene array structure

Early Southern blot experiments carried out on the Ann line (for genotyping purposes) suggested that the transgene array contained multiple transgene copies, most probably arranged in a 'head-to-tail' orientation. This was suggested by the presence of multiple, transgene-specific bands, of which at least one had a much higher level of intensity (suggestive of multiple copies). This created a problem when constructing and screening genomic libraries, in that using transgene sequence as a probe is at least as likely, if not more likely, to isolate clones containing only sequence internal to the transgene array and not flanking it.

To assist with attempts to clone genomic sequence flanking the inserted transgene it was decided to elucidate the structure of the transgene array by Southern blotting and hybridisation with a variety of transgene-specific probes. Transgenic and wild-type (control) DNA was digested with a variety of common restriction enzymes, which have sites within the transgene sequence, and Southern blotted. The same blot was probed serially with each of four probes recognising different parts of the transgene construct (see Fig. 7.1) and the probe completely removed following hybridisation with each one. From the examination of these blots (see Fig. 7.2) it was clear that the structure of the transgene array was likely to be extremely complex.

In each track one or more strong bands (depending on the position of restriction sites in relation to the hybridising probe) were present corresponding to the repeated units of a multiple copy, 'head-to-tail'

transgene array (Fig. 7.3.). Probes specific to the *H19* enhancer element found in the transgene also hybridised to at least one endogenous fragment. It was thought that any other bands present could correspond to fragments at the junction of the transgene and the surrounding genome (termed junction fragments).

Probing an *Eco*RI digest with the 5' Lux probe reveals the presence of a band of approximately 1.9kb. This same band was present in samples digested with *Eco*RI and either *Kpn*I, *Nhe*I or *Pst*I, but was ablated when samples were digested with *Eco*RI and *Xba*I or *Hin*dIII (Fig. 7.4). The 'A' construct sequence indicates the presence of single *Xba*I and *Hin*dIII sites downstream of the most 5' *Eco*RI site. No *Kpn*I, *Nhe*I or *Pst*I sites are found downstream of the *Eco*RI site.

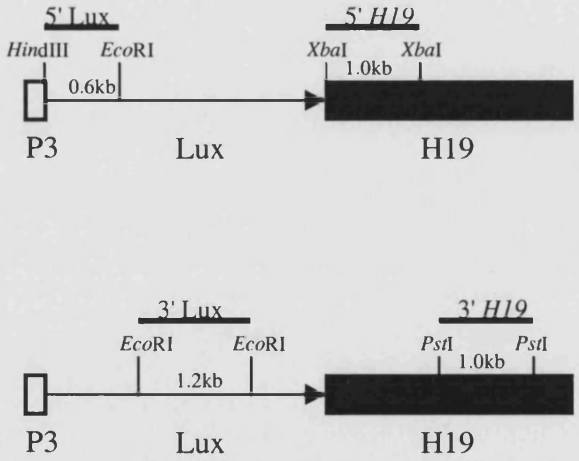

Fig. 7.1. 'A' transgene probes.
Segments of transgene constructs used as probes for hybridisation to Southern blots. 5′ and 3′ Lux probes consist of sequence specific to the firefly (*Photinus pyralis*) *luciferase* gene whilst the 5′ and 3′ *H19* probes consist of sequence specific to the murine *H19* enhancer element.

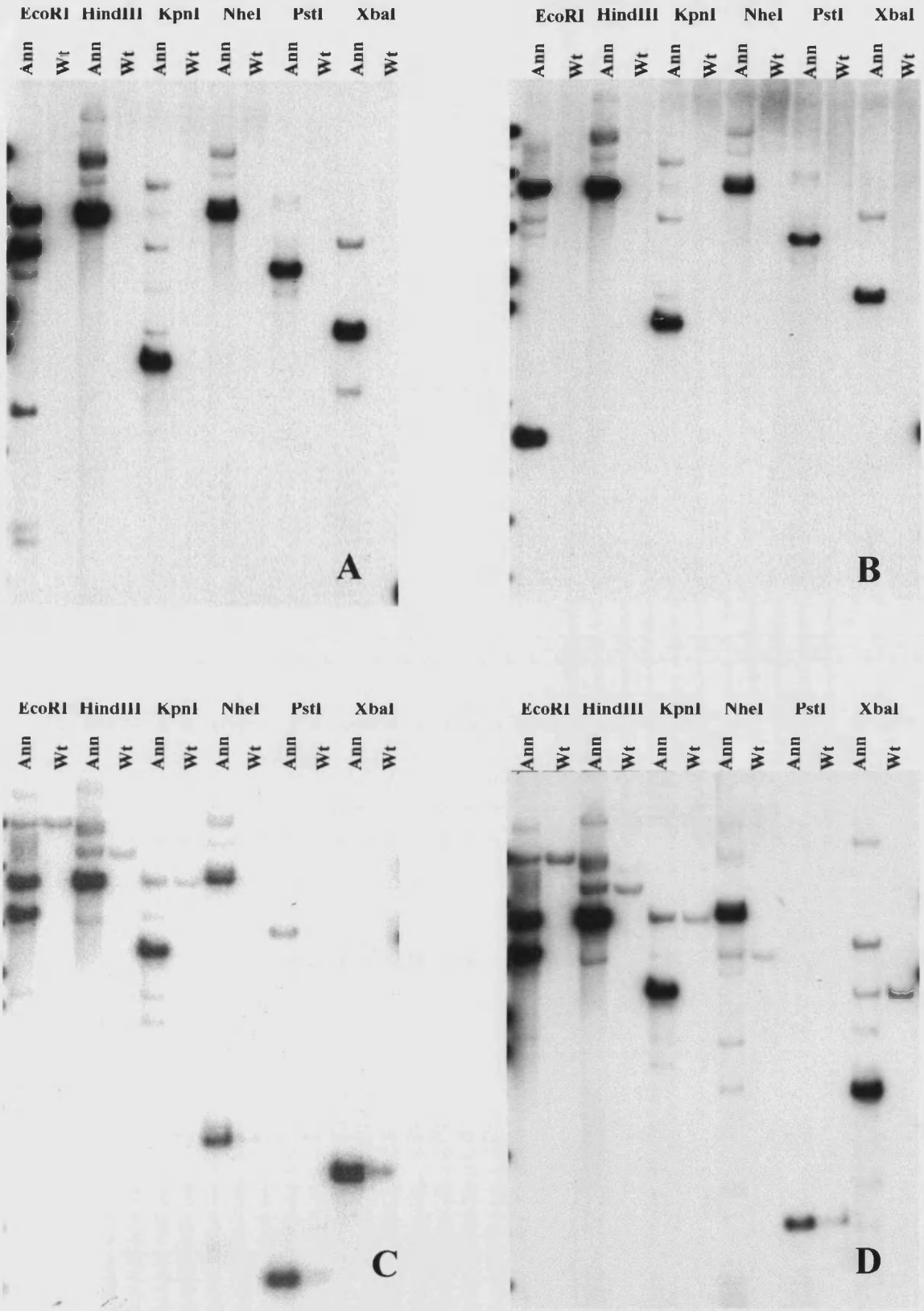

Fig. 7.2. Ann Southern blots probed with transgene fragments.
Southern blot autoradiographs showing restriction endonuclese digested Ann transgenic and wild-type control genomic DNA samples digested with a variety of restriction endonucleases prior to blotting and hybridisation with radiolabelled A) Lux 5' probe. The same blot was then stripped and reprobed consecutively with B) Lux 3', C) *H19* 5' and D) *H19* 3' radiolabelled probes.

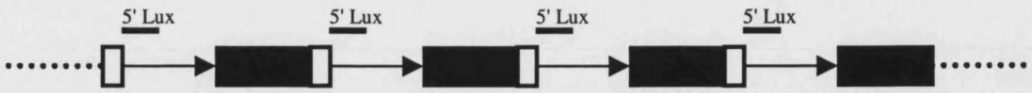

Fig. 7.3. A multiple copy transgene array.
A diagrammatic representation of a multiple A transgene copy, 'head-to-tail' array. The dotted line represents flanking genomic DNA, open boxes represent the P3 promoter, arrows represent the Luciferase reporter gene, filled boxes represent the *H19* enhancer. The 5′ Lux probe is also shown.

If two 'A' transgene copies were orientated with their 5' most ends abutting (in a head-to-head arrangement), one would expect an *Eco*RI band of approximately 1.8kb on hybridisation with the 5' Lux probe only (Fig. 7.5). This band would be ablated on double digestion with *Xba*I and *Hin*dIII (producing a variety of smaller fragments), but not *Kpn*I, *Nhe*I or *Pst*I. We can thus have a certain degree of confidence that such an arrangement does exist within the transgene array.

Two small bands (a 1.0kb and 1.1kb doublet) were observed in *Eco*RI digested samples, again probed with the 5' Lux probe. This doublet was also present in samples digested with *Eco*RI and *Eco*RI with either *Kpn*I, *Nhe*I or *Pst*I, but was ablated with *Xba*I. Digestion with *Eco*RI and *Hin*dIII removed the larger (approximately 1.1kb) band, but left the smaller (approximately 1.0kb) band intact (Fig.7.4).

Such results appear hard to reconcile, but one possibility does provide a suitable explanation. The small size of these bands would appear to limit the possibility of both, or at least one of them, being a 'junction fragment', whilst their persistence/disappearance upon double digestion suggests another 'head-to-head' arrangement. This would be possible if a stretch of

sequence containing at least one *Eco*RI site was situated between two 'head-to-head' transgene copies, resulting in 1.0kb and 1.1kb bands on 5' Lux probed *Eco*RI digests (see Fig.7.6).

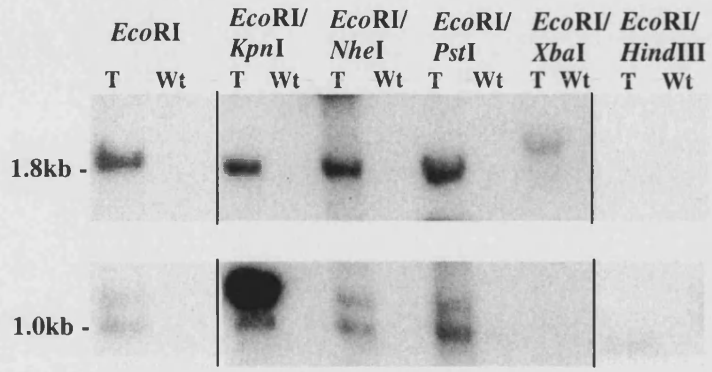

Fig. 7.4. Southern blot suggesting a 'head-to-head' transgene arrangement.
Overnight exposure of Southern blot autoradiograph showing restriction endonuclease digested Ann transgenic genomic DNA samples (plus wild-type control sample). DNA samples were digested with a variety of restriction endonucleases prior to blotting and hybridisation with radiolabelled Lux 5' probe. The band present in some of the samples at approximately 1.9kb represents a putative 'head-to-head transgene fragment whilst the doublet at approximately 1.0kb/1.1kb represents another putative 'head-to-head' fragment with intervening sequence.

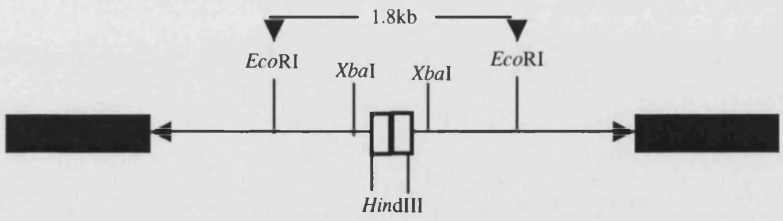

Fig. 7.5. Diagram of a putative 'head-to-head' transgene arrangement.
Such an arrangement may be present within the Ann multicopy transgene array. *Eco*RI digestion would produce a fragment of approximately 1.8kb, which would itself be cut into smaller fragments upon restriction endonuclease digestion with either *Xba*I or *Hin*dIII.

The persistance of such bands upon double digestion with *Kpn*I, *Nhe*I or *Pst*I would agree with this model, as would the ablation of both bands on digestion with *Eco*RI and *Xba*I. The loss of the 1.1kb band but not the 1.0kb band on *Eco*RI/*Hin*dIII double digestion can be explained by loss of the 5' most end of one of these transgene copies from a point somewhere between the *Xba*I and *Hin*dIII sites. In support of this, the 1.9kb (*Eco*RI digested) 'head-to-head' array band appears to have greater intensity (perhaps double) than the 1.0kb and the 1.1kb bands. This would be expected in this case since the 1.9kb band represents hybridisation of two probe units per fragment whereas only one probe unit hybridises per 1.0kb or 1.1kb fragment.

Extension of the above hypotheses leads one to resolve that at least one 'tail-to-tail' transgene copy arrangement must exist within the multiple copy array. For two 'head-to-head' arrangements to exist within one transgene array they must be interspersed by a single 'tail-to-tail' unit.

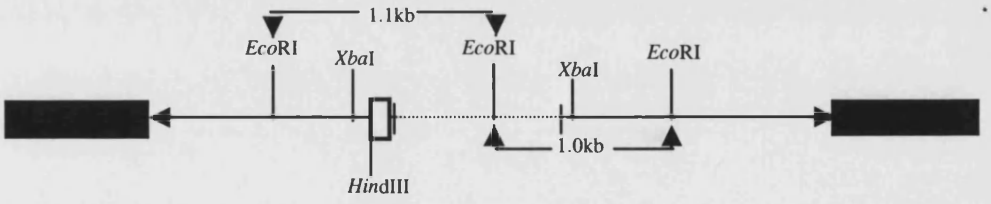

Fig. 7.6. Diagram of a modified putative 'head-to-head' transgene arrangement.
This may be present within the Ann multicopy transgene array. Owing to the presence of an *Eco*RI site between transgene copies, digestion with this restriction endonuclease would give fragments of approximately 1.0kb and 1.1kb. Both fragments would be digested further with *Xba*I treatment, but further digestion with *Hin*dIII would only cut the 1.1kb fragment leaving the smaller fragment intact.

Although the majority of bands on Southern blots can be explained as transgene repeats, 'head-to-tail', 'tail-to-tail' or endogenous DNA fragments, this still leaves the question of which fragments are candidate junction fragments. The fact that a majority of digests, on Southern blotting and hybridisation, still present more than one band which cannot be assigned to one of the above types, could suggest that some other transgene arrangement is present in the array.

Alternatively, if one or both of the terminal transgene copies was not completely intact this could allow the same probe to hybridise to both junction fragments on the same restriction digest, thus producing more than one junction fragment band on a Southern blot.

Thus far, there remains no way to conclusively distinguish between these possibilities. This creates a problem when attempting to isolate junction fragments away from other fragments internal to the transgene array in order to produce, for example, a size-restricted genomic library. The cloning of these fragments with such strategies remains a problem.

7.3.2 The array contains multiple transgene copies arranged 'head-to-tail'

An alternative to specifically isolating junction fragments, would be to clone the entire transgene array, including both junctions. Given the multiple copy nature of the transgene array, the probable size of the fragment one would need to clone would seem to exclude the use of a plasmid or bacteriophage λ library. It is more likely that either a cosmid, PAC, BAC or YAC library would be more suitable. Before deciding upon the most suitable cloning vector to use for library construction it is essential to elucidate the size of the transgene array fragment to be cloned. With this

in mind, it was decided to calculate the number of transgene copies arranged 'head-to-tail', which from existing Southern blot evidence, one would presume makes up the majority of the transgene array.

This was done by a copy number titration method, using *Kpn*I digested (hemizygous) transgenic DNA, Southern blotting and hybridisation with the 5' *H19* probe. By comparing the endogenous band of a test sample of known concentration with a transgene repeat specific band of a variety of dilutions of the same sample, the dilution factor which gives the endogenous, and transgene specific, bands the same intensity was estimated. Since the endogenous band is known to represent two gene copies, and the DNA used was from hemizygous transgenic mice, multiplication of this dilution factor by two gives an approximate value for the number of copies in a single transgene array. Dilution factors were calculated which gave a transgene-specific band corresponding to 5 to 20 transgene copies when equivalent to the endogenous band of the undiluted test sample (see Fig. 7.7).

The transgene array seemed to contain approximately 11 to 13 'head-to-tail' copies, although some difficulty in distinguishing bands in more dilute samples resulted from using smaller volumes of DNA. A more precise approach would have been to use identical volumes of serially diluted samples in order to minimise pipetting errors. Nevertheless, since the size of a single 'A' transgene unit is approximately 5.6kb, a transgene array containing at least 11 'head-to-tail' copies would be a minimum of approximately 60kb in length. If, as postulated, 'head-to-head' and 'tail-to-tail' transgene arrangements are also included, the array might be considerably larger. To clone a complete array of this nature, including

flanking sequences, a PAC, BAC or YAC library would have to be constructed. Such an operation requires considerably more expertise than that involved in making a plasmid or bacteriophage library. Furthermore, to unambiguously identify the size of fragment one would have to clone in order to obtain the complete transgene array and accompanying flanking sequence, it would be necessary to carry out Southern blotting on genomic DNA digested with a restriction endonuclease which does not cut within the transgene. Given its large size, it is probable that such a fragment would have to be separated by Pulsed Feld Gel Electrophoresis (PFGE).

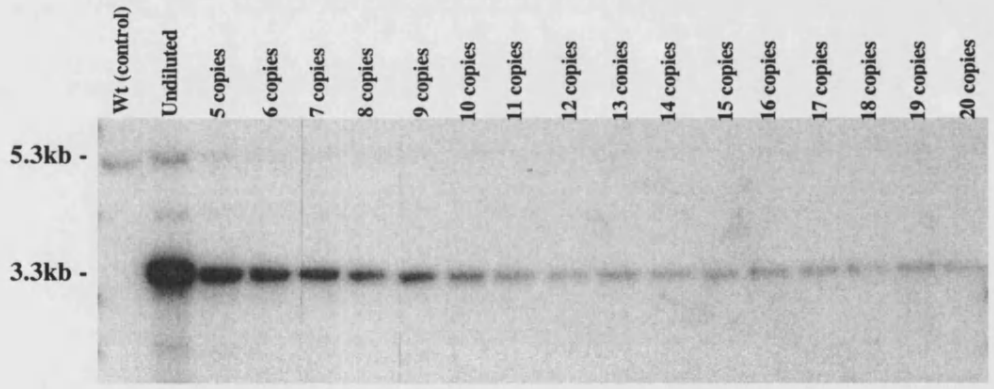

Fig. 7.7. Transgene copy number titration.
Copy number titration of 'head-to-tail' transgene copy number in the Ann transgene array. 48 hour exposure of Southern blot autoradiograph showing restriction endonuclease digested Ann hemizygote genomic DNA samples (plus wild-type control). DNA samples were digested with *Kpn*I prior to blotting and hybridisation with P^{32} labelled *H19* 5' probe. An indication of the number of copies can be obtained by comparing the 5.3kb endogenous *H19* band in the undiluted lane with the 3.3kb transgene specific band in the diluted sample lanes.

7.3.3 Attempts to clone genomic sequence flanking the transgene array were unsuccessful

Both PCR and library-based options for cloning the junctions between the transgene array and flanking genomic sequence were considered. A PCR approach was ruled out because the possible existence of 'head-to-head' and 'tail-to-tail' transgene arrangements within the array could result in the preferential amplification of internal sequence from the transgene-specific primer alone.

The most attractive alternative was that of a library from which junction-containing clones could be isolated in preference to those containing internal sequence. This precluded the use of a conventional library made from Ann total genomic DNA, since the majority of transgene-positive clones would carry only sequence internal to the multi-copy array. Instead it was decided to construct a size-restricted library in which the proportion of junction–containing clones was enriched. In this approach restriction digestion and Southern blotting of Ann genomic DNA was carried out to identify junction fragments of a suitable size for use in a plasmid library (between 2Kb and 5Kb was deemed to be an optimal trade-off between cloning efficiency and sequence length). Suitably digested DNA of the correct size range could then be purified and this used as insert material for cloning into an appropriate plasmid vector (pBluescript KS II+ (pBSKSII+) was chosen). Screening of this library with the same probe used to identify the junction fragment would be expected to yield a significant number of positive clones, especially since the library should be highly enriched for this fragment.

Endonuclease digestion was carried out on purified Ann transgenic and wild-type genomic DNAs, followed by Southern blotting and probing with a fragment specific to the 5′ end of the *H19* sequence used in the 'A' construct. A fragment of approximately 4kb, present in the *Kpn*I–digested sample, was identified as being suitable for isolation from a library enriched for *Kpn*I fragments of this size (see Fig. 7.2.). With this in mind it was decided to purify *Kpn*I-digested Ann genomic DNA of the 3 to 5kb size range for use as insert in generating a pBSKSII+ plasmid library which could then be screened using the *H19* 5′ fragment as a probe.

The first attempt at generating this library proved unsuccessful since a high proportion of the plasmids purified from surviving colonies (grown on Amp selective plates) were found to contain no insert (blue colonies on X-gal/IPTG). This is indicative of self-ligation of the pBSKS II+ plasmid.

To circumvent this problem it was decided to use plasmid vector digested with two endonucleases, rather than one. The 4kb *Kpn*I putative junction fragment was still used as the basis for the fragment to be isolated except on this occasion *Kpn*I-digested, Ann genomic DNA, in the 3 to 5kb size range was purified and then each of three aliquots re-digested with the restriction endonucleases *Apa*I, *Bam*HI and *Hin*dIII. Half of each double-digested sample was separated by gel electrophoresis, Southern blotted and hybridised with the *H19* 5′ probe fragment (see Fig. 7.8.). Following *Kpn*I, additional digestion with *Bam*HI or *Hin*dIII had no effect on the sizes of fragments identified by Southern blotting. In the sample subjected to additional digestion with *Apa*I, the 4kb putative junction fragment, as well as the 5.3kb endogenous *H19* band and the 3.3kb transgene-repeat band,

had all disappeared to be replaced by new bands of approximately 3kb, 2kb, 1.7kb and 1.5kb.

Comparison with a Southern blot performed on *Apa*I digested Ann transgenic and wild-type genomic DNA, hybridised with the *H19* 5′ fragment (Fig. 7.8), revealed that the 1.5kb band corresponded to the transgene repeat/*H19* endogenous fragment generated by *Apa*I. Furthermore, bands of approximately 1.7kb and 2.0kb were present in this blot. Whether these are identical in size to those seen in Figure 7.8. is difficult to discern. It is possible that in the *Apa*I/*Kpn*I digested sample, the bands of these sizes are generated purely by *Apa*I or alternatively these could be *bona fide Apa*I/*Kpn*I fragments, differing slightly in size from those seen in Fig. 7.8. If so, the cloning of these fragments into pBSKSII+, linearised with these enzymes, would be possible.

The band of approximately 3.0kb observed in the ApaI/KpnI digested sample is not present in that digested with *Apa*I alone, making it likely that this fragment is generated only through digestion with both endonucleases. Again, this fragment is suitable for cloning into *Apa*I/*Kpn*I digested pBSKSII+.

Having considered the possible origins of the fragments generated by the additional digestion of the purified *Kpn*I sample with *Apa*I, it was decided to attempt the generation of a pBSKSII+ library using the *Apa*I/*Kpn*I digested Ann DNA sample. A test transformation was carried out using approximately $1/10^{th}$ of a ligation reaction containing both 10ng of plasmid and insert DNA. Three quarters of the colonies surviving ampicillin

1.5 to 3.5kb (as revealed by *Apa*I/*Kpn*I digestion of miniprep DNA from 20 colonies picked).

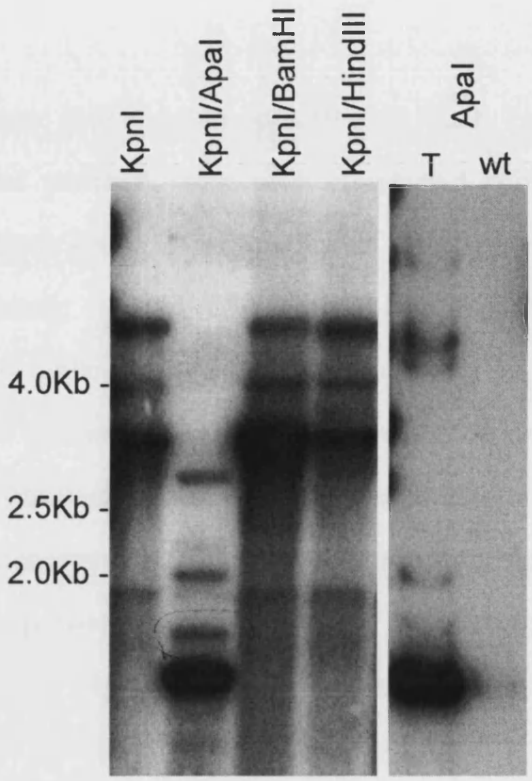

Fig. 7.8. Restricted library Southern blot.
Southern analysis of endonuclease digested Ann genomic DNA samples, purified for use in library construction. *Kpn*I digested Ann DNA of the 3 to 5kB size range was purified and redigested with either *Bam*HI, *Hin*dII or *Apa*I and samples. Hybridisation with the *H19* 5′ probe revealed novel fragments in only the *Apa*I/*Kpn*I digested sample that were also not present in Ann genomic DNA digested with *Apa*I alone.

The complete library was then transformed into electrocompetent DH5α *E. coli* and a total of 40,000 colonies plated. Of these, approximately 75% (as estimated from the test transformation), or 30,000 colonies, were predicted

to carry pBSKSII+ plasmid vector containing an insert in the desired size range. This library was screened using the *H19* 5′ probe fragment, identifying 12 positive colonies. Each of these was picked and re-plated to allow a second round of screening to be carried out using the same probe fragment

Four colonies were found to be positive in both rounds of screening. Plasmid DNA was purified from each clone and subjected to restriction digestion with *Apa*I/*Kpn*I. The results of this restriction analysis was somewhat surprising; instead of yielding two fragments: one of 2.9kb (corresponding to pBSKSII+) and another in the 1.5kb and 3.5kb (corresponding to genomic sequence), as would be expected, four bands were produced from each clone. This immediately suggested the presence of *Apa*I or *Kpn*I sites internal to the cloned genomic fragment. The positive clones could be separated into two groups depending upon the banding pattern produced by *Apa*I/*Kpn*I endonuclease digestion. Three of the clones belonged to group 1, in which bands of approximately 2.9kb, 1.4kb, 0.6kb and 0.2kb were present. Digestion of the remaining clone (group 2) yielded bands of 3kb, 1.4kb, 0.9kb and 0.2kb.

Nucleotide sequencing of the cloning junctions of a single clone from each of the two groups revealed that both inserts were derived entirely from the transgene itself, and contained no unknown sequence. The insert in the group 1 clones was an approximately 2.2kb fragment of the *H19* region found in the 'A' construct (see Fig. 7.9.) For this DNA fragment to be present in the purified *Apa*I/*Kpn*I digested genomic DNA sample, no restriction at the two internal *Apa*I sites (*Apa*I** and *Apa*I***) can have occurred.

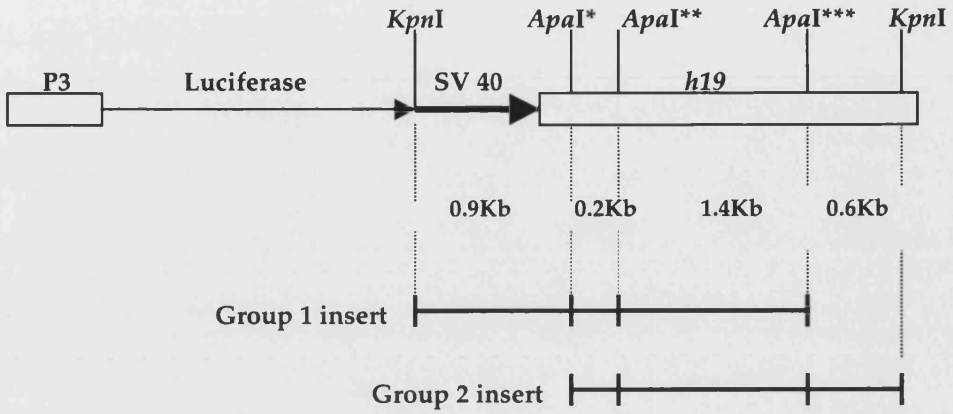

Fig. 7.9. Transgene fragments cloned by library screening.
Diagram outlining the regions present in the inserts of clones isolated by screening the Ann genomic library enriched for putative junction fragments. Inserts of both the group 1 and 2 types consisted only of sequence derived from the 'A' construct. In both cases *Apa*I sites present within the *H19* region resisted cleavage by this endonuclease.

The insert in the group 2 clone was a fragment of approximately 2.5Kb, again internal to the transgene array, except this time containing both *H19* sequence and the SV40 small t intron/polyadenylation signal present in the 'A' transgene construct. Again, to produce this DNA species in the purified *Apa*I/*Kpn*I sample, no digestion must have taken place at two ApaI sites in the *H19* region (in this case *Apa*I* and *Apa*I**).

At this stage, owing to the difficulties encountered in generating a suitable genomic library from which junction fragments could be isolated and taking into account the progress achieved in other studies through studying the location of the transgene array in the mouse genome (see Chapter 5), it was decided to abandon further attempts at that stage to clone genomic sequence flanking the transgene array.

7.4 Discussion

7.4.1 The nature of the transgene array made the cloning of flanking sequence difficult

The cloning of genomic sequence flanking the site of transgene integration can be of paramount importance, especially when a mutant phenotype results from the disruption of an endogenous gene's function by the transgene. In this case, isolation of flanking sequence is often the first step towards the identification of the gene involved.

A variety of strategies exist for the cloning of flanking sequence. In cases where multiple transgene copies are arranged in an array, a number of these strategies require prior knowledge of the structure of the array in order to allow the preferential isolation of flanking sequence rather than sequence internal to the array.

Southern blot analysis of endonuclease digested Ann genomic DNA, using transgene-specific DNA probes, indicated that the transgene in this line was present in multiple copies, and also that the structure of this multi-copy array might be extremely complicated.

One or more strongly hybridising bands were identified in each endonuclease digested sample, of a size which indicated that multiple transgene copies, arranged in a 'head-to-head' fashion, were present in the array, as is often the case in transgenic mouse lines [55]. Through a copy number titration, it was elucidated that at least 11 transgene copies were orientated in this fashion.

Further analysis and interpretation of bands present on Southern blots allowed us to elucidate that at least two 'head-to-head' and one 'tail-to-tail' transgene arrangements were likely to be present in the array. Despite this a large proportion of the bands present on the various Southern blots remained unaccounted for, although it was thought probable that a number of these bands represented junction fragments containing flanking genomic DNA.

The highly complex nature of the Ann transgene array, as revealed by Southern blotting, made selection of a strategy for isolating flanking sequence difficult. It was decided to construct a genomic DNA library in which the proportion of fragments, identified as containing flanking sequence, would be highly enriched. In this way the isolation of clones containing flanking sequence, rather than only sequence internal to the transgene array, should be highly favoured.

To do this, endonuclease digestion with a suitable enzyme was performed and DNA species of a specific size range, previously identified by Southern blotting as containing a putative junction fragment, were purified. This DNA sample was then further digested with another endonuclease, generating junction fragments with different end sequences, thus facilitating 'sticky-end' cloning and minimising self-ligation of plasmid vector. This library was then screened using a transgene-specific probe and positive clones were identified.

Unfortunately the insert sequences of all of the clones isolated were found to be internal to the transgene array, and did not contain any flanking genomic sequence. Furthermore, it was discovered that these inserts

contained *Apa*I restriction endonuclease target sites that escaped digestion during the preparation of the insert DNA. The reason for incomplete digestion of genomic DNA at these sites probably lies with a resistance of these specific sites to endonuclease digestion. This is a commonly observed phenomenon wherein specific endonucleases do not digest genomic DNA at 100% of their specific target sites. Indeed the *Apa*I restriction endonuclease is known to be sensitive to CpG methylation in certain cirumstances.

The identification of a number of restriction sites present in the transgene that are resistant to endonuclease cleavage poses as serious problem in the interpretation of the Southern blots used to elucidate the structure of the transgene array. Bands that cannot be attributed to either a transgene repeat or endogenous *H19* sequence could be either a junction fragment or may derive from incomplete digestion of genomic DNA, distinguishing these possibilities could be either impossible or at best extremely difficult and uncertain.

The substantial difficulities encountered in attempting to clone transgene flanking sequence was considered in relation to the progress achieved in studying the location of the transgene array in the mouse genome (see Chapter 5), it was thus decided to abandon further attempts to clone genomic sequence flanking the transgene array.

7.4.2 Alternative strategies could have been used to clone flanking sequence

That the transgene is present in the genome in a multiple-copy array and the structure of this array appears to be extremely complex ruled out a

number of possible strategies for isolating genomic sequence flanking the site of transgene insertion.

Owing to further uncertainties as to the nature of genomic fragments originally thought to contain flanking sequence, as revealed by our unsuccessful cloning attempts, it appears that PCR and library based methodologies that specifically target junction fragments and eliminate internal transgene sequence may well be inherently flawed. The successful isolation of such fragments may, rather than providing unknown flanking sequence, merely reveal that this fragment is generated through unsuccessful restriction digestion of internal transgene sequence.

Alternative strategies may provide a more straightforward route to the isolation of flanking sequence. For example the cloning of the complete array, including flanking regions, may be possible through the construction of either a PAC, BAC or YAC library. This would allow the isolation of both junctions that would be advantageous, for example, in elucidating whether any genomic sequence has been deleted at the site of transgene integration or by providing startpoints for chromosome walks out from the transgene in both directions.

CHAPTER 8 : A PUTATIVE MALE STERILITY MUTANT ARISING FROM TRANSGENE INSERTIONAL MUTAGENESIS

8.1 Introduction

8.1.1 An overview of spermatogenesis

The production of germ cells in the male, by the process of spermatogenesis, takes place in its entirety in the seminiferous tubules of the testes. Spermatogenesis can be divided into a number of stages essentially involving three distinct germ cell types: the spermatogonia, spermocytes and spermatids, with each cell type found concurrently but occupying a distinct position in the tubule (reviewed in [275]).

Found at the periphery of each seminiferous tubule are the spermatogonia. This is the earliest germ cell type and can itself be subdivided into three types: stem cells, mitotically dividing cells and cells undergoing differentiation. Formed by the differentiation of mature spermatogonia that have replicated their DNA, primary spermatocytes are located toward the lumen of the seminiferous tubule. Secondary spermatocytes are generated by meiotic division, a further round of which gives rise to the haploid round spermatids. This third germ cell type is found at the lumenal aspect of the tubule. Round spermatids differentiate into elongated spermatids and finally spermatozoa through the process of spermiogenesis, in which the genome is re-packaged with protamines.

A variety of somatic cell types are found in the testes and are important in spermatogenesis, including the Sertoli cells that reside towards the periphery of the seminiferous tubule. These cells play an important role in regulating spermatogenesis through paracrine interactions with germ cells [276].

8.1.2 Male infertility in humans

It has been estimated that 10% of couples are affected by infertility, with approximately half of all cases attributable to the male partner [277]. Infertility in males arises through a variety of mechanisms but it is often associated with a complete absence of sperm (azoospermia), a gross reduction in sperm numbers (oligozoospermia), or a loss of motility (asthenozoospermia). A high proportion of azoospermic, oligozoospermic and asthenozoospermic cases are said to be idiopathic, in that no obvious cause has been identified. Increasingly it is being found that many such cases can be attributed to genetic defects [278].

These findings take on an elevated level of importance given the advent of the intracytoplasmic sperm injection (ISCI) method for assisted reproduction, since this method may facilitate transmission of a genetically determined infertility trait to a male offspring [279].

8.1.3 Genetic causes of infertility in man

Recently, genetic abnormalities have been increasingly implicated in spermatogenic defects. Often, abnormal spermatogenesis is only one of a cohort of abnormalities associated with a particular genetic disease (e.g. Cystic fibrosis [280]) but in other cases this may be the sole phenotype. The genetic basis of such defects can involve either chromosomal aberrations or the mutation of a single gene.

Chromosomal defects both in number and in structure have been found to be involved in male sterility. Usually with such defects more than simply the fertility of the individual is abnormal. This is unsurprising given that chromosomal abnormalities often involve multiple genes. Illustrating the

fact that defects in both chromosomal number and structure can interfere with spermatogenesis, approximately 5% of azoospermic and 15% of oligozoospermic males exhibit an abnormal karyotype [281].

Numerical chromosomal disorders involving either polyploidy or aneuploidy are responsible for a number of syndromes in which male infertility is one of several abnormalities observed. Most such syndromes involve the sex chromosomes although a number involving only autosomes have been identified [282].

The most common chromosomal abnormality observed in azoospermic men (affecting 7 to 13% of the azoospermic population) is Klinefelters syndrome in which an XXY karyotype is classically seen [283]. Amongst the variety of abnormalities observed in these patients are sclerosis and hyalinization of the seminiferous tubules, an absence of spermatogenesis and a predomination of sertoli cells.

An example of an autosomal aneuploidy affecting spermatogenesis is Down's Syndrome in which male patients are almost always sterile. Histopathological defects include spermatogenic arrest, a reduction in germ cell numbers and hyalinized tubules [284].

Robertsonian translocations are the most common structural chromosomal abnormality found in infertile males, with an approximately ten-fold higher incidence in this subset of the population. In addition, paracentric and pericentric inversions are observed at an eight-fold higher incidence and reciprocal translocations at a five-fold higher incidence in infertile males as compared with normal individuals [282].

Deletions on the long arm of the Y chromosome have been associated with approximately 15% of azoospermic and 10% of oligozoospermic men [285]. The absence of genetic recombination (outwith the pseudoautosomal region) on the Y chromosome has meant that gene mapping in this region has relied upon cytogenetic analysis rather than linkage data [286, 287]. Cytogenetically-defined deletions identified in infertile men have been refined using Y-specific Southern blot probes and PCR-amplified STSs (sequence-tagged sites) [288], to show that rather than a single crucial locus, at least three regions of the human Y chromosome, and several genes therein, are essential for normal spermatogenesis [289]. These regions are termed AZFa, AZFb and AZFc and candidate spermatogenesis genes have been identified in both the AZFb and AZFc loci.

Located within the AZFc region is a gene family named DAZ/SPGY, and is the sequence most frequently deleted in azoospermic and oligozoospermic men [285, 290, 291]. As such, DAZ/SPGY appears a strong candidate for the gene located within the AZFc that is essential for normal spermatogenesis.

Amongst the genes located within the AZFb region are sequences belonging to the RBM gene family, with deletions of this region preventing the expression of the RBM protein [292, 293]. Strikingly, RBM and DAZ/SPGY both encode proteins that contain an RNA recognition motif (RRM) and are therefore likely to bind RNA [294]. It has thus been proposed that both proteins are involved in the processing of RNAs essential for spermatogenesis [295]. In support of this hypothesis, RBM protein is present in all transcriptionally active germ cell types, with levels peaking in spermatocytes [293] (the cellular location of DAZ has not been

described). Whether the two proteins are involved in the same process remains to be determined since the biological functions of both are unknown.

The DAZLA gene is an autosomally located DAZ/SPGY homologue and has a gonad-specific expression pattern [296]. No mutations in this gene have yet been identified in either man or mouse and as such the possible role of the DAZLA protein in spermatogenesis, although likely, remains unknown. In addition, RBM is closely related to the autosomal hnRNPG gene that is a member of the hnRNP protein family. Interestingly, these proteins are known to bind polyadenylated RNA in the nucleus and sometimes during nucleocytoplasmic transport [297]. It thus appears that the control of RNA metabolism could be extremely important in spermatogenesis and that a group of several proteins are likely to be involved in this process.

8.1.4 Using the laboratory mouse to investigate male infertility

The identification of genes important in spermatogenesis has been greatly aided by the availability of both spontaneous and targeted mouse mutants. The roles in human spermatogenesis of most of the genes identified in this way remains unknown, but the fact that these genes can now be tested for mutation in males suffering idiopathic infertility represents a significant advance in tackling this condition.

Similar to the situation in humans, a number of regions have been identified on the mouse Y Chromosome that are essential for spermatogenesis. Again, these regions have been mapped using mice bearing Y chromosome deletions and rearrangements [298].

Two critical regions have been defined, *Spy* and *Smy*, with the deletion of either leading to infertility as a result of abnormal spermatogenesis. The *Spy* region is required for spermatogonial proliferation and has been accurately mapped on the small arm of the mouse Y chromosome using an informative transposition event [298-300]. Although no *Spy* genes have been isolated, several good candidates have been identified. These include *Ube1y*, which encodes a ubiquitin-activating enzyme that may be involved in degrading histones during postmeiotic chromosome condensation in round spermatids [301, 302].

The *Smy* region, again defined by Y chromosome breakpoints, is required for normal sperm head morphology [303]. In mice lacking this region spermatogenesis does proceed through the meiotic stages but the animals are infertile due to the abnormality of sperm heads. In this case a candidate gene (*Ssty*), present in several copies in the Smy region, has been isolated [304].

A homologue of the human DAZ/SPY gene has not been identified on the murine Y chromosome, although an autosomal *Dazla* has been described [305, 306]. As with all mammalian species, including man, the mouse Y Chromosome contains the *Rbm* gene family, although its expression pattern in mice differs to that in man, suggesting possible different roles [307].

The fact that Y chromosome deletions have only been identified in 8 – 13% of idiopathic infertility cases suggests that the mutation of autosomal genes may make a significant contribution to the remainder of cases [288]. Descriptions of autosomal genes implicated in idiopathic male infertility however, remain limited to date. This is largely due to the fact that genetic

mutations causing male infertility are unlikely to be inherited and also because small family sizes make detailed genetic analysis of such mutations difficult.

Much has already been learned about the biological processes that are important to spermatogenesis and although a wide variety of gene products have been implicated in male sterility, many of which are involved in highly disparate biochemical pathways, it has become clear that certain pathways in particular (including, as described, the control of RNA metabolism) are critical at different stages of spermatogenesis in the mouse.

Meiosis is one of the key processes taking place during spermatogenesis and a number of processes exist that are specific to meisosis as opposed to mitosis. Spermatogenic defects arising from the targeted mutation of genes involved specifically in meiosis is therefore unsurprising. That the mutation of a number of meiosis-specific genes affects only spermatogenesis and not oogenesis [308, 309], is though rather more surprising and suggests sex-specific differences in meiosis.

Furthermore, a number of genes that are expressed outwith the testes have been mutated by gene targeting and male null mice found to be infertile due to defective meiosis. Included in this group are the DNA mismatch repair genes *Pms-2* [308] and *Mlh1* [309]. This suggests that although such genes are important in both germ cells and somatic cells, genetic redundancy may limit any phenotype only to meiosis.

As mentioned, the *Ube1y* gene, which encodes a ubiquitin-activating enzyme, represents a candidate for the Y Chromosome-specific *Spy* gene [301, 302]. Mice bearing a targeted deletion of the *mHR6B* gene are defective in postmeiotic chromosome condensation [310]. mHR6B is known to ubiquitinylate histones [311] and is thought to be involved in replacing histones with transition proteins prior to genome repackaging in round spermatids. That a number of other proteins involved in the ubiquitin pathway may be essential for spermatogenesis seems very probable.

A number of molecules involved in cell signalling pathways have been found to be essential to spermatogenesis, again through the generation of gene knockouts. Many of these molecules are expressed by the somatic sertoli cells but exert effects on the germ cell lineage. These include the signalling molecules BMP8B [312] and DHH[313] which, like the DNA mismatch genes, have widespread expression patterns but their deletion only affects spermatogenesis.

That the targeted deletion of a number of autosomal genes in the mouse affects only spermatogenesis reinforces the suggestion that a high proportion of idiopathic infertility cases in the human population may have a genetic basis. Such mouse mutants may prove to be invaluable mouse models for human infertility in man whilst also contributing to our understanding of the processes underlying spermatogenesis. The identification of further genes essential for spermatogenesis in this way also provides targets for mutational screening in infertile men.

8.1.5 A putative male sterility mutant identified from the screen for insertional mutants

Amongst the plethora of *bone fide* and putative transgene insertion mutants identified by the large scale screening programme (detailed in Chapter 3) were two lines, Ob and Grace in which the breeding of male homozygous transgenics proved impossible and it seems possible that homozygous transgenic males are infertile in these lines.

Studies to confirm male sterility in these lines has concentrated on Ob, with further breeding data reinforcing this suggestion. This chapter details these data and additional investigations carried out to further characterise both the molecular and physiological basis of the phenotype observed in this line.

8.2 Materials And Methods

8.2.1 Interphase FISH

Interphase FISH was carried out essentially in the same manner as FISH on metaphase chromosome spreads (as described in sections 2.2.18-2.2.22) except that the Giemsa banding stage was omitted. Additionally, interphase (rather than metaphase) chromosome spreads were chosen for image capture following FISH. Interphase spreads are always more abundant on slides generated by the method used.

8.2.2 Histological analysis

Histological analysis of mouse testis was carried out by W.R. Bennet, A. Ward, A. Melidou and N. Ridouta in the manner described in sections 2.2.23-2.2.25.

8.2.3 Linkage mappimg

Linkage mapping was carried out by A. Ward using the microsatellite markers D4Mit31, D6Mit16, D8Mit74 and D12Mit14 (described in section 5.2.1) and PCR conditions detailed in section 2.2.16. Samples were analysed by large-scale polyacrylamide gel electrophoresis (section 5.2.3) followed by silver staining (section 5.2.5).

8.3 Results

8.3.1 No Ob homozygous males have bred successfully

As discussed in Chapter 3, a two-step breeding strategy was adopted in order to screen for recessive mutations generated by transgene insertional mutagenesis. Intercrossing of hemizygous transgenic mice facilitated the generation of animals that were homozygous for the transgene whilst a second step involving backcrossing of transgenic offspring against a non-transgenic F1(C57/CBA) allowed the exact genotype of the transgenic parent (hemizygous or homozygous transgenic) to be identified. Confirmation of homozygosity required a transgenic animal, upon backcrossing against an F1(C57/CBA) partner, to produce at least 11 transgenic pups without any non-transgenics ($p=0.001$, using the χ^2 test). The identification of at least one homozygous mouse of each sex bearing no detectable phenotype was deemed enough to eliminate this line from further testing.

In the case of the Ob line, a homozygous female mouse was identified through backcrossing, whereas, despite the identification of 23 hemizygous males, no homozygotes successfully bred (see Table 8.1.). Interestingly, a further 13 male animals set up for backcrossing (36% of the total set up) failed to breed. Each of these non-breeding males did though succesfully mate with females as evidenced by the observation of copulation plugs. This immediately suggested male sterility, rather than a sex-linked embryonic lethality, as the cause of the failure to successfully identify male transgenic homozygotes.

♂		♀	
T/T	T/wt	T/T	T/wt
0	23	1	7

Table 8.1. Ob breeding data.
Breeding data for Ob transgenic mice tested for genotype by backcrossing. T/T = homozygous transgenic, T/wt = hemizygote.

According to Mendelian genetics, one would expect 2/3 of all transgenic males generated by intercrossing of transgenic hemizygotes, to themselves be hemizygous and 1/3 to be homozygous. The probability of generating no homozygous male mice from intercrossing by chance was calculated as less the 1 in 1000 ($\chi^2 = 11.50$ –for 1 degree of freedom this gives a $p<0.001$). In other words there is less than a 1 in 1000 chance that the failure to generate homozygous transgenic Ob null males by hemizygous intercrossing is not associated with their genotype.

8.3.2 Interphase FISH shows non-breeding males to be homozygous for the transgene

Despite statistical evidence that the inability to identify Ob homozygous males was not through chance, and even though 13 transgenic males (36% of the total set up) failed to breed, there was no solid evidence to support the hypothesis that this was due to male sterility rather than, for example, sex-linked embryonic lethality.

It was decided to confirm that the non-breeding Ob transgenic males were homozygous for the transgene by hybridisation of a transgene-specific probe to interphase chromosome spreads generated from these mice. In

the case of a homozygous transgenic mouse, one would expect to observe two transgene specific signals per chromosome spread as compared to one in spreads from hemizygous control mice (see Fig 8.1.).

Analysis of two non-breeding males in this manner confirmed that both were homozygous for the transgene. This not only proves that Ob male homozygotes are viable but also adds support to the hypothesis that such mice are sterile especially since the the hemizygous transgenic control animals were fertile.

8.3.3 Quantitative and histopathological analysis of non-breeding Ob males reveals a reduction in abundance of specific spermatogenic cell types

Testis from non-breeding (putative homozygous transgenic) and fertile (hemizygous transgenic) littermates were weighed and vas deferens squeezed in order to detect the presence of mature sperm (work carried out by W.R. Bennett, A. Melidou, N. Ridout and A. Ward). It was found that testis from two non-breeding (putative homozygous transgenic) animals examined were much reduced in mass (less than half that of fertile hemizygous transgenic littermates) and furthermore that mature sperm were either absent or present at very low levels in comparison to fertile hemizygous transgenic littermates.

A histological analysis was carried out on haematoxylin and eosin stained, transverse testis sections (work carried out by W.R. Bennett, A. Melidou, N. Ridout and A. Ward). Briefly, all spermatogenic cell types (spermatogonia, spermatocyctes, spermatids and spermatozoa) were identified although

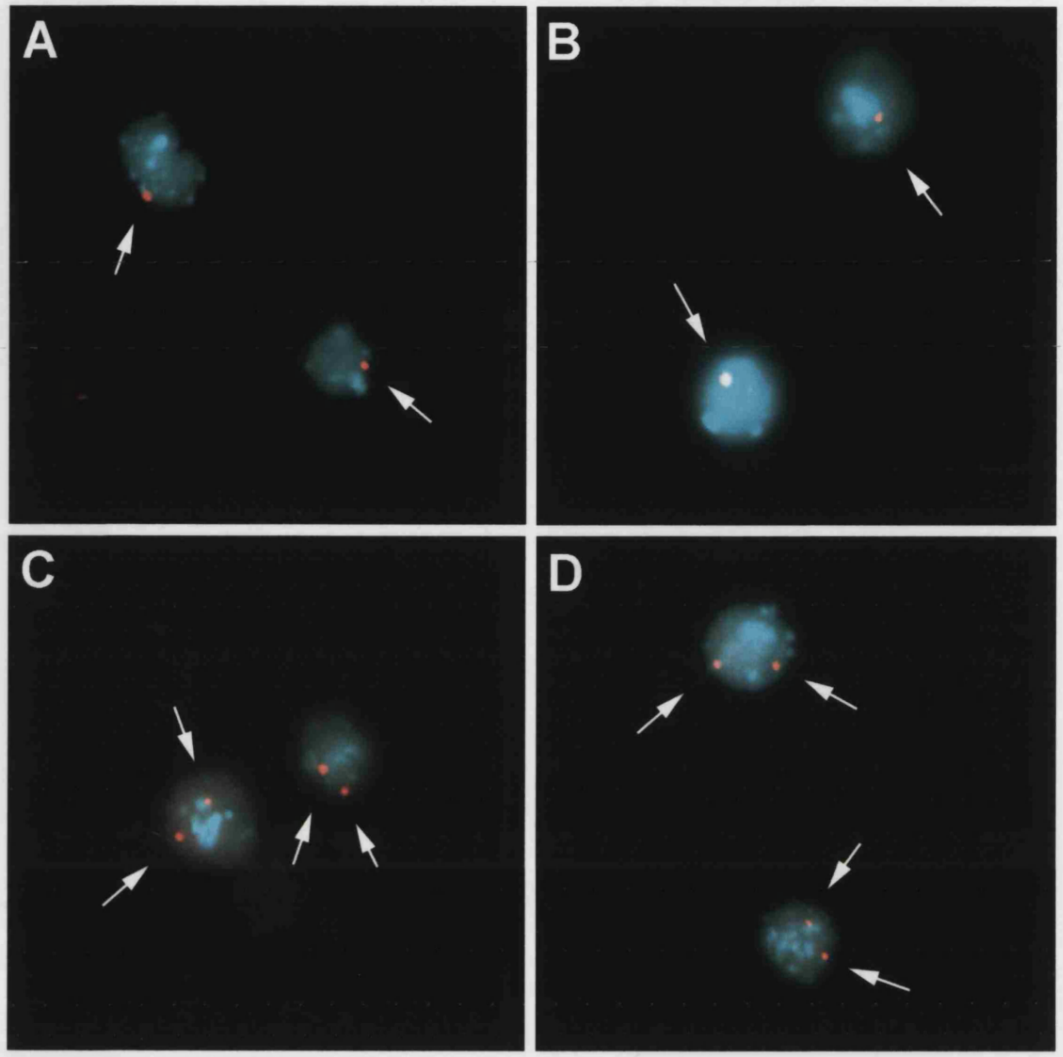

Fig. 8.1. Ob interphase FISH.
Interphase chromosome spreads from fertile Ob transgenic hemizygous males (A and B) and non-breeding transgenic littermates (C and D). An inserted transgene is identified by a fluorescent spot (indicated by an arrow) and is present on sister chromatids in spreads from non-breeding males but on only a single chromatid in spreads from the fertile transgenic animals.

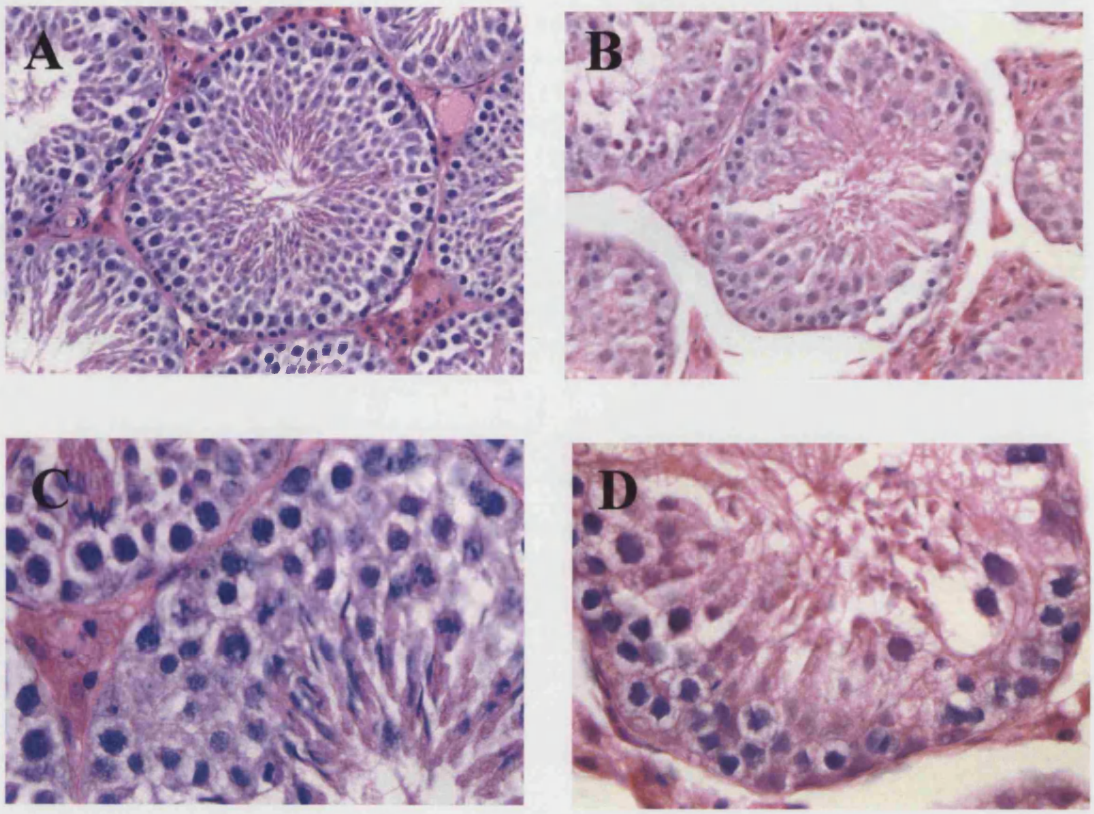

Fig. 8.2. H and E stained sections from wild-type (A and C) and mutant (B and D) Ob testis at 400x (A and B) and 1000x (C and D) magnification. Although a number of tubules from the mutant animals appear normal, a proportion display morphological abnormalities in the form of extracellular spaces as well as deficiencies in a variety spermatogenic cell-types.

some morphological abnormalities, in the form of numerous extracellular spaces, were observed (see Fig. 8.2.). In those tubules more severely affected, the organisation of spermatogenic cells was poor.

A variety of measurements were taken from the testis sections. In sterile males seminiferous tubule diameter was significantly reduced in comparison to sterile (hemizygous transgenic) littermates. Quantification of spermatogenic cell types (subdivided into four easily distinguishable classes: spermatogonia, spermatocytes, early spermatids and mature spermatozoa) identified a significant reduction in the total number of spermatogenic cells per tubule in sterile males as compared to wild-type littermates with a reduction in each of the four cell classes. Furthermore, when represented as a percentage of the total cell number, there was found to be a significant reduction in the relative abundance of spermatids and especially mature spermatozoa (with an accompanying increase in the relative abundance of the other two cell types).

8.3.4 Mapping the location of the transgene in the Ob line by G-banding and FISH

Given the strong likelihood that the spermatogenic defects and male sterility observed in the Ob line results from transgene insertional mutagenesis of an endogenous gene, it was decided to attempt mapping the site of transgene integration. Successful identification of a map position would allow an assessment to be made on possible candidate genes located around the site of transgene insertion.

A chromosomal mapping strategy was pursued using fluorescence *in-situ* hybridisation of Ob metaphase chromosome spreads with a transgene-

specific DNA probe fragment. This, carried out alongside karyotyping by G-banding, would allow a tentative identification of the chromosome and the particular chromosomal region into which the transgene had integrated. Production of metaphase chromosome spreads, G-banding and FISH was carried out as described in sections 2.2.18 – 2.2.22. A DNA probe containing the P3 Lux/CCD regions used in the 'O' construct was used for FISH.

Successful G-banding and FISH showed that in the Ob line, the 'O' construct had integrated slightly to the centomeric side of the middle third of a medium sized chromosome (see Fig. 8.3.). This chromosome appeared to have either one thick or two darkly staining bands in its centre and another located in its telomeric third. Comparison with standard mouse karyotypes and karyotype ideograms (see Fig. 5.4.) allowed the transgene-specific chromosome to be narrowed down to one of four strong possibilities: chromosomes 4, 6, 8 and 12.

8.3.5. Microsatellite linkage mapping confirms chromosome 8 as harbouring the transgene

In order to identify which of chromosomes 4, 6, 8 and 12 the transgene had integrated (if any) a linkage mapping strategy, using microsatellite markers, was employed. Microsatellite markers (D4Mit31, D6Mit16, D8Mit73 and D12Mit14) located on the central region of each of the four candidate chromosomes were selected. These markers had already been confirmed as size-polymorphic between the two founder strains as part of studies conducted on the Ann transgenic line (see section 5.2.1).

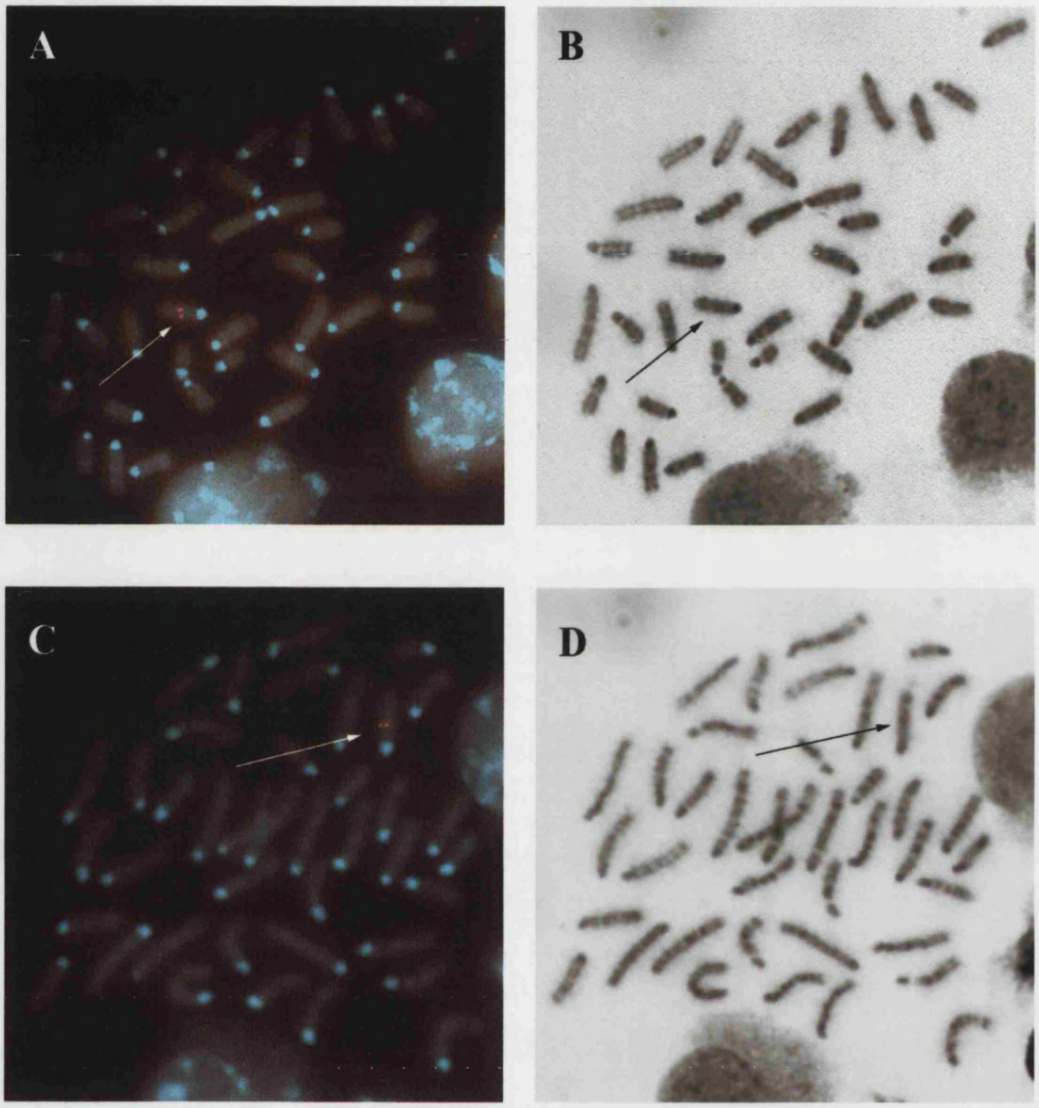

Fig. 8.3. Ob FISH and G-banding.

Chromosomal mapping of the transgene insertion by FISH and G-banding of Ob metaphase chromosome spreads. Fluorescence *in situ* hybridisation of Ob metaphase chromosome spreads using a transgene specific probe fragment, (A) and (C). The site of transgene insertion is identified by a fluorescent spot on sister chromatids of the same chromosome (indicated by arrow). G-banding of the same spreads is shown in (B) and (D), again the site of transgene insertion is indicated.

Transgenic founders had been generated using F1 embryos derived from crossing C57BL/6J and CBA/Ca mice. Interbreeding of subsequent generations meant that all available transgenic mice had genetic backgrounds of a mixed C57 and CBA constitution. To be informative for possible intercross mapping analysis, it was essential for breeding mice to have suitable haplotypes for the microsatellite markers being tested. Such mice were identified by marker typing and crosses set up. Transgenic parents confirmed as being of the F1(C57/CBA) haplotype for the marker being tested, were bred with non-transgenic parents, again of the F1(C57/CBA) haplotype for the marker (marker typing of parents and offspring was carried out by W.R. Bennett, A. Melidou, N. Ridout and A. Ward).

For the markers D4Mit31 and D12Mit74, not enough informative offspring were generated to allow statistical analysis to be conducted. The fact that hemizygous transgenic mice of both the C57/C57 and CBA/CBA haplotypes for each marker were identified within the small number of samples analysed, does though strongly suggest that these markers are not linked with the transgene. The possibility of partial linkage cannot be discounted but seems unlikely since the chromosomal position of the transgene (as determined by FISH) and the markers should correlate reasonably well.

Enough informative offspring were generated for the microsatellite markers D6Mit16 and D8Mit73 to allow a statistical analysis to be carried out. In the case of D6Mit16 a χ^2 value of 0.92 was calculated for the null hypothesis that this marker and the transgene are unlinked. This is less than the critical value at the p=0.05 level (critical value = 11.1, with 5

degrees of freedom), confirming there is no significant difference between the observed and expected values for non-linkage. We can thus conclude that the transgene and marker D6Mit16 are unlinked.

In the case of D8Mit73, using the observed and expected values for the null hypothesis of non-linkage with the transgene (following the Mendelian ratio of 1:2:1, see table 8.2.) a χ^2 value of 53.8 was calculated using the special χ^2 equation for intercrossing outlined in the book *Mouse Genetics* [1]. This suggests that the probability of non-linkage between the transgene and this microsatelite is <0.0001. We can therefore conclude that the transgene is linked with D8Mit73 and therefore that the transgene is located in the central portion of mouse chromosome 8.

Transgene status	No. offspring	D8Mit73		
		C57	F1	CBA
wt/wt	11	11	0	0
T/wt	4	0	4	0

Table 8.2. Ob intercross mapping data.
Small scale intercross analysis shows possible co-segregation of the transgene and the chromosome 8 microsatellite marker D8Mit73.

8.4 Discussion

8.4.1 Ob: a recessive male sterility mutant caused by transgene insertional mutagenesis

During the large-scale screening programme for insertional mutant phenotypes conducted on a group of transgenic mouse lines one line was identified in which male homozygous transgenic mice could never be identified by backcross breeding analysis. Sufficient numbers of Ob transgenic males were generated by hemizygous intercrossing to confirm that this lack of homozygotes was significant. The fact that 38% of transgenic males, set up for backcrossing mated successfully (as evidenced by coital plugs) but produced no offspring, strongly suggested that the failure to identify male homozygotes rested with their inability to breed, rather than a sex-linked lethality. In support of this hypothesis, two non-breeding male transgenics were genotyped by interphase FISH analysis that confirmed these mice as homozygous transgenics. In two other non-breeding males the testis mass was less than half that of fertile, hemizygous siblings, and mature sperm were either absent or found in very low numbers in the vas deferens of these non-breeding males. Thus the Ob line most likely represents a recessive male sterility phenotype caused by transgene insertional mutagenesis.

8.4.2 Histological analysis of Ob testis suggests a defect in spermatogenesis

A histological analysis was conducted on testis from infertile transgenic males. It was observed that the seminiferous tubules of infertile mice were not only significantly smaller in diameter than in their fertile siblings (a trait which has been associated with male sterility in the *weaver* mutant), but that they also exhibited a significant difference in the relative abundance of the various spermatogenic cell-types. Mature spermatozoa,

and to a lesser extent early spermatids, were found in much reduced numbers, relative to total spermatogenic cell numbers, when compared with fertile litter-mates. This suggests that the defect present in Ob homozygote transgenics may be specifically involved with the transition of immature spermatogenic cells, such as the spermatogonia or spermatocytes, to the more mature cell types found towards the lumen of the seminiferous tubule (i.e. the spermatids and spermatocytes).

As discussed in the introduction to this Chapter, the causes of male sterility, as identified through studies on mutant mice, often belong to specific processes which are of paramount importance to spermatogenesis and the maturation of spermatogenic cells. One such process is meiosis, which is actively occurring in the spermatocytic cell population. A number of male sterile mice have been identified which display defects in meiosis as a result of disruption to genes involved in this process (i.e the DNA missmatch repair genes *Pms-2* [308] and *Mlh-1* [309]). A disruption to meiotic divison could well be responsible for the reduction in post-meiotic spermatogenic cell types observed in Ob homozygous males.

Alternatively a defect in post-meiotic chromatin condensation, which takes place in the round spermatid cells, may be the source of the Ob phenotype. Indeed one noteable male-sterile line, mutated in the *mHR6B* gene (involved in the ubiquitinylation of histones) displays defects in this process [310].

The unexplained extracellular spaces observed in the seminiferous tubules of Ob mutant mice could result from the degeneration (and subsequent phagocytosis by Sertoli cells) of spermatogenic cells which cannot progress

to the next stage of spermatogenesis (e.g. due to meiotic arrest). That similar such extracellular spaces are also observed in ageing mice [314] means that studies must be carried out in Ob mice of a variety of ages to eliminate an age-related effect.

One realistic alternative to a spermatogenic-cell-specific defect in Ob homozygotes is the possibility that the phenotype may arise from an abnormality in Sertoli cell function. These cells are essential for spermatogenic cell survival and many cases of defective spermatogenesis have been associated with defects in the Sertoli cell population (e.g. the *weaver* mouse mutant [315]). Further such studies should therefore include an analysis of Sertoli cell numbers which would be aided through the use of Sertoli cell-specifc staining or antibodies (preliminary data has been obtained using an anti-WT1 antibody that reveals a normal number of Sertoli cells).

8.4.2 The transgene in Ob mice maps to the central region of Chromosome 8

Through a combination of FISH mapping on metaphase chromosome spreads, and linkage mapping using microsatellite markers, the location of the integrated transgene in the Ob line was identified as the central third of Chromosome 8.

Inspection of the mouse chromosome committee consensus map for this chromosome [219] reveals one obvious candidate. The *calmegin* gene maps at offset 38.0cM, in the central third of Chromosome 8 [316], and encodes a testis-specific endoplasmic reticular (ER) protein that is homologous to the ubiquitous ER chaperone calnexin [317]. Calmegin has itself been shown to bind to nascent polypeptides during spermatogenesis [318] and is

expressed in early pachytene spermatocytes and round and elongating spermatids [319]. Expression of Calmegin is undetectable from the spermatid maturation phase. Such an expression pattern would not be incompatible with the cell types affected in Ob mutants i.e. spermatid stages onwards.

Calmegin function has been disrupted by gene targeting and was found to be required for sperm fertility, with homozygous null males displaying reduced fertility [318]. Spermatogenesis in these mutants though, is morphologically normal, which is not in keeping with our observations of Ob mutants. The specific defect in Calmegin null mice was found to be one of adherance to the zona pellucida of the egg, suggesting that this protein acts as a chaperone for sperm-surface proteins which mediate interactions between sperm and egg.

Although the map position and expression pattern of the *calmegin* gene is compatible with it being the gene mutated in Ob mice, when mutated the resulting phenotype does not correlate strongly with that observed in Ob mutants. Despite this, testing of this gene as an Ob candidate by, for example, Northern analysis still seems warranted.

Elimination of *calmegin* as the gene mutated in Ob and the lack of other strong candidates in the region of Chromosome 8 to which the Ob transgene maps may indicate that a hitherto unidentified gene has been disrupted in this line. In this case, the isolation of genomic DNA flanking the site of transgene integration will be of paramount importance for the identifiction of the gene mutated in this line.

CHAPTER 9: DISCUSSION

A screen of 74 transgenic mouse lines for visible mutant phenotypes, resulting from transgene insertion, has been described. To date, four *bona fide* insertional mutants have been identified and characterised at both the phenotypic and molecular levels.

That at least three of these mutants represent new allelic forms of previously identified genes/mutations may provide an indication as to the percentage of mouse genes, that have already been discovered, which can be mutated to give a visible phenotype.

Additional putative insertional mutants, identified by the screen, are awaiting confirmation. Furthermore, the screen cannot be considered as exhaustive, since it is possible that subtle or partially-penetrant phenotypes might have eluded detection. Thus, the number of insertional mutants identified to date (currently at 5.4%) is unlikely to be final.

Homozygous transgenic Ann mutants were identified at an early age due to their sevre ataxic phenotype. Expression of the mouse *disabled 1* (*mdab1*) gene is ablated in these mutants as a result of transgene insertion. mDab1 is a cytosolic adaptor protein that functions as part of the reelin signalling pathway in the developing CNS. This pathway is essential for correct neuronal migration/positioning during the development of the cerebellum, cerebral cortex and hippocampus. Gross abnormalities of neural patterning in these brain structures are apparent in Ann mutants.

That *mdab1* mutant mice have already been described (*scrambler*, *yotari* and a gene-targeted mutation) means that the discovery of a novel mutation of this gene contributes to a pre-exisiting allelic series. A failure to detect any

disruption to a large section of the *mdab1* gene structure suggests that a promoter/enhancer sequence may be disrupted in the Ann line. This mutant could therefore serve as a useful tool in dissecting how the expression of this gene is controlled.

The identification and characterisation of a second insertional mutant line, Ob, has been described. Homozygous transgenic males of this line are found to be sterile. Testicular histology suggests that a reduction in numbers of a subset of spermatogenic cell-types may be responsible. The transgene insertion has been mapped to the centre of Chromosome 8.

One possible candidate gene, *calmegin*, located in this region, must be tested. Failure to identify any abnormalities in the expression of the *calmegin* gene orits corresponding protein may indicate that the Ob line represents a mutation of an, as yet, unidentified gene. Such a discovery would provide an important contribution to studies being conducted on the genetic basis of human infertility.

Systematic screening programmes of large numbers of transgenic mice for insertional mutation events, such as that described, can make a useful contribution to the array of mouse mutation/gene identification methods currently in use. The value of these methods in helping to elucidate the genetic basis of human development and disease cannot be understated.

BIBLIOGRAPHY

1. Silver, L.M., *Mouse Genetics: concepts and applications.* 1 ed. 1995: Oxford University Press.
2. Evans, M.J. and M.H. Kaufman, *Establishment in culture of pluripotential cells from mouse embryos.* Nature, 1981. **292**(5819): p. 154-6.
3. Martin, G.R., *Isolation of a pluripotent cell line from early mouse embryos cultured in medium conditioned by teratocarcinoma stem cells.* Proc Natl Acad Sci U S A, 1981. **78**(12): p. 7634-8.
4. Smith, A.G., *et al., Differentiation inhibiting activity (DIA/LIF) and mouse development.* Dev Biol, 1992. **151**(2): p. 339-51.
5. Bradley, A., *et al., Formation of germ-line chimaeras from embryo-derived teratocarcinoma cell lines.* Nature, 1984. **309**(5965): p. 255-6.
6. Capecchi, M.R., *The new mouse genetics: altering the genome by gene targeting.* Trends Genet, 1989. **5**(3): p. 70-6.
7. Thomas, K.R. and M.R. Capecchi, *Site-directed mutagenesis by gene targeting in mouse embryo-derived stem cells.* Cell, 1987. **51**(3): p. 503-12.
8. Wood, S.A., *et al., Non-injection methods for the production of embryonic stem cell-embryo chimaeras.* Nature, 1993. **365**(6441): p. 87-9.
9. Hasty, P., *et al., Introduction of a subtle mutation into the Hox-2.6 locus in embryonic stem cells [published erratum appears in Nature 1991 Sep 5;353(6339):94].* Nature, 1991. **350**(6315): p. 243-6.
10. Reid, L.H., *et al., Regulatory elements in the introns of the human HPRT gene are necessary for its expression in embryonic stem cells.* Proc Natl Acad Sci U S A, 1990. **87**(11): p. 4299-303.
11. Wu, H., X. Liu, and R. Jaenisch, *Double replacement: strategy for efficient introduction of subtle mutations into the murine Col1a-1 gene by*

homologous recombination in embryonic stem cells. Proc Natl Acad Sci U S A, 1994. **91**(7): p. 2819-23.

12. Gu, H., *et al., Deletion of a DNA polymerase beta gene segment in T cells using cell type-specific gene targeting.* Science, 1994. **265**(5168): p. 103-6.
13. Ramirez-Solis, R., P. Liu, and A. Bradley, *Chromosome engineering in mice.* Nature, 1995. **378**(6558): p. 720-4.
14. Zheng, B., *et al., Engineering a mouse balancer chromosome.* Nat Genet, 1999. **22**(4): p. 375-8.
15. Wang, Y., *et al., Functional redundancy of the muscle-specific transcription factors Myf5 and myogenin.* Nature, 1996. **379**(6568): p. 823-5.
16. Joyner, A.L., A. Auerbach, and W.C. Skarnes, *The gene trap approach in embryonic stem cells: the potential for genetic screens in mice.* Ciba Found Symp, 1992. **165**: p. 277-88.
17. Friedrich, G. and P. Soriano, *Promoter traps in embryonic stem cells: a genetic screen to identify and mutate developmental genes in mice.* Genes Dev, 1991. **5**(9): p. 1513-23.
18. Gossler, A., *et al., Mouse embryonic stem cells and reporter constructs to detect developmentally regulated genes.* Science, 1989. **244**(4903): p. 463-5.
19. Skarnes, W.C., B.A. Auerbach, and A.L. Joyner, *A gene trap approach in mouse embryonic stem cells: the lacZ reported is activated by splicing, reflects endogenous gene expression, and is mutagenic in mice.* Genes Dev, 1992. **6**(6): p. 903-18.
20. Frohman, M.A., M.K. Dush, and G.R. Martin, *Rapid production of full-length cDNAs from rare transcripts: amplification using a single gene-specific oligonucleotide primer.* Proc Natl Acad Sci U S A, 1988. **85**(23): p. 8998-9002.

21. Joyner, A.L., *Gene targeting and gene trap screens using embryonic stem cells: new approaches to mammalian development.* Bioessays, 1991. **13**(12): p. 649-56.

22. Skarnes, W.C., *et al., Capturing genes encoding membrane and secreted proteins important for mouse development.* Proc Natl Acad Sci U S A, 1995. **92**(14): p. 6592-6.

23. Gordon, J.W., *et al., Genetic transformation of mouse embryos by microinjection of purified DNA.* Proc Natl Acad Sci U S A, 1980. **77**(12): p. 7380-4.

24. Lovell-Badge, R.H., *et al., Transformation of embryonic stem cells with the human type-II collagen gene and its expression in chimeric mice.* Cold Spring Harb Symp Quant Biol, 1985. **50**: p. 707-11.

25. Jaenisch, R., *Germ line integration and Mendelian transmission of the exogenous Moloney leukemia virus.* Proc Natl Acad Sci U S A, 1976. **73**(4): p. 1260-4.

26. Meisler, M.H., *Insertional mutation of 'classical' and novel genes in transgenic mice.* Trends Genet, 1992. **8**(10): p. 341-4.

27. Popp, R.A., *et al., Analysis of a mouse alpha-globin gene mutation induced by ethylnitrosourea.* Genetics, 1983. **105**(1): p. 157-67.

28. Hardisty, R.E., P. Mburu, and S.D. Brown, *ENU mutagenesis and the search for deafness genes.* Br J Audiol, 1999. **33**(5): p. 279-83.

29. Bode, V.C., *Ethylnitrosourea mutagenesis and the isolation of mutant alleles for specific genes located in the T region of mouse chromosome 17.* Genetics, 1984. **108**(2): p. 457-70.

30. Nolan, P.M., *et al., Implementation of a large-scale ENU mutagenesis program: towards increasing the mouse mutant resource.* Mamm Genome, 2000. **11**(7): p. 500-6.

31. Shedlovsky, A., T.R. King, and W.F. Dove, *Saturation germ line mutagenesis of the murine t region including a lethal allele at the quaking locus.* Proc Natl Acad Sci U S A, 1988. **85**(1): p. 180-4.

32. Russell, L.B., *et al., Chlorambucil effectively induces deletion mutations in mouse germ cells.* Proc Natl Acad Sci U S A, 1989. **86**(10): p. 3704-8.

33. Nolan, P.M., *et al., A systematic, genome-wide, phenotype-driven mutagenesis programme for gene function studies in the mouse.* Nat Genet, 2000. **25**(4): p. 440-3.

34. Schena, M., *et al., Quantitative monitoring of gene expression patterns with a complementary DNA microarray.* Science, 1995. **270**(5235): p. 467-70.

35. Heller, R.A., *et al., Discovery and analysis of inflammatory disease-related genes using cDNA microarrays.* Proc Natl Acad Sci U S A, 1997. **94**(6): p. 2150-5.

36. Debouck, C. and P.N. Goodfellow, *DNA microarrays in drug discovery and development.* Nat Genet, 1999. **21**(1 Suppl): p. 48-50.

37. Rikke, B.A. and T.E. Johnson, *Towards the cloning of genes underlying murine QTLs.* Mamm Genome, 1998. **9**(12): p. 963-8.

38. Dietrich, W., *et al., A genetic map of the mouse suitable for typing intraspecific crosses.* Genetics, 1992. **131**(2): p. 423-47.

39. http://www.informatics.jax.org

40. Trask, B.J., *Gene mapping by in situ hybridization.* Curr Opin Genet Dev, 1991. **1**(1): p. 82-7.

41. Ruddle, F.H., *Linkage analysis using somatic cell hybrids.* Adv Hum Genet, 1972. **30**: p. 173-235.

42. Cox, D.R., *et al., Radiation hybrid mapping: a somatic cell genetic method for constructing high-resolution maps of mammalian chromosomes.* Science, 1990. **250**(4978): p. 245-50.

43. Burke, D.T., *et al., A mouse genomic library of yeast artificial chromosome clones.* Mamm Genome, 1991. **1**(1): p. 65.

44. Osoegawa, K., *et al., Bacterial artificial chromosome libraries for mouse sequencing and functional analysis.* Genome Res, 2000. **10**(1): p. 116-28.

45. Collins, F.S., *et al., New goals for the U.S. Human Genome Project: 1998-2003.* Science, 1998. **282**(5389): p. 682-9.

46. Nusbaum, C., *et al., A YAC-based physical map of the mouse genome.* Nat Genet, 1999. **22**(4): p. 388-93.

47. Buckler, A.J., *et al., Exon amplification: a strategy to isolate mammalian genes based on RNA splicing.* Proc Natl Acad Sci U S A, 1991. **88**(9): p. 4005-9.

48. Bird, A.P., *CpG-rich islands and the function of DNA methylation.* Nature, 1986. **321**(6067): p. 209-13.

49. Jaenisch, R. and B. Mintz, *Simian virus 40 DNA sequences in DNA of healthy adult mice derived from preimplantation blastocysts injected with viral DNA.* Proc Natl Acad Sci U S A, 1974. **71**(4): p. 1250-4.

50. Varmus, H., *Retroviruses.* Science, 1988. **240**(4858): p. 1427-35.

51. Stewart, C.L., M. Vanek, and E.F. Wagner, *Expression of foreign genes from retroviral vectors in mouse teratocarcinoma chimaeras.* Embo J, 1985. **4**(13B): p. 3701-9.

52. Palmiter, R.D., *et al., Dramatic growth of mice that develop from eggs microinjected with metallothionein-growth hormone fusion genes.* Nature, 1982. **300**(5893): p. 611-5.

53. Antoch, M.P., *et al., Functional identification of the mouse circadian Clock gene by transgenic BAC rescue.* Cell, 1997. **89**(4): p. 655-67.

54. Schedl, A., *et al., A yeast artificial chromosome covering the tyrosinase gene confers copy number-dependent expression in transgenic mice.* Nature, 1993. **362**(6417): p. 258-61.

55. Palmiter, R.D. and R.L. Brinster, *Germ-line transformation of mice.* Annu Rev Genet, 1986. **20**: p. 465-99.

56. Dellaire, G. and P. Chartrand, *Direct evidence that transgene integration is random in murine cells, implying that naturally occurring double-strand breaks may be distributed similarly within the genome.* Radiat Res, 1998. **149**(4): p. 325-9.

57. Lo, C.W., *Transformation by iontophoretic microinjection of DNA: multiple integrations without tandem insertions.* Mol Cell Biol, 1983. **3**(10): p. 1803-14.

58. Gordon, J.W. and F.H. Ruddle, *Gene transfer into mouse embryos: production of transgenic mice by pronuclear injection.* Methods Enzymol, 1983. **101**: p. 411-33.

59. Bishop, J.O., *Chromosomal insertion of foreign DNA.* Reprod Nutr Dev, 1996. **36**(6): p. 607-18.

60. Palmiter, R.D., Hammer, R.E. and Brinster, R.L., *Expression of growth hormone genes in transgenic mice.* Banbury report 20: Genetic manipulation of the early embryo. 1985, New York: Cold Spring Harbor Lab.

61. Brinster, R.L., *et al., Factors affecting the efficiency of introducing foreign DNA into mice by microinjecting eggs.* Proc Natl Acad Sci U S A, 1985. **82**(13): p. 4438-42.

62. Woychik, R.P., *et al., An inherited limb deformity created by insertional mutagenesis in a transgenic mouse.* Nature, 1985. **318**(6041): p. 36-40.

63. Ratty, A.K., *et al., Genetic mapping of two DNA markers, D16Ros1 and D16Ros2, flanking the mutation site in the chakragati mouse, a transgenic insertional mutant.* Mamm Genome, 1992. **3**(1): p. 5-10.

64. Francke, U., *et al., Induced reciprocal translocation in transgenic mice near sites of transgene integration.* Mamm Genome, 1992. **3**(4): p. 209-16.

65. Cory, S., *Activation of cellular oncogenes in hemopoietic cells by chromosome translocation.* Adv Cancer Res, 1986. **47**: p. 189-234.

66. Brinster, R.L., *et al., Transgenic mice harboring SV40 T-antigen genes develop characteristic brain tumors.* Cell, 1984. **37**(2): p. 367-79.

67. Palmiter, R.D., H.Y. Chen, and R.L. Brinster, *Differential regulation of metallothionein-thymidine kinase fusion genes in transgenic mice and their offspring.* Cell, 1982. **29**(2): p. 701-10.

68. Shani, M., *Tissue-specific and developmentally regulated expression of a chimeric actin-globin gene in transgenic mice.* Mol Cell Biol, 1986. **6**(7): p. 2624-31.

69. Xiang, X., K.F. Benson, and K. Chada, *Mini-mouse: disruption of the pygmy locus in a transgenic insertional mutant.* Science, 1990. **247**(4945): p. 967-9.

70. Soriano, P., T. Gridley, and R. Jaenisch, *Retroviruses and insertional mutagenesis in mice: proviral integration at the Mov 34 locus leads to early embryonic death.* Genes Dev, 1987. **1**(4): p. 366-75.

71. Wilkie, T.M., R.L. Brinster, and R.D. Palmiter, *Germline and somatic mosaicism in transgenic mice.* Dev Biol, 1986. **118**(1): p. 9-18.

72. Ward, A., *et al., Genomic regions regulating imprinting and insulin-like growth factor-II promoter 3 activity in transgenics: novel enhancer and silencer elements.* Genes Funct, 1997. **1**(1): p. 25-36.

73. Sambrook, J., E.F. Fritsch, and T. Maniatis, *Molecular Cloning: A laboratory manual.* 1989, New York: Cold Spring Harbor Laboratory Press.

74. Calvin, N.M. and P.C. Hanawalt, *High-efficiency transformation of bacterial cells by electroporation.* J Bacteriol, 1988. **170**(6): p. 2796-801.

75. Fiedler, S. and R. Wirth, *Transformation of bacteria with plasmid DNA by electroporation.* Anal Biochem, 1988. **170**(1): p. 38-44.

76. Hogan, B., *et al.*, *Manipulating The Mouse Embryo: A laboratory Manual.* 2 ed. 1994, New York: Cold Spring Harbor Laboratory Press.

77. Chomczynski, P. and N. Sacchi, *Single-step method of RNA isolation by acid guanidinium thiocyanate- phenol-chloroform extraction.* Anal Biochem, 1987. **162**(1): p. 156-9.

78. Church, G.M. and W. Gilbert, *Genomic sequencing.* Proc Natl Acad Sci U S A, 1984. **81**(7): p. 1991-5.

79. http://www.genome.wi.mi.edu

80. Bennett, W.R., *PhD Thesis.* 1999.

81. Wilkinson, D.G., *Whole mount in situ hybridisation of vertebrate embryos,* in *In situ hybridisation: A practical approach.* 1992, Oxford University Press: Oxford.

82. Bancroft, J.D. and A. Stevens, eds. *Theory And Practice Of Histological Techniques.*. 1977, Churchill Livingstone: New York.

83. DeChiara, T.M., E.J. Robertson, and A. Efstratiadis, *Parental imprinting of the mouse insulin-like growth factor II gene.* Cell, 1991. **64**(4): p. 849-59.

84. Bartolomei, M.S., S. Zemel, and S.M. Tilghman, *Parental imprinting of the mouse H19 gene.* Nature, 1991. **351**(6322): p. 153-5.

85. Caricasole, A. and A. Ward, *A luciferase-reporter vector with blue-white selection for rapid subcloning and mutational analysis of eukaryotic promoters.* Gene, 1993. **124**(1): p. 139-40.

86. Southard-Smith, E.M., L. Kos, and W.J. Pavan, *Sox10 mutation disrupts neural crest development in Dom Hirschsprung mouse model.* Nat Genet, 1998. **18**(1): p. 60-4.

87. Jiang, X., *et al.*, *Fate of the mammalian cardiac neural crest [In Process Citation].* Development, 2000. **127**(8): p. 1607-16.

88. Koide, T., *et al.*, *Comparative analysis of Igf-2/H19 imprinted domain: identification of a highly conserved intergenic DNase I hypersensitive region.* Genomics, 1994. **24**(1): p. 1-8.

89. Gridley, T., P. Soriano, and R. Jaenisch, *Insertional mutagenesis in mice.* Trends in Genetics, 1987. **3**(6): p. 162 - 166.

90. Weiher, H., *et al.*, *Transgenic mouse model of kidney disease: insertional inactivation of ubiquitously expressed gene leads to nephrotic syndrome.* Cell, 1990. **62**(3): p. 425-34.

91. http://www.mgu.har.mrc.ac.uk/mutabase

92. Kandel, E.R., J.H. Schwartz, and T.M. Jessell, *Principles of Neural Science.* 3 ed. 1991, Norwalk, CT.: Appleton and LAnge.

93. Hoffman, E.P. and L.M. Kunkel, *Dystrophin abnormalities in Duchenne/Becker muscular dystrophy.* Neuron, 1989. **2**(1): p. 1019-29.

94. Campbell, K.P., *Three muscular dystrophies: loss of cytoskeleton-extracellular matrix linkage.* Cell, 1995. **80**(5): p. 675-9.

95. Ozawa, E., *et al.*, *Dystrophin-associated proteins in muscular dystrophy.* Hum Mol Genet, 1995. **4**(Spec No): p. 1711-6.

96. Bulfield, G., *et al.*, *X chromosome-linked muscular dystrophy (mdx) in the mouse.* Proc Natl Acad Sci U S A, 1984. **81**(4): p. 1189-92.

97. Sicinski, P., *et al.*, *The molecular basis of muscular dystrophy in the mdx mouse: a point mutation.* Science, 1989. **244**(4912): p. 1578-80.

98. Deconinck, A.E., *et al.*, *Utrophin-dystrophin-deficient mice as a model for Duchenne muscular dystrophy.* Cell, 1997. **90**(4): p. 717-27.

99. Grady, R.M., *et al., Skeletal and cardiac myopathies in mice lacking utrophin and dystrophin: a model for Duchenne muscular dystrophy.* Cell, 1997. **90**(4): p. 729-38.

100. Michelson, A., E. Russell, and P. Harman, *Dystrophia Muscularis: a hereditary primary myopathy in the house mouse.* Proc Natl Acad Sci U S A, 1955. **41**: p. 1079-1084.

101. Sunada, Y., *et al., Deficiency of merosin in dystrophic dy mice and genetic linkage of laminin M chain gene to dy locus.* J Biol Chem, 1994. **269**(19): p. 13729-32.

102. Xu, H., *et al., Murine muscular dystrophy caused by a mutation in the laminin alpha 2 (Lama2) gene.* Nat Genet, 1994. 8(3): p. 297-302.

103. Lane, P.W., T.C. Beamer, and D.D. Myers, *Myodystrophy, a new myopathy on chromosome 8 of the mouse.* J Hered, 1976. **67**(3): p. 135-8.

104. Cote, P.D., *et al., Chimaeric mice deficient in dystroglycans develop muscular dystrophy and have disrupted myoneural synapses [see comments].* Nat Genet, 1999. **23**(3): p. 338-42.

105. Williamson, R.A., *et al., Dystroglycan is essential for early embryonic development: disruption of Reichert's membrane in Dag1-null mice.* Hum Mol Genet, 1997. **6**(6): p. 831-41.

106. Duclos, F., *et al., Progressive muscular dystrophy in alpha-sarcoglycan-deficient mice.* J Cell Biol, 1998. **142**(6): p. 1461-71.

107. Hack, A.A., *et al., Gamma-sarcoglycan deficiency leads to muscle membrane defects and apoptosis independent of dystrophin.* J Cell Biol, 1998. **142**(5): p. 1279-87.

108. DiMario, J.X., A. Uzman, and R.C. Strohman, *Fiber regeneration is not persistent in dystrophic (MDX) mouse skeletal muscle.* Dev Biol, 1991. **148**(1): p. 314-21.

109. Pons, F., *et al., Does utrophin expression in muscles of mdx mice during postnatal development functionally compensate for dystrophin deficiency?* J Neurol Sci, 1994. **122**(2): p. 162-70.

110. Crawford, T.O. and C.A. Pardo, *The neurobiology of childhood spinal muscular atrophy.* Neurobiol Dis, 1996. **3**(2): p. 97-110.

111. Schmalbruch, H., *et al., A new mouse mutant with progressive motor neuronopathy.* J Neuropathol Exp Neurol, 1991. **50**(3): p. 192-204.

112. Messer, A. and L. Flaherty, *Autosomal dominance in a late-onset motor neuron disease in the mouse.* J Neurogenet, 1986. **3**(6): p. 345-55.

113. Jones, J.M., *et al., mnd2: a new mouse model of inherited motor neuron disease.* Genomics, 1993. **16**(3): p. 669-77.

114. Wong, P.C. and D.R. Borchelt, *Motor neuron disease caused by mutations in superoxide dismutase 1.* Curr Opin Neurol, 1995. **8**(4): p. 294-301.

115. Rosen, D.R., *et al., Mutations in Cu/Zn superoxide dismutase gene are associated with familial amyotrophic lateral sclerosis [published erratum appears in Nature 1993 Jul 22;364(6435):362].* Nature, 1993. **362**(6415): p. 59-62.

116. Gurney, M.E., *et al., Motor neuron degeneration in mice that express a human Cu,Zn superoxide dismutase mutation [published erratum appears in Science 1995 Jul 14;269(5221):149].* Science, 1994. **264**(5166): p. 1772-5.

117. Cote, F., J.F. Collard, and J.P. Julien, *Progressive neuronopathy in transgenic mice expressing the human neurofilament heavy gene: a mouse model of amyotrophic lateral sclerosis.* Cell, 1993. **73**(1): p. 35-46.

118. Xu, Z., *et al., Increased expression of neurofilament subunit NF-L produces morphological alterations that resemble the pathology of human motor neuron disease.* Cell, 1993. **73**(1): p. 23-33.

119. Duchen, L.W. and S.J. Strich, *An hereditary motor neurone disease with progressive denervation of muscle in the mouse: the mutant 'wobbler'.* J Neurol Neurosurg Psychiatry, 1968. **31**(6): p. 535-42.

120. Ripps, M.E., *et al., Transgenic mice expressing an altered murine superoxide dismutase gene provide an animal model of amyotrophic lateral sclerosis.* Proc Natl Acad Sci U S A, 1995. **92**(3): p. 689-93.

121. Doyle, J.L. and L. Stubbs, *Ataxia, arrhythmia and ion-channel gene defects.* Trends Genet, 1998. **14**(3): p. 92-8.

122. Patil, N., *et al., A potassium channel mutation in weaver mice implicates membrane excitability in granule cell differentiation [see comments].* Nat Genet, 1995. **11**(2): p. 126-9.

123. Sidman, R., M. Green, and S. Appel, *Catalog of the Neurological Mutants of the Mouse.* 1965: Harvard University Press.

124. Zhuchenko, O., *et al., Autosomal dominant cerebellar ataxia (SCA6) associated with small polyglutamine expansions in the alpha 1A-voltage-dependent calcium channel.* Nat Genet, 1997. **15**(1): p. 62-9.

125. Smart, S.L., *et al., Deletion of the K(V)1.1 potassium channel causes epilepsy in mice.* Neuron, 1998. **20**(4): p. 809-19.

126. Ho, C.S., R.W. Grange, and R.H. Joho, *Pleiotropic effects of a disrupted K+ channel gene: reduced body weight, impaired motor skill and muscle contraction, but no seizures.* Proc Natl Acad Sci U S A, 1997. **94**(4): p. 1533-8.

127. Pai, A., *Developmental genetics of a lethal mutation, muscular dysgenesis (mdg), in the mouse. II. Developmental analysis.* Dev Biol, 1965. **11**: p. 93-109.

128. Chaudhari, N., *A single nucleotide deletion in the skeletal muscle-specific calcium channel transcript of muscular dysgenesis (mdg) mice.* J Biol Chem, 1992. **267**(36): p. 25636-9.

129. Green, M. and R. Sidman, *Tottering - a neuromuscular mutation in the mouse.* J Hered, 1962. **53**: p. 233-237.

130. Fletcher, C.F., *et al., Absence epilepsy in tottering mutant mice is associated with calcium channel defects.* Cell, 1996. **87**(4): p. 607-17.

131. Burgess, D.L., *et al., Mutation of the Ca2+ channel beta subunit gene Cchb4 is associated with ataxia and seizures in the lethargic (lh) mouse.* Cell, 1997. **88**(3): p. 385-92.

132. Duchen, L.W., *Hereditary motor end-plate disease in the mouse: light and electron microscopic studies.* J Neurol Neurosurg Psychiatry, 1970. **33**(2): p. 238-50.

133. Burgess, D.L., *et al., Mutation of a new sodium channel gene, Scn8a, in the mouse mutant 'motor endplate disease'.* Nat Genet, 1995. **10**(4): p. 461-5.

134. Griffiths, I.R., *Myelin mutants: model systems for the study of normal and abnormal myelination.* Bioessays, 1996. **18**(10): p. 789-97.

135. Nave, K.A., *Neurological mouse mutants and the genes of myelin.* J Neurosci Res, 1994. **38**(6): p. 607-12.

136. Snipes, G.J., U. Suter, and E.M. Shooter, *The genetics of myelin.* Curr Opin Neurobiol, 1993. **3**(5): p. 694-702.

137. Baechner, D., *et al., Widespread expression of the peripheral myelin protein-22 gene (PMP22) in neural and non-neural tissues during murine development.* J Neurosci Res, 1995. **42**(6): p. 733-41.

138. Suter, U. and G.J. Snipes, *Peripheral myelin protein 22: facts and hypotheses.* J Neurosci Res, 1995. **40**(2): p. 145-51.

139. Low, P.A., *Hereditary hypertrophic neuropathy in the trembler mouse. Part 1. Histopathological studies: light microscopy.* J Neurol Sci, 1976. **30**(2-3): p. 327-41.

140. Falconer, D., *Two new mutants "Trembler" and "Reeler", with neurological actions in the house mouse (Mus musculus L.).* J Genetics, 1951. **50**: p. 192-201.

141. Chernoff, G.F., *Shiverer: an autosomal recessive mutant mouse with myelin deficiency.* J Hered, 1981. **72**(2): p. 128.

142. Roach, A., *et al., Chromosomal mapping of mouse myelin basic protein gene and structure and transcription of the partially deleted gene in shiverer mutant mice.* Cell, 1985. **42**(1): p. 149-55.

143. Phillips, R., *Jimpy, a new totally sex-linked gene in the house mouse.* Z Indukt Abstamm Vererbungsl, 1954. **86**: p. 322-326.

144. Nave, K.A., F.E. Bloom, and R.J. Milner, *A single nucleotide difference in the gene for myelin proteolipid protein defines the jimpy mutation in mouse.* J Neurochem, 1987. **49**(6): p. 1873-7.

145. Suter, U., *et al., Trembler mouse carries a point mutation in a myelin gene.* Nature, 1992. **356**(6366): p. 241-4.

146. Giese, K.P., *et al., Mouse P0 gene disruption leads to hypomyelination, abnormal expression of recognition molecules, and degeneration of myelin and axons.* Cell, 1992. **71**(4): p. 565-76.

147. Sidman, R., M. Dickie, and S. Appel, *Mutant mice (quaking and jimpy) with deficient myelination in the central nervous system.* Science, 1964. **144**: p. 309-311.

148. Li, C., *et al., Myelination in the absence of myelin-associated glycoprotein.* Nature, 1994. **369**(6483): p. 747-50.

149. Matsunami, N., *et al., Peripheral myelin protein-22 gene maps in the duplication in chromosome 17p11.2 associated with Charcot-Marie-Tooth 1A.* Nat Genet, 1992. **1**(3): p. 176-9.

150. Martini, R., *Expression and functional roles of neural cell surface molecules and extracellular matrix components during development and regeneration of peripheral nerves.* J Neurocytol, 1994. **23**(1): p. 1-28.

151. Hayasaka, K., G. Takada, and V.V. Ionasescu, *Mutation of the myelin P0 gene in Charcot-Marie-Tooth neuropathy type 1B.* Hum Mol Genet, 1993. **2**(9): p. 1369-72.

152. Hayasaka, K., *et al., De novo mutation of the myelin P0 gene in Dejerine-Sottas disease (hereditary motor and sensory neuropathy type III).* Nat Genet, 1993. **5**(3): p. 266-8.

153. Herrup, K., *Role of staggerer gene in determining cell number in cerebellar cortex. I. Granule cell death is an indirect consequence of staggerer gene action.* Brain Res, 1983. **313**(2): p. 267-74.

154. Wetts, R. and K. Herrup, *Interaction of granule, Purkinje and inferior olivary neurons in lurcher chimeric mice. II. Granule cell death.* Brain Res, 1982. **250**(2): p. 358-62.

155. Mullen, R.J., E.M. Eicher, and R.L. Sidman, *Purkinje cell degeneration, a new neurological mutation in the mouse.* Proc Natl Acad Sci U S A, 1976. **73**(1): p. 208-12.

156. Phillips, R., *"Lurcher", a new gene in linkage group XI of the house mouse.* J Genet, 1960. **57**: p. 35-42.

157. Lalouette, A., J.L. Guenet, and S. Vriz, *Hotfoot mouse mutations affect the delta 2 glutamate receptor gene and are allelic to lurcher.* Genomics, 1998. **50**(1): p. 9-13.

158. Sidman, R., P. Lane, and M. Dickie, *Staggerer, a new mutation in the house mouse affecting the cerebellum.* Science, 1962. **137**: p. 610-612.

159. Hamilton, B.A., *et al., Disruption of the nuclear hormone receptor RORalpha in staggerer mice [published erratum appears in Nature 1996 May 23;381(6580):346].* Nature, 1996. **379**(6567): p. 736-9.

160. Caddy, K.W., R.L. Sidman, and E.M. Eicher, *Stumbler, a new mutant mouse with cerebellar disease.* Brain Res, 1981. **208**(1): p. 251-5.

161. Shultz, L.D., *et al., 'Wasted', a new mutant of the mouse with abnormalities characteristic to ataxia telangiectasia.* Nature, 1982. **297**(5865): p. 402-4.

162. Chambers, D.M., J. Peters, and C.M. Abbott, *The lethal mutation of the mouse wasted (wst) is a deletion that abolishes expression of a tissue-specific isoform of translation elongation factor 1alpha, encoded by the Eef1a2 gene.* Proc Natl Acad Sci U S A, 1998. **95**(8): p. 4463-8.

163. Sidman, R. and M. Green, *"Nervous", a new mutant mouse with cerebellar disease.* Coll Int Centre Natl Recherche Sci, 1970. **924**: p. 69-79.

164. D'Arcangelo, G., *et al., A protein related to extracellular matrix proteins deleted in the mouse mutant reeler.* Nature, 1995. **374**(6524): p. 719-23.

165. Sweet, H.O., *et al., Scrambler, a new neurological mutation of the mouse with abnormalities of neuronal migration.* Mamm Genome, 1996. **7**(11): p. 798-802.

166. Sheldon, M.e.a., *Scrambler and yotari disrupt the disabled gene and produce a reeler-like phenotype in mice.* Nature, 1997. **389**: p. 730-733.

167. Caddy, K.W. and R.L. Sidman, *Purkinje cells and granule cells in the cerebellum of the Stumbler mutant mouse.* Brain Res, 1981. **227**(2): p. 221-36.

168. Mishra, P.R., *et al., DNA loss in the developing cerebellum of nervous mouse: a flow cytometric study.* Brain Res, 1983. **282**(2): p. 193-6.

169. Rice, D.S., et al., *Disabled-1 acts downstream of Reelin in a signaling pathway that controls laminar organization in the mammalian brain.* Development, 1998. **125**: p. 3719-3729.

170. Goldowitz, D., et al., *Cerebellar disorganization characteristic of reeler in scrambler mutant mice despite presence of reelin.* J. Neurosci., 1997. **17**(22): p. 8767-8777.

171. Howell, B.W., et al., *Neuronal positioning in the developing brain is regulated by mouse disabled-1.* Nature, 1997. **389**: p. 733-737.

172. Mariani, J., *et al., Anatomical, physiological and biochemical studies of the cerebellum from Reeler mutant mouse.* Philos Trans R Soc Lond B Biol Sci, 1977. **281**(978): p. 1-28.

173. http://www.neuro.wustl.ed/neuromuscular/pathol

174. Carnwath, J.W. and D.M. Shotton, *Muscular dystrophy in the mdx mouse: histopathology of the soleus and extensor digitorum longus muscles.* J Neurol Sci, 1987. **80**(1): p. 39-54.

175. D'Arcangelo, G. and T. Curran, *Reeler: new tales on an old mutant mouse.* Bioessays, 1998. **20**(3): p. 235-44.

176. Rakic, P., *Neuron-glia relationship during granule cell migration in developing cerebellar cortex. A Golgi and electronmicroscopic study in Macacus Rhesus.* J Comp Neurol, 1971. **141**(3): p. 283-312.

177. Miao, G.G., *et al., Isolation of an allele of reeler by insertional mutagenesis.* Proc Natl Acad Sci U S A, 1994. **91**(23): p. 11050-4.

178. Ogawa, M., *et al., The reeler gene-associated antigen on Cajal-Retzius neurons is a crucial molecule for laminar organization of cortical neurons.* Neuron, 1995. **14**(5): p. 899-912.

179. Caviness, V.S., Jr., D.K. So, and R.L. Sidman, *The hybrid reeler mouse.* J Hered, 1972. **63**(5): p. 241-6.

180. Ware, M.L., *et al., Aberrant splicing of a mouse disabled homolog, mdab1, in the scrambler mouse.* Neuron, 1997. **19**(2): p. 239-49.

181. Rice, D.S. and T. Curran, *Mutant mice with scrambled brains: understanding the signaling pathways that control cell positioning in the CNS.* Genes Dev, 1999. **13**(21): p. 2758-73.

182. Campuzano, V., *et al., Frataxin is reduced in Friedreich ataxia patients and is associated with mitochondrial membranes.* Hum Mol Genet, 1997. **6**(11): p. 1771-80.

183. Koeppen, A.H., *The hereditary ataxias.* J Neuropathol Exp Neurol, 1998. **57**(6): p. 531-43.

184. Rosenberg, R.N., *Autosomal dominant cerebellar phenotypes: the genotype has settled the issue.* Neurology, 1995. **45**(1): p. 1-5.

185. Ranum, L.P., *et al., Spinocerebellar ataxia type 1 and Machado-Joseph disease: incidence of CAG expansions among adult-onset ataxia patients from 311 families with dominant, recessive, or sporadic ataxia.* Am J Hum Genet, 1995. **57**(3): p. 603-8.

186. Pulst, S.M., *et al., Moderate expansion of a normally biallelic trinucleotide repeat in spinocerebellar ataxia type 2.* Nat Genet, 1996. **14**(3): p. 269-76.

187. Kawaguchi, Y., *et al., CAG expansions in a novel gene for Machado-Joseph disease at chromosome 14q32.1 [see comments].* Nat Genet, 1994. 8(3): p. 221-8.

188. Caviness, V.S., Jr., *Neocortical histogenesis in normal and reeler mice: a developmental study based upon [3H]thymidine autoradiography.* Brain Res, 1982. **256**(3): p. 293-302.

189. Gonzalez, J.L., *et al., Birthdate and cell marker analysis of scrambler: a novel mutation affecting cortical development with a reeler-like phenotype.* J Neurosci, 1997. **17**(23): p. 9204-11.

190. Angevine, J.B. and R.L. Sidman, *Autoradiographic study of cell migration during histogenesis of cerebral cortex in the mouse.* Nature, 1961(192): p. 766-768.

191. Hoffarth, R.M., *et al., The mouse mutation reeler causes increased adhesion within a subpopulation of early postmitotic cortical neurons.* J Neurosci, 1995. **15**(7 Pt 1): p. 4838-50.

192. Aicardi, J., *The agyria-pachygyria complex: a spectrum of cortical malformations.* Brain Dev, 1991. **13**(1): p. 1-8.

193. Norman, M.G., *et al., Congenital Malformations of the Brain: Pathological, Embryological, Clinical, Radiological and Genetic Aspects.* 1995, New York: Oxford University Press.

194. Barkovich, A.J., *et al., Band heterotopia: correlation of outcome with magnetic resonance imaging parameters.* Ann Neurol, 1994. **36**(4): p. 609-17.

195. Pinard, J.M., *et al., Subcortical laminar heterotopia and lissencephaly in two families: a single X linked dominant gene.* J Neurol Neurosurg Psychiatry, 1994. **57**(8): p. 914-20.

196. Gleeson, J.G., *et al., Doublecortin, a brain-specific gene mutated in human X-linked lissencephaly and double cortex syndrome, encodes a putative signaling protein.* Cell, 1998. **92**(1): p. 63-72.

197. Howell, B.W., F.B. Gertler, and J.A. Cooper, *Mouse disabled (mDab1): a Src binding protein implicated in neuronal development.* Embo J, 1997. **16**(1): p. 121-32.

198. Reiner, O., *et al., Isolation of a Miller-Dieker lissencephaly gene containing G protein beta-subunit-like repeats.* Nature, 1993. **364**(6439): p. 717-21.

199. Hattori, M., *et al., Miller-Dieker lissencephaly gene encodes a subunit of brain platelet-activating factor acetylhydrolase. [published erratum appears in Nature 1994 Aug 4;370(6488):391].* Nature, 1994. **370**(6486): p. 216-8.

200. Neer, E.J., *Heterotrimeric G proteins: organizers of transmembrane signals.* Cell, 1995. **80**(2): p. 249-57.

201. Hirotsune, S., *et al., Graded reduction of Pafah1b1 (Lis1) activity results in neuronal migration defects and early embryonic lethality.* Nat Genet, 1998. **19**(4): p. 333-9.

202. Allen, K.M. and C.A. Walsh, *Genes that regulate neuronal migration in the cerebral cortex.* Epilepsy Res, 1999. **36**(2-3): p. 143-54.

203. Stanfield, B.B. and W.M. Cowan, *The morphology of the hippocampus and dentate gyrus in normal and reeler mice.* J Comp Neurol, 1979. **185**(3): p. 393-422.

204. Stanfield, B.B. and W.M. Cowan, *The development of the hippocampus and dentate gyrus in normal and reeler mice.* J Comp Neurol, 1979. **185**(3): p. 423-59.

205. Del Rio, J.A., *et al., A role for Cajal-Retzius cells and reelin in the development of hippocampal connections.* Nature, 1997. **385**(6611): p. 70-4.

206. Hearne, C.M., S. Ghosh, and J.A. Todd, *Microsatellites for linkage analysis of genetic traits.* Trends Genet, 1992. **8**(8): p. 288-94.

207. Avner, P., *et al., Genetic analysis of the mouse using interspecific crosses.* Trends Genet, 1988. **4**(1): p. 18-23.

208. Taylor, B.A., *Recombinant inbred strains: use in gene mapping.*, in *Origins of Inbred Mice.* 1978, Academic Press: New York. p. 423 - 438.

209. Craig, J.M. and W.A. Bickmore, *Chromosome bands--flavours to savour.* Bioessays, 1993. **15**(5): p. 349-54.

210. Gall, J.G. and M.L. Pardue, *Formation and detection of RNA-DNA hybrid molecules in cytological preparations.* Proc Natl Acad Sci U S A, 1969. **63**(2): p. 378-83.

211. John, H.A., M.L. Birnstiel, and K.W. Jones, *RNA-DNA hybrids at the cytological level.* Nature, 1969. **223**(206): p. 582-7.

212. Abbott, C., *Characterization of mouse-hamster somatic cell hybrids by PCR: a panel of mouse-specific primers for each chromosome.* Mamm Genome, 1992. **2**(2): p. 106-9.

213. Cox, R.D., *et al., Genome mapping and cloning of mutations using yeast artificial chromosomes.* Methods Enzymol, 1993. **225**: p. 637-53.

214. Riley, J., *et al., A novel, rapid method for the isolation of terminal sequences from yeast artificial chromosome (YAC) clones.* Nucleic Acids Res, 1990. **18**(10): p. 2887-90.

215. Zoghbi, H.Y.a.C., A.C., *Generation of YAC contigs by walking.*, in *YAC Libraries, A User's Guide*, D.L.a.B. Nelson, B.H., Editor. 1994, W.H. Freeman and Company: New York. p. 93 - 112.

216. Hoffman, E.P., *et al., Conservation of the Duchenne muscular dystrophy gene in mice and humans.* Science, 1987. **238**(4825): p. 347-50.

217. Hoffman, E.P., R.H. Brown, Jr., and L.M. Kunkel, *Dystrophin: the protein product of the Duchenne muscular dystrophy locus.* Cell, 1987. **51**(6): p. 919-28.

218. Florijn, R.J., *et al., High-resolution DNA Fiber-FISH for genomic DNA mapping and colour bar- coding of large genes.* Hum Mol Genet, 1995. **4**(5): p. 831-6.

219. http://www.informatics.jax.org

220. Montagutelli, X., *GENE-LINK: a program in PASCAL for backcross genetic analysis.* J Hered, 1990. **81**(6): p. 490-1.

221. Sweet, H.O., et al., *Scrambler a new neurological mutation of the mouse with abnormalities of neuronal migration.* Mammalian Genome, 1996. **7**: p. 798-802.

222. Kim, K.M., *et al., Cloning of the human glycine transporter type 1: molecular and pharmacological characterization of novel isoform variants and chromosomal localization of the gene in the human and mouse genomes.* Mol Pharmacol, 1994. **45**(4): p. 608-17.

223. Wan, M., *et al., Conserved chromosomal location and genomic structure of human and mouse fatty-acid amide hydrolase genes and evaluation of clasper as a candidate neurological mutation.* Genomics, 1998. **54**(3): p. 408-14.

224. Adams, R.H., *et al., Gene structure and glial expression of the glycine transporter GlyT1 in embryonic and adult rodents.* J Neurosci, 1995. **15**(3 Pt 2): p. 2524-32.

225. Liu, Q.R., *et al., Cloning and expression of a glycine transporter from mouse brain.* FEBS Lett, 1992. **305**(2): p. 110-4.

226. Thomas, E.A., *et al., Fatty acid amide hydrolase, the degradative enzyme for anandamide and oleamide, has selective distribution in neurons within the rat central nervous system.* J Neurosci Res, 1997. **50**(6): p. 1047-52.

227. Mechoulam, R., *et al., Anandamide may mediate sleep induction.* Nature, 1997. **389**(6646): p. 25-6.

228. Schloss, P., A.W. Puschel, and H. Betz, *Neurotransmitter transporters: new members of known families.* Curr Opin Cell Biol, 1994. **6**(4): p. 595-9.

229. Sweet, H.O., *Clapser (cla).* Mouse News Letter, 1985. **75**: p. 18.

230. Singh, G., *et al., legless insertional mutation: morphological, molecular, and genetic characterization.* Genes Dev, 1991. **5**(12A): p. 2245-55.

231. Woychik, R.P., *et al., 'Formins': proteins deduced from the alternative transcripts of the limb deformity gene.* Nature, 1990. **346**(6287): p. 850-3.

232. Borowsky, B., E. Mezey, and B.J. Hoffman, *Two glycine transporter variants with distinct localization in the CNS and peripheral tissues are encoded by a common gene.* Neuron, 1993. **10**(5): p. 851-63.

233. Hall, P.V., *et al., Glycine and experimental spinal spasticity.* Neurology, 1979. **29**(2): p. 262-7.

234. White, W.F. and A.H. Heller, *Glycine receptor alteration in the mutant mouse spastic.* Nature, 1982. **298**(5875): p. 655-7.

235. Hayashi, H., *et al., Reduced glycine receptor in the spinal cord in amyotrophic lateral sclerosis.* Ann Neurol, 1981. **9**(3): p. 292-4.

236. Lloyd, K.G., *et al., Neurochemical and neuropharmacological indications for the involvement of GABA and glycine receptors in neuropsychiatric disorders.* Adv Biochem Psychopharmacol, 1983. **37**: p. 137-48.

237. Cravatt, B.F., *et al., Chemical characterization of a family of brain lipids that induce sleep.* Science, 1995. **268**(5216): p. 1506-9.

238. Cravatt, B.F., *et al., Molecular characterization of an enzyme that degrades neuromodulatory fatty-acid amides.* Nature, 1996. **384**(6604): p. 83-7.

239. Giang, D.K. and B.F. Cravatt, *Molecular characterization of human and mouse fatty acid amide hydrolases.* Proc Natl Acad Sci U S A, 1997. **94**(6): p. 2238-42.

240. Howell, B.W., *et al., Neuronal position in the developing brain is regulated by mouse disabled-1.* Nature, 1997. **389**(6652): p. 733-7.

241. Sheldon, M., *et al., Scrambler and yotari disrupt the disabled gene and produce a reeler- like phenotype in mice.* Nature, 1997. **389**(6652): p. 730-3.

242. Xu, X.X., *et al., Disabled-2 (Dab2) is an SH3 domain-binding partner of Grb2.* Oncogene, 1998. **16**(12): p. 1561-9.

243. Gertler, F.B., *et al., Dosage-sensitive modifiers of Drosophila abl tyrosine kinase function: prospero, a regulator of axonal outgrowth, and disabled, a*

novel tyrosine kinase substrate [published erratum appears in Genes Dev 1996 Sep 1;10(17):2234]. Genes Dev, 1993. 7(3): p. 441-53.

244. Pawson, T. and J.D. Scott, *Signaling through scaffold, anchoring, and adaptor proteins.* Science, 1997. **278**(5346): p. 2075-80.

245. Gustafson, T.A., *et al., Phosphotyrosine-dependent interaction of SHC and insulin receptor substrate 1 with the NPEY motif of the insulin receptor via a novel non- SH2 domain.* Mol Cell Biol, 1995. **15**(5): p. 2500-8.

246. Fiore, F., *et al., The regions of the Fe65 protein homologous to the phosphotyrosine interaction/phosphotyrosine binding domain of Shc bind the intracellular domain of the Alzheimer's amyloid precursor protein.* J Biol Chem, 1995. **270**(52): p. 30853-6.

247. Trommsdorff, M., *et al., Interaction of cytosolic adaptor proteins with neuronal apolipoprotein E receptors and the amyloid precursor protein.* J Biol Chem, 1998. **273**(50): p. 33556-60.

248. Yoneshima, H., *et al., A novel neurological mutant mouse, yotari, which exhibits reeler-like phenotype but expresses CR-50 antigen/reelin.* Neurosci Res, 1997. **29**(3): p. 217-23.

249. Kuff, E.L. and K.K. Lueders, *The intracisternal A-particle gene family: structure and functional aspects.* Adv Cancer Res, 1988. **51**: p. 183-276.

250. Lueders, K.K. and E.L. Kuff, *Intracisternal A-particle genes: identification in the genome of Mus musculus and comparison of multiple isolates from a mouse gene library.* Proc Natl Acad Sci U S A, 1980. 77(6): p. 3571-5.

251. Royaux, I., *et al., Reln(rl-Alb2), an allele of reeler isolated from a chlorambucil screen, is due to an IAP insertion with exon skipping.* Genomics, 1997. **42**(3): p. 479-82.

252. Goldowitz, D., *et al., Cerebellar disorganization characteristic of reeler in scrambler mutant mice despite presence of reelin.* J Neurosci, 1997. **17**(22): p. 8767-77.

253. Rice, D.S., *et al., Disabled-1 acts downstream of Reelin in a signaling pathway that controls laminar organization in the mammalian brain.* Development, 1998. **125**(18): p. 3719-29.

254. Falconer, D.S., *Two new mutants trembler and reeler, with neurological actions in the house mouse.* Journal of Genetics, 1951. **50**: p. 192-201.

255. Miao, G.G., *et al., Isolation of an allele of reeler by insertional mutagenesis.* Proc Natl Acad Sci U S A, 1994. **91**(23): p. 11050-4.

256. Howell, B.W., T.M. Herrick, and J.A. Cooper, *Reelin-induced tryosine phosphorylation of disabled 1 during neuronal positioning.* Genes Dev, 1999. **13**(6): p. 643-8.

257. Chen, W.J., J.L. Goldstein, and M.S. Brown, *NPXY, a sequence often found in cytoplasmic tails, is required for coated pit-mediated internalization of the low density lipoprotein receptor.* J Biol Chem, 1990. **265**(6): p. 3116-23.

258. Krieger, M. and J. Herz, *Structures and functions of multiligand lipoprotein receptors: macrophage scavenger receptors and LDL receptor-related protein (LRP).* Annu Rev Biochem, 1994. **63**: p. 601-37.

259. Trommsdorff, M., *et al., Reeler/Disabled-like disruption of neuronal migration in knockout mice lacking the VLDL receptor and ApoE receptor 2.* Cell, 1999. **97**(6): p. 689-701.

260. Hiesberger, T., *et al., Direct binding of Reelin to VLDL receptor and ApoE receptor 2 induces tyrosine phosphorylation of disabled-1 and modulates tau phosphorylation.* Neuron, 1999. **24**(2): p. 481-9.

261. Gilmore, E.C., *et al.*, *Cyclin-dependent kinase 5-deficient mice demonstrate novel developmental arrest in cerebral cortex.* J Neurosci, 1998. **18**(16): p. 6370-7.

262. Kwon, Y.T. and L.H. Tsai, *A novel disruption of cortical development in p35(-/-) mice distinct from reeler.* J Comp Neurol, 1998. **395**(4): p. 510-22.

263. Davis, A.P. and M.J. Justice, *Mouse alleles: if you've seen one, you haven't seen them all.* Trends Genet, 1998. **14**(11): p. 438-41.

264. Huang, J.D., *et al.*, *Molecular genetic dissection of mouse unconventional myosin-VA: tail region mutations [published erratum appears in Genetics 1998 Nov;150(3):1332].* Genetics, 1998. **148**(4): p. 1963-72.

265. Huang, J.D., *et al.*, *Molecular genetic dissection of mouse unconventional myosin-VA: head region mutations.* Genetics, 1998. **148**(4): p. 1951-61.

266. DiLeone, R.J., L.B. Russell, and D.M. Kingsley, *An extensive 3' regulatory region controls expression of Bmp5 in specific anatomical structures of the mouse embryo.* Genetics, 1998. **148**(1): p. 401-8.

267. Hamada, T., *et al.*, *Mechanism of chromosomal integration of transgenes in microinjected mouse eggs: sequence analysis of genome-transgene and transgene-transgene junctions at two loci.* Gene, 1993. **128**(2): p. 197-202.

268. Triglia, T., M.G. Peterson, and D.J. Kemp, *A procedure for in vitro amplification of DNA segments that lie outside the boundaries of known sequences.* Nucleic Acids Res, 1988. **16**(16): p. 8186.

269. Lagerstrom, M., *et al.*, *Capture PCR: efficient amplification of DNA fragments adjacent to a known sequence in human and YAC DNA.* PCR Methods Appl, 1991. **1**(2): p. 111-9.

270. Arnold, C. and I.J. Hodgson, *Vectorette PCR: a novel approach to genomic walking.* PCR Methods Appl, 1991. **1**(1): p. 39-42.

271. Allen, M.J., A. Collick, and A.J. Jeffreys, *Use of vectorette and subvectorette PCR to isolate transgene flanking DNA.* PCR Methods Appl, 1994. **4**(2): p. 71-5.

272. Liu, Y.G. and R.F. Whittier, *Thermal asymmetric interlaced PCR: automatable amplification and sequencing of insert end fragments from P1 and YAC clones for chromosome walking.* Genomics, 1995. **25**(3): p. 674-81.

273. Sarkar, G., R.T. Turner, and M.E. Bolander, *Restriction-site PCR: a direct method of unknown sequence retrieval adjacent to a known locus by using universal primers.* PCR Methods Appl, 1993. **2**(4): p. 318-22.

274. Minami, M., *et al., A novel PCR technique using Alu-specific primers to identify unknown flanking sequences from the human genome.* Genomics, 1995. **29**(2): p. 403-8.

275. de Krester, D.M. and J.B. Kerr, *The cytology of the testis,* in *The physiology of reproduction,* E. Knobil and J.D. Neill, Editors. 1994, Raven Press: New York. p. 1177 - 1290.

276. Bremner, W.J., *et al., Immunohistochemical localization of androgen receptors in the rat testis: evidence for stage-dependent expression and regulation by androgens.* Endocrinology, 1994. **135**(3): p. 1227-34.

277. Okabe, M., M. Ikawa, and J. Ashkenas, *Male infertility and the genetics of spermatogenesis.* Am J Hum Genet, 1998. **62**(6): p. 1274-81.

278. Hargreave, T.B., *Human infertility,* in *Male Infertility,* T.B. Hargreave, Editor. 1997, Springer Verlag. p. 1 - 16.

279. Palermo, G., *et al., Pregnancies after intracytoplasmic injection of single spermatozoon into an oocyte.* Lancet, 1992. **340**(8810): p. 17-8.

280. Patrizio, P. and J. Zielenski, *Congenital absence of the vas deferens: a mild form of cystic fibrosis.* Mol Med Today, 1996. **2**(1): p. 24-31.

281. Van Assche, E., *et al.*, *Cytogenetics of infertile men.* Hum Reprod, 1996. **11 Suppl 4**: p. 1-24; discussion 25-6.

282. Patrizio, P. and D. Broomfield, *The genetic basis of male infertility*, in *male fertility and infertility*, T.D. Glover and C.L.R. Barratt, Editors. 1999, Cambridge University Press: Cambridge. p. 162 - 179.

283. Mak, V. and K.A. Jarvi, *The genetics of male infertility.* J Urol, 1996. **156**(4): p. 1245-56; discussion 1256-7.

284. Hulten, M. and J. Lindsten, *Cytogenetic aspects of human male meiosis.* Adv Hum Genet, 1973. **4**: p. 327-87.

285. Reijo, R., *et al.*, *Diverse spermatogenic defects in humans caused by Y chromosome deletions encompassing a novel RNA-binding protein gene.* Nat Genet, 1995. **10**(4): p. 383-93.

286. Vergnaud, G., *et al.*, *A deletion map of the human Y chromosome based on DNA hybridization.* Am J Hum Genet, 1986. **38**(2): p. 109-24.

287. Vollrath, D., *et al.*, *The human Y chromosome: a 43-interval map based on naturally occurring deletions.* Science, 1992. **258**(5079): p. 52-9.

288. Qureshi, S.J., *et al.*, *Polymerase chain reaction screening for Y chromosome microdeletions: a first step towards the diagnosis of genetically-determined spermatogenic failure in men.* Mol Hum Reprod, 1996. **2**(10): p. 775-9.

289. Vogt, P.H., *et al.*, *Human Y chromosome azoospermia factors (AZF) mapped to different subregions in Yq11.* Hum Mol Genet, 1996. **5**(7): p. 933-43.

290. Lahn, B.T. and D.C. Page, *Functional coherence of the human Y chromosome.* Science, 1997. **278**(5338): p. 675-80.

291. Vogt, P.H., *Human Y chromosome deletions in Yq11 and male fertility.* Adv Exp Med Biol, 1997. **424**: p. 17-30.

292. Ma, K., *et al., A Y chromosome gene family with RNA-binding protein homology: candidates for the azoospermia factor AZF controlling human spermatogenesis.* Cell, 1993. **75**(7): p. 1287-95.

293. Elliott, D.J., *et al., Expression of RBM in the nuclei of human germ cells is dependent on a critical region of the Y chromosome long arm.* Proc Natl Acad Sci U S A, 1997. **94**(8): p. 3848-53.

294. Kenan, D.J., C.C. Query, and J.D. Keene, *RNA recognition: towards identifying determinants of specificity.* Trends Biochem Sci, 1991. **16**(6): p. 214-20.

295. Elliott, D.J. and H.J. Cooke, *The molecular genetics of male infertility.* Bioessays, 1997. **19**(9): p. 801-9.

296. Yen, P.H., N.N. Chai, and E.C. Salido, *The human autosomal gene DAZLA: testis specificity and a candidate for male infertility.* Hum Mol Genet, 1996. **5**(12): p. 2013-7.

297. Weighardt, F., G. Biamonti, and S. Riva, *The roles of heterogeneous nuclear ribonucleoproteins (hnRNP) in RNA metabolism.* Bioessays, 1996. **18**(9): p. 747-56.

298. Bishop, C.E. and M.J. Mitchell, *Mouse Y Chromosome.* Mamm Genome, 1996. **6**(13): p. 331-3.

299. Bishop, C.E., *Mouse Y chromosome.* Mamm Genome, 1992. **3 Spec No**: p. S289-93.

300. Levy, E.R. and P.S. Burgoyne, *The fate of XO germ cells in the testes of XO/XY and XO/XY/XYY mouse mosaics: evidence for a spermatogenesis gene on the mouse Y chromosome.* Cytogenet Cell Genet, 1986. **42**(4): p. 208-13.

301. Kay, G.F., *et al., A candidate spermatogenesis gene on the mouse Y chromosome is homologous to ubiquitin-activating enzyme E1.* Nature, 1991. **354**(6353): p. 486-9.

302. Mitchell, M.J., *et al., Homology of a candidate spermatogenic gene from the mouse Y chromosome to the ubiquitin-activating enzyme E1.* Nature, 1991. **354**(6353): p. 483-6.

303. Burgoyne, P.S., *et al., Fertility in mice requires X-Y pairing and a Y-chromosomal "spermiogenesis" gene mapping to the long arm.* Cell, 1992. **71**(3): p. 391-8.

304. Conway, S.J., *et al., Y353/B: a candidate multiple-copy spermiogenesis gene on the mouse Y chromosome.* Mamm Genome, 1994. **5**(4): p. 203-10.

305. Cooke, H.J., *et al., A murine homologue of the human DAZ gene is autosomal and expressed only in male and female gonads.* Hum Mol Genet, 1996. **5**(4): p. 513-6.

306. Reijo, R., *et al., Mouse autosomal homolog of DAZ, a candidate male sterility gene in humans, is expressed in male germ cells before and after puberty.* Genomics, 1996. **35**(2): p. 346-52.

307. Elliott, D.J., *et al., An RBM homologue maps to the mouse Y chromosome and is expressed in germ cells.* Hum Mol Genet, 1996. **5**(7): p. 869-74.

308. Baker, S.M., *et al., Male mice defective in the DNA mismatch repair gene PMS2 exhibit abnormal chromosome synapsis in meiosis.* Cell, 1995. **82**(2): p. 309-19.

309. Edelmann, W., *et al., Meiotic pachytene arrest in MLH1-deficient mice.* Cell, 1996. **85**(7): p. 1125-34.

310. Roest, H.P., *et al., Inactivation of the HR6B ubiquitin-conjugating DNA repair enzyme in mice causes male sterility associated with chromatin modification.* Cell, 1996. **86**(5): p. 799-810.

311. Koken, M.H., *et al., Structural and functional conservation of two human homologs of the yeast DNA repair gene RAD6.* Proc Natl Acad Sci U S A, 1991. **88**(20): p. 8865-9.